

INDIAN INSTITUTE OF TECHNOLOGY GANDHINAGAR

DOCTORAL THESIS

Some Novel Studies of Black holes in General Relativity and Modified Theories

Author:

Akash K. MISHRA

Supervisor:

Dr. Sudipta SARKAR



*A thesis submitted in fulfillment of the requirements
for the degree of Doctor of Philosophy
in the*

Department of Physics
IIT Gandhinagar

Declaration

I, **Akash K. MISHRA**, declare that this thesis titled, Some Novel Studies of Black holes in General Relativity and Modified Theories represents my ideas in my own words and where other's ideas or words incorporated, I have adequately cited and referenced the original sources. Also, I declare that I have adhered to all principles of academic honesty and integrity and have not falsified or fabricated any idea/fact/source in this submission. I understand that any violation of the above can cause disciplinary action by the Institute and can also summon penal action from the sources which have thus not been properly cited or from whom proper permission has not been taken.

Signed: Akash K. Mishra

Date: 31. 05. 2021

CERTIFICATE

It is certified that the work contained in the thesis titled Some Novel Studies of Black holes in General Relativity and Modified Theories by Mr. **Akash K. MISHRA** (Roll No. 14510035), has been carried out under my supervision and that this work has not been submitted elsewhere for a degree.

Dr. Sudipta SARKAR
(Thesis Supervisor)
Department of Physics
IIT Gandhinagar
Date: 31. 05. 2021

Dedicated To...

My Mother (Kalpana Mishra)

and

In the memory of my grandfather (Late Bhagawat Mishra)

Acknowledgements

Looking back at last few years of my graduate studies, it gives me immense pleasure to acknowledge the help and support of several people involved in my research work and personal life directly or indirectly.

First and foremost, I express my immeasurable sense of gratitude and appreciation towards my doctoral supervisor Prof. Sudipta Sarkar for his patient guidance and encouragement throughout this thesis work. It has been an excellent opportunity as well as a great learning experience to work under his mentorship. I sincerely thank him for suggesting me many interesting problems and his help and support at various stages of my PhD. Certainly, I could not have asked for a better supervisor.

I wish to thank Dr Sumanta Chakraborty (IACS, Kolkata) for his wonderful collaboration and guidance through several projects. His suggestions and advice have always helped me greatly in my research. I also thank him for hosting me at IACS several times during my visits. I thank Prof. Maulik Parikh for being my host supervisor at Arizona State University (ASU) during my visit. Discussions with him have immensely helped me in understanding various concepts of quantum field theory and black holes.

A sincere note of gratitude towards my Doctoral Study Committee members Prof. Baradhwaj Coleppa and Prof. Sanjay Amrutiya for their valuable inputs and comments on my work. It has enormously helped me in my research. I am also grateful to you for the opportunity to work under your guidance on several projects in quantum field theory and differential geometry. I have learned a lot from you.

I want to thank our previous group member and collaborator Avirup Ghosh for his inputs in my research projects during the early part of my PhD. Also, for patiently listening to my questions and help me to understand several difficult concepts of my research area. I thank my senior colleague Fairoos for his help and support. He has always been an elder brother to me. I also thank Rakesh Ghosh for many useful discussions. In addition, I acknowledge my co-authors Abhirup Ghosh, Soumya Jana and Mostafizur Rahman, for collaborations. Over time, Mostafizur has become one of my best friends.

I also take this opportunity to thank the entire physics discipline of IIT Gandhinagar for being so supportive and offering such a friendly and research-oriented atmosphere to the students. Thanks to my teachers, Professor Puri, Anand, Rupak and Vinod, for guiding me through many interesting courses. I acknowledge the help of Prof. Krishna on several academic-related matters. He was always easily approachable whenever I needed any guidance. A special thanks to Prasanna for several physics and beyond physics (cricket, politics etc.) discussions.

I am forever thankful to my friends and PhD colleagues Agnivo, Ashish, Manu, Utsav and Kaushik, with whom I have shared some of the most memorable moments of my life. Thanks for several group discussions and journal clubs which has undoubtedly helped me in my research. I have learned a lot from all of you. Your friendship is one of the most important takeaways of my PhD career. I wish you all the best in your future ambitions. I am also thankful to Soumen and Lalit for patiently explaining various concepts of gravitational wave research. Thanks to Rahul and Gokul for challenging chess

games.

To my best friends Debasish and Sumit for their lifelong friendship and standing with me in tough times. Thanks for your encouragement. A special mention of my good friend Bidhan for all of our discussions on politics, cricket and life. I fondly remember my friends Eva and Callum from Tempe. Thank you very much for your wonderful friendship and for making my stay comfortable in the US.

Lastly, I would like to thank my family and relatives for their continuous support and encouragement. My mother has always been the greatest source of inspiration to me. I owe her everything. She struggled and sacrificed a lot in raising us. It is her guidance and blessings that has driven me to this point. Thanks to my brother Alok for carrying all the burden and responsibility of the family in my absence. I have dedicated this thesis to my grandparents (Bhagawat and Sudeshna) for their unconditional affection and blessings for me. Also for all the valuable life lessons that were crucial in shaping my character. My uncle Pradeep and aunt Kalyani have been an integral part of my family. I thank them for standing with us in tough times. Finally, my sister Jasmin, you are always special to me.

I gratefully acknowledge the financial support provided by my institute IIT Gandhinagar during my PhD tenure. I also thank the institute for the overseas research fellowship and fully funding my visit to Arizona State University.

Akash K. Mishra

Abstract

The primary motivation of this thesis is to study certain theoretical and observational aspects of theories beyond general relativity. This includes the horizon topology, thermodynamics of black holes, cosmic censorship conjectures, gravitational lensing, gravitational waves etc.

The topology theorem by Hawking is considered as one of the most important results in classical black hole physics. The theorem asserts that the admissible topology of the event horizon cross-section of black holes in general relativity is either spherical (S^2) or toroidal ($S^1 \times S^1$). However, this result is specific to four-dimensional black hole solutions in general relativity. In this thesis, we have studied the topology theorem in the context of $f(R)$ theory of gravity. We have obtained a sufficient differential condition on the function $f(R)$ for which the allowed topological structures in $f(R)$ theory is identical to that of general relativity. We also extend this result to higher dimensions.

Further, we study the Physical Process First Law (PPFL) of black hole thermodynamics in an arbitrary diffeomorphism invariant theory of gravity. We have obtained the most general form of the variation of horizon entropy and use the result to understand the effects of the ambiguities present in the Wald entropy on the formulation of PPFL. We show that, for linear order perturbation, when the variation of entropy is computed between a past bifurcation surface and a future stationary slice, the PPFL is independent of the ambiguity terms. Finally, we calculate the change in entropy between two arbitrary non-equilibrium cross-sections of the event horizon. In this setting, we could express the variation of entropy as the first law by identifying the additional boundary term to be horizon membrane energy. We have explicitly illustrated this result in the context of Einstein-Gauss-Bonnet gravity and arbitrary order Lovelock theory.

This thesis also addresses the validity of cosmic censorship conjectures (weak and strong) in various non-trivial settings. The weak cosmic censorship negates the formation of naked singularity as the final state of a gravitational collapse. This is essential to ensure the stability of black holes under small perturbations. We examine the Gedanken experiment of overcharging a system of two extremal black holes via the process of charged particle absorption to test the validity of weak cosmic censorship. We show that, even for such a non-trivial system, the conjecture remains valid. Also, our work represents the first-ever study of weak cosmic censorship in a multi black hole setting. Furthermore, we study the strong cosmic censorship conjecture in higher curvature theories, which is a statement regarding the deterministic nature of the underlying theory of gravity. The primary motivation of this work is to understand the effects of higher curvature couplings on the violation of strong cosmic censorship conjecture. Our results indicate that the violation seems to be stronger in the presence of higher curvature terms. We demonstrate this result for charged de Sitter black holes in Einstein-Gauss-Bonnet gravity and pure Lovelock gravity.

Because of the strong gravitational lensing effect, light can follow a circular path in the vicinity of black holes known as photon orbits. This gives rise to the formation of shadow structure around a black hole. Surprisingly, most of the previous studies of black hole shadow consider the spacetime to be stationary. This is only an idealization since an astrophysical black hole strongly interacts with the surrounding matter distribution and, as a result, cannot be represented by a stationary spacetime ansatz. In this thesis, for the first time, we study the evolution of the photon sphere and shadow radius around several black hole solutions in general relativity and Einstein-Gauss-Bonnet gravity. We obtained a general second-order differential equation that governs the dynamics of the photon

sphere and illustrates some interesting results by applying it to various dynamical models.

Setting constraints on theories of gravity beyond general relativity has been of growing interest in recent years. With the recent advancement of gravitational wave detectors, we can access the previously unexplored strong and dynamical regime of gravity. The gravitational-wave observation provides an unprecedented opportunity to test the predictions of general relativity and constrain modified theories. The second part of this thesis attempts to connect theory and observations in gravitational physics. In particular, we have developed two general methodologies to obtain constraints on the parameters of modified gravity theories from gravitational-wave observations. Firstly, using the observed time delay between the gravitational-wave and electromagnetic signal in the GW 170817 event, we constrain the coupling of the quadratic gravity in four dimensions. Finally, using the observed quasi-normal mode spectrum of the GW 150914 event, we were able to constrain the tidal charge parameter of a rotating braneworld black hole. These formalism are entirely general and can be employed in several other class of modified gravity models.

List of Publications

The results presented in this thesis are based on the following publications,

- **Akash Mishra**, S. Chakraborty, A. Ghosh, S. Sarkar, "On the physical process first law for dynamical black holes," *JHEP* 09 (2018) 034, arXiv:1709.08925.
- **Akash K. Mishra**, M. Rahman, S. Sarkar, "Black hole topology in $f(R)$ gravity," *Class.Quant.Grav.* 35 (2018) 14, 145011, arXiv:1806.06596.
- **Akash K. Mishra**, S. Chakraborty, S. Sarkar, "Understanding photon sphere and black hole shadow in dynamically evolving spacetimes," *Phys.Rev.D* 99 (2019) 10, 104080, arXiv:1903.06376.
- **Akash K. Mishra**, S. Sarkar, "Overcharging a multi black hole system and cosmic censorship," *Phys.Rev.D* 100 (2019) 2, 024030, arXiv:1905.00394.
- A. Ghosh, S. Jana, **Akash K. Mishra**, S. Sarkar, "Constraints on higher curvature gravity from time delay between GW170817 and GRB 170817A," *Phys.Rev.D* 100 (2019) 8, 084054, arXiv:1906.08014.
- **Akash K. Mishra**, S. Chakraborty, "Strong Cosmic Censorship in higher curvature gravity," *Phys.Rev.D* 101 (2020) 6, 064041, arXiv:1911.09855.
- **Akash K. Mishra**, "Quasinormal modes and strong cosmic censorship in the regularised 4D Einstein–Gauss–Bonnet gravity," *Gen.Rel.Grav.* 52 (2020) 11, 106, arXiv:2004.01243.
- **Akash K. Mishra**, A. Ghosh, S. Chakraborty, "Constraining extra dimensions using observations of black hole quasi-normal modes," arXiv:2106.05558.

Contents

Acknowledgements	ix
Abstract	xi
1 Introduction	1
1.1 Einstein's Theory of General Relativity	1
1.2 Limitations of General Relativity & Motivation for Modified Theories	2
1.2.1 Presence of Spacetime Singularity	3
1.2.2 The Cosmological Constant Problem	3
1.2.3 Incompatibility with Quantum Theory	4
1.3 A General Overview of Higher Curvature Theories	4
1.3.1 Lanczos-Lovelock Theories	5
1.3.2 $f(R)$ Theories	5
1.3.3 Quadratic-Curvature Theories in Four-Dimensions	6
1.4 Classical Black holes and their Properties	6
1.4.1 Horizon Geometry	6
1.4.2 Black hole Thermodynamics	7
1.4.3 Photon Sphere and Black hole Shadow	8
1.4.4 Cosmic Censorship Conjectures	11
1.5 Confronting Theories with Observations	12
1.6 An Overview of the Thesis	13
2 Black Hole Topology in $f(R)$ Gravity	17
2.1 Topology of a stationary black hole horizon in $3 + 1$ dimensions	18
2.2 Generalization to Higher Dimensions	24
2.3 Summary	26
3 On the General Structure of Physical Process first Law	29
3.1 General Structure of PPFL	31
3.2 Black hole Entropy and Ambiguities	35
3.3 Membrane Paradigm for Black holes	37
3.4 Physical process first law and the membrane paradigm	37
3.5 First law for dynamical black holes in Einstein-Gauss-Bonnet gravity	39
3.6 Summary	41

4 Photon Sphere and Black hole Shadow in Dynamically Evolving Spacetimes	43
4.1 Evolution of Photon Sphere in a Spherically Symmetric Dynamical Spacetime	44
4.2 Application: Photon Sphere in Vaidya and Reissner-Nordström-Vaidya Spacetimes . .	45
4.2.1 Photon Sphere in Vaidya Space time	46
4.2.2 Reissner-Nordström-Vaidya Space-time	49
4.2.3 Schwarzschild-de Sitter Spacetime	54
4.3 Shadow of a Spherically Symmetric Dynamical Black Hole	55
4.4 Kerr-Vaidya in the Slow Rotation Limit	58
4.4.1 Evolution of Photon Circular Orbit	58
4.4.2 Shadow Casted by Slowly-Rotating Kerr-Vaidya Black Hole	61
4.5 Effective Graviton Metric in Gauss-Bonnet Gravity	63
4.5.1 Photon Vs. Graviton Sphere	65
4.6 Summary	69
5 Overcharging a multi black hole system and the Weak Cosmic Censorship	71
5.1 Introduction and Motivation	71
5.2 Overcharging a Majumdar-Papapetrou configuration	72
5.3 Summary	76
6 Strong Cosmic Censorship in Higher Curvature Gravity	77
6.1 Introduction and Motivation	77
6.2 Strong cosmic censorship conjecture and Quasi-normal modes: A brief overview . . .	79
6.3 Numerical Analysis: Computation of quasi-normal modes	82
6.3.1 Frequency Domain	82
6.3.2 Time Domain	83
6.4 Validity of Strong Cosmic Censorship	84
6.4.1 Higher dimensional Einstein-Gauss-Bonnet Gravity	84
6.4.2 Pure Lovelock Gravity	88
6.4.3 Four dimensional Einstein-Gauss-Bonnet Gravity	90
Scalar perturbation	91
Electromagnetic perturbation	92
6.5 Summary	94
7 Constraints on Higher Curvature Theories from Gravitational Wave Observations	97
7.1 A general framework for the time delay between Gravitational Wave and Electromagnetic signal	98
7.2 Time delay in higher curvature gravity	100
7.3 Summary	103
8 Constraining the tidal charge parameter of a Braneworld Black hole	105
8.1 Introduction and Motivation	105
8.2 Brief review of rotating braneworld black hole	106
8.3 Quasi-normal modes of a rotating braneworld black hole	107
8.4 Bounds from GW 150914	110
8.5 Conclusion	112
9 Conclusion and Future Outlook	113

A Derivation of the Evolution Equation for photon sphere (Chapter 4)	119
B Derivation of the effective graviton metric (Chapter 4)	121

List of Figures

1.1	In the left panel we have shown the shadow cast by a Kerr black hole for various spin parameter. In the right panel, we have shown the recent image of the supermassive object at the centre of M87 galaxy captured by the event horizon telescope.	11
3.1	A geometric illustration of the physical process first law	30
3.2	The point \mathcal{B} ($U = 0, V = 0$), a $(d - 2)$ -dimensional cross-section of the Horizon represents the Bifurcation surface, where $\theta_k, \theta_l = 0$	32
4.1	Evolution of the photon sphere, event horizon and apparent horizon for the mass function $\frac{M_0}{2} \{1 + \tanh(v)\}$	47
4.2	Evolution of the photon sphere radius for various other mass function	48
4.3	Evolution of the photon sphere radius for radiating black hole	49
4.4	Evolution of the photon sphere, event horizon and apparent horizon for mass and charge profile in Eq. (4.2.8)	51
4.5	Dynamics of the photon sphere in the presence of a critical surface corresponding to mass and charge functions are given in Eq. (4.2.9)	51
4.6	Dynamical evolution of the photon sphere in the presence of a critical surface for the choice of $M(v) = 0.95 + (0.05/2)\{1 + \tanh(v)\}$ and $Q(v) = (0.9/2)\{1 + \tanh(v)\}$. . .	52
4.7	Evolution of the photon sphere, event horizon and apparent horizon for $M(v) = 0.5\{1 + \tanh(v)\}$ and $Q(v) = 0.45\{1 - \tanh(1 - v)\}$	53
4.8	Evolution of the photon sphere, event horizon and apparent horizon for $M(v) = 0.5\{1 + \tanh(v)\}$ as well as $Q(v) = 0.3\{1 - \tanh(1 - v)\}$	54
4.9	In this figure we have shown the evolution of the photon sphere for dynamical Schwarzschild de Sitter spacetime. The mass functions are chosen to be $M(v) = M_0\{1 + \tanh(v)\}$ (left panel) and $M(v) = M_0\{2 - \operatorname{sech}(v)\}$ (right panel) with $M_0 = 1$	55
4.10	Dynamical evolution of black hole shadow for various mass and charge functions . .	57
4.11	This figure illustrates the evolution of prograde photon orbits for the choice of mass functions $M(v) = 1 + \tanh(v)$ [left panel] and $M(v) = 2 - \operatorname{sech}(v)$ [right panel]. The rotation parameter ‘ a ’ has been chosen to be 0.01.	60
4.12	Shadow of slowly rotating Kerr Vaidya black hole.	62

4.13 In this figure we depict the evolution of the photon sphere and shadow around a Gauss-Bonnet black hole in five-dimensions for various choice of coupling constants α . The top left and right panel shows the evolution of photon sphere for $m(v) = 1 + \tanh(v)$ and $m(v) = 1 - \tanh(u)$ respectively. In the bottom left and right panel we have plotted the corresponding evolution of shadow.	66
4.14 In this figure we compare the evolution of photon and graviton sphere around a five-dimensional Gauss-Bonnet black hole for the choice of mass function $M(v) = 1 + \tanh(v)$ and the coupling constant $\alpha = 0.01$ (top left), 0.001 (top right), 0.00001 (bottom) respectvelly.	68
4.15 This figure represents a snapshot of the evolution of graviton and photon shadow at in-going time $v = 2$ w.r.t the mass function $M(v) = 1 + \tanh(v)$ and coupling constant $\alpha = 0.01$	69
 6.1 Time domain evolution of a scalar field perturbation on a charged de Sitter black hole background in five-dimensional Einstein-Gauss-Bonnet theory.	84
6.2 Plot of β for the photon sphere , de Sitter and near extremal modes corresponding to five-dimensional Einstein-Gauss-Bonnet gravity.	87
6.3 Violation of strong cosmic censorship in the context of five and higher dimensional Einstein-Gauss-Bonnet gravity.	88
6.4 Violation of strong cosmic censorship conjecture in seven-dimensional pure Gauss-Bonnet gravity.	89
6.5 In this figure we demonstrate the variation of $\{-(\text{Im } \omega_n)/\kappa_{\text{ch}}\}$ against (Q/Q_m) for all three family of modes in the contest of scalar perturbation for various choice of cosmological constant(Λ) and the Gauss-Bonnet coupling constant(α). Mass of the black hole is taken to be unity.	92
6.6 The variation of β is presented corresponding to electromagnetic perturbation for the de Sitter modes(green) and the photon sphere modes(blue) for various choice of cosmological constant(Λ) and the Gauss-Bonnet coupling constant(α). The vertical line represents the value of Q/Q_m where the violation of strong cosmic censorship conjecture occurs for the first time. The Mass parameter of the black hole is taken to be unity.	93
 8.1 Quasi-normal modes of rotating brane world black hole.	110
8.2 90% credible interval of the 2D posterior probability distributions of the frequency and damping time of the (2,2) quasi-normal modes. The labels refers to the LIGO-Virgo analysis used for the corresponding distribution. For the 'PyRing' distributions, the mass and spin samples from the GW150914 PyRing analysis were used to predict the distributions on (f_{220}, τ_{220}) for a given value of β . The pSEOBNRv4HM posterior is from [1] and the 'IMR' posterior is from [2].	111

List of Tables

6.1	Numerical values of $\{-(\text{Im } \omega_{n,\ell})/\kappa_{\text{ch}}\}$ for photon sphere , de Sitter and near extremal modes corresponding to scalar perturbation in five-dimensional Einstein-Gauss-Bonnet gravity.	86
6.2	Numerical values of $\{-\min. (\text{Im } \omega_n)/\kappa_{\text{ch}}\}$ is presented for photon sphere , de Sitter and near extremal modes corresponding to scalar perturbation in four-dimensional Einstein-Gauss-Bonnet gravity.	91
6.3	Numerical values of $\{-\min. (\text{Im } \omega_n)/\kappa_{\text{ch}}\}$ is presented for photon sphere and de Sitter mode corresponding to electromagnetic perturbation in the four-dimensional Einstein-Gauss-Bonnet gravity.	93
8.1	In this table we present the numerical values of the quasi-normal frequency corresponding to the modes $(n=0,l=m=2)$ and $(n=0,l=m=3)$ for gravitational perturbation($s=-2$). We have taken the spin parameter to be $a = 0.67$ and mass of the remnant as $M = 62M_\odot$. The redshift factor (z) here is 0.093.	109

List of Abbreviations

GR	General Relativity
EGB	Einstein - Gauss - Bonnet
GW	Gravitational Wave
GRB	Gamma Ray Burst
QNM	Quasi - Normal Mode
ΛCDM	Lambda Cold Dark Matter
CMBR	Cosmic Microwave Background Radiation
PPFL	Physical Process First Law

Notations and Conventions

Throughout this thesis we adopt the following notations and conventions. If used otherwise, it will be specified explicitly.

- The d dimensional spacetime metric is denoted as $g_{\mu\nu}$ and the induced metric on a co-dimension two surface is h_{AB} . We work with the metric signature $(-, +, +, +)$. Einstein's convention is assumed to sum over repeated indices.
- The Latin indices ($a, b, \dots h$) and Greek indices ($\alpha, \beta, \mu, \nu, \dots$ etc.) represents the full d -dimensional spacetime index. Coordinates over a co-dimension two surface are denoted by the indices (i, j, \dots etc.) or (A, B, \dots etc.).
- We shall use the geometrized units, in which the speed of light and gravitational constant can be set to unity ($c = 1, G = 1$).

Chapter **1**

Introduction

1.1 Einstein's Theory of General Relativity

Newtonian gravity was well accepted as the fundamental theory of gravitation for more than two hundred years until Einstein formulated the theory of general relativity in 1915. Our modern understanding of gravitational interaction is based in the framework of general relativity, that describes gravity as the curvature of spacetime rather as a force. Such an elegant description of gravitation in the language of differential geometry has revolutionized our understanding of how gravity works at a fundamental level and widely regarded as one of the greatest scientific achievement in the history of mankind. In the framework of general relativity, the spacetime is a pseudo-Riemannian differential manifold equipped with a metric governed by Einstein's equations that relates the matter content and spacetime curvature [3–5],

$$G_{\mu\nu} = R_{\mu\nu} - \frac{1}{2}Rg_{\mu\nu} = 8\pi G T_{\mu\nu} \quad (1.1.1)$$

The interplay of matter and curvature in this context is best described by John Wheeler as "*Spacetime tells matter how to move; matter tells spacetime how to curve*". Even after a century of its discovery, general relativity remains as one of the most successful physical theory of nature.

Einstein's equation is composed of a set of non-linear coupled partial differential equations of the spacetime metric. Such a system can not be exactly solved unless certain spacetime symmetries are assumed. The first solution of Einstein's equation was derived by Karl Schwarzschild with the assumption of spherical symmetry, which reads [6],

$$ds^2 = - \left(1 - \frac{2M}{r}\right) dt^2 + \left(1 - \frac{2M}{r}\right)^{-1} dr^2 + r^2 d\theta^2 + r^2 \sin^2 \theta d\phi^2 \quad (1.1.2)$$

This describes the spacetime geometry exterior to a spherically symmetric matter distribution of mass M and represents the unique asymptotically flat spherically symmetric vacuum solution of Einstein's equation in four dimensions. One can use the Schwarzschild solution outside the Sun to predict the perihelion precession of Mercury, which is considered as one of the classical tests of general relativity [7].

The surface $r = 2M$ behaves like a one-way membrane that causally separates the interior from

the exterior and known as the event horizon. Also, the Schwarzschild solution provided the first suggestion towards the existence of spacetime horizons. However, the Schwarzschild metric only represents the simplest possible one-parameter family of solution of Einstein's equation and completely determined by the mass. Apart from this, several other non-trivial solutions exist in general relativity [8]. For instance, black holes with charge and rotation are represented by Reissner-Nordström and Kerr solution respectively [5, 9]. In four dimensions, according to the uniqueness theorem [10], the Kerr-Newmann family represents the unique stationary asymptotically flat electro-vacuum black hole solution of Einstein's equation. The no-hair theorem further guarantees that all black hole solutions of Einstein-Maxwell equations are characterized by only three parameters, namely the mass (M), electric charge (Q), and angular momentum (J) [11, 12]. The no-hair theorem, along with the uniqueness theorem, severely constrains the solution space of Einstein's equation.

In the past several decades, studies of black holes have revealed various interesting results and have been one of the central themes of research in gravitational physics. We provide a brief overview of some of these results in subsequent sections. The generation of gravitational wave as ripples of spacetime from the coalescence of several binary sources has been recently confirmed by the LIGO-Virgo detectors [13–18]. This is a milestone in astronomy and provides strong evidence for the existence of real astrophysical black holes. Also, the image of the super-massive compact object at the centre of the M87 galaxy captured by the even horizon telescope a year ago resembles the structure of a rotating Kerr black hole [19–22]. These discoveries provide an excellent platform to perform tests of general relativity and alternative theories of gravity in the strong gravity limit.

Like any other physical theory of nature, general relativity has also been put under scrutiny against observations ever since its formulation. The outstanding success of Einstein's theory is not only because of its mathematical beauty but also due to observational consistencies. The main approach to test general relativity from observation can be broadly classified into two categories; a) verifying various predictions of general relativity , b) setting constraints on the parameters of various modified gravity theories. Such tests may include local experiments as well as observations at cosmological length scales. From solar system tests to the evolution of stars and galaxies or measurement of the cosmic microwave background radiation, the predictions of general relativity are in excellent agreement with observations. The classical tests of general relativity include the measurement of the perihelion precession of the Mercury, bending of light by gravity, gravitational red-shift etc., dates back to the days of Einstein and Eddington [7].

The key intuition of Einstein behind the formulation of such a masterpiece was the '*Equivalence Principle*': equivalence between homogeneous gravity and uniform acceleration. In recent years the principle of equivalence has been tested in the laboratory with arbitrary accuracy. For an extensive review of the experimental aspects of general relativity, I refer the reader to Ref. [7] and references therein.

1.2 Limitations of General Relativity & Motivation for Modified Theories

In the previous section, we briefly summarized general relativity, particularly focusing on its theoretical and experimental predictions. However, a theory as successful and appealing as general

relativity also possesses several shortcomings, suggesting it to be an incomplete theory. These limitations can be traced to the fact that general relativity breaks down at small enough length scales. Also, most of the tests of general relativity consider the situation of weak gravity, while analogous tests in the strong gravity regime are still limited. This further suggests that general relativity could be a low energy limit of a more general theory of gravity. In this section, we discuss some of such issues with the theory of general relativity and highlight the motivations to consider alternative theories of gravity.

1.2.1 Presence of Spacetime Singularity

General relativity predicts the existence of spacetime singularities. Singularities are generic features of Einstein's equation and best described in terms of geodesic incompleteness of causal curves [3,4]. The occurrence of a spacetime singularity at the end state of a gravitational collapse (black hole singularity) and at the beginning of the Universe (big bang singularity) are inevitable consequences of general relativity as shown by Hawking-Penrose singularity theorems [3,23]. At the singularities, the spacetime curvature becomes infinite, which leads to the breakdown of the theory. Therefore, the deterministic nature of general relativity crucially depends on the conjecture that singularities that can causally influence regions of spacetime are censored out. This is known as Penrose's weak cosmic censorship conjecture [4,24]. However, a desirable property of any well behaved physical theory should be a singularity free description. It is therefore believed that at small enough length scales, general relativity would be replaced by a quantum theory of gravity, which will ultimately overcome the singularity problem. Results from loop quantum gravity also hint towards this possibility [25,26].

1.2.2 The Cosmological Constant Problem

The current picture of our Universe is well described by the Λ CDM (Λ -Cold Dark Matter) model of cosmology preceded by an era of inflation [27,28]. Modern cosmology is a data starved science where observations play a crucial role. Observations from the Cosmic Microwave Background Radiation (CMBR) and Supernova data suggest that the energy content of our Universe is approximately comprised of 4% of ordinary matter, 20% of dark matter and 76% of dark energy [29]. Although the Λ CDM model is in strong agreement with these observational data, it is still plagued with several theoretical challenges. Apart from not explaining the nature of dark matter and dark energy, the Λ CDM model also cannot explain the origin of inflation and the big bang. Observations also indicate that our Universe is currently going through an accelerated phase of expansion [30,31]. Such a late-time acceleration can be explained within the framework of general relativity with the inclusion of a positive cosmological constant (Λ), which can be accounted for the dark energy density. However, the existence of a positive cosmological constant in the standard model of cosmology also leads to one of the most enigmatic puzzles in theoretical physics, i.e., the cosmological constant problem [32–35]. Broadly, the problem has to do with the large disagreement between the observed value of the cosmological constant ($\Lambda/8\pi G \sim 10^{-47} GeV^4$) and the vacuum energy density inferred from quantum field theory ($10^{71} GeV^4$). This is the largest discrepancy between theory and observation ever recorded and considered by many authors to be the most critical challenge in modern physics. Such severe limitations of the Λ CDM model leads to the speculation that our current picture of the evolution of the Universe requires modifications. This has motivated cosmologists to propose several alternatives to the cosmological constant as a candidate for dark energy over the years. Another perspective to approach the problem that has been extensively studied in the literature is to consider

modification of general relativity [36–44]. Note that all these alternatives are not problem-free, and we shall not attempt to rank one above another. Such models are studied in the literature with the spirit that, in the absence of a solution exploring all possible alternatives are worth pursuing.

1.2.3 Incompatibility with Quantum Theory

Modern physics is based on two pillars: quantum field theory and general relativity. Three of the fundamental interactions (weak, strong and electromagnetic) are well described in the framework of quantum field theory. On the other hand, general relativity is a classical field theory. Any attempt to reconcile gravity with quantum theory leads to non-renormalizable ultra-violet divergences. This can be realized by studying linearized perturbation over a fixed curved geometry. Such an approach gives rise to new divergent terms appearing at every order in the loop expansion. Making sense out of these divergences further requires the inclusion of an infinite number of counter-terms in the effective action and subsequently an infinite number of coupling constants, suggesting that quantum general relativity is a perturbatively non-renormalizable theory. However, by truncating the expansion at a particular loop order, one can remove the divergences by renormalization of a finite number of parameters. For instance, the one-loop effective action of perturbative quantum gravity is of the form [45],

$$\mathcal{A}_{\text{1-loop}} = \frac{1}{16\pi G} \int d^4x \sqrt{-g} \left[R - 2\Lambda + \alpha R^2 + \beta R_{\mu\nu}R^{\mu\nu} + \gamma R_{\mu\nu\sigma\delta}R^{\mu\nu\sigma\delta} \right] \quad (1.2.1)$$

In this case, renormalization of Newton's constant (G), cosmological constant (Λ) along with the couplings (α, β, γ) is sufficient to remove the divergence at one-loop. This was first shown by Utiyama and De Witt [46] and later by Stelle [47]. Results from string theory also show that the effective low energy corrections to Einstein-Hilbert action involve similar higher curvature invariants [48, 49].

The above structure of the one-loop effective action clearly suggests that general relativity may only make sense as a low energy effective theory which must be supplemented by higher curvature terms as one approaches the ultra-violet scale. But what do we learn from such effective field theories? The answer to this question has to do with one of the most remarkable properties of nature, i.e., interesting physical phenomena occur in nature over a wide range of length scales that is independent of each other. For example, the dynamics of fluid inside a tube can be studied via the Navier Stokes equation without any reference to the fluid's quantum mechanical composition. The standard model of particle physics is also an effective field theory. This is the case with any physical theory of nature since the validity of a theory is subjected to the relevant domain of length scale. Hence it indeed makes sense to study effective gravitational theories of the form Eq. (1.2.1). We explore some fascinating properties of such higher curvature theories, including black holes, gravitational waves, quasi-normal modes, shadow etc., in the subsequent chapters.

1.3 A General Overview of Higher Curvature Theories

Exploring several limitations of general relativity in the previous section leads us to conclude that it may have modification at relevant length scales. The structure of physical theories are often governed by symmetries, and general relativity is no exception. The underlying symmetry for gravitational theories is the diffeomorphism invariance, i.e., symmetry with respect to arbitrary coordinate transformations. Modelling gravitational theories beyond general relativity is not an easy task since

there exist several ways to deviate from general relativity, and any modifications consistent with the diffeomorphism invariance may be present in the classical action. Nevertheless, approaches to modify general relativity can be broadly classified into two categories: (a) modification of the gravity sector and (b) modification of the matter sector. The former mostly includes higher curvature corrections to the Einstein-Hilbert action, while the latter refers to the presence of additional fields (scalar or vector). In this dissertation, we have carried out a detailed analysis of several interesting aspects of black holes in the context of general relativity and higher curvature theories. These involve the study of black hole thermodynamics, black hole shadow, quasi-normal modes, horizon topology, cosmic censorship conjectures etc. Before diving into the technical part, which we shall present in the subsequent chapters, it would be instructive to overview some of the most commonly studied higher curvature alternatives to general relativity that are also studied in this thesis.

1.3.1 Lanczos-Lovelock Theories

A gravitational action may contain arbitrary combinations of diffeomorphism invariant terms involving higher powers of curvatures. However, in this thesis, we have worked extensively on a particular class of such higher curvature theory, namely the Lanczos-Lovelock theory of gravity [50,51]. Lanczos-Lovelock theories represents the unique generalization over the Einstein-Hilbert action in dimensions higher than four, with the field equation containing at most second derivative of the metric [51,52]. The Lanczos-Lovelock Lagrangian is of the form,

$$\mathcal{L} = \sum_{k=0}^{k_{\max}} \lambda_k \mathcal{L}_k \quad \text{where} \quad \mathcal{L}_k = \frac{1}{2^k} \delta_{cd c_1 d_1 \dots c_k d_k}^{ab a_1 b_1 \dots a_k b_k} R_{ab}^{cd} R_{a_1 b_1}^{c_1 d_1} \dots R_{a_k b_k}^{c_k d_k} \quad (1.3.1)$$

Here R_{ab}^{cd} is the d dimensional Riemann tensor and $\delta_{c_1 d_1 \dots c_k d_k}^{ab a_1 b_1 \dots a_k b_k}$ denotes the totally antisymmetric Kronecker delta. The zeroth order ($k = 0$) term of the Lanczos-Lovelock polynomial is the cosmological constant, while the first order term ($k = 1$) represents the Einstein-Hilbert Lagrangian and the second order term ($k = 2$) is the Gauss-Bonnet Lagrangian. Further, k_{\max} appearing in the Lanczos-Lovelock Lagrangian is related to the spacetime dimensions (d) as $2k_{\max} \leq d$. The action for such a theory involving the first three non-trivial contributions to the Lanczos-Lovelock Lagrangian is of the following form [52],

$$\mathcal{A} = \frac{1}{16\pi} \int d^d x \sqrt{-g} \left[R + \alpha \left(R^2 - 4R_{\mu\nu}R^{\mu\nu} + R_{\mu\nu\alpha\beta}R^{\mu\nu\alpha\beta} \right) - 2\Lambda + \mathcal{L}_M \right] \quad (1.3.2)$$

This is known as the Einstein-Gauss-Bonnet theory of gravity. Here \mathcal{L}_M denotes the matter Lagrangian. The Gauss-Bonnet term in four-dimensions turns out to be pure topological and doesn't contribute to the field equation. Note that, the Gauss-Bonnet term is a special case of the one-loop effective Lagrangian with $\alpha = -(\beta/4) = \gamma$, where α is the Gauss-Bonnet coupling constant. We have carried out extensive studies on several aspects of this theory, including black hole thermodynamics, shadow, strong cosmic censorship etc., in the subsequent chapters.

1.3.2 $f(R)$ Theories

Another special class of higher curvature theory that involves polynomial expansion in the power of Ricci scalar is the $f(R)$ theory of gravity and the action is of the form [53,54],

$$\mathcal{A} = \int d^d x \sqrt{-g} \left[\frac{f(R)}{16\pi} + \mathcal{L}_M \right] \quad \text{where} \quad f(R) = R + \alpha R^2 + \beta R^3 + \dots \quad (1.3.3)$$

Here \mathcal{L}_m represents the matter field Lagrangian. $f(R)$ theories have been extensively studied in the literature as one of the simplest alternatives to general relativity. The primary motivation for the $f(R)$ theory comes from cosmology. This has to do with one of the most interesting properties of $f(R)$ gravity, i.e., its relation with general relativity via a conformal transformation. More precisely, in the conformal frame, the action takes the form of Einstein-Hilbert action with an additional scalar field. This has been discussed in great detail in [Chapter 2](#). The scalar field can be further modelled as a source of inflation as well as late-time acceleration. For example, the theory $f(R) = R + \alpha R^2$ with $\alpha > 0$ is a viable model for the accelerated expansion of the Universe [53, 55]. Also, recall that this was one of the earliest models of inflation proposed by Starobinski [56]. In [Chapter 2](#), we present an analysis of Hawking's topology theorem in the context of $f(R)$ gravity in four and higher dimensions.

1.3.3 Quadratic-Curvature Theories in Four-Dimensions

Action for the most general form of higher curvature theory with terms up to quadratic order in curvature is of the form [Eq. \(1.2.1\)](#). However, in four dimensions, one can employ the Gauss-Bonnet theorem to express one of the quadratic curvature invariants in terms of the other two, and the action finally takes the form [57–62],

$$\mathcal{A}_{\text{quad}} = \frac{1}{16\pi G} \int d^4x \sqrt{-g} \left[R - 2\Lambda + \alpha R^2 + \beta R_{\mu\nu} R^{\mu\nu} + \mathcal{L}_M \right] \quad (1.3.4)$$

Variation of this action with respect to the spacetime metric $g^{\mu\nu}$ leads to the following field equation [57],

$$(1 + 2\alpha R) \left(R_{\mu\nu} - \frac{1}{2} R g_{\mu\nu} \right) + \frac{\alpha}{2} R^2 g_{\mu\nu} + \left(2\alpha + \frac{\beta}{2} \right) g_{\mu\nu} \square R - (2\alpha + \beta) \nabla_\mu \nabla_\nu R + \beta \square R_{\mu\nu} - \frac{\beta}{2} R_{\alpha\beta} R^{\alpha\beta} g_{\mu\nu} + 2\beta R_{\alpha\beta} R^\mu_\mu R^\beta_\nu = 8\pi G T_{\mu\nu} \quad (1.3.5)$$

The coupling constants α and β here must obey the no tachyon conditions $(3\alpha + \beta) \geq 0$ and $\beta \leq 0$, that ensures the absence of tachyonic modes [57, 58]. Since the theory is four-dimensional, it has been extensively studied in the literature as a potential alternative to general relativity. In particular, obtaining stringent bounds on the couplings α and β from both the theoretical and observational side has been one of the major themes of research along this line. We shall discuss some of these bounds in subsequent sections.

1.4 Classical Black holes and their Properties

1.4.1 Horizon Geometry

Black holes are complicated mathematical solutions of Einstein's equation, yet they possess some remarkably simple universal properties. Several such results are often expressed in the form of elegant mathematical theorems. In one of his remarkable work [63], Hawking illustrated some general properties of the black hole event horizon in general relativity. Firstly, he established the strong rigidity theorem, which is essentially the statement that the event horizon in a stationary spacetime in general relativity is also a Killing horizon. Furthermore, most importantly, Hawking proved the area theorem, which states that the area of the event horizon of a black hole always increases, provided

the matter-energy tensor obeys the null energy condition. Later, this result turned out to be the foundation in the development of black hole thermodynamics. Lastly, another intriguing result of [63] is the topology theorem by Hawking. The theorem states that in four dimensions, the topology of the event horizon cross-section is either spherical or toroidal, provided the stress-energy tensor obeys the dominant energy condition. The toroidal case is further ruled out by the topology censorship theorem [64]. This is one of the most important theorems in mathematical relativity. By using the Gauss-Bonnet theorem in four dimensions, the proof relates the Euler characteristics (χ) associated with the event horizon to the spacetime curvature as follows [10, 63],

$$\chi(\mathcal{H}) = \int_{\mathcal{B}} \left(2R_{\mu\nu}k^\mu l^\nu - 2R_{\mu\nu\alpha\beta}k^\mu l^\nu k^\alpha l^\beta \right) dA + \int_{\mathcal{B}} 16\pi T_{\mu\nu}k^\mu l^\nu dA \quad (1.4.1)$$

where k^μ is the horizon generating null vector, l^μ is the auxiliary null normal, and $T_{\mu\nu}$ represents the stress-energy tensor. The second term is positive if $T_{\mu\nu}$ satisfies the dominant energy condition, while the first term can be shown to be positive from the existence of trapped surfaces (see [Chapter 2](#) for more details). Extension of this result to higher dimensions is not trivial since the Gauss-Bonnet theorem is no longer applicable. However, instead of Euler characteristics, in higher dimensions, one can work with the Yamabe invariant associated with the horizon cross-section to restrict possible topologies. It was first studied by Galloway and Schoen [65, 66]. In this thesis, we present an extension of Hawking's topology theorem to $f(R)$ gravity in four and higher dimensions [67].

1.4.2 Black hole Thermodynamics

Black holes have often been proved to be a useful tool in understanding the fundamental nature of spacetime. The last century, especially the second half, witnessed significant advancement of the subject. The discovery of the rotating black hole solution by Roy Kerr was one of the stepping stone in black hole physics [9]. Pioneering works of Hawking, Bekenstein, Penrose and others established several important results in mathematical relativity [23, 24, 68–71]. One such result is the striking similarity between black holes and a thermodynamic system [71]. In other words, classical black holes in general relativity follow a particular set of laws analogous to the four laws of thermodynamics. Studies of quantum fields on a black hole background have revealed that the analogy is not just a mere mathematical artefact rather an intrinsic property of black holes. More precisely, in this context, a black hole can be attributed with entropy (proportional to the surface area of the event horizon) [68, 69], temperature (proportional to the surface gravity, κ of the event horizon) [70] analogous to a thermodynamic system and expressed as,

$$T_H = \frac{\hbar c^3}{2\pi G k_B} \kappa_H \quad \text{and} \quad S_H = \frac{k_B c^3}{4G\hbar} A_H \quad (1.4.2)$$

The presence of Planck constant in the Hawking temperature indicates that the process is quantum mechanical. This is also evident from the fact that classically a black hole is a perfect absorber and hence does not radiate. The inclusion of quantum mechanics leads to the emission of thermal radiation at Hawking temperature. However, unlike thermodynamic entropy, the statistical origin of the black hole entropy is not fully known and still stands as an open problem.

One of the primary focus of this thesis would be to study the *first law* of black hole thermodynamics for an arbitrary diffeomorphism invariant theory of gravity. The first law can be expressed in the following two forms,

- **Stationary State Version:**

Also known as the equilibrium state version of the first law, it compares the ADM mass, and angular momentum of two stationary black holes separated infinitesimally in the space of solutions of Einstein's equation. More precisely, it relates two black hole solutions of Einstein's equation with masses ($M, M + dM$), angular momentum ($J, J + dJ$) and horizon area ($A, A + dA$) using the Smarr formula [72] as,

$$\left(\frac{\kappa}{8\pi}\right) dA = dM - \Omega_H dJ \quad (1.4.3)$$

where κ and Ω_H represents the surface gravity and angular velocity of the event horizon, respectively. This clearly resembles the structure of the first law of thermodynamics. The stationary state version of the first law is a global statement since the ADM energies are defined at infinity with respect to some asymptotic symmetries.

- **Physical Process version:**

Unlike the equilibrium state version, the physical process version of the first law is local and dynamical in nature. In this case, instead of comparing two global solutions, one simply perturb a stationary black hole with some influx of matter and computes the corresponding change in horizon area [73–76]. If $T_{\mu\nu}$ is the stress-energy tensor of the influx matter, the physical process first law takes the form,

$$\frac{\kappa}{2\pi} \delta \left(\frac{A_H}{4} \right) = \int_{\mathcal{H}} T_{\mu\nu} \xi^{\mu} d\Sigma^{\nu} \quad (1.4.4)$$

where κ is the surface gravity of the stationary background horizon. Also, $d\Sigma^{\mu} = k^{\mu} dA$ with k^b being the horizon generating null vector and ξ^a is the Killing vector of the stationary background spacetime.

Note that if the influx matter-energy tensor obeys the null energy condition, the area of the black hole horizon always increases.

1.4.3 Photon Sphere and Black hole Shadow

The bending of light by a strong gravitational field is one of the fascinating features of general relativity. This phenomenon is known as gravitational lensing, and it is one of the extensively pursued research subjects in gravitational physics [77–85]. Huge concentration of matter such as clusters of galaxies or super-massive stars and black holes distort the spacetime geometry strongly, which acts as a gravitational lens that can deflect and magnify light rays approaching from distant sources. These lensed images can further be analyzed to extract important information about the source as well as the surrounding matter distribution along the line of sight. This effect further leads to the existence of circular null orbits in the vicinity of black holes, namely the photon sphere. For an illustration, we start with a static spherically symmetric spacetime,

$$ds^2 = -f(r) dt^2 + f(r)^{-1} dr^2 + r^2(d\theta^2 + \sin^2 \theta d\phi^2) \quad (1.4.5)$$

For later use, it is convenient to switch to the Eddington-Finkelstein coordinate system in which the above static spacetime line element takes the form,

$$ds^2 = -f(r) dv^2 + 2dv dr + r^2(d\theta^2 + \sin^2 \theta d\phi^2) \quad (1.4.6)$$

where $u = t - r_*$, and $v = t + r_*$ represents the light cone coordinates and r_* denotes the tortoise coordinate defined by $dr_* = dr/f(r)$.

Since the spacetime under consideration is spherically symmetric, we can choose a particular plane for geodesic motion, which for convenience can be chosen to be at $\theta = \pi/2$. Also, for circular orbit one has $r = \text{constant} \equiv r_{\text{ph}}$ and $\dot{r} = \ddot{r} = 0$. Additionally, for null curves one has, $ds^2 = 0$ and we finally get,

$$\left(\frac{d\phi}{dv}\right)^2 = \frac{1}{r_{\text{ph}}^2} f(r_{\text{ph}}). \quad (1.4.7)$$

Further, the radial null geodesic is of the form,

$$\frac{d^2r}{d\lambda^2} - \frac{\partial f}{\partial r} \left(\frac{dr}{d\lambda} \right) \left(\frac{dv}{d\lambda} \right) + \frac{1}{2} f \frac{\partial f}{\partial r} \left(\frac{dv}{d\lambda} \right)^2 - rf \left(\frac{d\phi}{d\lambda} \right)^2 = 0 \quad (1.4.8)$$

However, since we are interested in circular null geodesic we may use the fact that $r = r_{\text{ph}}$, leading to both $\dot{r} = 0$ and $\ddot{r} = 0$. Thus with these results taken into account, Eq. (1.4.8) for circular null geodesics become,

$$\left(\frac{d\phi}{dv}\right)^2 = \frac{1}{2r_{\text{ph}}} \frac{\partial f(r)}{\partial r} \Big|_{r_{\text{ph}}} \quad (1.4.9)$$

Now, one can immediately equate Eq. (1.4.7) and Eq. (1.4.9), to get an algebraic equation for the location of photon sphere r_{ph} , which reads [86],

$$r_{\text{ph}} \frac{\partial f(r)}{\partial r} \Big|_{r_{\text{ph}}} = 2f(r_{\text{ph}}). \quad (1.4.10)$$

This is the most general equation governing the location of the photon sphere around a static spherically symmetric black hole solution. For the case of Schwarzschild spacetime (Eq. (1.1.2)), the above equation leads to $r_{\text{ph}} = 3M$. However, note that astrophysical black holes are never static since they strongly interact with the surrounding matter distribution present in the form of an accretion disc. As a result, the above analysis carried out for the static spacetime (Eq. (1.4.5)) does not correspond to an astrophysically realistic situation. One of the central goals of this thesis is to study the evolution of the photon sphere around dynamical black holes that are constantly accreting matter.

As far as observational implications are concerned, the photon sphere further leads to the existence of an unobservable dark patch around the black hole, known as shadow [87–99]. More precisely, the black hole shadow is defined as the set of directions in the observer's sky from which light from distant sources does not reach the observer. Such an optical property of the black hole has several interesting consequences. For instance, observation of such shadow structure may be considered as direct evidence for the existence of black holes. Furthermore, the shadow carries an intrinsic fingerprint of the super-massive central object and can be analyzed to extract interesting information. The structure of a shadow around a black hole also depends on the underlying theory of gravity. As a result, such observation can further lead to interesting constraints on several alternative theories of gravity. The recent image captured by the event horizon telescope strongly suggests the super-massive object at the centre of the M87 galaxy to be a rotating Kerr black hole [19–22].

To understand the concept of black hole shadow, let us start with the Lagrangian of a massless test particle (photon) on a static spherically symmetric black hole background,

$$\mathcal{L} = \frac{1}{2} \left\{ -f(r) \left(\frac{dv}{d\lambda} \right)^2 + 2 \left(\frac{dv}{d\lambda} \right) \left(\frac{dr}{d\lambda} \right) + r^2 \left(\frac{d\theta}{d\lambda} \right)^2 + r^2 \sin^2 \theta \left(\frac{d\phi}{d\lambda} \right)^2 \right\} \quad (1.4.11)$$

As per our notation, a ‘prime’ and a ‘dot’ over any quantity represents derivative with respect to the radial coordinate r and the in-going time v respectively, and λ denotes the affine parameter along the particle’s geodesic. From the symmetry of the Lagrangian, it is evident that the angular momentum and energy are conserved.

$$E = -f(r) \left(\frac{dv}{d\lambda} \right) + \left(\frac{dr}{d\lambda} \right) \quad \text{and} \quad L = r^2 \sin^2 \theta \left(\frac{d\phi}{d\lambda} \right) \quad (1.4.12)$$

Solving these equations for $dv/d\lambda$ and $d\phi/d\lambda$ leads to,

$$\left(\frac{dv}{d\lambda} \right) = \frac{1}{f(r)} \left\{ \left(\frac{dr}{d\lambda} \right) - E \right\} \quad \text{and} \quad \left(\frac{d\phi}{d\lambda} \right) = \frac{L}{r^2 \sin^2 \theta} \quad (1.4.13)$$

For photon trajectories, we have to work with the condition $ds^2 = 0$, which further leads to the vanishing of the Lagrangian ‘ \mathcal{L} ’ in Eq. (6.2.3). Using the above expressions, we obtain,

$$r^2 \left(\frac{dr}{d\lambda} \right)^2 - r^2 E^2 + r^4 \left(\frac{d\theta}{d\lambda} \right)^2 f(r) + \frac{L^2 f(r)}{\sin^2 \theta} = 0 \quad (1.4.14)$$

The radial and the angular part of the above equation can be separated by introducing the Carter Constant K [100],

$$r^4 \left(\frac{d\theta}{d\lambda} \right)^2 = K - \cot^2 \theta L^2; \quad r^2 \left(\frac{dr}{d\lambda} \right)^2 = E^2 r^2 - (K + L^2) f(r). \quad (1.4.15)$$

Now, for circular null orbit, one has $r = \text{constant} = r_{\text{ph}}$ and $dr_{\text{ph}}/d\lambda = 0$. This leads to the general expression for the shadow radius around a static spherically symmetric black hole.

$$K + L^2 = \frac{E^2 r_{\text{ph}}^2}{f(r_{\text{ph}})} \quad \Rightarrow \quad \eta + \xi^2 = \alpha^2 + \beta^2 = \frac{r_{\text{ph}}^2}{f(r_{\text{ph}})} \quad (1.4.16)$$

where, by following the traditional convention, we have expressed the shadow radius in terms of celestial coordinates α and β [5, 101]. For Schwarzschild black hole, the above expression reduces to $\alpha^2 + \beta^2 = 27 M^2$. Since, in this work, we have only studied the dynamics of shadow in the spherically symmetric case, we do not engage ourselves in presenting any details for rotating black holes. However, a similar calculation can be extended straightforwardly to axially symmetric spacetimes. For a Kerr black hole, the shadow radius in the celestial coordinate takes the form [101],

$$\alpha^2 + \beta^2 = \frac{4M(2r^3 - 3Mr^2 + Ma^2)}{(r - M)^2} \quad (1.4.17)$$

In Fig. 1.1, we have plotted the outer boundary of the shadow around a rotating black hole. As one would expect, for Schwarzschild case ($a = 0$), the shadow is spherically symmetric. However, as the rotation parameter increases, the shape of the shadow changes. Such an asymmetry is a result of the rotation of the black hole. We have also shown the image of the supermassive object at the centre of the M87 galaxy captured by the event horizon telescope [19–22], which resembles the shadow structure of a rotating Kerr black hole. In the subsequent chapters, we study the dynamical evolution of the photon sphere and shadow around black holes. In particular, we restrict to spherically

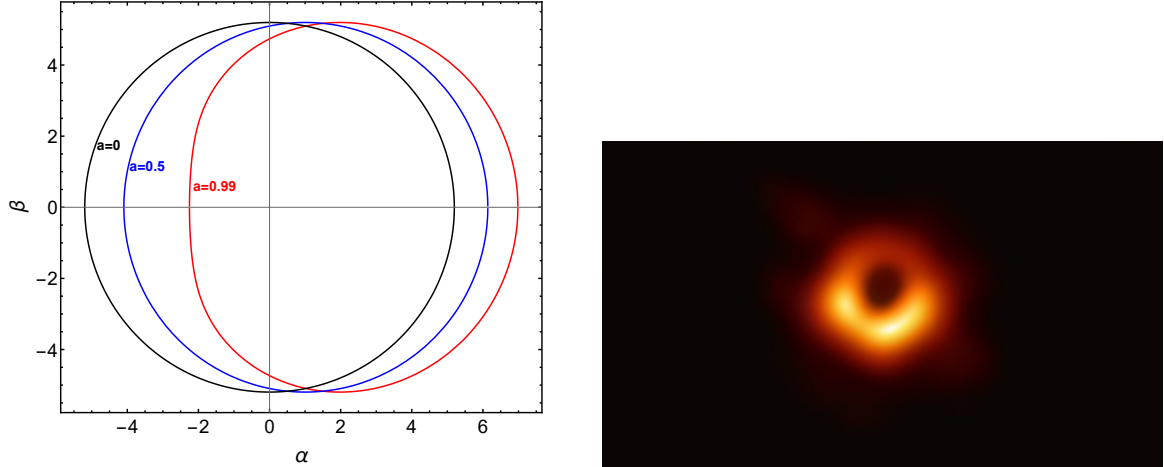


FIGURE 1.1: In the left panel we have shown the shadow cast by a Kerr black hole for various spin parameter. In the right panel, we have shown the recent image of the supermassive object at the centre of M87 galaxy captured by the event horizon telescope.

symmetric black holes in general relativity and Einstein-Gauss-Bonnet theories.

1.4.4 Cosmic Censorship Conjectures

As discussed previously, the existence of spacetime singularity is considered to be one of the severe challenges to the foundation of general relativity. Even the fundamental notion of spacetime breaks down at the singularities. The cosmic censorship conjectures are mathematical statements regarding the predictability of general relativity. The conjecture comes in two versions, namely the weak and strong cosmic censorship, initially proposed by Roger Penrose [24]. The *weak cosmic censorship* conjecture simply negates the existence of a naked singularity in the universe, i.e., it asserts that singularities are always cloaked by an event horizon. In technical terms, a singularity is not visible to an observer at null infinity [4,24]. The statement has no general proof and often studied in the literature by analyzing possible counterexamples. Initial research along this line dates back to the seminal work of Wald [102], where he proved that extremal Reissner-Nordström and Kerr-Newmann black holes of general relativity cannot be overcharged or overspin by test particle absorption. This is a remarkable result since the exposure of the singularity would lead to severe violation of physical laws. For a detailed review on this subject, we refer the reader to Ref. [103]. This thesis presents an analysis of this conjecture for a multi charged black hole configuration [104].

The *strong cosmic censorship* conjecture is a statement about the deterministic nature of general relativity. It asserts that spacetimes in general relativity are globally hyperbolic, i.e., the future of any event is uniquely determined from regular initial data [3, 4, 105]. However, the existence of Cauchy horizons may lead to a potential violation of the conjecture since it is considered to be the boundary of the domain of dependence of an initial hypersurface. Therefore, the validity of strong cosmic censorship is intrinsically related to the question of whether a perturbation can be extended beyond the Cauchy horizon. Recent studies strongly indicate a violation of the conjecture to occur for charged black hole spacetimes in the presence of a positive cosmological constant [106]. It is indeed an interesting question to ask, what would be the fate of strong cosmic censorship in theories beyond general relativity? Or, would it be possible to negate the strength of violation by the addition of higher curvature terms to Einstein Hilbert action? Motivated by these questions, in this thesis, we extend the analysis of the strong cosmic censorship to several class of higher curvature theories [107].

1.5 Confronting Theories with Observations

As discussed previously, any correction consistent with the diffeomorphism symmetry may contribute to the gravitational field equation, leaving us with a plethora of higher curvature alternatives. It is difficult to restrict these corrections only from the theoretical side. In the absence of a unique approach, an effective way to study these problems could be to perform several consistency checks of the low energy theory, possibly by comparing with observations. Such tests are expected to provide novel bounds on the strength of corrections over general relativity. Some of the low energy tests include the measurement of the Newtonian potential locally in laboratories using torsion balance experiments or solar system tests like measuring the Shapiro time delay, etc [7]. Inclusion of higher curvature corrections to Einstein-Hilbert action often leads to Yukawa type correction over the gravitational potential in the Newtonian limit [108–110]. For example, for a quadratic curvature Lagrangian of the type $\mathcal{L} = R + \alpha \mathcal{O}(R^2)$, the Newtonian potential takes the form,

$$V(r) \propto \frac{G M}{r} \exp\left[\frac{-r}{\alpha}\right] \quad (1.5.1)$$

Such small scale corrections to Newton's force law has been termed by many authors to be the '*fifth force*' and can be tested using astrophysical as well as local laboratory experiments, which often leads to interesting bounds on the coupling constant (α) of the modified theory [110–116]. The Eöt-Wash experiment bounds the coupling constant by comparing the strength of the above Yukawa correction with the locally measured value of gravitational potential using a torsion balance. Some of the astrophysical tests also involve the measurement of the deflection of light and orbit of Mercury. However, the Eöt-Wash experiment provides the strongest bound ($\alpha \leq 2 \times 10^{-6} m^2$) [111, 112]. We discuss some of these constraints on various higher curvature theories in [Chapter 7](#).

Note that most of these tests consider the situation of weak gravitational field, where the space-time curvature is small, and characteristics velocities of objects are small as compared to the speed of light. As a result, the effects of higher curvature corrections are often negligible, and higher-order post-Newtonian terms can be ignored. Since corrections to general relativity are apparently relevant at high energies, it is desirable to compare predictions of these theories with some strong gravity observations. After the recent detection of gravitational waves, theories of gravity are conferred with observations in the strong gravity regime. The most likely source of gravitational wave generation is the rapidly inspiraling compact binaries involving neutron stars or black holes. These observations allow us to probe previously unexplored regions where the spacetime curvature is strong, as well as the velocities of involved objects, are comparable to the speed of light. So far, all the LIGO observations are consistent with the predictions of Einstein's theory. However, there still exists ample parameter space where classical general relativity may require modifications.

Gravitational waves carry several interesting information about the source as well as the underlying theory of gravity and can be used as an excellent observational tool to perform strong-field tests of general relativity. Testing theories using gravitational wave observations mainly includes the parameterized test, the inspiral merger ringdown (IMR) consistency test and gravitational wave propagation test [117]. The first one, i.e., the parameterized test, involves the inclusion of a non general relativity parameter in the theory, and one attempts to constraint this parameter by comparing it with the gravitational wave data [118–122]. The IMR consistency check is a test for the validity of general relativity. This involves the independent estimation of final mass and spin of the remnant using the inspiral and post-inspiral data separately and checks for consistency between the

two [123–127]. Observation suggests that the final remnant of binary black hole mergers is consistent with the Kerr black hole of general relativity [14, 15]. Lastly, in the gravitational wave propagation test, one studies various non general relativity effects present in the signal, i.e., modified dispersion relations, presence of more than two polarizations, difference in the propagation speed of gravitational wave and electromagnetic wave etc.

General relativity represents the unique four-dimensional theory of Lorentz invariant massless helicity-2 particle. In other words, gravitational waves in general relativity have two states of polarization, namely the cross and plus modes. Any higher curvature modification over general relativity often leads to the presence of additional degrees of freedom, which may affect the gravitational physics even at low energy. These additional degrees of freedom could be massless or massive and scalar, vector or tensor type. Detection of such additional polarization in the gravitational wave signal in the future by LIGO-Virgo detectors would be catastrophic for general relativity. Also note that general relativity predicts the mass of graviton to be exactly zero, which may not be the case in modified gravity theories. Observation of gravitational wave signal from compact binary coalescence sets strong bound on the mass of graviton ($m_g \leq 10^{-22} \text{ eV}/c^2$) [15, 128–131].

Another distinctive feature of higher curvature gravity is the difference in the propagation speed of gravity and light. In higher curvature theories, gravitational perturbation propagates as a null ray with respect to an *effective graviton metric* (refer to [Chapter 4](#) and [Chapter 7](#) for more details). Such an effect has interesting observational consequences. For instance, in the event GW170817 [18], i.e., the coalescence of a binary neutron star system, the electromagnetic signal was detected ~ 1.7 second after the gravitational wave. This constrains the difference in speed of electromagnetic and gravitational wave signals to less than $10^{-15}c$. This bound gives rise to several interesting constraints on various theories beyond general relativity [132–142]. In this thesis, we extend these ideas further and provide a general framework to obtain observational bounds on the most general higher curvature theory in four dimensions.

1.6 An Overview of the Thesis

Broadly, the thesis presents several interesting studies of black hole and gravitational wave physics in the context of general relativity and higher curvature theories. We establish these results by employing various analytical and numerical techniques. The thesis is classified into two parts. The first part deals with the studies of some general properties of black holes and their extensions beyond general relativity. This includes analysis of black hole thermodynamics, black hole shadow, validity cosmic censorship conjectures (weak and strong), horizon topology etc. The second part of this thesis deals with obtaining observational constraints on modified gravity theories from gravitational wave observations. A chapter-wise overview of the thesis is as follows,

Part I

- In [Chapter 2](#) we study the Hawking topology theorem in the context of $f(R)$ gravity in $3 + 1$ and higher dimensions. In particular, we obtain a sufficient condition for the topology of horizon cross-section being spherical.
- In [Chapter 3](#) we perform detail analysis of the physical process first law for an arbitrary diffeomorphism invariant theory of gravity. We further analyse the effect of ambiguity present in the Wald entropy on the physical process first law.
- In [Chapter 4](#), we study the evolution of the photon sphere and black hole shadow in a dynamical black hole spacetime. We also extend this result to higher curvature theory and study the motion of photon and graviton separately.
- In [Chapter 5](#), we demonstrate the validity of the weak cosmic censorship conjecture for a multi-black hole system. We extend the earlier work of Wald to show that over-charging is not possible for a Majumdar-Papapetrou black hole.
- [Chapter 6](#) deals with the study of strong cosmic censorship conjecture in higher curvature gravity. We find that the violation of strong cosmic censorship is stronger in the presence of higher curvature terms. We illustrate this result in the context of Einstein-Gauss-Bonnet and pure Lovelock theories.

Part II

- Lastly, in [Chapter 7](#) and [Chapter 8](#), we develop two general frameworks to constrain theories beyond general relativity consistent with gravitational wave observations. In particular, we have used the GW 170817 and GW 150914 observations to constrain parameters of modified gravity. The formalism developed here is completely general and can be used in the context of several classes of modified gravity theories.

Part I

**Black holes in General Relativity and
Higher Curvature Theories**

Chapter **2**

Black Hole Topology in $f(R)$ Gravity

This Chapter is based on, A. K. Mishra, M. Rahman, S. Sarkar, Classical and Quantum Gravity, Volume 35, Number 14 [67].

The topology theorem by Hawking is one of the most intriguing results of mathematical relativity [3, 63]. The theorem is a statement regarding the topology of the event horizon of black holes in general relativity. It beautifully relates the intrinsic geometry of the event horizon to the matter content of spacetime. It states that the cross-section of the event horizon in a stationary, asymptotically flat spacetime in four-dimensions, with matter stress-energy tensor obeying dominant energy condition, is always topologically spherical (S^2) or toroidal ($S^1 \times S^1$). The case of toroidal topology is further ruled out by the topology censorship theorem [64]. Hawking's proof uses the Gauss-Bonnet theorem in four dimensions to relate the Euler characteristic (χ , a quantity intrinsic to any geometric surface) to the spacetime curvature and consequently the matter-energy tensor via Einstein's equation. The Euler characteristic can be proved to be positive from the non-existence of trapped surfaces outside the event horizon. Note that a non-negative Euler number guarantees the co-dimension two surface, i.e., the horizon cross-section to be either spherical ($\chi = 2$) or toroidal ($\chi = 0$).

The theorem, however, is specific to $3 + 1$ dimensional black hole spacetimes in general relativity. Generalization of this result to higher dimensions and theories beyond general relativity is not a straightforward exercise. The root of the complication is related to the non-applicability of the Gauss-Bonnet theorem in higher dimensions. In $3 + 1$ dimensions, the horizon cross-section is a co-dimension two surface, and the Euler number can be related to the intrinsic curvature by the Gauss-Bonnet theorem. In contrast, in higher dimensions, the theorem can not be applied in the identical form. Nevertheless, instead of the Euler characteristic, one can work with the Yamabe number, a geometric invariant associated with a co-dimension two surface in any dimensions. Galloway and Schoen have demonstrated that it is indeed possible to restrict the sign of the Yamabe invariant, and as a result, even in higher dimensional spacetimes, only certain class of topologies are allowed [65, 66]. For instance, in five dimensions, the topology of the horizon cross-section has been shown to be either S^3 or $S^2 \times S^1$. The former one is the familiar spherical geometry, while the latter type corresponds to a new horizon structure, known as black ring solution. Such results also illustrate that the topological structure of higher-dimensional black holes is richer as compared to the lower-dimensional ones. I refer the reader to Ref. [143] for an extensive review. Notice that the topology theorem of Hawking and its higher-dimensional proof by Galloway and Schoen assumes

the spacetime to be stationary. However, the theorem also extends to non-stationary spacetimes as well [144].

Surprisingly, the possible topological structure of horizon in modified gravity, such as $f(R)$ theories, are still unexplored. Since the field equation is different, it is expected that the imposition of the dominant energy condition may not lead to a definite topology of the horizon cross-sections. One of the simplest higher curvature extension of general relativity is the case where the correction is a polynomial expansion in Ricci scalar ($f(R) = R + \alpha_1 R^2 + \alpha_2 R^3 \dots$) [53, 54]. Interestingly, the $f(R)$ theory is related to Einstein's gravity with an additional scalar field via conformal transformation. Also, note that the causal structure of spacetime is invariant under conformal transformation, and as a result, the stationary horizon is mapped to itself [145]. Therefore, one way to approach the topology theorem could be to formulate the problem entirely in the conformal frame and understand the possible restrictions on horizon topology in $f(R)$ gravity from the analogous results in general relativity.

Understanding the topological structure of black hole horizons beyond general relativity could be an important theoretical tool to distinguish certain classes of modified theories from general relativity. Also, in general, the solution space of a modified theory is expected to be richer and could admit black hole solutions with no parallel in general relativity. In Ref. [67], we presented an extension of the Hawking topology theorem to $f(R)$ gravity by studying the possible topology of a stationary horizon cross-section. In $3+1$ dimensional case, we obtained a sufficient differential condition on the form of the function $f(R)$ (along with dominant energy condition) that ensures the topology of stationary black holes to be the same as that of general relativity. By following the procedure as in [65, 66], we further show that the same condition also restricts the sign of Yamabe invariant associated with the horizon cross-section of stationary black holes in higher dimensions. This is an interesting result as it gives a sufficient condition on the choice of $f(R)$ theories for which the topology of the black hole event horizon is the same as general relativity, irrespective of the dimension of spacetime. Firstly, we obtain our result via a direct approach, i.e., without performing any conformal transformation (physical frame) and subsequently reproduce the same result in the conformal frame.

2.1 Topology of a stationary black hole horizon in $3+1$ dimensions

Let us start by considering a black hole event horizon in $3+1$ dimensions in a stationary spacetime with metric $g_{\mu\nu}$. The event horizon \mathcal{H} in a stationary spacetime is also a Killing horizon on which the norm of a Killing vector (which is timelike outside) vanishes. We consider the null Killing vector filed k^μ to be the generator of the event horizon which obeys the non-affine geodesic equation: $k^\mu \nabla_\mu k^\nu = \kappa k^\nu$, where κ represents the surface gravity. The cross-section of the event horizon is a compact spacelike surface \mathcal{B} . If l^μ is the auxiliary null normal to the horizon then the intrinsic metric of the cross-section is: $h_{\mu\nu} = g_{\mu\nu} + k_\mu l_\nu + k_\nu l_\mu$ where we have used the normalization condition $k_\mu l^\mu = -1$. The Euler characteristic of such a surface is then given by,

$$\chi(\mathcal{B}) = \int_{\mathcal{B}} \mathcal{K}_G d\mathcal{A} \quad (2.1.1)$$

Here \mathcal{K}_G denotes the Gaussian curvature of the co-dimension two surface \mathcal{B} . For a stationary spacetime, the horizon has vanishing expansion and shear. In this case, the intrinsic Gaussian curvature can be related to the full spacetime curvature [10, 146] and correspondingly, the Euler characteristic takes the form,

$$\chi(\mathcal{B}) = \int_{\mathcal{B}} \left(R + 4R_{\mu\nu}k^\mu l^\nu - 2R_{\mu\nu\alpha\beta}k^\mu l^\nu k^\alpha l^\beta \right) dA \quad (2.1.2)$$

This equation relates topological information of the horizon cross-section, i.e., the Euler characteristic, to the spacetime curvature. Now, by following an identical line of calculation as general relativity, we study the possible topology of the horizon in $f(R)$ theories of gravity. In particular, we expect to obtain constraints on the topological structure of the horizon from the constraint on the stress-energy tensor.

Hawking's Topology theorem assumes that the stress-energy tensor to obey the dominant energy condition and spacetime metric to be a stationary solution of Einstein's field equations. With these assumptions, the Euler characteristic can be shown to be positive semi-definite. For a time orientable compact co-dimension two surface, this leads to the only possibility of a sphere (S^2) and torus ($S^1 \times S^1$). Interestingly, the horizon with toroidal topology is ruled out by the topology censorship theorem, which leaves us with the only physical possibility of spherical case.

In the present work, we are interested in the topological structure of horizon cross-section arising from higher curvature theories of the form,

$$I_0 = \int d^4x \sqrt{-g} \left[\frac{f(R)}{16\pi} + \mathcal{L}_m \right] \quad (2.1.3)$$

Here \mathcal{L}_m denotes the Lagrangian for matter fields, and as discussed previously, $f(R)$ is some polynomial of Ricci scalar. The field equation arising from the variation of this action with respect to the metric is of the form [53, 54],

$$f'(R)R_{\mu\nu} - \frac{1}{2}g_{\mu\nu}f(R) + g_{\mu\nu}\square f'(R) - \nabla_\mu \nabla_\nu f'(R) = 8\pi T_{\mu\nu} \quad (2.1.4)$$

$f'(R)$ represents the derivative of the function $f(R)$ with respect to the Ricci scalar R . Now using Eq. (2.1.2) and the above field equation, the Euler characteristics for the horizon cross-section in $f(R)$ gravity takes the form,

$$\begin{aligned} \chi(\mathcal{H}) &= \int_{\mathcal{B}} \left(2R_{\mu\nu}k^\mu l^\nu - 2R_{\mu\nu\alpha\beta}k^\mu l^\nu k^\alpha l^\beta \right) dA \\ &+ \int_{\mathcal{B}} \left[\frac{Rf'(R) - f(R)}{f'(R)} + \frac{2k^\mu l^\nu \nabla_\mu \nabla_\nu f'(R) + 2\square f'(R)}{f'(R)} + \left(\frac{16\pi T_{\mu\nu}k^\mu l^\nu}{f'(R)} \right) \right] dA \end{aligned} \quad (2.1.5)$$

In the limit of general relativity, we have $f(R) = R$ and the expression for Euler characteristics reduces to Eq. (1.4.1). Notice that the above expression of the Euler characteristics is composed of two parts. The first term on the right-hand side is independent of the structure of the field equation, while the second term explicitly depends on the theory under consideration [10]. To tackle the first term, we start with the variation of the null expansion $\theta = h_\mu^\nu \nabla_\nu k^\mu$, of an outgoing null congruence generated by null vector k^μ , along the ingoing null geodesic generated by l^μ (parametrized by s). A straightforward calculation leads to [10],

$$R_{\mu\nu}k^\mu l^\nu - R_{\mu\nu\alpha\beta}k^\mu l^\nu k^\alpha l^\beta = -\frac{d\theta}{ds} - h_\sigma^\mu h_\rho^\nu \nabla_\mu l^\rho \nabla_\nu k^\sigma + p_\mu p^\mu - d^\dagger p \quad (2.1.6)$$

where $p^\mu = -l^\sigma h^{\mu\nu} \nabla_\nu k_\sigma$ and $d^\dagger p = -h^{\mu\nu} \nabla_\mu p_\nu$. Also p^μ is a space like vector field and as a result $p_\mu p^\mu$ is positive definite. Furthermore, the second term on the right hand side of Eq. (2.1.6), represents sheer and expansion on the horizon. Such terms do not contribute, as we are considering the spacetime to be stationary. Integrating Eq. (2.1.6) over the cross section \mathcal{B} finally gives,

$$\int_{\mathcal{B}} [R_{\mu\nu} k^\mu l^\nu - R_{\mu\nu\alpha\beta} k^\mu l^\nu k^\alpha l^\beta] dA = \int_{\mathcal{B}} \left[p_\mu p^\mu - \frac{d\theta}{ds} \right] dA$$

Now, using the above expression for the variation of expansion along l^μ , the Euler characteristics of \mathcal{B} , reduces to,

$$\begin{aligned} \chi(\mathcal{H}) &= \int_{\mathcal{B}} 2 \left[p_\mu p^\mu - \frac{d\theta}{ds} \right] dA \\ &+ \int_{\mathcal{B}} \left[\frac{Rf'(R) - f(R)}{f'(R)} + \frac{2k^\mu l^\nu \nabla_\mu \nabla_\nu f'(R) + 2\Box f'(R)}{f'(R)} + \left(\frac{16\pi T_{\mu\nu} k^\mu l^\nu}{f'(R)} \right) \right] dA \end{aligned} \quad (2.1.7)$$

For a stationary black hole, the event horizon is also the limit to the existence of outer trapped surfaces. Therefore, when we approach the horizon from the domain of outer communication, the expansion coefficient θ takes positive value outside and vanishes on the horizon. As a result $d\theta/ds$ is strictly negative on \mathcal{B} and consequently the first term in the above expression of Euler characteristics (Eq. (2.1.7)) turn out to be positive definite, irrespective of the field equation [10, 63].

Now let us consider the second integral of Eq. (2.1.7), which clearly contain terms that are explicitly dependent on the structure of the field equation. Assuming the stress-energy tensor to satisfy the dominant energy condition, we have $T_{\mu\nu} k^\mu l^\nu > 0$, while one can not in general comment on the sign of any other terms. To proceed further, we employ a field redefinition technique as follows to identify some of the terms to be positive. This can be achieved by rewriting the action I_0 in a slightly different form, where an auxiliary scalar field ϕ is coupled to Ricci scalar as,

$$I_1 = \int d^4x \sqrt{-g} \left[\frac{f(\phi) + (R - \phi)f'(\phi)}{16\pi} + \mathcal{L}_m \right]$$

Note that the equation of motion of the auxiliary scalar field is $\dot{\phi} = R$, which ensures the redefined action to be identical to I_0 , i.e., $I_1(\phi = R) = I_0$. In other words, the dynamics of the field equation obtained from I_0 is equivalent to that of I_1 [147]. The action I_1 can now be easily transformed into Einstein gravity coupled to a scalar field by a conformal transformation,

$$\bar{g}_{\mu\nu} = f'(\phi) g_{\mu\nu} \quad (2.1.8)$$

The resulting action is of the form [148],

$$I_2 = \int d^4x \sqrt{-\bar{g}} \frac{1}{16\pi} \left[\bar{R} - \frac{3}{2} \left(\frac{f''(\phi)}{f'(\phi)} \right)^2 \bar{\nabla}_\mu \phi \bar{\nabla}^\mu \phi + \frac{1}{f'(\phi)} \{ [f(\phi) - \phi f'(\phi)] + 16\pi L_m \} \right] \quad (2.1.9)$$

Taking variation with respect to the metric $\bar{g}_{\mu\nu}$, one can obtain the field equation corresponding to the action I_2 , which is of the form,

$$\begin{aligned} \bar{R}_{\mu\nu} - \frac{1}{2} \bar{g}_{\mu\nu} \bar{R} &= \frac{8\pi}{f'(\phi)} T_{\mu\nu} + \frac{3}{2} \left[\frac{f''(\phi)}{f'(\phi)} \right]^2 \bar{\nabla}_\mu \phi \bar{\nabla}_\nu \phi - \frac{3}{4} \bar{g}_{\mu\nu} \left[\frac{f''(\phi)}{f'(\phi)} \right]^2 \bar{\nabla}_\alpha \phi \bar{\nabla}^\alpha \phi \\ &+ \frac{1}{2} \bar{g}_{\mu\nu} \frac{f(\phi) - \phi f'(\phi)}{f'(\phi)^2} \end{aligned} \quad (2.1.10)$$

Now, if we consider the entire expression on the right-hand side of Eq. (2.1.10) to be an effective stress-energy tensor, it can be shown to obey dominant energy condition, provided that, $f'(\phi) > 0$ and $\phi f'(\phi) - f(\phi) > 0$. Since the equation for the auxiliary scalar field ϕ is just, $\phi = R$, the above two conditions translates to $f'(R) > 0$ and $Rf'(R) - f(R) > 0$ in the physical frame [148]. Note that, in the process of conformal transformation, we have used the conformal factor to be $f'(R)$ (Eq. (2.1.8)). Hence, the first inequality, i.e., $f'(R) > 0$, must hold in order to have a smooth conformal mapping between $f(R)$ gravity and Einstein plus a scalar field theory. Also, recall that $f'(R)$ represents the local entropy density of a black hole horizon in $f(R)$ gravity and has to be positive. Note that, if this condition is violated, i.e., for any process, the black hole spacetime, starting with a configuration $f'(R) > 0$, evolves to $f'(R) < 0$, then $f'(R)$ has to be zero at some point in between and for that case, not only the matter-energy tensor in Eq. (2.1.10) becomes singular, but also the entropy density takes negative value. So, these kinds of processes have to be ruled out from the theory. This is ensured by the second condition $Rf'(R) - f(R) > 0$ [148, 149]. For $f(R) = R + \alpha R^2$ theory, this condition translates to be $\alpha > 0$, which ensures the stability of the theory.

Furthermore, by a change of variable [149] $\varphi = \beta \ln f'(\phi)$, with $\beta = \sqrt{3/16\pi G}$, Eq. (2.1.9) becomes,

$$I_3 = \int d^4x \sqrt{-\bar{g}} \left[\frac{1}{16\pi G} \bar{R} - \frac{1}{2} \bar{\nabla}_\mu \varphi \bar{\nabla}_\nu \varphi - V(\varphi) + e^{-2\beta^{-1}\varphi} L_m(\psi, e^{-2\beta^{-1}\varphi} \bar{g}) \right]$$

where $V(\varphi) = \frac{1}{16\pi G} e^{2\beta^{-1}\varphi} (Rf'(\phi) - f(\phi))$ is some effective potential. In the absence of matter the last term of I_3 vanishes and the theory reduces to a Einstein-scalar theory with a minimally coupled potential $V(\varphi)$. In this case, the positivity of the potential $V(\varphi) \geq 0$ or $Rf'(\phi) - f(\phi) \geq 0$ leads to the no-hair theorem for asymptotically flat black holes [150]. However, when the above condition is not satisfied, one must check numerically for the existence of possible scalar hair. For the particular case of spherically symmetric asymptotically flat black holes in various $f(R)$ models of interest, numerical studies show the non-existence of scalar hair [150]. These results assume spherical symmetry and can not be generalized unless the topology is known a priori. In the presence of matter, the minimal coupling breaks down and in general, the no-hair theorem may not hold. This is not surprising since even in general relativity one can have black holes with scalar hair [151–153], which doesn't obey any energy conditions. The topology theorem doesn't hold in such cases. However, such solutions are ruled out when one assumes the matter-energy tensor to obey the dominant energy condition. Also, most of such hairy solutions are unstable and hence are not considered as strong counterexamples to the no-hair theorem [153].

Therefore, under these two physically reasonable conditions ($f'(R) > 0$ and $Rf'(R) - f(R) > 0$), the Euler characteristic take the form,

$$\begin{aligned} \chi(\mathcal{H}) &= \int_{\mathcal{B}} \left[2 \left(p_\mu p^\mu - \frac{d\theta}{ds} \right) + \frac{Rf'(R) - f(R)}{f'(R)} + \left(\frac{16\pi T_{\mu\nu} k^\mu l^\nu}{f'(R)} \right) \right] dA \\ &\quad + \int_{\mathcal{B}} \left[\frac{2k^\mu l^\nu \nabla_\mu \nabla_\nu f'(R) + 2\Box f'(R)}{f'(R)} \right] dA \end{aligned} \quad (2.1.11)$$

In the above expression, we have collectively written the positive definite terms in the first integral. Further, using the form of the induced metric \mathcal{B} , the second integral can be simplified as follows,

$$2k^\mu l^\nu \nabla_\mu \nabla_\nu f'(R) + 2\Box f'(R) = (k^\mu l^\nu + k^\nu l^\mu + 2g^{\mu\nu}) \nabla_\mu \nabla_\nu f'(R) = h^{\mu\nu} \nabla_\mu \nabla_\nu f'(R) + \Box f'(R)$$

Extending the calculation further, one can easily show that,

$$\int_{\mathcal{B}} \frac{h^{\mu\nu} \nabla_\mu \nabla_\nu f'(R)}{f'(R)} dA = \int_{\mathcal{B}} \frac{[\nabla^\mu f'(R)] [\nabla_\mu f'(R)]}{f'(R)^2} dA \quad (2.1.12)$$

Since k^μ is a killing field along the horizon, i.e., $k^\mu \nabla_\mu f'(R)|_{\mathcal{H}} = 0$, the integrand on the right-hand side of the above equation can be shown to be strictly positive. And, finally, the Euler characteristics becomes,

$$\begin{aligned} \chi(\mathcal{H}) &= \int_{\mathcal{B}} \left[2 \left(p_\mu p^\mu - \frac{d\theta}{ds} \right) + \frac{R f'(R) - f(R)}{f'(R)} + \frac{\nabla^\mu f'(R) \nabla_\mu f'(R)}{f'(R)^2} + \left(\frac{16\pi T_{\mu\nu} k^\mu l^\nu}{f'(R)} \right) \right] dA \\ &\quad + \int_{\mathcal{B}} \left[\frac{\square f'(R)}{f'(R)} \right] dA \end{aligned} \quad (2.1.13)$$

The above equation represents the final form of the Euler characteristics associated with the horizon cross-section in the physical frame. The first integral is positive definite since the integrand is positive and integrated over a compact surface \mathcal{B} gives a positive contribution. But, in general, the sign of $\square f'(R)$ is not certain. However, under the assumption, $\square f'(R) \geq 0$, χ becomes positive, and the topology turns out to be either toroidal or spherical.

Now a few comments in order. Note that the above differential condition on the function $f(R)$, i.e., $\square f' \geq 0$ is a sufficient condition, which ensures the Euler characteristics to be positive semi-definite. This does not rule out the possibility of toroidal horizon topology, for which one may require proof of the topology censorship theorem [64, 144] in $f(R)$ gravity. Another possible way to rule out the toroidal case could be to prove the instability of the horizon with such topology in $f(R)$ theories. Also, we need this condition to be valid only at the location of the horizon.

So far, we have shown our result in the physical frame. However, as emphasized earlier, now we proceed further to reproduce the result in the conformal frame. As we know, the $f(R)$ gravity can be transformed into Einstein gravity with an effective energy-momentum tensor by a conformal transformation. The effective energy-momentum tensor can be shown to obey the dominant energy condition. Such a technique has been used in the literature earlier to understand certain aspects of $f(R)$ gravity in a simpler framework. For instance, in Ref. [148], the conformal transformation technique is used to derive a classical second law for black holes in $f(R)$ gravity. Our aim is to understand the emergence of the sufficient condition $\square f'(R) \geq 0$ in the conformal frame. For future use, below we list down the transformation of certain terms of interest under the transformation ($\bar{g}_{\mu\nu} = \omega^2 g_{\mu\nu}$),

$$\left\{ \begin{array}{l} k^\mu \rightarrow \bar{k}^\mu = \frac{1}{\omega^2} k^\mu \\ l^\mu \rightarrow \bar{l}^\mu = l^\mu, h_{\mu\nu} \rightarrow \bar{h}_{\mu\nu} = \omega^2 h_{\mu\nu} \\ R \rightarrow \bar{R} = \frac{1}{\omega^2} R - \frac{6}{\omega^3} g^{\mu\nu} \nabla_\mu \nabla_\nu \omega \\ R(k, l) \rightarrow \bar{R}(\bar{k}, \bar{l}) = \frac{1}{\omega^2} R(k, l) - \frac{1}{\omega^3} [2k^\mu l^\nu \nabla_\mu \nabla_\nu \omega - \square \omega] - \frac{1}{\omega^4} (\nabla_\mu \omega)(\nabla^\mu \omega) \\ R(k, l, k, l) \rightarrow \bar{R}(\bar{k}, \bar{l}, \bar{k}, \bar{l}) = \frac{1}{\omega^2} R(k, l, k, l) - \frac{2}{\omega^3} (k^\mu l^\nu) \nabla_\mu \nabla_\nu \omega + \frac{1}{\omega^4} (\nabla_\mu \omega)(\nabla^\mu \omega) \\ \theta \rightarrow \bar{\theta} = \frac{1}{\omega^2} \theta + \frac{1}{\omega^4} k^\mu \nabla_\mu f'(R) \end{array} \right.$$

It is important to notice that the conformal transformation preserves the causal structure of space-time. Since the event horizon is a null surface, the topology and Euler characteristics of the horizon remains invariant under such a transformation. Therefore, the positivity of χ in the physical frame

should guarantee the positivity of $\bar{\chi}$ in the conformal frame, and one should expect to reproduce the same sufficient condition for the positivity of $\bar{\chi}$ as well. Since k^μ is a killing field only on the horizon, $k^\mu \nabla_\mu f'(R)|_{\mathcal{H}}$ identically vanishes. Also, θ and the shear σ_{ab} remains zero under conformal transformation from a stationary spacetime, and a stationary killing horizon remains stationary under conformal transformation. However, since the killing property of k^μ is specific to the horizon only, quantities that are defined away from the horizon may attain a different form in the conformal frame. For instance, the rate of change of expansion along the auxiliary null normal l^μ non-homogeneously changes under conformal transformation as,

$$\frac{d\bar{\theta}}{ds} = \frac{1}{\omega^2} \frac{d\theta}{ds} + \frac{1}{\omega^4} l^\alpha \nabla_\alpha (k^\mu \nabla_\mu f'(R)) \quad (2.1.14)$$

We emphasize that the last term on the right-hand side of the above equation need not vanish even on a stationary killing horizon since it represents the change along the auxiliary null direction, i.e., away from the horizon. Also, under conformal transformation we have,

$$\int \left[\bar{p}^\mu \bar{p}_\mu - \frac{d\bar{\theta}}{ds} \right] d\bar{A} \longrightarrow \int \left[p^\mu p_\mu - \frac{d\theta}{ds} + \frac{\square\omega}{\omega} \right] dA \quad (2.1.15)$$

This expression is derived upto a total divergence term of the type $d^\dagger p$. Finally, in the conformal frame, the Euler characteristics takes the form,

$$\bar{\chi}(\bar{\mathcal{B}}) = \int_{\bar{\mathcal{B}}} 2 \left[(\bar{p}|\bar{p}) - \frac{d\bar{\theta}}{ds} \right] d\bar{A} + \int_{\bar{\mathcal{B}}} \bar{\mathcal{T}}(\bar{k}, \bar{l}) d\bar{A} \quad (2.1.16)$$

Here $\bar{\mathcal{T}}(\bar{k}, \bar{l})$ represents the (\bar{k}, \bar{l}) component of the effective energy-momentum tensor that appears in the $f(R)$ equation and it involves higher-order curvature terms. However, as discussed previously, under the physically well motivated conditions $f'(R) > 0$ and $Rf'(R) - f(R) > 0$, the effective energy-momentum tensor satisfies the dominant energy condition. With this, the Euler characteristic $\bar{\chi}$ in the conformal frame will turn out to be positive, provided that \bar{p}^μ is a space-like vector field and the event horizon in the conformal frame is the limit to the existence of outer trapped surfaces, i.e $\frac{d\bar{\theta}}{ds}|_{\bar{\mathcal{B}}} < 0$. These two conditions, if satisfied, ensures the positivity of Euler characteristic in the conformal frame without the requirement of the sufficient differential condition we obtained by a direct approach in the physical frame, which seems to be contradictory. To resolve this apparent contradiction, we first note that the quantities $\frac{d\bar{\theta}}{ds}$ and $(\bar{p}|\bar{p})$ doesn't transform homogeneously under conformal transformation. This suggests that the condition for the non-existence of trapped surfaces outside the horizon is not a conformal invariant statement, which can also be realized from Eq. (2.1.15). Finally, by substituting various conformal transformations, one can show that,

$$\begin{aligned} \bar{\chi}(\bar{\mathcal{B}}) &= \int_{\bar{\mathcal{B}}} 2 \left[(p|p) - \frac{d\theta}{ds} + \frac{1}{2} \frac{\square f'(\phi)}{f'(\phi)} \right] dA \\ &+ \int_{\bar{\mathcal{B}}} \left[\frac{16\pi}{f'(\phi)} T(k, l) + \left(\frac{f''(\phi)}{f'(\phi)} \right)^2 (\nabla_a \phi)(\nabla^a \phi) + \frac{\phi f'(\phi) - f(\phi)}{f(\phi)} \right] dA \end{aligned} \quad (2.1.17)$$

With the field equation of the auxiliary scalar field, $\phi = R$, the above expression of $\bar{\chi}$ in the conformal frame reduces to χ in Eq. (2.1.13), as one should expect. This also proves the invariance of Euler characteristics under conformal transformations. Again, note that each term in the second integral

is individually positive definite and, when integrated over a compact surface, yields a positive contribution. Now consider the first integral. As discussed earlier, the product $(p|p)$ is positive since p is a spacelike vector field. Also, $\frac{d\theta}{ds}$ is negative on the horizon and as a result combinedly we have $(p|p) - \frac{d\theta}{ds} > 0$ on the horizon. Therefore, the same sufficient condition $\square f'(R) \geq 0$ is needed if we impose no trapped surface condition in the physical frame.

2.2 Generalization to Higher Dimensions

In the previous section, we presented an extension of Hawking's topology theorem to $f(R)$ gravity in $3+1$ dimensions. Now we want to explore the case of higher-dimensional black holes. As discussed previously, the Gauss-Bonnet theorem can not be used in higher dimensions, and as a result, the expression for Euler characteristics associated with the horizon is no longer given by Eq. (2.1.1). This is a subtle issue since the topological classification is richer as compared to $3+1$ dimensions, and one needs to be careful while commenting on the topology of surfaces. However, Hawking's theorem has been previously extended to higher dimensions by Galloway and Schoen [65, 66]. Following this work, we look for the Yamabe invariant associated with the stationary horizon cross-section instead of Euler characteristics, which is defined as,

$$\mathcal{Y}[\sigma] = \sup_{[\gamma]} \inf_{\tilde{\gamma} \in [\gamma]} \frac{\int_{\sigma} S_{\tilde{\gamma}} d\bar{\Sigma}}{\int_{\sigma} d\bar{\Sigma}} \quad (2.2.1)$$

Before proceeding further with the proof, a few words on the notation. Here σ represents a compact co-dimension two surface in a d -dimensional manifold (\mathcal{M}^d, g) . The induced metric on σ is denoted by γ , and $[\gamma]$ represents the conformal class of metric of γ , i.e., the set of all possible metrics related to γ by a conformal transformation. S_{γ} is the scalar curvature of the co-dimension two surface σ . The central result of [65] is as follows: if σ^{d-2} is a marginally outer trapped surface and g is a solution of Einstein's equation with the matter-energy tensor obeying dominant energy condition, then σ admits positive scalar curvature. As a result, the Yamabe invariant is positive definite. In our work, we follow an identical approach in the context of $f(R)$ gravity to explore possible topological structures of the stationary horizon. Firstly, we provide a brief overview of the steps carried out in [65] and further use $f(R)$ equation to obtain our result. To our surprise, we find that the same sufficient condition we obtained for the $3+1$ dimensional case turns out to be enough to ensure the positivity of the Yamabe invariant in higher dimensions.

To that end, let us start by considering σ (horizon cross-section) to be a marginally outer trapped surface. This implies, the expansion θ vanishes on σ and positive outside. Since σ is a co-dimension two surface, it has two normal directions. Let u and v be the time like and space like normal to σ . The strategy is to deform the horizon cross-section σ along v in the n -dimensional space like hypersurface V^{d-1} . This is done with an initial deformation velocity $v = \phi v$ to get a surface σ_t at some later time t , where ϕ is some smooth function defined on σ . With this setup, the variation of the null expansion takes the form [65, 66, 154],

$$\frac{\partial \theta}{\partial t} = \square \phi + 2 \langle X, \nabla \phi \rangle + \left(\frac{1}{2} S - G(u, k) - \frac{1}{2} |\chi_k|^2 + \text{div } X - |X|^2 \right) \phi \quad (2.2.2)$$

Further defining $Q = \frac{1}{2} S - G(u, k) - \frac{1}{2} |\chi_k|^2$, we get,

$$\frac{\partial \theta}{\partial t} = \square \phi + 2 \langle X, \nabla \phi \rangle + (Q + \text{div } X - |X|^2) \phi \quad (2.2.3)$$

Here, the derivatives are taken on the horizon cross-section with respect to the induced metric γ . χ_{ab} represents the extrinsic curvature of σ with respect to the outgoing null vector $k = u + v$. S denotes the scalar curvature of σ and $G(u, k) = G_{\mu\nu}u^\mu k^\nu$ is the (u, k) component of the Einstein's tensor. Also, $X = -l_a \nabla_A k^a$, where ' A ' represents the spatial indices. Note that, Eq. (5.2.22) represents an eigenvalue equation of the form,

$$\frac{\partial \theta}{\partial t} = L(\phi) = \lambda \phi \quad (2.2.4)$$

where L denotes the stability operator. Although L is in general not an self adjoint operator, the principal eigenvalue of L is always real and the corresponding principal eigenfunction ϕ is positive definite [155]. Since σ is defined to be a marginally outer trapped surface we have $\frac{\partial \theta}{\partial t} > 0$, i.e, $L(\phi) > 0$. With this, we can show,

$$\int_\sigma |\nabla \phi|^2 + Q\phi^2 \geq 0, \forall \phi \in C^\infty(\sigma) \quad (2.2.5)$$

To proceed further, we consider the operator $L_1 = -\square + Q$ with the eigenvalue equation, $L_1\phi = \lambda_1\phi$. The principal eigenvalue of L_1 is given by,

$$\lambda_1(p) = \inf \frac{\int_\sigma \phi L_1(\phi) d\Sigma}{\int_\sigma \phi^2 d\Sigma} = \inf \frac{\int_\sigma |\nabla \phi|^2 + Q\phi^2 d\Sigma}{\int_\sigma \phi^2 d\Sigma} \quad (2.2.6)$$

The principal eigen function ϕ_p can be choosen to be strictly positive. The scalar curvature \bar{S} of surface σ , with respect to a metric $\bar{\gamma} = \phi_p^{2/d-3}\gamma$ is of the form [66];

$$\begin{aligned} \bar{S} &= \phi_p^{-2/d-3} \left[(-2\square + 2Q)\phi_p + 2G(u, k)\phi_p + |\chi_k|^2\phi_p + \frac{d-2}{d-3} \frac{|\nabla \phi_p|^2}{\phi_p^2} \right] \\ &= \phi_p^{-2/d-3} \left[\lambda_1(p)\phi_p + 2G(u, k)\phi_p + |\chi_k|^2\phi_p + \frac{d-2}{d-3} \frac{|\nabla \phi_p|^2}{\phi_p} \right] \end{aligned} \quad (2.2.7)$$

Note that, in Eq. (2.2.7), all other term except $G(u, k)$ are strictly positive definite. In the general relativity limit, $G(u, k)$ would be replaced by $T(u, k)$, and the imposition of the dominant energy condition would be sufficient to guarantee the positivity of $G(u, k)$. However, for $f(R)$ gravity, it is not the case since the field equation contains additional higher curvature terms. Using the field equation of $f(R)$ gravity we obtain,

$$G(k+l, k) = \frac{8\pi T(u, k) + k^\mu k^\nu \nabla_\mu \nabla_\nu f'(R) + (Rf'(R) - f(R)) + \square f'(R) + k^\mu l^\nu \nabla_\mu \nabla_\nu f'(R)}{f'(R)}$$

Now, on the horizon we find that,

$$k^\mu k^\nu \nabla_\mu \nabla_\nu f'(R) = k^\mu \nabla_\mu (k^\nu \nabla_\nu f') - (k^\mu \nabla_\mu k^\nu) \nabla_\nu f' = 0$$

As similar to the $3+1$ dimensional case, the last two terms on the right hand side can be simplified as,

$$\frac{\square f'(R) + k^\mu l^\nu \nabla_\mu \nabla_\nu f'(R)}{f'(R)} = \frac{1}{2} \frac{\square f'(R)}{f'(R)} + \frac{h^{\mu\nu} \nabla_\mu \nabla_\nu f'(R)}{f'(R)}$$

The last term in the above expression given a positive contribution to the Yamabe invariant when integrated over a compact surface(see Eq. (2.1.12)). Therefore, using the same argument presented in previous section, we conclude that, the scalar curvature of σ defined for a conformal class of metric

is strictly positive, provided $\square f'(R) \geq 0$. As a result the Yamabe invariant is positive.

Manifolds with positive scalar curvature and hence positive Yamabe invariant is of great mathematical interest and has been extensively studied previously by several authors [156–158]. In higher dimensions, the possible class of topology is richer as compared to lower dimensions. Although there are not many restrictions on the horizon topology in higher dimensions, as shown in Ref. [66], in five dimensions, the admissible topology is limited, i.e., either S^3 or $S^1 \times S^2$. The sufficient differential condition $\square f'(R) \geq 0$ obtained in this work restricts the possible topology of black horizons in five-dimensional $f(R)$ gravity to be either S^3 or $S^1 \times S^2$ or connected sum of these.

2.3 Summary

Hawking's topology theorem strictly restricts the admissible topology of four-dimensional asymptotically flat black holes in general relativity. Such a result may not hold for theories beyond general relativity. Therefore, black holes in such theories can admit different topological structure. This further could lead to several interesting properties of black holes with no parallel in general relativity. For example, the quasinormal mode spectrum of a black hole is sensitive to the horizon topology. As a result, deviation in the quasinormal mode spectrum may indicate a possible violation of general relativity. This motivates us to generalize Hawking's topology theorem to $f(R)$ theory of gravity. We obtained a sufficient differential equation $\square f'(R) \geq 0$, which, along with the dominant energy condition, ensures the positivity of Euler number [67]. In order to understand this condition further, let us consider the case where $f(R) = R + \alpha R^n$. Then the sufficient condition reduces to,

$$\square(R^{n-1}) = \frac{8\pi T + R + \alpha(2-n)R^n}{3\alpha n} \quad (2.3.1)$$

Where T represents the trace of the energy-momentum tensor. The case of $n = 2$, i.e for $f(R) = R + \alpha R^2$ theory is of cosmological interest since it has been extensively studied as a viable model for the inflation [159–162]. For this theory, the above condition takes the form,

$$\square R = \frac{R + 8\pi T}{6\alpha} > 0 \quad (2.3.2)$$

Further note that, in this case from $f'(R) = 1 + 2\alpha R > 0$, we have $R > -1/2\alpha$, i.e., the Ricci scalar is bounded from below. From this bound, Eq. (2.3.2) yields positive value of $\square R$, provided a sufficient condition $T \geq (1/16\pi\alpha)$ holds. So the condition on curvature is now reduced to a condition on the matter, given in terms of the coupling constant. Therefore, the topology of black holes in $R + \alpha R^2$ theory is completely determined from the matter sector, i.e., by the dominant energy condition and the trace energy condition derived above. In higher dimensions, the same condition makes the Yamabe invariant positive. However, as one can see from Eq. (2.3.1), such a simplification doesn't happen for $n > 2$.

Also, note that in our derivation, we have assumed the rigidity theorem [3, 4] to hold in $f(R)$ gravity, i.e., the event horizon of stationary black hole spacetime is also a killing horizon. To the best of our knowledge, no generalization of the rigidity theorem exists in higher curvature theories, including the $f(R)$ gravity. However, this is a reasonable assumption since $f(R)$ theory is conformal to general relativity, and Hawking's original proof may be extended to $f(R)$ gravity by conformal

transformations. Finally, even with the differential condition, we can not rule out the Toroidal topology, and a detailed study involving the generalization of the topology censorship theorems is needed to settle this issue.

Chapter **3**

On the General Structure of Physical Process first Law

This Chapter is based on, A. Mishra, S. Chakraborty, A. Ghosh, S. Sarkar, JHEP 1809 (2018) 034 [163].

Black holes are one of the fascinating prediction of Einstein's theory of general relativity. Studies in the past several decades have revealed strong fundamental connections among gravity, thermodynamics and quantum theory. The remarkable resemblance between the laws of thermodynamics and black hole mechanics [68, 69, 71] is one of the most significant theoretical achievement of the last century. The discovery of Hawking radiation [70] has further revealed that such a gravity-thermodynamics correspondence is not just a mathematical analogy. Therefore, the properties of the event horizon may provide several deep insights into the fundamental nature of black holes and particularly towards a theory of quantum gravity. Several follow up works also suggest that the connection between spacetime and thermodynamics is not specific to black holes only, and one can indeed relate various thermodynamic parameters to several geometric quantities associated with any null surface acting as a causal boundary (eg. Rindler horizon) [164–167].

In this chapter, we discuss the mathematical structure of the first law of black hole mechanics. As explained in [Chapter 1](#), in general, the first law can be expressed in two separate forms, namely the stationary state version and the physical process version. The stationary state version relates the variation of ADM charges at asymptotic infinity with the difference in horizon area of two stationary black holes infinitesimally separated in the solution space of Einstein's equation. This is a global statement that requires prior knowledge of the asymptotic structure of spacetime. On the other hand, the physical process first law (PPFL) involves the computation of change in horizon area with respect to some influx matter [73]. For illustration, we have depicted such a process in [Fig. 3.1](#). In contrast to the stationary state version, the PPFL is a local statement and does not require any information of the asymptotic structure of spacetime. Interestingly the PPFL is also valid for any bifurcate killing horizon [165, 166].

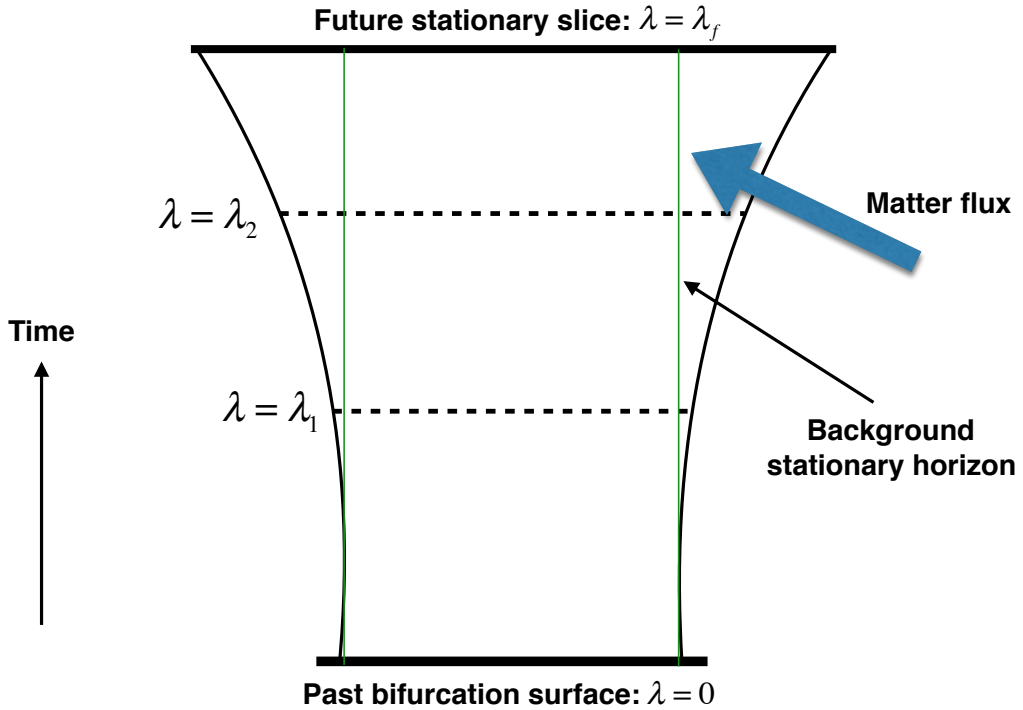


FIGURE 3.1: This figure represents a geometric illustration of the physical process first law. The green lines depict the stationary event horizon, while the black curves represent the evolution of the horizon with respect to matter perturbation. The change in area is computed between the two slices $\lambda = 0$ (the bifurcation surface) and $\lambda = \lambda_f$ (a final stationary slice). We want to generalize this and calculate the change between two arbitrary slices $\lambda = \lambda_1$ and $\lambda = \lambda_2$.

In order to provide a precise formulation of the PPFL, let us start by perturbing a black hole with some influx of matter having stress-energy tensor $T_{\mu\nu}$. We further assume that the black hole settles down to a final stationary state. Such a requirement is necessary to ensure the stability of the black hole under small perturbations. In this setting, the PPFL determines the change of the horizon area A_H , that is given by,

$$\frac{\kappa}{2\pi} \Delta \left(\frac{A_H}{4} \right) = \int_{\mathcal{H}} T_{\mu\nu} \xi^\mu d\Sigma^\nu . \quad (3.0.1)$$

Here $d\Sigma^\mu = k^\mu dA d\lambda$ represents the surface element of the event horizon and $k^\mu = (\partial/\partial\lambda)^\mu$ denotes the null generator of the horizon. The integration has been carried out over the horizon cross-section and along the affine parameter λ that varies from $\lambda = 0$ (bifurcation surface) to $\lambda = \lambda_f$ (final stationary state). The background event horizon is also a killing horizon with respect to the killing vector field ξ^μ , which is related to the null generator of the horizon as $\xi^\mu = \lambda \kappa k^\mu$. κ denotes the surface gravity of the background Killing horizon. The presence of terms quadratic in expansion and shear are neglected in Eq. (3.0.1) since the process we are considering is sufficiently stationary. This also ensures that no caustics will form within the range of integration. For a stationary spacetime, one has, $\xi^\mu = t^\mu + \Omega_H \phi^\mu$, where (t, ϕ) represents the time like and angular killing vector, with Ω_H being the angular velocity of the horizon.

Now, for the generalization of these results to theories beyond general relativity, one needs to define a suitable notion of horizon entropy. For the case of the stationary horizon with a regular bifurcation surface, the Wald entropy turns out to be an appropriate candidate for the black hole entropy [168,169]. However, in the context of the PPFL, where the black hole is involved in a dynamical process, Wald's entropy becomes ambiguous and can not be used as a good measure of entropy [170]. Therefore, it is important to understand how the ambiguities present in Wald's construction affects the PPFL at various order in perturbation. One of the primary results of this work is to show that the ambiguities of Wald's entropy do not affect the PPFL at first order when the integration is carried out from an initial bifurcation surface to a final stationary surface. In other words, the Wald entropy can be used in the context of PPFL as far as the dynamics of the black hole is quasi-stationary. However, this result does not hold at second order in perturbation.

Further note that, in the context of membrane paradigm, the coefficient of θ^2 and σ^2 in the Raychaudhuri equation can be interpreted as the bulk and shear viscosity respectively associated with the fictitious fluid living on the horizon. Therefore, a detailed analysis of the general structure of PPFL would be helpful to understand various properties of the membrane fluid in a general context [171].

One of the essential assumptions that goes into the derivation of the PPFL is the stability of black holes with respect to small perturbations. This allows one to choose the final state to be stationary. In this work, we also study the PPFL when the variation of the horizon entropy is computed between two non-stationary cross-sections and properly interpret the additional boundary terms appearing in Eq. (3.0.1). We will show how these boundary terms are related to the energy of the horizon membrane arising in the context of the black hole membrane paradigm. Moreover, we will establish that such a correspondence transcends beyond general relativity and also holds true for Lanczos-Lovelock theories of gravity.

This chapter is organized as follows: We start by describing the geometry of the event horizon and set up the notations and conventions. Then we present the most general form of the PPFL for an arbitrary diffeomorphism invariant theory of gravity and subsequently discuss several limiting cases. Then we briefly discuss the ambiguities present in Wald's Noether charge construction and further study its effect on the PPFL at various order in perturbation. We also derive the dynamical version of the PPFL, i.e., by integrating between two non-equilibrium cross-sections. Lastly, we derive the dynamical version of the PPFL for Einstein-Gauss-Bonnet and arbitrary order Lanczos-Lovelock theories of gravity. We conclude with a brief summary of the present chapter.

3.1 General Structure of PPFL

We start by describing the geometry of the event horizon and setting up our notations and conventions. Let H denotes the event horizon in a d -dimensional black hole spacetime generated by the null vector k^μ and λ is the affine parameter along the horizon. The horizon cross-section \mathcal{H} is a co-dimension two surface with two normal direction k^μ (horizon generator) and l^μ (an auxiliary null vector) such that $k_\mu l^\mu = -1$. The induced metric on \mathcal{H} is of the form $h_{\mu\nu} = g_{\mu\nu} + k_\mu l_\nu + k_\nu l_\mu$. If x^A ($A = 1, 2, \dots, d-2$) represent the coordinates on \mathcal{H} , then (λ, x^A) spans the horizon. The event horizon of a stationary black hole is also a killing horizon, where the killing vector (ξ^μ) is proportional to the horizon generator, i.e., $\xi^\mu = \lambda \kappa k^\mu$. Here κ denotes the surface gravity of the horizon and defined as

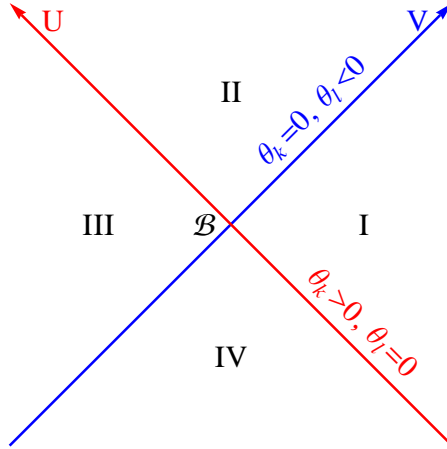


FIGURE 3.2: The point \mathcal{B} ($U = 0, V = 0$), a $(d - 2)$ -dimensional cross-section of the Horizon represents the Bifurcation surface, where $\theta_k, \theta_l = 0$.

$\xi^\mu \nabla_\mu \xi^\nu \stackrel{\mathcal{H}}{=} \kappa \xi^\nu$. Now, the expansion and shear associated with the horizon are defined to be the trace and traceless symmetric part of the extrinsic curvature of \mathcal{H} , i.e., $(\theta_k, \sigma_{\mu\nu}^k)$ and $(\theta_l, \sigma_{\mu\nu}^l)$ with respect to k^μ and l^ν respectively. If h represents the determinant of the induced metric $h_{\mu\nu}$, then the expansion θ_k is of the form,

$$\theta_k = \frac{1}{\sqrt{h}} \frac{d}{d\lambda} \sqrt{h} \quad (3.1.1)$$

The dynamics of θ_k is governed by the Raychaudhuri equation which reads,

$$\frac{d\theta_k}{d\lambda} = -\frac{1}{d-2} \theta_k^2 - \sigma_{\mu\nu}^k \sigma_k^{\mu\nu} - R_{\mu\nu} k^\mu k^\nu \quad (3.1.2)$$

An important notion that will play a crucial role throughout our discussion is a bifurcation surface. The bifurcation surface is a $(d - 2)$ dimensional spacelike surface \mathcal{B} , on which the killing vector ξ^μ vanishes identically. At the bifurcation surface (\mathcal{B}), the past and future horizon intersect, and for convenience, we choose it to be at $\lambda = 0$. The conventional derivation of the PPFL extensively relies on the existence of a bifurcation surface. Note that, in general, the bifurcation surface is not part of a black hole spacetime formed by the gravitational collapse process. However, if the horizon generating geodesics can be extended to the past, then one can always have a bifurcation surface at some earlier λ . For example, the Schwarzschild spacetime does not have a bifurcation surface. Nevertheless, in its maximal extension, i.e., in the Kruskal spacetime, the co-dimension two surface $U = 0, V = 0$ represents a bifurcation surface (Fig. 3.2). Here (U, V) represents the Kruskal coordinates.

A simple calculation leads to the following expressions of the expansion coefficients along k and l ,

$$\theta_k \propto U; \quad \theta_l \propto V \quad (3.1.3)$$

Therefore, at the future horizon ($U = 0$), the expansion with respect to the null vector k vanishes, i.e., $\theta_k = 0$, while at the past horizon ($V = 0$), $\theta_l = 0$. And, at the bifurcation surface ($U = 0, V = 0$) both θ_k and θ_l vanishes. Also the shear can be shown to be vanishing on \mathcal{B} . As a result, on the future horizon we have $\theta_k, \sigma_k \sim \mathcal{O}(\epsilon)$, while θ_l and σ_l are of zeroth order. Here ϵ represents the strength of the perturbation, which in our case refers to the influx matter. However, since θ_l and σ_l both identically vanishes at the bifurcation surface \mathcal{B} , they must be of at least $\mathcal{O}(\epsilon)$ only at \mathcal{B} . This result is indeed

a property of the bifurcation surface itself and independent of the physical theory one considers. Hence it also generalizes beyond general relativity and holds for higher curvature theories as well. In summary we have, $\theta_k, \sigma_k, R_{\mu\nu}k^\mu k^\nu, d\rho/d\lambda \sim \mathcal{O}(\epsilon)$ and $\theta_l, \sigma_l \sim \mathcal{O}(\epsilon)$ at \mathcal{B} . As a result, terms like $\theta_k \theta_l \sim \mathcal{O}(\epsilon^2)$ only at the bifurcation surface of the background stationary horizon.

Having defined the geometry of the event horizon, we now illustrate the most general structure of PPFL for an arbitrary diffeomorphism invariant theory of gravity. To that end, we start with the horizon entropy and study its variation with respect to some matter influx. Since we consider theories beyond general relativity here, the standard formula for entropy, as being proportional to area, no longer holds. However, one can always express the horizon entropy as some local density function integrated over the horizon cross-section, which can be written as,

$$S = \frac{1}{4} \int_{\mathcal{H}} (1 + \rho) \sqrt{h} d^{d-2}x, \quad (3.1.4)$$

where ρ represents the entropy density constructed locally on the horizon and contains the higher curvature contributions. In the general relativity limit ($\rho = 0$), one recovers the area-entropy relation. The field equation in such a general theory can always be written as,

$$R(k, k) + H(k, k) = 8\pi T(k, k) \quad (3.1.5)$$

where, $R(k, k) \equiv R_{\mu\nu}k^\mu k^\nu$ and $T(k, k) = T_{\mu\nu}k^\mu k^\nu$. Also, $H(k, k) \equiv H_{\mu\nu}k^\mu k^\nu$, which represents the deviation from general relativity. With this setting, let us now compute the variation of the entropy along the horizon generator k^μ , in response to some influx of matter,

$$\Delta S(\rho) = \frac{1}{4} \int_{\mathcal{H}} d^{d-2}x \int \frac{d}{d\lambda} [(1 + \rho) \sqrt{h}] d\lambda \quad (3.1.6)$$

Furthermore, integrating by parts and using the field equation, one can simplify the above expression to,

$$\begin{aligned} \Delta S(\rho) &= \frac{1}{4} \left(\int dA \lambda \Theta_k \right)_{\lambda_1}^{\lambda_2} + 2\pi \int dA d\lambda \lambda T(k, k) + \frac{1}{4} \int dA d\lambda \lambda \left[- \left(\frac{d-3}{d-2} \right) (1 + \rho) \theta_k^2 + (1 + \rho) \sigma^2 \right] \\ &\quad - \frac{1}{4} \int dA d\lambda \lambda \left(\frac{d^2 \rho}{d\lambda^2} + 2\theta_k \frac{d\rho}{d\lambda} - \rho R(k, k) + H(k, k) \right) \end{aligned} \quad (3.1.7)$$

Here $\Theta_k = \theta_k + \rho \theta_k + \frac{d\rho}{d\lambda}$ is the generalized expansion. We would like to emphasize that Eq. (3.1.7) represents the most general form of the variation of entropy along the null generator, and no assumption regarding the strength of the perturbation or the range of integration has been made throughout the derivation. By truncating this general result to linear order in the perturbation, we further obtain,

$$\Delta S^{(1)}(\rho) = \frac{1}{4} \left(\int dA \lambda \Theta_k \right)_{\lambda_1}^{\lambda_2} + 2\pi \int dA d\lambda \lambda T(k, k) - \frac{1}{4} \int dA d\lambda \lambda \left(\frac{d^2 \rho}{d\lambda^2} - \rho R(k, k) + H(k, k) \right) \quad (3.1.8)$$

Now, to understand this result further, we evaluate the last term on the right hand side for some simplified models. For instance, let us consider the $f(R)$ theory, for which, the field equation is given by Eq. (2.1.4),

$$f'(R)R_{\mu\nu} - \frac{1}{2}g_{\mu\nu}f(R) + g_{\mu\nu}\square f'(R) - \nabla_\mu \nabla_\nu f'(R) = 8\pi T_{\mu\nu} \quad (3.1.9)$$

For this particular case, $\rho = f'(R) - 1$ represents the modification to entropy density, where a prime

denotes derivative with respect to the Ricci scalar R . Note that, for general relativity $f(R) = R$ and as a result $\rho = 0$. Also, one can always rewrite the field equation for $f(R)$ theory in the form of Eq. (3.1.5), with

$$H(k, k) = f'(R)R(k, k) - k^a k^b \nabla_a \nabla_b f'(R) \quad (3.1.10)$$

Substitution of the above expression for $H(k, k)$ results into the following identity for $f(R)$ theories,

$$\frac{d^2\rho}{d\lambda^2} - \rho R(k, k) + H(k, k) = 0 \quad (3.1.11)$$

If Eq. (3.1.11) is a property of the entropy density itself, then our If Eq. (3.1.11) is a property of the entropy density itself, then our expression for the change in entropy up to first order as given in Eq. (3.1.8) will take a very simplified form. At this stage, it seems a mere coincidence, but one can show the above equation to hold for arbitrary order Lovelock theory. Motivated by these results, we argue that Eq. (3.1.11) is a general property of the entropy density and holds in an arbitrary diffeomorphism invariant theory of gravity. Note that the above equation for the flow of entropy density is a result that holds only up to first order in perturbation, i.e., it may be proportional to terms that are quadratic in expansion and shear. Hence in general Eq. (3.1.11) is indeed of the form,

$$\frac{d^2\rho}{d\lambda^2} - \rho R(k, k) + H(k, k) = O(\epsilon^2) \quad (3.1.12)$$

Therefore, at least up to linear order, the variation of the entropy simplifies to,

$$\Delta S^{(1)}(\rho) = \frac{1}{4} \left(\int dA \lambda \Theta_k \right)_{\lambda_1}^{\lambda_2} + 2\pi \int dA d\lambda \lambda T(k, k) \quad (3.1.13)$$

As one would expect, the final form of the variation of horizon entropy up to linear order is comprised of a boundary term and a bulk integral. The traditional derivation of the PPFL is based on the following two assumptions,

- The horizon possesses a regular bifurcation surface in the asymptotic past, which is set at $\lambda = 0$ for convenience.
- The horizon is stable under perturbation and eventually settle down to a new stationary black hole.

The first assumption is technical in nature. In general, the bifurcation surface is not part of the black hole spacetime formed by gravitational collapse. Therefore, it is desirable to have a formulation of the physical process first law without this assumption. The second assumption is motivated by cosmic censorship conjectures, which asserts that the event horizon must be stable under small perturbation. More precisely, it is a requirement for the stability of the black hole.

Under these assumptions, the first term vanishes when the integration is carried out between the bifurcation surface (λ_1) and a final stationary cross-section (λ_2). This is because at the bifurcation surface $\lambda \rightarrow 0$ and for a stationary cross-section $\Theta_k \rightarrow 0$. However, when the PPFL is evaluated between two non equilibrium slice λ_1 and λ_2 , the boundary term turns out to be non vanishing. We will discuss this situation in subsequent sections. Finally the linear order variation of entropy takes the form,

$$\Delta S = 2\pi \int_{\lambda=0}^{\lambda_f} \lambda d\lambda d^{d-2}x \sqrt{h} T_{\mu\nu} k^\mu k^\nu . \quad (3.1.14)$$

The background killing field $\xi^\mu = \lambda \kappa k^\mu$ and one can rewrite the above equation as,

$$\frac{\kappa}{2\pi} \Delta S = \int_{\mathcal{H}} T_{\mu\nu} \xi^\mu d\Sigma^\nu . \quad (3.1.15)$$

This completes the standard derivation of what is known as the integrated version of the physical process first law described by Eq. (3.0.1). If the matter field satisfies the null energy condition, then one will have $T_{\mu\nu} k^\mu k^\nu \geq 0$, and as a result, the entropy change between the two cross-sections is positive semi-definite.

3.2 Black hole Entropy and Ambiguities

For stationary black holes with a regular bifurcation surface in an arbitrary diffeomorphism invariant theory of gravity, the entropy associated with the horizon is given by Wald's formula [168],

$$S_W = -2\pi \int_B \frac{\partial L}{\partial R_{\mu\nu\alpha\beta}} \epsilon_{\mu\nu} \epsilon_{\alpha\beta} \sqrt{h} d^{d-2}x = \int_B (1 + \rho_w) \sqrt{h} d^{d-2}x \quad (3.2.1)$$

Where $\epsilon_{\mu\nu} = k_\mu l_\nu - k_\nu l_\mu$ is the bi-normal to the bifurcation surface. In the general relativity limit, the Lagrangian is given by the Einstein-Hilbert term, and the Wald entropy reduces to Bekenstein-Hawking entropy. Note that the construction of Wald entropy crucially depends on the existence of a bifurcation surface. However, as shown in [170], the Wald entropy remains unaffected when computed on an arbitrary stationary cross-section of the event horizon. This is not surprising since, in a stationary black hole spacetime, every cross-section of the horizon is isomorphic to others. As a result, one would naturally expect to obtain an identical expression for the Wald entropy irrespective of the choice of horizon cross-section.

Also, like any other Noether charge construction in field theory, the Wald entropy is known to be affected by ambiguities [169]. But, as discussed in [169,170], these ambiguities doesn't affect the Wald entropy in the case of stationary black holes. This is not the case when the black hole is involved in a dynamical process. In fact, for non-stationary black holes, the Wald entropy formula no longer holds and turns out to be ambiguous up to addition of terms of the form,

$$\Delta S_w = \int \Omega dA , \quad (3.2.2)$$

where $\Omega = (p\theta_k\theta_l + q\sigma_k\sigma_l)$ and $\sigma_k\sigma_l = \sigma_{\mu\nu}^k \sigma_l^{\mu\nu}$. The coefficients p and q in this expression are fixed by demanding the entropy to be locally increasing [61,172]. Comparing Eq. (3.1.4) and Eq. (3.2.1), we can identify that $\rho = \rho_w + \Omega$. This essentially means that the entropy of a non-stationary horizon cross-section can always be written as the entropy of the stationary case with ambiguities. In the stationary limit, the ambiguity term vanishes, and the black hole entropy coincides with the Wald entropy. Now, we would like to understand how these ambiguity terms affect the PPFL. We shall prove that, for linear perturbations, the PPFL is independent of these ambiguities, provided we integrate from an initial bifurcation surface to a final stationary cross-section. To illustrate this result, we start from

the first-order variation of the Wald entropy,

$$\begin{aligned}\Delta S^{(1)}(\rho_w) = & \frac{1}{4} \left(\int dA \lambda \Theta_k(\rho_w) \right)_{\lambda_1}^{\lambda_2} + 2\pi \int dA d\lambda \lambda T(k, k) \\ & - \frac{1}{4} \int dA d\lambda \lambda \left(\frac{d^2 \rho_w}{d\lambda^2} - \rho_w R(k, k) + H(k, k) \right)\end{aligned}\quad (3.2.3)$$

It is important to emphasize that, the differential equation for the entropy density obeyed by ρ (Eq. (3.1.12)) may not hold for ρ_w because of the presence of additional ambiguity terms. The difference between the change in black hole entropy to the change in Wald entropy upto linear order takes the form,

$$\Delta S^{(1)}(\rho) - \Delta S^{(1)}(\rho_w) = \frac{1}{4} \int dA \lambda \left(\frac{d\Omega}{d\lambda} + \Omega \theta_k \right) \Big|_{\lambda_1}^{\lambda_2} - \frac{1}{4} \int dA d\lambda \left(\lambda \frac{d^2 \Omega}{d\lambda^2} \right)\quad (3.2.4)$$

Also, one can neglect the term $\Omega \theta_k$, which is of $\mathcal{O}(\epsilon^2)$. Therefore, finally, up to $\mathcal{O}(\epsilon)$, we get

$$\Delta S^{(1)}(\rho) - \Delta S^{(1)}(\rho_w) = \frac{1}{4} \int dA \Omega \Big|_{\lambda_1}^{\lambda_2} + \mathcal{O}(\epsilon^2)\quad (3.2.5)$$

Eq. (3.2.5) represents the difference between the change in Wald entropy and black hole entropy evaluated between two arbitrary non-stationary cross-section (λ_1 and λ_2). Note that, in general the boundary term Ω does not vanishes on a non-stationary horizon slice, as it contains terms proportional to expansion and shear. However, consider the situation when the background stationary black hole spacetime has a regular bifurcation surface (say at $\lambda_1 = 0$). In this case, as as discussed previously, terms like $\theta_k \theta_l$ and $\sigma_k \sigma_l$ are of second order in perturbation. As a result we have $\Omega \sim \mathcal{O}(\epsilon^2)$ at the bifurcation surface and we are left with,

$$\Delta S^{(1)}(\rho) - \Delta S^{(1)}(\rho_w) = \mathcal{O}(\epsilon^2)\quad (3.2.6)$$

Therefore, if the perturbations are considered to be sufficiently small such that one can neglect terms beyond linear order, the ambiguities does not affect the PPFL when integrated from a bifurcation surface to a stationary surface. However, this result doesn't hold when second order perturbations are considered. Up to $\mathcal{O}(\epsilon^2)$, the difference between $\Delta S(\rho)$ and $\Delta S(\rho_w)$ is of the form,

$$\Delta S^{(2)}(\rho) - \Delta S^{(2)}(\rho_w) = \frac{1}{4} \int dA (\lambda \theta_k \Omega + \Omega) \Big|_{\lambda_1}^{\lambda_2} + \frac{1}{4} \int dA d\lambda \left(\lambda \theta_k \frac{d\Delta}{d\lambda} + \lambda \Omega R(k, k) - \Omega \theta_k \right)\quad (3.2.7)$$

Note that, unlike linear order, the expression for the difference in the variation of Wald entropy and black hole entropy is comprised of a boundary term and a bulk integral that explicitly contains ambiguities. As a result, the PPFL is clearly affected by the ambiguity terms beyond linear order.

So far, we have only considered the integrated version of PPFL, where the variation of entropy is computed between the past bifurcation surface and the future stationary slice. Now we would like to understand the PPFL, when integrated between two arbitrary non-stationary horizon cross-section. As we shall show in the subsequent section, the boundary term, in this case, can be identified with the horizon membrane energy. However, for this illustration, we would require some preliminary results from the membrane paradigm formulation of the black hole. Therefore we briefly describe the membrane construction for the event horizon in the next section.

3.3 Membrane Paradigm for Black holes

The membrane paradigm is an effective description of the event horizon of a black hole from the point of view of an external observer. In this framework, the black hole horizon is modelled by a membrane of fictitious fluid living on the horizon surface. The interaction of the black hole with external matter fields is mimicked by the interaction between exterior matter and the horizon fluid and are often expressed in terms of the transport coefficients associated with the fluid [173].

The stress-energy tensor associated with the membrane fluid can be derived using a variational principle. As an example, consider the variation of Einstein-Hilbert action with a Gibbons-Hawking surface term [174, 175]. In the presence of a horizon as an inner boundary, the contribution at the inner boundary makes the variational principle ill-defined. Therefore, one needs to add an additional contribution at the horizon. This new contribution can be interpreted as some fictitious matter living on the stretched horizon, a time like surface just outside the horizon [176]. Then, in the limit when the stretch horizon approaches the true horizon, the stress-energy tensor on the horizon cross-section can be expressed in terms of parameter intrinsic to the horizon as [173, 176, 177]:

$$t^{\mu\nu} = p h^{\mu\nu} + 2\eta \sigma^{\mu\nu} + \zeta \theta_k h^{\mu\nu} \quad (3.3.1)$$

Let us recall that, here $t_{\mu\nu} e_A^\mu e_B^\nu = t_{AB}$, where e_A^μ represents the projection into the horizon cross-section and $A = 1, 2, \dots, (d-2)$ is the coordinate index of the co-dimension two surface. Note that the above expression of the stress-energy tensor resembles that of a viscous fluid with pressure p , shear viscosity η and a negative bulk viscosity ζ . For general relativity, we have $p = \kappa$, $\eta = 1/16\pi$ and $\zeta = -1/16\pi$. However, for other theories, although the form of the stress-energy tensor remains unchanged, the coefficients get modified [178–180].

Now, by considering a tangent vector to the stretched horizon u^μ , one can obtain the energy density associated with the membrane fluid as $\Sigma \equiv t_{\mu\nu} u^\mu u^\nu = -\theta_k/8\pi$. Since the expansion θ_k is always positive (from Hawking's area theorem), the membrane energy turns out to be negative. The negativity of the membrane energy is related to the teleological nature of the event horizon [173]. Because of the teleological property, the horizon tends to expand even before the influx of matter hits the horizon. Since the influx matter is assumed to obey the null energy condition, it has a positive energy density. As a result, the expanding horizon must have negative energy to attain equilibrium. The same teleological condition also results in the negative bulk viscosity [181–184].

3.4 Physical process first law and the membrane paradigm

One of the primary focus of the present chapter is to formulate a generalization of the PPFL for the arbitrary dynamical cross-sections of the event horizon. When the change in entropy is evaluated between a past bifurcation surface and a future stationary slice, the boundary term does not contribute. We would like to understand the physics behind the above process when the variation of entropy is computed between two arbitrary slices (λ_1 and λ_2). It is convenient to work with the non-affine parametrization of the null generators and use the following relation between the expansion scalars in different parametrization,

$$\theta_k^{(\text{affine})} = \frac{1}{\kappa\lambda}\theta, \quad (3.4.1)$$

where κ denotes the surface gravity of the background stationary horizon and can be treated as constant. θ represents the expansion in the non-affine parametrization ¹. In this setting, the entropy change between two arbitrary horizon cross-section takes the form,

$$\frac{\kappa}{2\pi}\Delta S = \Delta \left[\frac{1}{8\pi} \int d^{d-2}x \theta \sqrt{h} \right] + \int_{\mathcal{H}} T_{\mu\nu} \xi^\mu d\Sigma^\nu, \quad (3.4.2)$$

Recall that when the integration range is from a bifurcation surface to a future stationary slice, the first term vanishes, which is not the case otherwise. The last term on the right-hand side is identified as the energy flux ΔQ flowing into the horizon. It is now clear that the above equation indeed has a thermodynamic interpretation provided one can interpret θ to be proportional to some sort of energy. It can be shown in connection with the black hole membrane paradigm. This will enable us to write down a thermodynamic physical process first law for the entropy change between two arbitrary dynamical slices of the horizon. A look at the first term on the right-hand side of Eq. (3.4.2) is sufficient to convince that it is the change of this membrane energy. Using the expression of the membrane energy, $\Sigma = -\theta/8\pi$, we obtain,

$$\frac{\kappa}{2\pi}\Delta S = \Delta E + \int_{\mathcal{H}} T_{\mu\nu} \xi^\mu d\Sigma^\nu; \quad E = - \int d^{d-2}x \sqrt{h} \Sigma, \quad (3.4.3)$$

Eq. (3.4.3) is the first law in a dynamical context. Furthermore, unlike Eq. (3.0.1), we have an additional energy term E , which has its origin in the energy of the horizon fluid arising from the membrane paradigm. Since the membrane energy density Σ is negative, it immediately follows that the energy E defined here is positive.

Further, if we identify $\kappa/2\pi$ as the Hawking temperature T_H of the background stationary horizon, the PPFL when integrated between two arbitrary horizon cross-section reduces to the following form,

$$T_H \Delta S = \Delta E + \Delta Q \quad (3.4.4)$$

This explicitly shows that one can indeed write down a well defined physical process version of the first law for any two arbitrary cross-sections of the horizon. In this analysis, the energy density of the membrane fluid plays a crucial role. This result illustrates a connection between the laws of black hole mechanics and the membrane paradigm in a dynamical context.

So far, we have only considered the first law for general relativity. As a result, our horizon entropy is taken to be a quarter of the area. But, the integrated version of the physical process law can be generalized beyond Einstein gravity, in particular to higher curvature theories of gravity as well. For example, it is possible to write down a physical process first law for Lanczos-Lovelock class of theories [185] where the entropy is no longer proportional to the area, rather is a complicated function of the horizon geometry [186]. Therefore, the additional term appearing in the expression of entropy change, which we have identified as the membrane energy, is different. It would be an interesting exercise to understand whether our interpretation of the boundary term as the horizon

¹This will be the general strategy followed in the rest of the paper. The quantity without the subscript k will correspond to the quantity in non-affine parametrization.

membrane energy holds even for higher curvature theories. We carry out this analysis in the context of Lanczos-Lovelock gravity and show that the boundary terms in such theories can also be interpreted as the energy associated with the corresponding membrane at the horizon. This result shows that our generalization transcends beyond general relativity and have much broader applicability.

In the next section, we will consider the case of Einstein-Gauss Bonnet gravity, the first non-trivial Lanczos-Lovelock term. We will show how the physical process first law for arbitrary cross-sections can be obtained for Einstein-Gauss-Bonnet gravity and shall establish its relationship with the corresponding membrane energy. We will extend our analysis to the full Lanczos-Lovelock gravity in subsequent sections.

3.5 First law for dynamical black holes in Einstein-Gauss-Bonnet gravity

We have derived the PPFL for dynamical black holes in a quasi-stationary scenario in the context of general relativity. It will be worthwhile to explore whether the same result applies to other gravity theories as well. Even though there can be a large class of theories that would satisfy the diffeomorphism invariance property and qualify as a gravitational Lagrangian, they can be distinguished by the additional criteria of providing second-order field equations under variation. As discussed in [Chapter 1](#), the Lanczos-Lovelock Lagrangians represents a unique class of higher curvature theory having second-order field equations [51]. The Lanczos-Lovelock Lagrangians are polynomials in the Riemann curvature tensor, suitably contracted with the completely antisymmetric determinant tensor ([Eq. \(1.3.1\)](#)). A Lanczos-Lovelock Lagrangian of order m will involve the product of m Riemann curvature tensors. The first order ($m = 1$) term in the expansion corresponds to Einstein gravity, while the second-order ($m = 2$) term represents the Gauss-Bonnet gravity. The Gauss-Bonnet term naturally appears as a special case of the low energy effective action of string theory [49]. We would like to generalize the results for Einstein gravity derived in the previous section to Gauss-Bonnet gravity. The action for the Einstein-Gauss-Bonnet gravity in d spacetime dimensions reads,

$$\mathcal{A} = \int d^d x \sqrt{-g} \frac{1}{16\pi} \left\{ R + \alpha \left(R^2 - 4R_{\mu\nu}R^{\mu\nu} + R_{\mu\nu\alpha\beta}R^{\mu\nu\alpha\beta} \right) \right\}, \quad (3.5.1)$$

where α is a dimensionful coupling constant with dimension (length)². One can write down an expression for the entropy associated with black holes in Einstein-Gauss-Bonnet gravity as [186],

$$S_{\text{EGB}} \equiv \frac{1}{4} \int d^{d-2} x \sqrt{h} (1 + \rho); \quad \rho = 2\alpha^{(d-2)} R, \quad (3.5.2)$$

Here $^{(d-2)}R$ represents the intrinsic Ricci scalar of the $(d - 2)$ dimensional horizon cross-section. In the general relativity limit we have $\alpha = 0$ and ρ vanishes. One can compute the variation of entropy with respect to some influx of matter along the horizon generator k (parameterized by the affine parameter λ), which further leads to the following expression,

$$\Delta S_{\text{EGB}} = \frac{1}{4} \int d^{d-2} x \int_{\lambda_1}^{\lambda_2} d\lambda \sqrt{h} \left[(1 + \rho) \theta_{(k)} + \frac{d\rho}{d\lambda} \right] \equiv \frac{1}{4} \int d^{d-2} x \int_{\lambda_1}^{\lambda_2} d\lambda \sqrt{h} \vartheta_k, \quad (3.5.3)$$

where ϑ_k is the analog of the expansion θ_k in Einstein-Gauss-Bonnet gravity. Now, we can integrate by parts and separate out a total divergence term to obtain,

$$\Delta S_{\text{EGB}} = \Delta \left\{ \frac{1}{4} \int d^{d-2}x \lambda \sqrt{h} \vartheta_k \right\} - \frac{1}{4} \int d^{d-2}x \int_{\lambda_1}^{\lambda_2} d\lambda \lambda \sqrt{h} \frac{d\vartheta_k}{d\lambda}. \quad (3.5.4)$$

Note that, in order to arrive at the above expression, we have neglected all the quadratic terms in $\vartheta_{(k)}$, since we are working under quasi-stationary approximation. Among the terms in the boundary, the $d\rho/d\lambda$ term essentially depends on how ${}^{(d-2)}R$ changes along the null generators. Since ${}^{(d-2)}R$ depends on the metric $h_{\mu\nu}$ projected on to the $(d-2)$ dimensional cross-section of the horizon it follows that change of ${}^{(d-2)}R$ is essentially related to $dh^{\mu\nu}/d\lambda$. This is nothing but the extrinsic curvature of the surface generated by the space of null generators. Thus one obtains,

$$\frac{d}{d\lambda} {}^{(d-2)}R = -2 {}^{(d-2)}R_{\mu\nu} \left(\sigma_{(k)}^{\mu\nu} + \frac{\vartheta_{(k)}}{d-2} h^{\mu\nu} \right), \quad (3.5.5)$$

Further, one can considerably simplify the bulk term $d\vartheta_k/d\lambda$, and up to linear order, it is nothing but $-8\pi T_{\mu\nu} k^\mu k^\nu$ [185], similar to general relativity. Finally, we arrive at the following expression for the change in entropy for the Einstein-Gauss-Bonnet gravity,

$$\Delta S_{\text{EGB}} = \frac{1}{4} \Delta \left\{ \int d^{d-2}x \sqrt{h} \lambda \vartheta_k \right\} + 2\pi \int d^{d-2}x \int_{\lambda_1}^{\lambda_2} d\lambda \lambda \sqrt{h} T_{\mu\nu} k^\mu k^\nu. \quad (3.5.6)$$

In the non-affine parametrization the change in entropy takes the following form,

$$\frac{\kappa}{2\pi} \Delta S_{\text{EGB}} = \Delta \left\{ \frac{1}{8\pi} \int d^{d-2}x \sqrt{h} \vartheta \right\} + \int_{\mathcal{H}} T_{\mu\nu} \xi^\mu d\Sigma^\nu. \quad (3.5.7)$$

Note that when the evolution of the horizon entropy is computed between a past bifurcation surface and a future stationary slice, the boundary term vanishes as in the case of general relativity. This is the integrated version of PPFL for Einstein-Gauss-Bonnet gravity [187]. However, when we compute the entropy change between arbitrary cross-sections, the boundary term contributes. We are interested in understanding whether the boundary term appearing, in this case, has any thermodynamic interpretation. Before venturing into such an analysis, we note that the term ϑ also represent the analogue of expansion in this case, measuring the change in entropy per unit cross-section. For Einstein-Gauss Bonnet theory, the entropy has been shown to be increasing at any arbitrary slice for linearized perturbations with positive energy matter. Therefore, analogous to general relativity, ϑ is also positive semi-definite, at least for linearized perturbations of the horizon. Next, we compare the boundary term with the energy of the horizon membrane fluid for Einstein-Gauss-Bonnet gravity. The membrane stress-energy tensor t_{ab} for Einstein-Gauss-Bonnet gravity has been obtained in [178] for perturbations over a spherically symmetric black hole horizon, and the corresponding energy density $\Sigma = t_{\mu\nu} u^\mu u^\nu$ associated with an evolving horizon in the membrane paradigm is,

$$\Sigma_{\text{EGB}} = -\frac{\theta}{8\pi} \left[1 + 2\alpha \frac{d-4}{d-2} {}^{(d-2)}R \right]. \quad (3.5.8)$$

In the general relativity limit ($\alpha \rightarrow 0$), $\Sigma_{\text{EGB}} \rightarrow \Sigma_{\text{GR}} = -\theta/8\pi$. Also, when $d = 4$, the Gauss-Bonnet contribution to the energy density vanishes. We then evaluate ϑ for the case of linearized perturbations around a spherically symmetric horizon leading to:

$$\frac{\vartheta}{8\pi} = -\Sigma_{\text{EGB}} = \frac{\theta}{8\pi} \left[1 + 2\alpha \frac{d-4}{d-2} {}^{(d-2)}R \right]. \quad (3.5.9)$$

This allows us to finally write down the first law for entropy change between two arbitrary cross-sections of the dynamical horizon in Einstein-Gauss Bonnet theory as,

$$\frac{\kappa}{2\pi} \Delta S = \Delta E + \int_{\mathcal{H}} T_{\mu\nu} \xi^\mu d\Sigma^\nu; \quad E = - \int d^{d-2}x \sqrt{h} \Sigma_{\text{EGB}}. \quad (3.5.10)$$

We have illustrated the integrated version of the PPFL between two arbitrary dynamical horizon cross-section in Einstein-Gauss-Bonnet gravity. This again coincides with the interpretation put forward in the context of general relativity. This further prompts us to see whether such an interpretation can be put forward for any other higher curvature theories. We have carried out this analysis explicitly in the context of the full Lanczos-Lovelock class of theories and pure Lovelock theories. Refer to [163] for a detailed calculation.

3.6 Summary

In general, astrophysical black holes are not stationary due to the presence of flux across the horizon. Hence, the notion of a stationary global solution of the field equations does not exist in reality. Also, the assumption of the existence of a bifurcation surface for every non-extremal black hole is only an idealization. As a result, it is not at all clear how to define the entropy of black holes in such situations. As we have discussed previously, such difficulties are due to the ambiguities present in the Wald entropy when the black hole is dynamical. Therefore, it is important to understand the extent to which these ambiguities affects the PPFL. With such motivations, we started by obtaining a general expression of the variation of entropy in an arbitrary diffeomorphism invariant theory of gravity. Further, we have shown that up to linear order in perturbations, the ambiguities in the Wald entropy do not affect the PPFL as long as the integration range is from the initial bifurcation surface to the final stationary horizon cross-section. However, the second-order variation of entropy turns out to be affected by ambiguities.

In the second part of this chapter, we studied the variation of entropy between two arbitrary non-equilibrium horizon cross-section. Interestingly, in this setting, we were able to express the change in entropy in the form of first law by introducing an extra term ΔE which has been interpreted as the change in horizon membrane energy. We have extended this result in the context of Lanczos-Lovelock theories of gravity. Note that we can not assert the sign of the membrane energy unless we demand that the expansion is positive at every cross-section. This is true because of Hawking's area theorem, which requires the assumption of cosmic censorship. Therefore, although we compute the change in entropy between two intermediate cross-sections, we indirectly require the stability of the black hole under perturbation.

In general relativity, the focusing theorem along with the null energy condition ensures that the rate of change of expansion is negative as the matter flux perturbs the horizon. Therefore, the expansion remains positive and decreases to zero in the future. In this process, the matter flux is used to increase the entropy as well as the membrane energy (from negative to zero). It is indeed interesting that all these can be easily extended to higher curvature theories like Lanczos-Lovelock gravity. This indicates that the thermodynamic nature of the horizon is a universal property independent of the detailed dynamics of gravity.

Chapter **4**

Photon Sphere and Black hole Shadow in Dynamically Evolving Spacetimes

This Chapter is based on, A. K. Mishra, S. Chakraborty, S. Sarkar, Phys. Rev. D 99, 104080 (2019) [86].

Black holes are interesting predictions of general relativity. Ever since the pioneering work of Hawking, Bekenstein, Penrose and others, black hole physics has received tremendous amount of attention and theoretical success [3, 63, 68–71]. As a result, studies of black holes in general relativity and modified theory has been one of the major themes of research in gravitational physics. Astrophysical observations provide strong evidence for the existence of super-massive objects (possibly black holes) at the centre of most of the galaxies [188–190]. However, all these tests including the detection of gravitational waves are indirect evidences, while a direct detection of black hole must correspond to the observation of black hole shadow [87–98].

The strong gravitational lensing effect leads to the existence of circular photon orbits around black holes. The shadow is defined as the region around the back hole from which no light from distant source reaches the observer [77–85]. Several interesting aspects of photon sphere and shadow has been extensively studied by numerous authors [191–201]. The recent shadow image of the supermassive object at the center of M87 galaxy, captured by the event horizon telescope resembles that of a rotating Kerr black hole. This is an important observation in gravitational physics. We have provided a preliminary review of the photon sphere and shadow for the case of static and spherically symmetric black hole spacetime in Section 1.4.3. Note that, black holes are in general not static since they continuously interact with the surrounding and accrete matter. Therefore, it would be interesting to understand how the photon orbit evolves when one goes beyond the stationary consideration [191]. Following this motivation, we want to extend the notion of a photon sphere when the spacetime is dynamical. In particular, we want to obtain a generalization of Eq. (1.4.10). In the dynamical case, we find that the radius of the photon sphere turns out to be governed by a second-order differential equation, unlike Eq. (1.4.10), which is an algebraic equation. In this chapter, we shall study the evolution of the photon sphere and shadow around slowly rotating and non-rotating black holes by solving the associated differential equation for various dynamical black hole models and illustrate some interesting results.

Furthermore, we extend our analysis to theories beyond general relativity. As we have discussed in [Section 1.3.1](#), the Lanczos-Lovelock gravity represents one possible generalization of Einstein's theory with the field equations containing at most second derivative of the metric [50–52]. The causal structure of spacetimes in Lovelock theories are vastly different than that of general relativity [202–209]. Unlike general relativity, the characteristics hypersurface of Lovelock theories are non-null. As a result, gravity propagates at a speed different from light since they follow null geodesic with respect to a different metric. Hence, it is interesting to ask how the circular null orbit corresponding to the graviton is different from the photon sphere. This difference is an intrinsic feature of any higher curvature theory. In this chapter, we shall study these effects in the context of Einstein-Gauss-Bonnet gravity by obtaining the effective graviton metric explicitly.

The rest of the chapter is organised as follows: In [Section 4.1](#), we start by deriving the evolution equation for the photon sphere radius for a spherically symmetric dynamical black hole spacetime. In [Section 4.2](#), we illustrate the dynamical evolution of the photon sphere for various spacetime by solving the differential equation numerically. More specifically, we study the Vaidya, Reissner-Nordström-Vaidya and Schwarzschild de-Sitter Vaidya black hole w.r.t. suitable choices of mass and charge functions. Interestingly, we obtain a novel relation between the evolution of the radius of the photon sphere and the null energy condition of the influx matter. Further, in [Section 4.3](#), we obtain an expression for the shadow radius of a dynamical spherically symmetric black hole and present the evolution by plotting the shadow at various instance of time. In [Section 4.4](#), we extend these studies to slowly rotating case, i.e., the Kerr-Vaidya black hole in the slow rotation limit. Finally, in [Section 4.5](#) we generalize our analysis to Einstein-Gauss-Bonnet theory and provide a derivation of the effective graviton metric in the dynamical context and studied the evolution of the graviton sphere and corresponding shadow, which has been contrasted with the photon sphere.

Notations and Conventions: In this chapter, a ‘prime’ will denote derivative with respect to the radial coordinate ‘ r ’ while a ‘dot’ over a quantity implies derivative with respect to ‘ v ’. All the derivatives with respect to the affine parameter ‘ λ ’ along the null geodesic will be displayed explicitly.

4.1 Evolution of Photon Sphere in a Spherically Symmetric Dynamical Spacetime

In [Section 1.4.3](#), we presented a brief calculation to obtain the general equation for the photon sphere radius in a static black hole spacetime. In this section, we will generalize [Eq. \(1.4.10\)](#) by deriving a second-order differential equation that governs the evolution of the photon sphere. To that end, let us start with the following spacetime metric ansatz,

$$ds^2 = -f(r, v)dv^2 + 2dv\,dr + r^2d\Omega^2. \quad (4.1.1)$$

Although the structure of the metric is very much similar to the one presented in [Section 1.4.3](#), as we shall see, the photon orbits will be completely different. This is because the spacetime is no longer static, and the radius of the circular photon orbit must vary with time. In this situation, we can model the photon sphere radius as a function of the in-going time to coordinate (v) for accreting matter and out-going time (u) for radiating matter. Since the spacetime is still spherically symmetric, the photon sphere does not depend on any other coordinates. Let us start with the in-going case first, where we have $r_{\text{ph}} = r_{\text{ph}}(v)$. We can follow an identical line of approach as in the static case, i.e., by starting

with $ds^2 = 0$ and then couple it with the radial null geodesic equation. This gives rise to the desired evolution equation for the radius of circular photon orbits in the equatorial plane, which reads (for a derivation see [Appendix A](#)),

$$\ddot{r}_{\text{ph}}(v) + \dot{r}_{\text{ph}}(v) \left[\frac{3}{r_{\text{ph}}(v)} f(r_{\text{ph}}(v), v) - \frac{3}{2} \frac{\partial f}{\partial r} \Big|_{r_{\text{ph}}(v), v} \right] - \frac{2}{r_{\text{ph}}(v)} \left\{ \dot{r}_{\text{ph}}(v) \right\}^2 + \frac{1}{2} \left(f(r_{\text{ph}}(v), v) \frac{\partial f}{\partial r} \Big|_{r_{\text{ph}}(v), v} - \frac{\partial f}{\partial v} \Big|_{r_{\text{ph}}(v), v} \right) - \frac{1}{r_{\text{ph}}(v)} f(r_{\text{ph}}(v), v)^2 = 0 \quad (4.1.2)$$

Similarly, for a radiating black hole spacetime, the metric is expressed in terms of the out-going coordinate u as,

$$ds^2 = -f(r, u) du^2 - 2dudr + r^2 d\Omega^2. \quad (4.1.3)$$

In this case, we can model the photon sphere radius as, $r = r_{\text{ph}}(u)$. Following a similar calculation as the accreting case, it is straightforward to obtain the differential equation governing $r_{\text{ph}}(u)$ for radiating black hole spacetime, which is of the form,

$$\ddot{r}_{\text{ph}}(u) - \dot{r}_{\text{ph}}(u) \left[\frac{3}{r_{\text{ph}}(u)} f(r_{\text{ph}}(u), u) - \frac{3}{2} \frac{\partial f}{\partial r} \Big|_{r_{\text{ph}}(u), u} \right] - \frac{2}{r_{\text{ph}}(u)} \left\{ \dot{r}_{\text{ph}}(u) \right\}^2 + \frac{1}{2} \left\{ f(r_{\text{ph}}(u), u) \frac{\partial f}{\partial r} \Big|_{r_{\text{ph}}(u), u} + \frac{\partial f}{\partial u} \Big|_{r_{\text{ph}}(u), u} \right\} - \frac{1}{r_{\text{ph}}(u)} f(r_{\text{ph}}(u), u)^2 = 0. \quad (4.1.4)$$

[Eq. \(4.1.2\)](#) and [Eq. \(4.1.4\)](#) represent the general equations governing the evolution of the photon sphere around a dynamically evolving black hole, either accreting or radiating. An entirely different approach has been taken in Ref. [191] to arrive at the same second-order differential equation. We want to solve the above equations to study further the evolution of the photon sphere for various choices of $f(r, v)$.

As an aside, let us point out two more radii of significant interest in the context of a dynamical black hole spacetime. Firstly, the apparent horizon, which can be determined by solving the equation $f(r, v) = 0$, leading to $r_{\text{ah}} = r_{\text{ah}}(v)$. Secondly, the event horizon, whose location is governed by the differential equation $(dr/dv) = (1/2)f(r, v)$ [72,210]. It is important to make the distinction between these two surfaces in a dynamical black hole spacetime. The event horizon is a null surface, while the apparent horizon is spacelike. However, if the spacetime is stationary, the event and apparent horizon coincide. So given a particular spacetime, with a specific $f(r, v)$, one can immediately determine the location of the event and apparent horizon, besides the circular photon orbit. We will explore these results as well in the following sections.

4.2 Application: Photon Sphere in Vaidya and Reissner-Nordström-Vaidya Spacetimes

In the previous section, we have derived a second-order differential equation that governs the evolution of photon sphere in dynamical black hole spacetime. Now we apply this formalism in the context

of two well known dynamical black holes, namely the Vaidya spacetime and Reissner-Nordström-Vaidya spacetime. For the Vaidya spacetime, the mass is a function of time, while for the Reissner-Nordström-Vaidya case, both mass and charge varies with time. We will first consider the Vaidya spacetime and determine the circular photon orbit along with the event and apparent horizon in it before taking up the Reissner-Nordström-Vaidya case. Finally, we will study possible modifications in the presence of a cosmological constant.

4.2.1 Photon Sphere in Vaidya Space time

As a first illustration of the method developed above, let us consider the case of Vaidya spacetime, which is basically a black hole spacetime accreting null fluid. Since we are primarily interested in an accreting black hole, we can write down the Vaidya spacetime in the in-going null coordinate as [211],

$$ds^2 = - \left(1 - \frac{2M(v)}{r} \right) dv^2 + 2dv dr + r^2 d\Omega^2. \quad (4.2.1)$$

The corresponding energy-momentum tensor associated with the null fluid can be obtained from the Einstein equation, which takes the form,

$$T_{ab} = \frac{1}{4\pi r^2} \frac{dM(v)}{dv} \delta_{va} \delta_{vb}. \quad (4.2.2)$$

The above energy-momentum tensor satisfies the null energy condition if $dM(v)/dv \geq 0$. This is expected as the flow of matter satisfying energy condition increases the black hole mass. Now, one can immediately write down the differential equation governing the evolution of the photon sphere in this spacetime. As anticipated, this equation has no analytical solution possible, and we must resort to numerical techniques. To solve the above second-order differential equation, we require two boundary conditions. For the accreting scenario, we must use future boundary conditions. Throughout this work we shall assume that at late time the black hole settles down to a stationary configuration and we may use the following boundary conditions: (a) $r_{ph}(v_0) = 3M(v_0)$ and (b) $\dot{r}_{ph}(v_0) = 0$, where v_0 is some future time where the mass function approaches a constant value, i.e., $\dot{M}(v_0) = 0$. Moreover, the location of the apparent horizon corresponds to $r_{ap} = 2M(v)$, while event horizon can be determined by solving $(dr/dv) = (1/2)\{1 - (2M(v)/r)\}$ with appropriate future boundary conditions [210].

Having developed the necessary theoretical framework, we want to solve the differential equation for the evolution of the photon sphere, starting with the Vaidya spacetime. To illustrate the evolution explicitly, we focus our attention on smoothly varying mass functions. For that matter, we begin with the following choice,

$$M(v) = \frac{M_0}{2} \{1 + \tanh(v)\}, \quad (4.2.3)$$

The above mass function approaches to a constant value M_0 , in the asymptotic future ($v \rightarrow \infty$) and as a result one can impose the future boundary conditions $r_{ph}(v \rightarrow \infty) = 3M_0$ and $\dot{r}_{ph}(v \rightarrow \infty) = 0$, which uniquely determines the evolution of the photon sphere. Similarly, we can also study the behaviour of the event and apparent horizon in Vaidya spacetime. We have depicted these results in Fig. 4.1. As evident, the photon sphere radius along with the event and apparent horizon increases initially and approaches to constant values at asymptotic time. Also, the apparent horizon, in the dynamical context, lies within the event horizon and ultimately coincides with the event horizon.

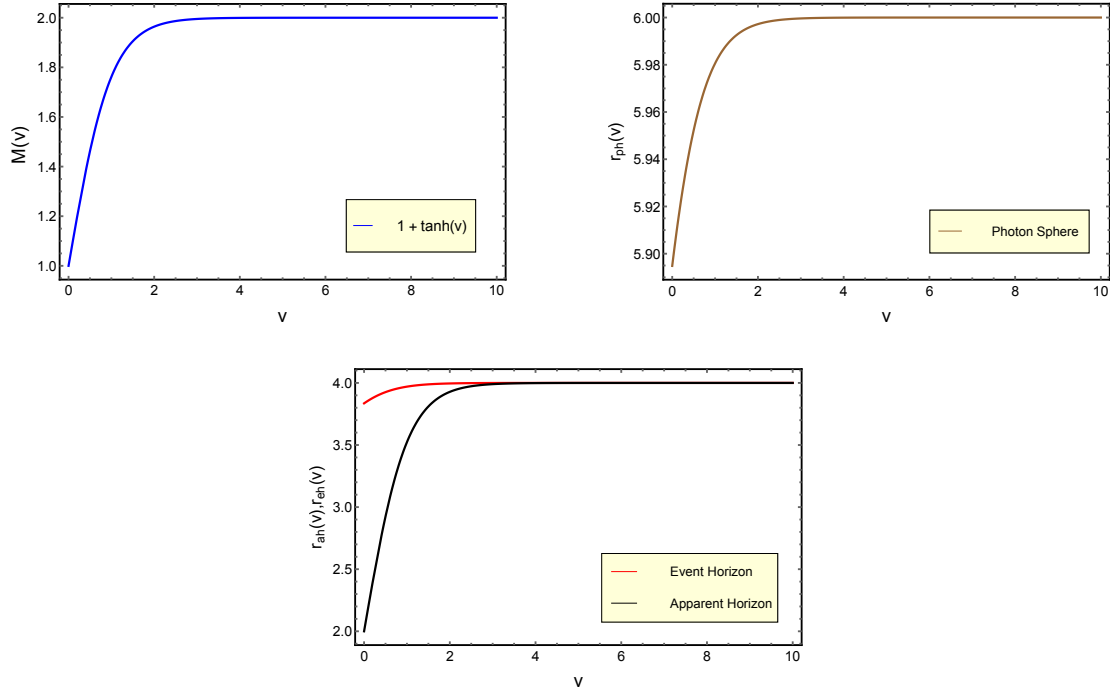


FIGURE 4.1: Evolution of the radius of the photon sphere (top right), event, and apparent horizon (bottom) as a function of the in-going time (v) has been presented for the mass function (top left) written down in Eq. (4.2.3).

To further grasp the theoretical result derived earlier, we have considered a few other examples of smoothly increasing mass functions, e.g., $M(v) = (M_0/2)\{2 - \text{sech}(v)\}$, which asymptotically approaches M_0 . Imposing the future boundary conditions $r_{ph}(v \rightarrow \infty) = 3M_0$ and $\dot{r}_{ph}(v \rightarrow \infty) = 0$ in Eq. (4.1.2), we can obtain the corresponding evolution of the photon sphere. We illustrate the result for the mass function presented above along with some other mass functions in Fig. 4.2. As one would expect, the photon sphere radius in all these case initially increases and finally settles down to a constant radius $3M_0$.

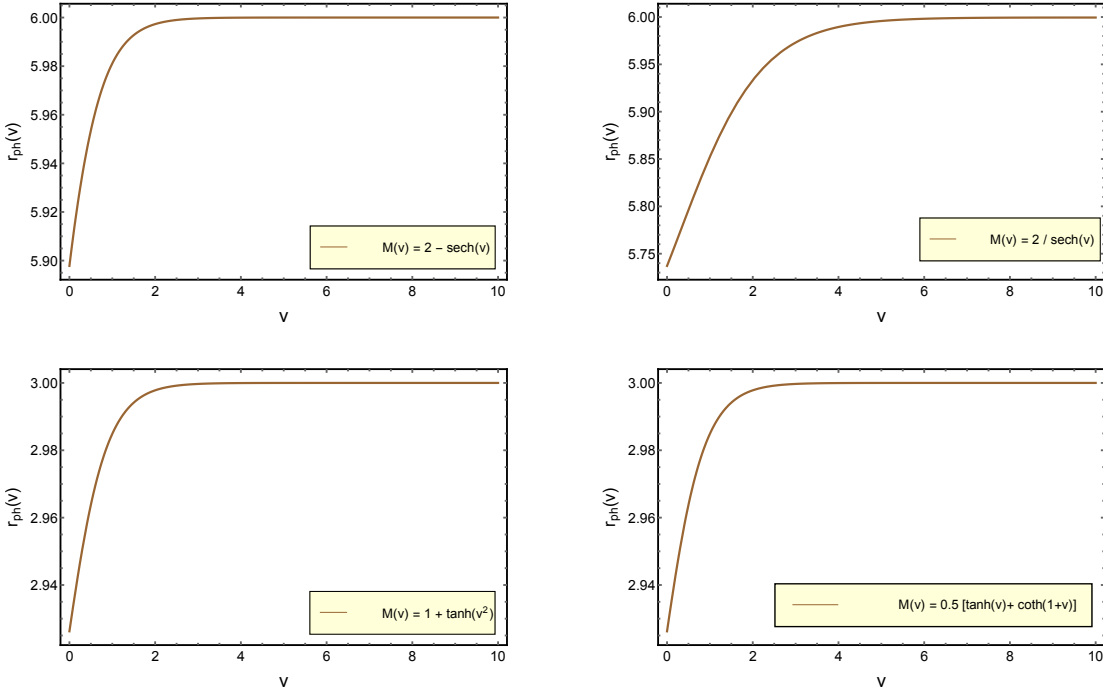


FIGURE 4.2: This figure shows the evolution of the photon sphere for $M(v) = M_0\{2 - \text{sech}(v)\}$ (top left), $M(v) = 2/\{1 + \text{sech}(v)\}$ (top right), $M(v) = 1 + \tanh(v^2)$ (bottom left) and $M(v) = 0.5\{\tanh(v) + \coth(1+v)\}$ (bottom right) respectively.

Now let us consider the case of a black hole that is radiating matter, which can be modelled by a smoothly decreasing mass function. It is important to emphasize that such a process doesn't occur classically since the black hole evaporation is a quantum process. However, to understand the evolution of the photon sphere in such a scenario, we can model the radiating black hole spacetime by a smoothly decreasing mass function without worrying about the underlying quantum mechanical phenomenon. We can obtain the evolution of the photon sphere radius by solving Eq. (4.1.4), but this time with a past boundary condition, i.e., one assumes the black hole to be static to start with. One such radiating mass function takes the following form,

$$M(u) = \left(\frac{M_0}{2}\right) [1 - \tanh(u)] \quad (4.2.4)$$

The black hole starts with a constant value of mass, M_0 in the far past (denoted by $u \rightarrow -\infty$) and allows one to impose past boundary conditions $r_{\text{ph}}(u \rightarrow -\infty) = 3M_0$ and $\dot{r}_{\text{ph}}(u \rightarrow -\infty) = 0$, to obtain the evolution of the photon sphere. We illustrate this result along with the evolution of the event horizon and apparent horizon in Fig. 4.3. As expected, all the radii start with some initial values and decrease as the black hole radiates matter. This is expected, as the size of the photon sphere must decrease as the mass function decreases. In the next section, we shall extend this result to a Reissner-Nordström-Vaidya spacetime, involving a time-dependent mass and charge function.

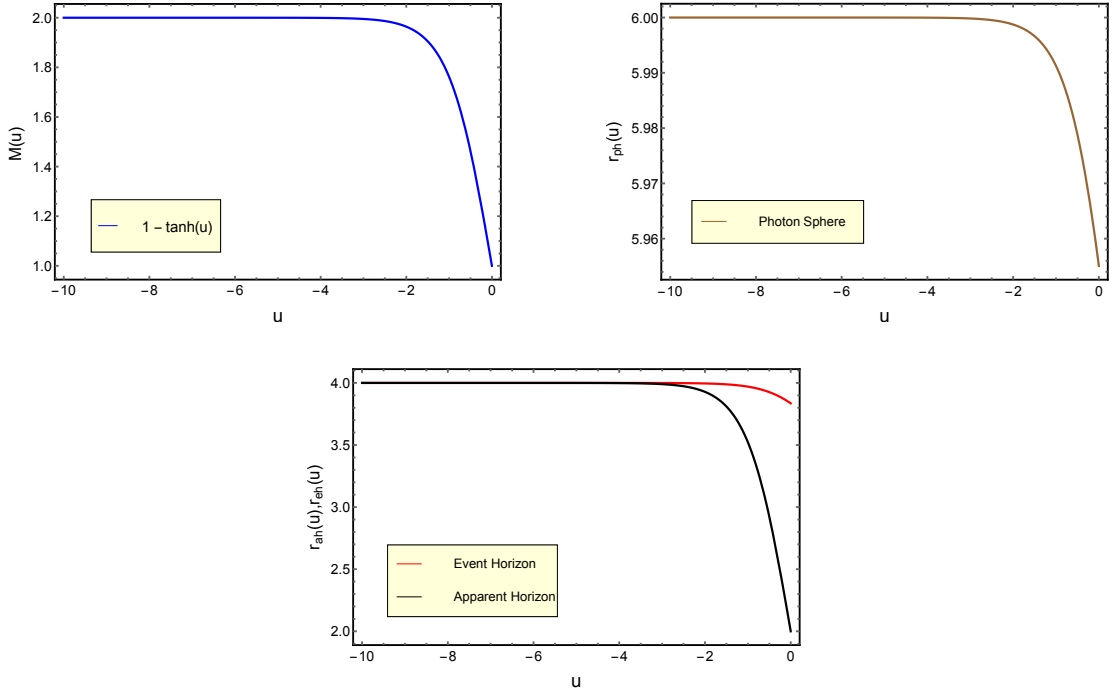


FIGURE 4.3: In this figure we have demonstrated the evolution of the photon sphere as function of the outgoing time u for the mass profile Eq. (4.2.4). The top left panel shows the variation of the mass function with u , while that on the top right panel shows the evolution of the radius of the photon sphere. We have also plotted the event and apparent horizon in the bottom panel.

4.2.2 Reissner-Nordström-Vaidya Space-time

Having understood the evolution of the photon sphere in the context of Vaidya spacetime, we shall now turn our attention to black holes with time-dependent charge and mass, i.e., the Reissner-Nordström-Vaidya spacetime. A physical scenario where this may arise is in the case of a black hole accreting both mass and charge. In this case, it is more natural to describe the black hole in the in-going coordinate, in which the spacetime geometry is given by Eq. (4.1.1), with the following identifications,

$$f(r, v) = 1 - \frac{2M(v)}{r} + \frac{Q(v)^2}{r^2}, \quad A_v = \frac{Q(v)}{r}. \quad (4.2.5)$$

where $M(v)$ and $Q(v)$ represents the mass and charge profile, with A_v being $U(1)$ gauge field. In this case, besides the Maxwell field, the energy-momentum tensor also receives an additional contribution from the matter sector, which is of the form,

$$8\pi T_{\mu\nu}^{\text{ext}} = \frac{1}{r^3} \{2r \dot{M}(v) - 2Q(v)\dot{Q}(v)\} \delta_\mu^v \delta_\nu^v. \quad (4.2.6)$$

As evident the above energy-momentum tensor is associated with some sort of charged null fluid and it obeys the null energy condition, i.e., $T_{\mu\nu}^{\text{ext}} k^\mu k^\nu \geq 0$ for the null vector $k^\mu = (\partial/\partial v)^\mu$ if the following condition holds [212].

$$2r \dot{M}(v) - 2Q(v)\dot{Q}(v) \geq 0, \quad (4.2.7)$$

Clearly the null energy condition is obeyed for all $r \geq (Q\dot{Q}/\dot{M}) \equiv r_{\text{cs}}$, where r_{cs} denotes the critical surface within which the Null Energy Condition may get violated. Thus for such spacetime, where Eq. (4.2.7) is not satisfied, there exist regions where the null energy condition is violated as well.

Hawking's area theorem suggests that the radius of the event horizon decreases when the infalling matter violates the null energy condition. Therefore, in the presence of a critical surface r_{cs} , this essentially boils down to the question of whether the event horizon lies inside or outside the critical surface and it would evolve accordingly. One can also choose the mass and charge function so that the critical surface crosses the event horizon at some value of the in-going null time. In such situations, one would expect the event horizon to increase first and later decrease when the critical surface crosses it. Interestingly, it turns out that the evolution of the photon sphere is also affected by the violation of the null energy condition. We will explicitly demonstrate this interesting phenomenon in this section. In particular, we will show that the evolution of the photon sphere is related to the location of the critical surface. Therefore, since an external observer can probe the photon spheres, it may possibly provide observational evidence of the violation of the null energy condition, if any.

Having described the necessary technical details, now let us study the evolution of the photon sphere by considering various mass and charge function. As discussed previously, we restrict our attention to smoothly varying mass and charge profiles. Our choice of mass and charge functions are particularly motivated from [212] and in addition, we have studied some different mass and charge functions as well. One can consider the following choice,

$$M(v) = \frac{M_0}{2} \left[1 + \frac{1}{2} \{1 + \tanh(v)\} \right] \quad \text{and} \quad Q(v) = Q_0 \{1 - \tanh(v)\} \quad (4.2.8)$$

By substituting the above mass and charge functions in Eq. (4.2.7), we can see that the null energy condition is satisfied for arbitrary choices of M_0 and Q_0 . As a result, the critical surface doesn't exist in this case. This, in turn, implies that the photon sphere along with the apparent and the event horizon smoothly increases. Now one can impose the future boundary conditions $r_{\text{ph}}(v \rightarrow \infty) = (1/2)(3M_0 + \sqrt{9M_0^2 - 8Q_0^2})$ and $\dot{r}_{\text{ph}}(v \rightarrow \infty) = 0$ to solve the differential equation for the photon sphere radius. The evolution of the photon sphere associated with the above mass and charge functions along with boundary conditions have been presented in Fig. 4.4.

For completeness, let us consider another situation in which both the mass and charge function, namely $M(v)$ and $Q(v)$, are such that there exists a critical surface but lies within the event horizon. In this case, the critical surface and consequently the violation of the null energy condition can not be probed by an external observer. This can be achieved by the following choice of mass and charge profile,

$$M(v) = \frac{M_0}{2} [1 + \tanh(v)] \quad \text{and} \quad Q(v) = Q_0 M(v)^{2/3} \quad (4.2.9)$$

Again, we solve the differential equation presented in Eq. (4.1.2) using the future boundary conditions to obtain the evolution of the photon sphere, and the result is illustrated in Fig. 4.5. The presence of a critical surface is evident from Fig. 4.5; however, it remains within the event horizon. In this case, the radius of the photon sphere, along with the event and apparent horizon increases.

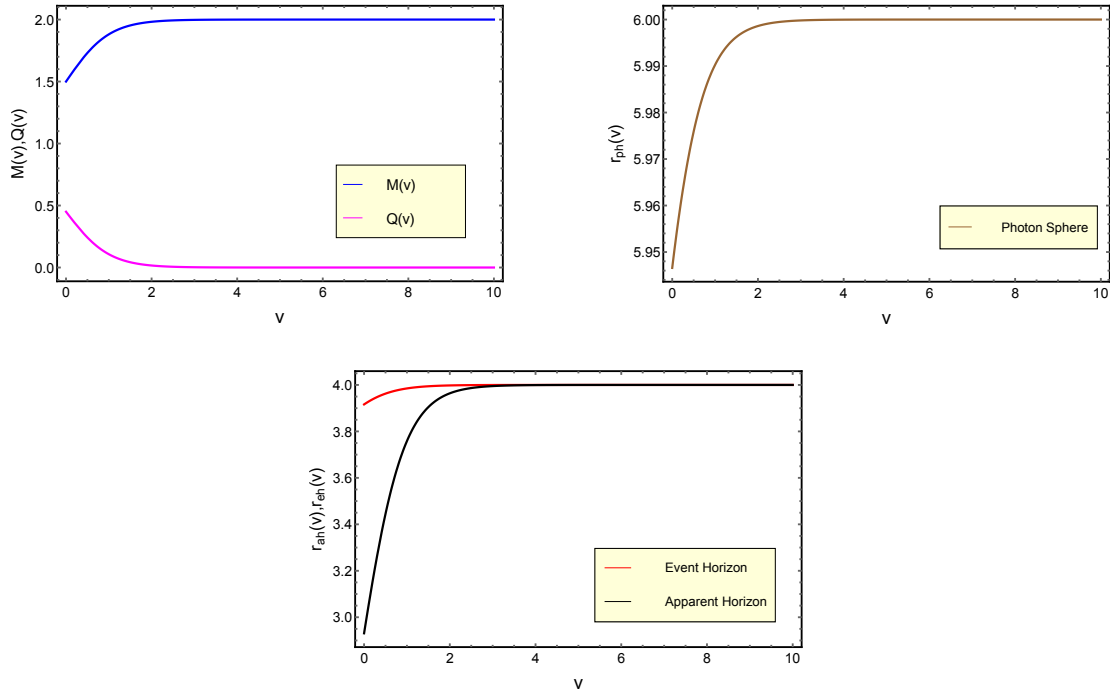


FIGURE 4.4: In this figure we have depicted the mass and charge function (top left), evolution of the photon sphere (top right) and the event and apparent horizon (bottom) for the choice of Eq. (4.2.8).

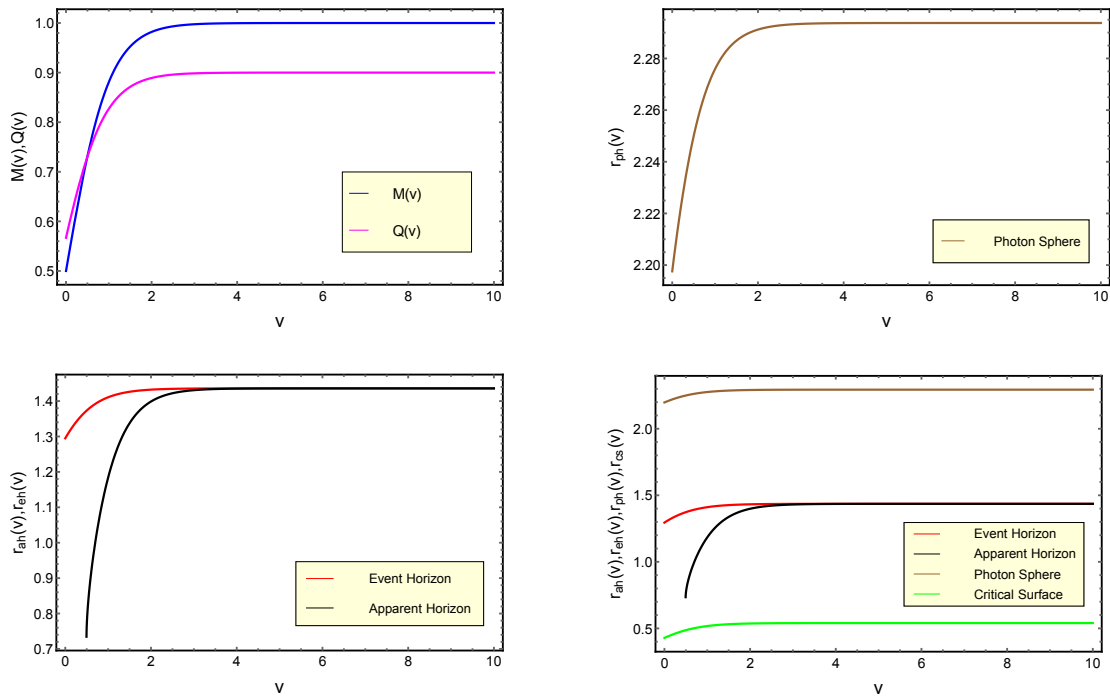


FIGURE 4.5: The top left panel shows the mass and charge function. The top right panel shows the evolution of the radius of photon sphere . In the bottom left panel, we've plotted the evolution of event horizon and apparent horizon . The bottom right panel shows the evolution of photon sphere , apparent horizon , event horizon and critical surface together for the choice of mass and charge profile in Eq. (4.2.9)

Now let us consider a situation where the critical surface lies completely outside the photon sphere and can be probed by an exterior observer. In this case, both the photon sphere and the event horizon decreases as they evolve. This is because both of the surfaces lie in a region where the null energy condition is violated. This can be achieved by choosing both $M(v)$ and $Q(v)$ to be proportional to $1 + \tanh(v)$, as given in Fig. 4.6. We have illustrated this particular case in Fig. 4.6. The photon sphere, along with the event and apparent horizon, decreases with the advanced null coordinate v for certain choices of the mass and charge function, which is also evident from Fig. 4.6.

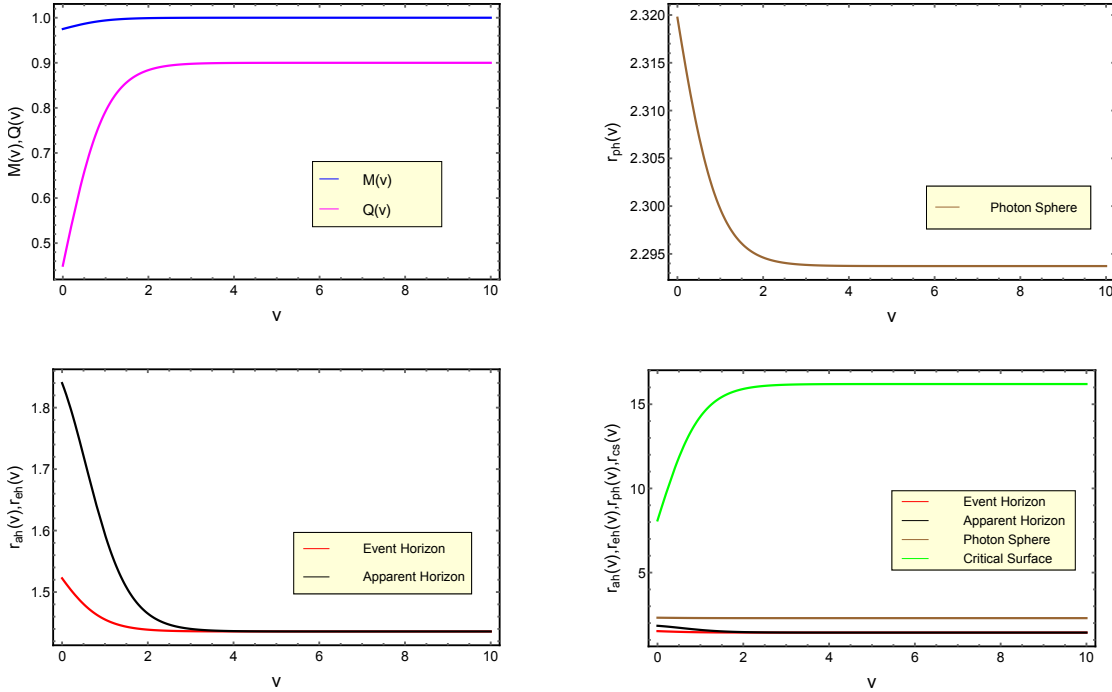


FIGURE 4.6: In this figure we have illustrated the evolution of photon sphere, event horizon and apparent horizon for the following mass and charge functions: $M(v) = 0.95 + (0.05/2)\{1 + \tanh(v)\}$ and $Q(v) = (0.9/2)\{1 + \tanh(v)\}$ (top left panel). The top right panel shows the evolution of the radius of photon sphere, while the bottom left panel shows the evolution of both the event horizon and the apparent horizon . Finally, the bottom right panel presents the evolution of the photon sphere, apparent horizon, event horizon, and critical surface together for the above choice of mass and charge functions.

In the previous examples we have considered, the location of the critical surface was such that the photon sphere and the event horizon were either completely outside or inside the critical surface. It is certainly possible to come up with certain $M(v)$ and $Q(v)$, such that the critical surface initially starts being within the event horizon and eventually crosses both event horizon and the photon sphere. In this case, one would expect the event horizon first to grow (since null energy condition is satisfied for some time) and eventually starts decreasing. Also, we should expect to observe the teleological property of the event horizon in this case [210], i.e., to see the event horizon decreasing even before it crosses the critical surface. An identical result can also be seen for the photon sphere, i.e., initially, it grows for some time and then starts decreasing. We have depicted this result in Fig. 4.7.

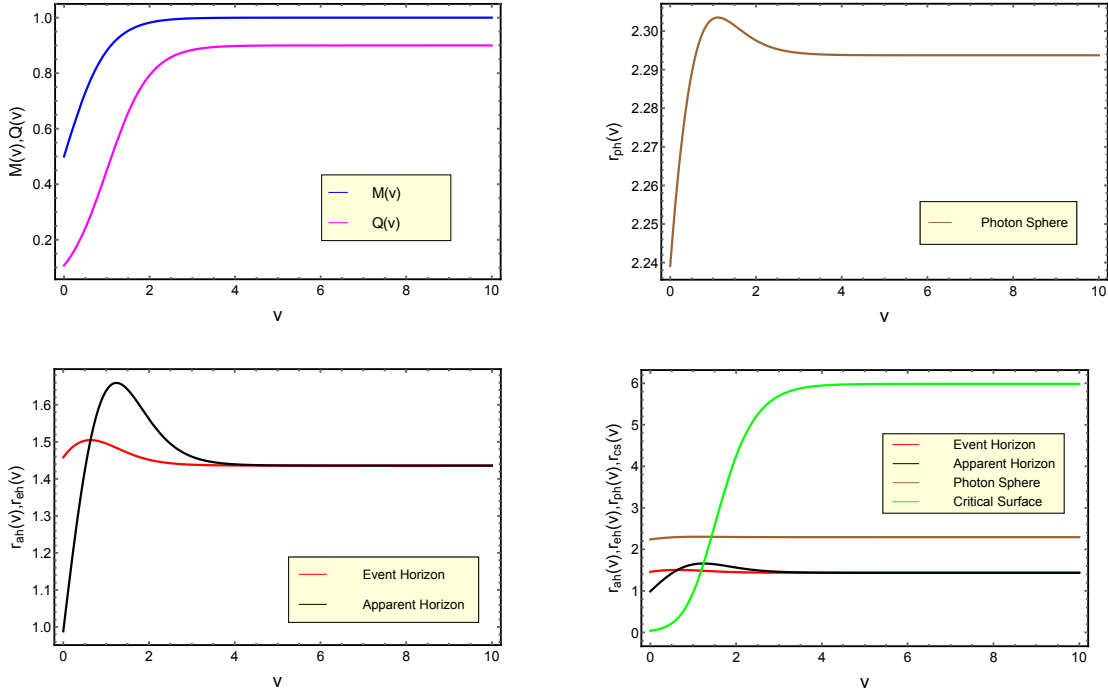


FIGURE 4.7: In the top left panel we show the mass and charge profile ($M(v) = 0.5\{1 + \tanh(v)\}$ and $Q(v) = 0.45\{1 - \tanh(1 - v)\}$) for which the critical surface crosses the photon sphere and event horizon. Further we plot the evolution of the photon sphere, event horizon and apparent horizon separately. It is evident that, the radius of all these surfaces initially increases and later starts to decrease when the critical surface crosses.

As a final illustration of the relation between null energy condition of the external matter and evolution of photon sphere for Reissner-Nordström-Vaidya black holes, let us consider the mass and charge function such that the critical surface crosses the event horizon, but not the photon sphere. We choose the mass and charge functions to be $M(v) = 0.5\{1 + \tanh(v)\}$ as well as $Q(v) = 0.3\{1 - \tanh(1 - v)\}$ respectively. As demonstrated in Fig. 4.8, the critical surface initially starts within the event horizon and eventually crosses it. As a result, the event horizon grows for some time and then decreases. However, the critical surface for this case doesn't cross the photon sphere at any point in the future. Hence the photon sphere lies in a region where the null energy condition is always satisfied. Therefore the photon sphere can not probe this violation and always increases. This result is illustrated in Fig. 4.8.

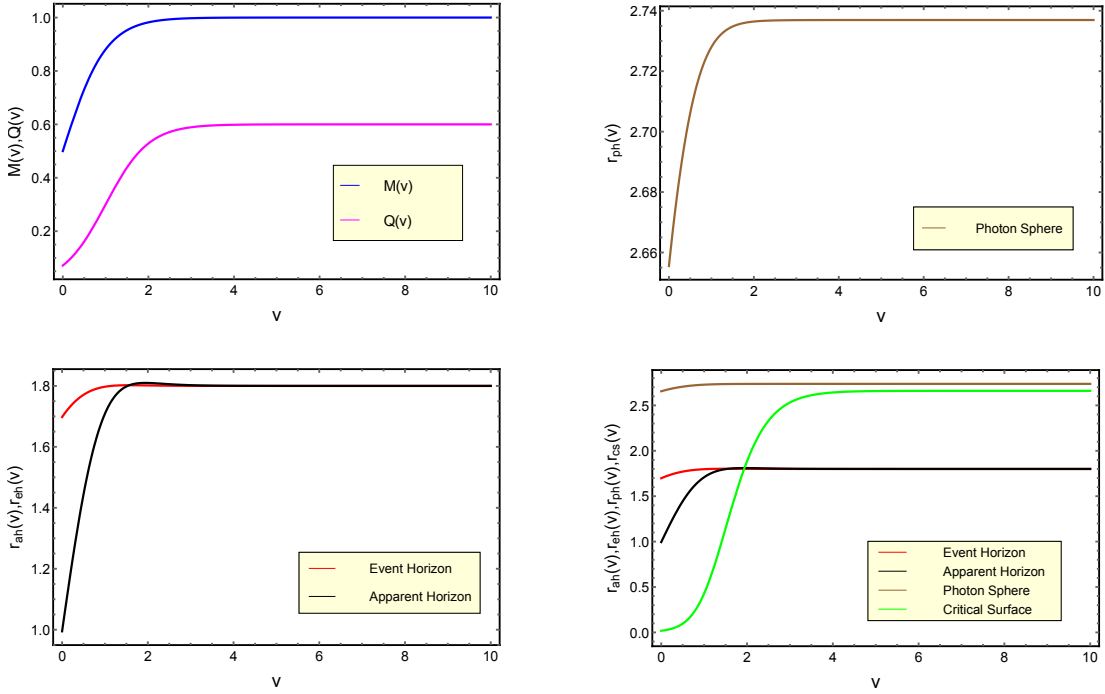


FIGURE 4.8: In the top left panel we have shown the mass and charge functions $M(v) = 0.5\{1 + \tanh(v)\}$ as well as $Q(v) = 0.3\{1 - \tanh(1 - v)\}$ as a function of the advanced null coordinate v . The evolution of photon sphere is depicted in the top right panel. In the bottom left panel we have plotted the evolution of event horizon and apparent horizon, while the bottom right panel shows the evolution of photon sphere, apparent horizon, event horizon and critical surface together.

4.2.3 Schwarzschild-de Sitter Spacetime

Finally, let us employ the method developed in Section 4.1 of this chapter to study the evolution of photon sphere around a black hole in the presence of a positive cosmological constant, with its mass being a function of time. The metric structure is identical to Eq. (4.1.1), with $f(r, v) = 1 - \{2M(v)/r\} + (\Lambda/3)r^2$. Note that, for the static case with constant mass, the radius of the photon sphere doesn't depend on the cosmological constant [213]. Therefore, it would be interesting to look for any effect of the cosmological constant on the photon sphere in the dynamical case. To our surprise, it turns out that for a dynamical Schwarzschild-de Sitter black hole, i.e., for black hole mass changing with time, the evolution of the photon sphere indeed depends on the value of the cosmological constant Λ . Again, an analytic solution for the evolution of the photon sphere turns out to be difficult to achieve. We can solve the equation numerically and obtain the evolution of the photon sphere for suitable choices of mass functions.

As an example of the Schwarzschild de Sitter black hole accreting matter, we consider the mass to be a smoothly increasing function of the in-going time v and using which we solve Eq. (4.1.2) to obtain the evolution of the photon sphere for different values of the cosmological constant. We take the mass functions $M(v) = (M_0/2)\{1 + \tanh(v)\}$ and $M(v) = (M_0/2)\{2 - \operatorname{sech}(v)\}$ and impose the future boundary conditions, $r_{ph}(v \rightarrow \infty) = 3M_0$ and $\dot{r}_{ph}(v \rightarrow \infty) = 0$. We illustrate this result in Fig. 4.9 for different choices of the cosmological constant Λ .

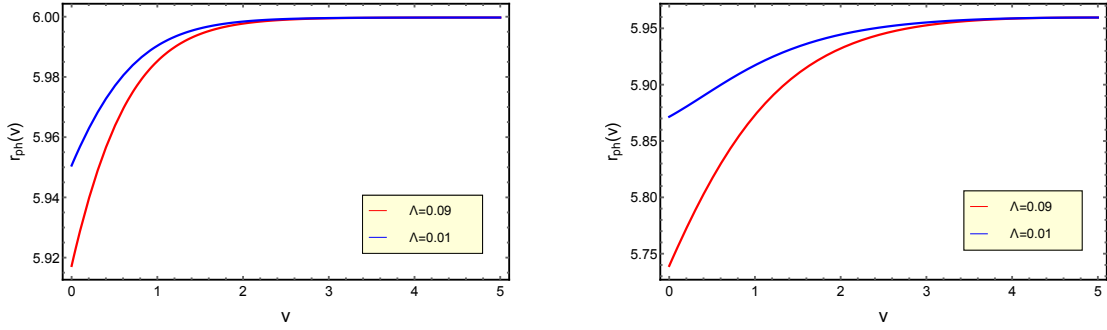


FIGURE 4.9: In this figure we have shown the evolution of the photon sphere for dynamical Schwarzschild de Sitter spacetime. The mass functions are chosen to be $M(v) = M_0\{1 + \tanh(v)\}$ (left panel) and $M(v) = M_0\{2 - \text{sech}(v)\}$ (right panel) with $M_0 = 1$.

This is an interesting result since, unlike the static scenario, the photon sphere in the dynamical case explicitly depends on the choice of the cosmological constant. Moreover, black holes are never in perfect equilibrium. Thus, a dynamical study of the photon sphere can be considered as an effective tool to explore the value of the cosmological constant of the universe. This result also extends to Reissner-Nordström -de Sitter black hole as well with a time-dependent charge.

4.3 Shadow of a Spherically Symmetric Dynamical Black Hole

In the previous section, we have studied the dynamical evolution of the photon sphere in the context of several spherically symmetric black hole spacetimes. Now we want to understand the dynamics of shadow around such black holes. The existence of shadow is an immediate consequence of the presence of circular photon orbits. Therefore, the evolution of the photon sphere would be ultimately reflected in the dynamics of shadow. In this section, we shall illustrate the time evolution of shadow around a spherically symmetric black hole as the mass and/or charge of the black hole varies with time. We start by presenting a detailed calculation of the equation that governs the time evolution of shadow in the in-going null coordinate v with an arbitrary choice of $f(r, v)$. Later we demonstrate our result for the particular cases of Schwarzschild Vaidya and Reissner-Nordström-Vaidya spacetimes. This can also be generalized in a simple manner to the case of out-going null coordinate u . In the next section, we generalize this result to slowly rotating black holes. The geometry of the spacetime we are interested in is given by Eq. (4.1.1) in which the motion of a test particle is described by the following Lagrangian,

$$\mathcal{L} = \frac{1}{2} \left\{ -f(r, v) \left(\frac{dv}{d\lambda} \right)^2 + 2 \left(\frac{dv}{d\lambda} \right) \left(\frac{dr}{d\lambda} \right) + r^2 \left(\frac{d\theta}{d\lambda} \right)^2 + r^2 \sin^2 \theta \left(\frac{d\phi}{d\lambda} \right)^2 \right\} \quad (4.3.1)$$

As mentioned previously, a ‘prime’ and ‘dot’ denotes differentiation with respect to the radial coordinate r and the in-going time v , respectively. The Lagrangian is independent of the azimuthal coordinate ϕ but depends on the in-going null coordinate v . As a result, the angular momentum of the particle is conserved while the energy is not. However, we can still define a quantity $E(r, v)$, such that,

$$E(r, v) = -f(r, v) \left(\frac{dv}{d\lambda} \right) + \left(\frac{dr}{d\lambda} \right) \quad \text{and} \quad L = r^2 \sin^2 \theta \left(\frac{d\phi}{d\lambda} \right) \quad (4.3.2)$$

From these two equations, one can obtain $dv/d\lambda$ and $d\phi/d\lambda$ in terms of $E(r, v)$ and L , which leads to the following expressions,

$$\left(\frac{dv}{d\lambda}\right) = \frac{1}{f(r, v)} \left\{ \left(\frac{dr}{d\lambda}\right) - E(r, v) \right\} \quad \text{and} \quad \left(\frac{d\phi}{d\lambda}\right) = \frac{L}{r^2 \sin^2 \theta} \quad (4.3.3)$$

Also, for photons we have $ds^2 = 0$, which implies vanishing of the Lagrangian ' \mathcal{L} ' in Eq. (6.2.3) and using the above expressions for $(dr/d\lambda)$ and $(d\theta/d\lambda)$ one can finally obtain,

$$r^2 \left(\frac{dr}{d\lambda}\right)^2 - r^2 E^2(r, v) + r^4 \left(\frac{d\theta}{d\lambda}\right)^2 f(r, v) + \frac{L^2 f(r, v)}{\sin^2 \theta} = 0 \quad (4.3.4)$$

The radial and the angular part of the above equation separates out naturally, which is basically achieved by introducing the Carter Constant K [100], such that the evolution equations for θ and r becomes,

$$r^4 \left(\frac{d\theta}{d\lambda}\right)^2 = K - \cot^2 \theta L^2; \quad r^2 \left(\frac{dr}{d\lambda}\right)^2 = E^2 r^2 - (K + L^2) f(r, v). \quad (4.3.5)$$

Let us recall that, for the static case one has $r = \text{constant} = r_{\text{ph}}$ and hence $dr_{\text{ph}}/d\lambda = 0$. This would further give rise to the shadow radius of static spherically symmetric black holes. However, since we are considering dynamical situations, we have $r = r_{\text{ph}}(v)$ and hence $(dr_{\text{ph}}(v)/d\lambda) = \dot{r}_{\text{ph}}(v) \{dv/d\lambda\}$. Then using Eq. (4.3.3) we obtain,

$$K + L^2 = \frac{E(r_{\text{ph}}(v), v)^2 r_{\text{ph}}(v)^2}{f(r_{\text{ph}}(v), v)} \left[1 - \left\{ \frac{\dot{r}_{\text{ph}}(v)}{f(r_{\text{ph}}(v), v) - \dot{r}_{\text{ph}}(v)} \right\}^2 \right] \quad (4.3.6)$$

where we have defined $\eta(v) \equiv K/E(r_{\text{ph}}(v), v)^2$ and $\xi(v) \equiv L/E(r_{\text{ph}}(v), v)$ and the above equation reduces to,

$$\eta(v) + \xi(v)^2 = \alpha(v)^2 + \beta(v)^2 = \frac{r_{\text{ph}}(v)^2}{f(r_{\text{ph}}(v), v)} \left[1 - \left\{ \frac{\dot{r}_{\text{ph}}(v)}{f(r_{\text{ph}}(v), v) - \dot{r}_{\text{ph}}(v)} \right\}^2 \right] \quad (4.3.7)$$

We have expressed the shadow in terms of the celestial coordinates α and β that span the two-dimensional celestial plane perpendicular to the line of sight with respect to the observer and defined at spatial infinity [87]. More precisely, each ray of light reaching the observer from the distant source corresponds to a point (α_0, β_0) in the celestial plane. The complement of these set of points in the celestial plane defines the shadow. For consistency, one might check that in the static limit, i.e., $\dot{r}_{\text{ph}} = 0$, we recover the expression of shadow around the static black hole. For a Schwarzschild black hole (Eq. (1.1.2)) it reduces to $\alpha(v)^2 + \beta(v)^2 = 27 M^2$ In Fig. 4.10, we have presented an illustration of the dynamics of shadow radius in the context of Schwarzschild-Vaidya and Reissner-Nordström-Vaidya black holes for various choices of mass and charge function.

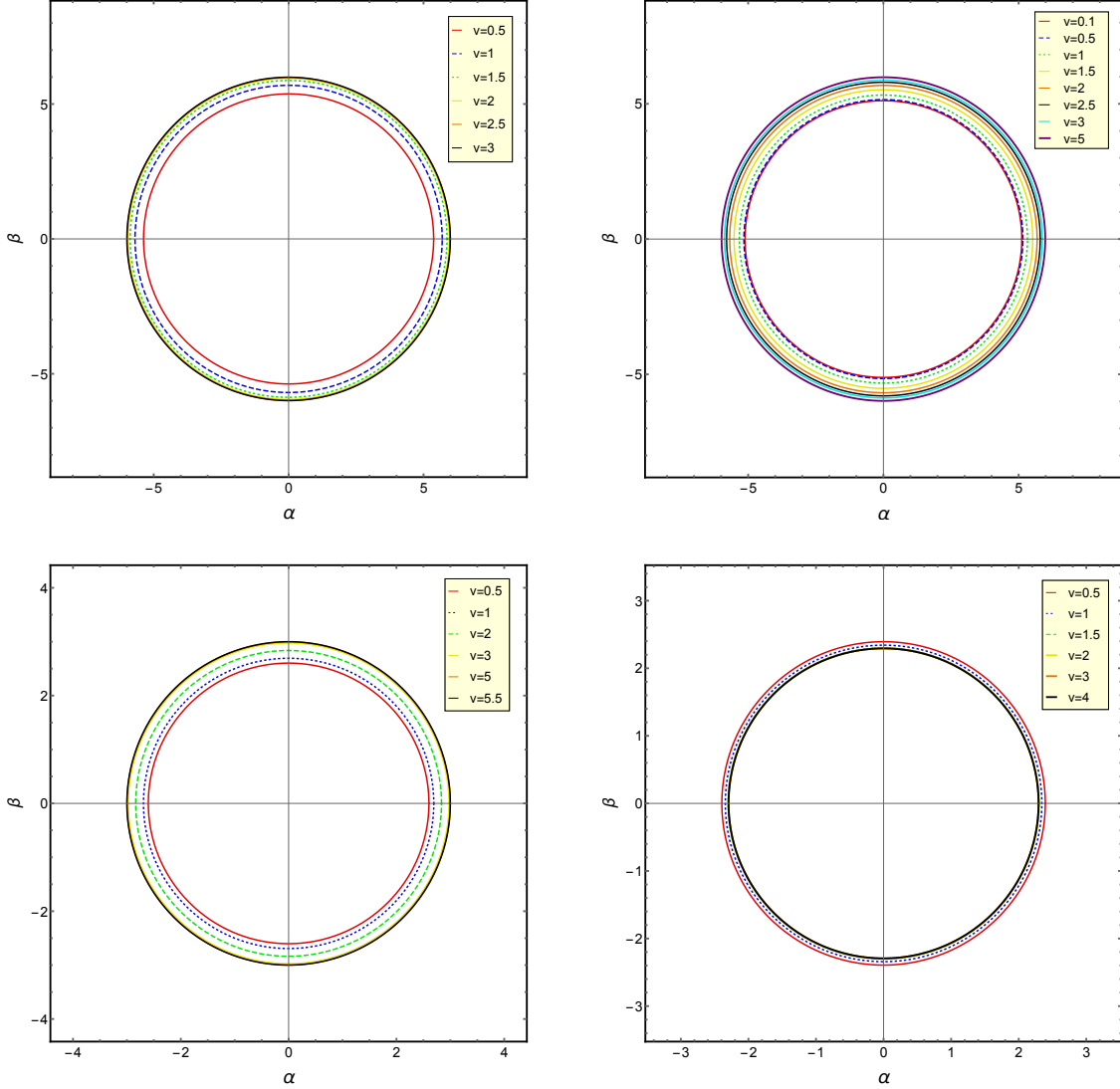


FIGURE 4.10: In this figure we demonstrate the time evolution of shadow around a spherically symmetric dynamical spacetime w.r.t various mass and charge functions. The top left and right panel are for mass functions $1 + \tanh(v)$, $2 - \text{sech}(v)$. In the bottom left panel we've shown the evolution of shadow for $M(v) = 0.5[1 + \tanh(v)]$, $Q(v) = \frac{0.9}{2}[\tanh(v) - \tanh(v - 1)]$. The bottom right panel shows the evolution of shadow for $M(v) = 0.95 + \frac{0.05}{2}[1 + \tanh(v)]$, $Q(v) = \frac{0.9}{2}[1 + \tanh(v)]$.

4.4 Kerr-Vaidya in the Slow Rotation Limit

In this section, we would like to understand the evolution of the circular photon orbit as well as that of black hole shadow for a dynamical black hole with rotation. In particular, we shall study the Kerr-Vaidya metric. However, a general computation is difficult in this case, since the radial and angular part in the Hamilton-Jacobi equation does not separate. This is because the Kerr-Vaidya spacetime admits only one Killing vector field, related to the angular coordinate ϕ . This prompts us to consider the slow rotation limit [214], where such a separation is achievable. Under this assumption, we will discuss the evolution of the circular photon orbit and the nature of the shadow it casts.

4.4.1 Evolution of Photon Circular Orbit

This section aims to provide the desired equation governing the dynamics of the photon sphere on the equatorial plane for Kerr-Vaidya spacetime. As discussed earlier, it is difficult to determine the governing differential equation for arbitrary values of rotation parameter since the Hamilton-Jacobi equation does not separate. Therefore, here we shall concentrate on the situation in which the rotation parameter is constant and small so that terms of $\mathcal{O}(a^2)$ can be neglected. In this approximation, the Kerr-Vaidya metric on the equatorial plane takes the following form [214],

$$ds^2 = - \left(1 - \frac{2M(v)}{r}\right) dv^2 + 2dv dr - 2a dr d\phi - \frac{4M(v)a}{r} dv d\phi + r^2 d\phi^2. \quad (4.4.1)$$

For the equatorial plane, we have substituted $\theta = \pi/2$ in the general form of the metric to arrive at Eq. (4.4.1). Also, since we are interested in null trajectories, we start by setting $ds^2 = 0$. This results in the following differential equation,

$$r^2 \left(\frac{d\phi}{dv}\right)^2 + \left(\frac{d\phi}{d\phi}\right) \left\{ -2a \left(\frac{dr}{dv}\right) - \frac{4M(v)a}{r} \right\} + 2 \left(\frac{dr}{dv}\right) - \left(1 - \frac{2M(v)}{r}\right) = 0. \quad (4.4.2)$$

The above result holds for any null trajectory, geodesic or not. However, we are interested in the null geodesics on the equatorial plane of the Kerr-Vaidya solution, for which it is important to write down the corresponding Lagrangian, which takes the following form,

$$\begin{aligned} L = & -\frac{1}{2} \left\{ 1 - \frac{2M(v)}{r} \right\} \left(\frac{dv}{d\lambda}\right)^2 + \left(\frac{dv}{d\lambda}\right) \left(\frac{dr}{d\lambda}\right) - a \left(\frac{dr}{d\lambda}\right) \left(\frac{d\phi}{d\lambda}\right) \\ & - \frac{2M(v)a}{r} \left(\frac{dv}{d\lambda}\right) \left(\frac{d\phi}{d\lambda}\right) + \frac{1}{2} r^2 \left(\frac{d\phi}{d\lambda}\right)^2 \end{aligned} \quad (4.4.3)$$

Where λ denotes the affine parameter along the null geodesics. From the above Lagrangian, one can immediately obtain the following geodesic equations,

$$\frac{d^2v}{d\lambda^2} - a \frac{d^2\phi}{d\lambda^2} = -\frac{1}{r^2} M(v) \left(\frac{dv}{d\lambda}\right)^2 + \frac{2aM(v)}{r^2} \left(\frac{dv}{d\lambda}\right) \left(\frac{d\phi}{d\lambda}\right) + r \left(\frac{d\phi}{d\lambda}\right)^2 \quad (4.4.4)$$

$$\begin{aligned} \frac{d^2r}{d\lambda^2} - \left(1 - \frac{2m(v)}{r}\right) \frac{d^2v}{d\lambda^2} - \frac{2aM(v)}{r} \frac{d^2\phi}{d\lambda^2} = & -\frac{1}{r} \frac{dM}{dv} \left(\frac{dv}{d\lambda}\right)^2 + \frac{2M(v)}{r^2} \left(\frac{dv}{d\lambda}\right) \left(\frac{dr}{d\lambda}\right) \\ & - \frac{2M(v)a}{r^2} \left(\frac{dr}{d\lambda}\right) \left(\frac{d\phi}{d\lambda}\right) \end{aligned} \quad (4.4.5)$$

$$r^2 \frac{d^2\phi}{d\lambda^2} - a \frac{d^2r}{d\lambda^2} - \frac{2M(v)a}{r} \frac{d^2v}{d\lambda^2} = \frac{2a}{r} \frac{dM}{dv} \left(\frac{dv}{d\lambda} \right)^2 - \frac{2M(v)a}{r^2} \left(\frac{dv}{d\lambda} \right) \left(\frac{dr}{d\lambda} \right) - 2r \left(\frac{dr}{d\lambda} \right) \left(\frac{d\phi}{d\lambda} \right) \quad (4.4.6)$$

Recall that, our aim is to construct a differential equation involving double derivative of the radial coordinate r with respect to the in-going null coordinate v , which will not involve terms like $\ddot{\phi}$. So, we first eliminate terms involving $(d^2r/d\lambda^2)$ in Eq. (4.4.5) and Eq. (4.4.6) to arrive at,

$$-a \frac{d^2v}{d\lambda^2} + \left(r^2 - \frac{2M(v)a^2}{r} \right) \frac{d^2\phi}{d\lambda^2} - \frac{a}{r} \frac{dM}{dv} \left(\frac{dv}{d\lambda} \right)^2 + \left(2r + \frac{2Ma^2}{r^2} \right) \left(\frac{dr}{d\lambda} \right) \left(\frac{d\phi}{d\lambda} \right) = 0 \quad (4.4.7)$$

Further, eliminating $(d^2\phi/d\lambda^2)$ between Eq. (4.4.7) and Eq. (4.4.4), one can finally obtain the following differential equation for $v(\lambda)$ at the lowest order in the rotation parameter,

$$\frac{d^2v}{d\lambda^2} + \frac{M(v)}{r^2} \left(\frac{dv}{d\lambda} \right)^2 - \frac{2M(v)a}{r^2} \left(\frac{dv}{d\lambda} \right) \left(\frac{d\phi}{d\lambda} \right) - r \left(\frac{d\phi}{d\lambda} \right)^2 + \frac{2a}{r} \left(\frac{dr}{d\lambda} \right) \left(\frac{d\phi}{d\lambda} \right) = 0 \quad (4.4.8)$$

From the above equation it is straightforward to read off the expression for $(d^2v/d\lambda^2)$, which as substituted in Eq. (4.4.4), yields,

$$a \frac{d^2\phi}{d\lambda^2} = -\frac{2a}{r} \left(\frac{dr}{d\lambda} \right) \left(\frac{d\phi}{d\lambda} \right) \quad (4.4.9)$$

Finally, we can use both the expressions for $(d^2v/d\lambda^2)$ along with $(d^2\phi/d\lambda^2)$ from Eq. (4.4.8) and Eq. (4.4.9) in order to rewrite Eq. (4.4.5) in the following form,

$$\begin{aligned} \frac{d^2r}{d\lambda^2} &= \left\{ -\frac{M(v)}{r^2} \left(1 - \frac{2M(v)}{r} \right) - \frac{1}{r} \frac{dM}{dv} \right\} \left(\frac{dv}{d\lambda} \right)^2 + \frac{2M}{r^2} \left(\frac{dr}{d\lambda} \right) \left(\frac{dv}{d\lambda} \right) - \frac{2M(v)a}{r^2} \left(\frac{dr}{d\lambda} \right) \left(\frac{d\phi}{d\lambda} \right) \\ &\quad + \frac{2M(v)a}{r^2} \left(1 - \frac{2M(v)}{r} \right) \left(\frac{dv}{d\lambda} \right) \left(\frac{d\phi}{d\lambda} \right) + (r - 2M) \left(\frac{d\phi}{d\lambda} \right)^2 - \frac{2a}{r} \left(\frac{dr}{d\lambda} \right) \left(\frac{d\phi}{d\lambda} \right) \end{aligned} \quad (4.4.10)$$

As required, the above equation does not involves terms like $(d^2v/d\lambda^2)$ or $(d^2\phi/d\lambda^2)$. Now we change the variable of differentiation from the affine parameter λ to the in-going null coordinate v , such that $(d^2r/d\lambda^2) = (dv/d\lambda)^2(d^2r/dv^2) + (dr/dv)(d^2v/d\lambda^2)$. This leads us to the following differential equation for the evolution of the photon sphere ($r_{\text{ph}} = r_{\text{ph}}(v)$) on the equatorial plane,

$$\begin{aligned} \frac{d^2r_{\text{ph}}(v)}{dv^2} &+ \left\{ \frac{M}{r_{\text{ph}}(v)^2} \left(1 - \frac{2M(v)}{r_{\text{ph}}(v)} \right) + \frac{1}{r_{\text{ph}}(v)} \frac{dM}{dv} - \frac{3M}{r_{\text{ph}}(v)^2} \frac{dr_{\text{ph}}(v)}{dv} \right\} \\ &+ \left\{ \frac{4M(v)a}{r_{\text{ph}}(v)^2} \frac{dr_{\text{ph}}(v)}{dv} - \frac{2a}{r_{\text{ph}}(v)} \left(\frac{dr_{\text{ph}}(v)}{dv} \right)^2 + \frac{2a}{r_{\text{ph}}(v)} \left(\frac{dr_{\text{ph}}(v)}{dv} \right) - \frac{2Ma}{r_{\text{ph}}(v)^2} \left(1 - \frac{2M(v)}{r_{\text{ph}}(v)} \right) \right\} \left(\frac{d\phi}{dv} \right) \\ &+ \left\{ r_{\text{ph}}(v) \left(\frac{dr_{\text{ph}}(v)}{dv} \right) - [r_{\text{ph}}(v) - 2M] \right\} \left(\frac{d\phi}{dv} \right)^2 = 0 \end{aligned} \quad (4.4.11)$$

Note that the above equation is not sufficient to determine the dynamics of the photon sphere since the differential equation depends on $(d\phi/dv)$. Thus we need to determine $(d\phi/dv)$ in terms of r and (dr/dv) , which can be derived separately from Eq. (4.4.2). This yields,

$$\frac{d\phi}{dv} = \frac{a}{r_{\text{ph}}(v)^2} \frac{dr_{\text{ph}}(v)}{dv} + \frac{2Ma}{r_{\text{ph}}(v)^3} \pm \frac{1}{r_{\text{ph}}(v)} \sqrt{1 - \frac{2M}{r_{\text{ph}}(v)} - 2 \left(\frac{dr_{\text{ph}}(v)}{dv} \right)} \quad (4.4.12)$$

Furthermore, combining Eq. (4.4.12) and Eq. (4.4.11) and keeping terms up to linear order in the rotation parameter, we finally arrive at the following differential equation of the circular photon orbit in the slow rotation approximation,

$$\begin{aligned} \ddot{r}_{\text{ph}}(v) + \frac{3\dot{r}_{\text{ph}}(v)}{r_{\text{ph}}(v)} + \frac{\dot{M}(v)}{r_{\text{ph}}(v)} - \frac{9M(v)\dot{r}_{\text{ph}}(v)}{r_{\text{ph}}(v)^2} - \frac{2\dot{r}_{\text{ph}}(v)^2}{r_{\text{ph}}(v)} - \frac{1}{r_{\text{ph}}(v)} + \frac{5M(v)}{r_{\text{ph}}(v)^2} - \frac{6M(v)^2}{r_{\text{ph}}(v)^3} \\ \pm \frac{6a}{r_{\text{ph}}(v)^3} \left[\left(2M(v)^2 - M(v)r_{\text{ph}}(v) + 2M(v)r_{\text{ph}}(v)\dot{r}_{\text{ph}}(v) \right) \sqrt{\frac{r_{\text{ph}}(v) - 2M(v) - 2r_{\text{ph}}(v)\dot{r}_{\text{ph}}(v)}{r_{\text{ph}}(v)^3}} \right] \\ + \mathcal{O}(a^2) = 0 \end{aligned} \quad (4.4.13)$$

The above differential equation governs the dynamics of the photon sphere radius on the equatorial plane. This can be numerically solved for various choices of mass functions by imposing future boundary conditions, i.e., at asymptotic infinity, the photon sphere radius must coincide with that of the Kerr black hole. This must hold for both the retrograde orbit and the prograde orbit. Moreover, in the slow rotation limit, one can work out the matter stress tensor responsible for the evolution of the black hole mass with time. This can be obtained by computing Einstein's tensor for the slowly rotating metric (Eq. (4.4.1)), which is of the following form [214],

$$T_{ij} = \frac{\dot{M}}{4\pi r^2} v_i v_j \quad (4.4.14)$$

where $v_i = (1, 0, 0, (3/2)a \sin^2 \theta)$ such that $v_i v^i \sim \mathcal{O}(a^2) \sim 0$. Thus up to $\mathcal{O}(a)$, the Kerr-Vaidya model indeed represents a rotating black hole accreting null fluid and hence just like the Reissner-Nordström-Vaidya spacetime, the evolution of photon sphere in this slowly rotating Kerr-Vaidya geometry is intimately connected to the null energy condition.

To illustrate our result we solve Eq. (4.4.13) numerically by imposing appropriate boundary conditions for various choice of smoothly increasing mass functions. For prograde photon orbits one may set the boundary conditions to be $r_{\text{ph}}(v \rightarrow \infty) = r_-$ and $\dot{r}_{\text{ph}}(v \rightarrow \infty) = 0$, where r_{\mp} correspond to the location of the photon circular orbit for prograde (or, retrograde) motion in stationary context [215, 216]. With these boundary conditions, the evolution of the photon sphere has been depicted in Fig. 4.11.

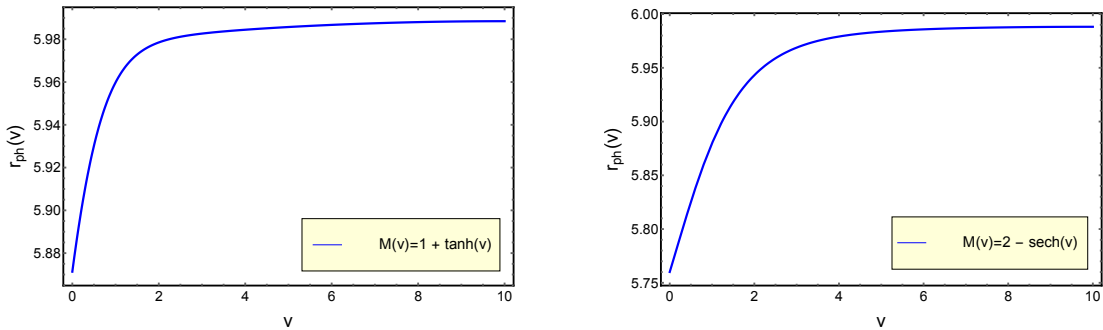


FIGURE 4.11: This figure illustrates the evolution of prograde photon orbits for the choice of mass functions $M(v) = 1 + \tanh(v)$ [left panel] and $M(v) = 2 - \operatorname{sech}(v)$ [right panel]. The rotation parameter 'a' has been chosen to be 0.01.

4.4.2 Shadow Casted by Slowly-Rotating Kerr-Vaidya Black Hole

Having studied the dynamics of photon circular orbit in the previous section, now we move to the shadow of the Kerr Vaidya black hole in the slow rotation limit. As in the spherically symmetric case, here also we start with the Lagrangian of a particle in the Kerr Vaidya spacetime up to $\mathcal{O}(a)$,

$$\mathcal{L} = \frac{1}{2} \left\{ -f(r, v) \left(\frac{dv}{d\lambda} \right)^2 + 2 \left(\frac{dv}{d\lambda} \right) \left(\frac{dr}{d\lambda} \right) - 2a \sin^2 \theta \left(\frac{dr}{d\lambda} \right) \left(\frac{d\phi}{d\lambda} \right) - \frac{4Ma}{r} \sin^2 \theta \left(\frac{dv}{d\lambda} \right) \left(\frac{d\phi}{d\lambda} \right) + r^2 \left(\frac{d\theta}{d\lambda} \right)^2 + r^2 \sin^2 \theta \left(\frac{d\phi}{d\lambda} \right)^2 \right\} \quad (4.4.15)$$

As evident, the above Lagrangian is independent of the azimuthal coordinate ϕ , and as a result, the angular momentum is conserved. However, since we are considering dynamical situations, in general, there is no conserved energy. Still, we can introduce a quantity E , which in this context is dependent on both r and v , such that

$$E(r, v) = \frac{\partial \mathcal{L}}{\partial (dv/d\lambda)} = -f(r, v) \left(\frac{dv}{d\lambda} \right) + \left(\frac{dr}{d\lambda} \right) - \frac{2Ma}{r} \sin^2 \theta \left(\frac{d\phi}{d\lambda} \right) \quad (4.4.16)$$

$$L = \frac{\partial \mathcal{L}}{\partial (d\phi/d\lambda)} = -a \sin^2 \theta - \frac{2Ma}{r} \sin^2 \theta \left(\frac{dv}{d\lambda} \right) + r^2 \sin^2 \theta \left(\frac{d\phi}{d\lambda} \right) \quad (4.4.17)$$

In the static limit, the Lagrangian is independent of v and $E(r, v)$ turns out to be a constant of motion. One can immediately solve Eq. (4.4.16) and Eq. (4.4.17) and obtain $(dv/d\lambda)$ and $(d\phi/d\lambda)$ in terms of $E(r, v)$ and L as,

$$\frac{dv}{d\lambda} = \frac{(dr/d\lambda) - E(r, v)}{f(r, v)} - \frac{2MaL}{f(r, v)r^3} \quad (4.4.18)$$

$$\frac{d\phi}{d\lambda} = \frac{L}{r^2 \sin^2 \theta} + \frac{a}{r^2} \left(\frac{dr}{d\lambda} \right) + \frac{2Ma[(dr/d\lambda) - E(r, v)]}{f(r, v)r^3} \quad (4.4.19)$$

Also for null orbit we have to set $ds^2 = 0$, which consequently results into \mathcal{L} being zero. Then we can substitute Eq. (4.4.18) and Eq. (4.4.19) in the $\mathcal{L} = 0$ equation to express everything in terms of $(dr/d\lambda)$, $(d\theta/d\lambda)$, $E(r, v)$ and L . Hence up to $\mathcal{O}(a)$, we obtain,

$$r^2 \left(\frac{dr}{d\lambda} \right)^2 - r^2 E(r, v) \left[E(r, v) + \frac{4MaL}{r^3} \right] + r^4 f(r, v) \left(\frac{d\theta}{d\lambda} \right)^2 + \frac{f(r, v)L^2}{\sin^2 \theta} = 0 \quad (4.4.20)$$

One can separate the above equation into radial and angular part by introducing the Carter constant K [100], such that the angular part takes the form,

$$r^4 \left(\frac{d\theta}{d\lambda} \right)^2 = K - L^2 \cot^2 \theta \quad (4.4.21)$$

Further, substituting this in Eq. (4.4.20) and re-arranging terms, we obtain the radial equation to be,

$$\left(\frac{dr}{d\lambda} \right)^2 = E(r, v) \left[E(r, v) + \frac{4MaL}{r^3} \right] - \frac{f(r, v)}{r^2} (K + L^2) \quad (4.4.22)$$

In the static limit, for circular orbit one would set $r = r_{\text{ph}}$ and $\dot{r} = 0$. However, in the dynamical case, the photon sphere radius depends on the in-going null coordinate v and we have $r = r_{\text{ph}}(v)$

and hence $(dr/d\lambda) = \dot{r}_{\text{ph}}(v)(dv/d\lambda)$. We can substitute this in Eq. (4.4.18) to obtain the following expression,

$$\left(\frac{dr}{d\lambda}\right)^2 = \frac{E(r_{\text{ph}}, v)^2}{[f(r_{\text{ph}}, v) - \dot{r}_{\text{ph}}(v)]^2} + \frac{4MaL E(r_{\text{ph}}, v)}{r_{\text{ph}}(v)^3 [f(r_{\text{ph}}, v) - \dot{r}_{\text{ph}}(v)]^2} \quad (4.4.23)$$

where we have kept terms up to $\mathcal{O}(a)$. Finally substituting this result in Eq. (4.4.22) we obtain,

$$\frac{f(r_p, v)}{r_p(v)^2} \left\{ \eta + \xi^2 \right\} = 1 + \frac{4Ma}{r_p(v)^3} \xi \left[1 - \frac{\dot{r}_p(v)^2}{[f(r_p, v) - \dot{r}_p(v)]^2} \right] - \frac{\dot{r}_p(v)^2}{[f(r_p, v) - \dot{r}_p(v)]^2} \quad (4.4.24)$$

Just as the spherically symmetric case, here we have introduced two parameters, namely, $\eta = K/E(r, v)^2$ and $\xi = L/E(r, v)$. In terms of the celestial coordinates α and β as introduced in the previous section, the above equation takes the following form,

$$\alpha^2 + \beta^2 = \frac{r_p(v)^2}{f(r, v)} \left[1 - \frac{4Ma}{r_p(v)^3} \alpha \left(1 - \frac{\dot{r}_p(v)^2}{[f(r, v) - \dot{r}_p(v)]^2} \right) - \frac{\dot{r}_p(v)^2}{[f(r, v) - \dot{r}_p(v)]^2} \right] \quad (4.4.25)$$

The above equation represents the dynamics of shadow of a Kerr-Vaidya black hole in the slow rotation limit. It is important to emphasize here that, the shape of the shadow in this limit is still circular, as the spherically symmetric case. This is because the Kerr-Vaidya metric in the slow rotation approximation is spherically symmetric, i.e., $r = \text{const}$ and $v = \text{const}$ surfaces are still sphere. However, due to the presence of small (non-zero) rotation parameter, the shadow of a slowly rotating Kerr-Vaidya black hole is different than the Schwarzschild-Vaidya case. We have illustrated this result in Fig. 4.12 for a smoothly increasing mass function.

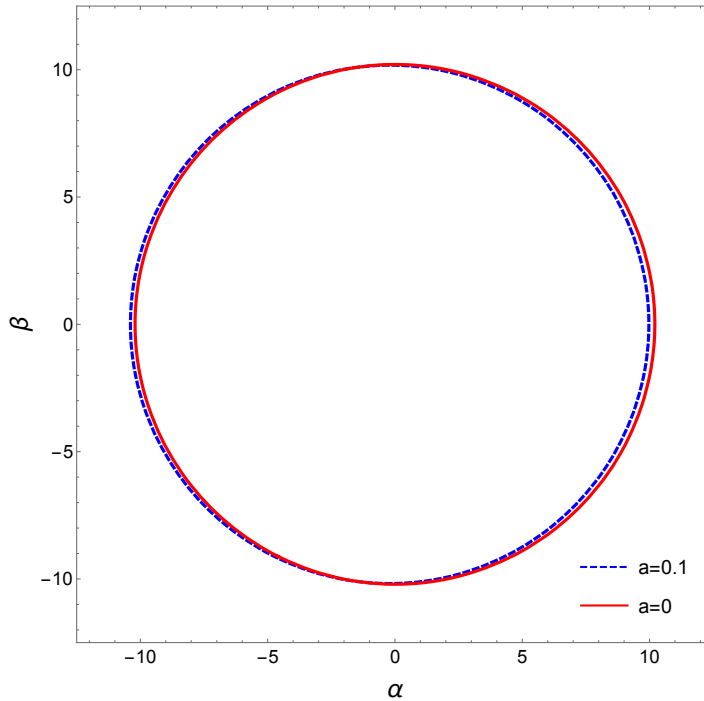


FIGURE 4.12: In this figure we compare the shadow casted by a Kerr-Vaidya black hole with rotation parameter $a = 0.1$ to that of a Vaidya black hole ($a = 0$) for the choice of mass function $M(v) = 1 + \tanh(v)$ at the in-going time $v = 2$. Note that, the shadow of slowly rotating Kerr black hole is still spherical, but with centre shifted.

Now let us perform some consistency check of the above expression, governing the dynamical evolution of shadow radius in the slow rotation limit.

- The first consistency check corresponds to the non-rotating case, i.e., with $a = 0$, where Eq. (4.4.25) becomes,

$$\alpha^2 + \beta^2 = \frac{r_p(v)^2 [f(r_p, v) - 2\dot{r}_p(v)]}{[f(r_p, v) - \dot{r}_p(v)]^2} \quad (4.4.26)$$

which which exactly matches with Eq. (4.3.7), the expression for the non-rotating dynamical black hole.

- Secondly, one can consider the stationary slowly rotating limit, i.e., $\dot{r}_{\text{ph}}(v) = 0$ and the above expression reduces to,

$$\alpha(v)^2 + \beta(v)^2 = \frac{r_p^2}{f(r_p)} \left(1 - \frac{4Ma}{r_p^3} \alpha \right) \quad (4.4.27)$$

One can immediately verify this expression exactly matches with the shadow radius of a stationary black hole in the slow rotation limit [90].

- Finally, we can also study the case of static non-rotating limit ($\dot{r}_{\text{ph}}(v) = 0$ and $a = 0$), where we recover Eq. (1.4.16), i.e., $\alpha^2 + \beta^2 = (r_{\text{ph}}^2/f(r_{\text{ph}}))$.

4.5 Effective Graviton Metric in Gauss-Bonnet Gravity

So far, our discussion has been in the context of general relativity, i.e., we have studied the time evolution of photon sphere and shadow around dynamical black hole solutions of Einstein's equation. Now we would like to extend this analysis to theories beyond general relativity. In particular, we would be interested in the Lanczos-Lovelock theories of gravity. As discussed explicitly in earlier sections, the Lanczos-Lovelock theory represents the unique generalization of the Einstein-Hilbert action in higher dimensions, with the field equation containing at the most second derivative of the metric [51, 52]. Lanczos-Lovelock theories possess several unique properties that are not present in general relativity. One such distinctive feature is the existence of superluminal propagating modes, and as a result, the issue of causality is very interesting in such theories..

It is well known that, in higher curvature theories of gravity, the gravitational degree of freedoms propagates at a different speed than that of the background ones. Here we shall refer to the background metric as the photon metric and its correction due to the higher curvature terms as the effective graviton metric. Such studies have been extensively carried out by several authors in the static case [202–209], by obtaining the effective graviton metric. Such a unique feature is intrinsic to higher curvature theories of gravity. The causal structure of a system of PDE (partial differential equation) is ultimately determined by the characteristics hyper-surface, which turns out to be null for Einstein's equations and non-null for Lanczos-Lovelock theories [204, 207]. Therefore, photon and graviton in such theories have different propagation speeds and consequently results into different circular null orbit and shadow. In this section, we would like to understand how these results generalize when the spacetime is dynamical, which will enable us to further compare the evolution of photon and graviton sphere.

We start by presenting an explicit calculation of the effective graviton metric for five-dimensional Einstein-Gauss-Bonnet gravity, which admits exact black hole solutions. For computational simplicity and without giving up any physical insights, we restrict ourselves to the case of small Gauss-Bonnet coupling constant and study the evolution of photon and graviton sphere, respectively. Gauss-Bonnet coupling constant. Let us start with the Lanczos-Lovelock Lagrangian,

$$\mathcal{L} = \sum_{k=0}^{k_{max}} \lambda_k \mathcal{L}_k \quad (4.5.1)$$

where,

$$\mathcal{L}_k = \frac{1}{2^k} \delta_{cd_1 d_1 \dots c_k d_k}^{ab a_1 b_1 \dots a_k b_k} R_{ab}^{cd} R_{a_1 b_1}^{c_1 d_1} \dots R_{a_k b_k}^{c_k d_k} \quad (4.5.2)$$

For this type of higher curvature corrections, the form of the effective graviton metric has been obtained for arbitrary order Lovelock terms in Ref. [208] (Eqn 2.24). The general strategy developed in [208] for deriving the effective metric is to start with a background metric and consider tensor perturbations. The effective metric is then identified by looking for the coefficient of the second-order derivative of the transverse-traceless perturbation h_{ab} in the linearized theory, which represents the gravitational degrees of freedom. For the Einstein-Gauss-Bonnet case, the effective metric takes the form,

$$\left[G^b_d \right] \nabla_b \nabla^d h_q^p = \left[(\delta_{qcd}^{pab} - \delta_q^p \delta_{cd}^{ab}) - \lambda_2 (\delta_{qdc_1 d_1}^{paba_1 b_1} R_{a_1 b_1}^{c_1 d_1} - \delta_q^p \delta_{cdc_1 d_1}^{ab a_1 b_1} R_{a_1 b_1}^{c_1 d_1}) \right] \nabla_b \nabla^d h_a^c \quad (4.5.3)$$

Note that the first term on the right-hand side is the background metric g_b^a while the second term, i.e., the coefficient of λ_2 represents the correction due to the presence of Gauss-Bonnet terms. The above form of the effective metric was derived in Ref. [208], by assuming the background spacetime to be static. In our analysis, we are interested in the dynamical case, and hence we start with the following background metric ansatz,

$$ds^2 = -f(r, v) dv^2 + 2dvdr + r^2 d\Omega_{d-2}^2 \quad (4.5.4)$$

The non-vanishing components of the Riemann tensor for this line element are given by,

$$R_{vr}^{vr} = -\frac{f''(r, v)}{2} \quad (4.5.5)$$

$$R_{ij}^{kl} = \frac{1-f(r, v)}{r^2} \delta_{ij}^{kl} \quad (4.5.6)$$

$$R_{\alpha i}^{\alpha j} = -\frac{f'(r, v)}{2r} \delta_i^j \quad (4.5.7)$$

$$R_{vi}^{vj} = -\frac{\dot{f}(r, v)}{2r} \delta_i^j \quad (4.5.8)$$

As per our notations, the indices i, j, k, l , etc = 1, 2, ..., (d - 2) denotes the angular coordinates on S^{d-2} , while $\alpha = (v, r)$. Eq. (4.5.8) represents the additional contribution to the Riemann tensor due to the time dependence of the metric, which vanishes in the static limit. Now, we follow an identical calculation as Ref. [208] to obtain various components of the effective graviton metric ¹,

¹Refer to Appendix B for more details.

$$G_v^v = 1 - 2\lambda_2 \left[(d-4) \left(\frac{f'(r,v)}{r} \right) - (d-4)(d-5) \left(\frac{1-f(r,v)}{r^2} \right) \right] \quad (4.5.9)$$

$$G_v^r = 2\lambda_2(d-4) \frac{\dot{f}(r,v)}{r} \quad (4.5.10)$$

All the other components of the effective metric are same as that of the static case derived in [208]. Note that, $G_{vv} = G_v^v g_{vv} + G_v^r g_{rv}$ and $G_{rv} = G_v^v$. The line element corresponding the above metric components finally takes the form,

$$ds_{eff}^2 = G_{vv} dv^2 + 2G_{rv} dv dr + G_{ij} dx^i dx^j \quad (4.5.11)$$

Since we are interested in the graviton circular null orbit, we start with the condition $ds_{eff}^2 = 0$, which can be further re-expressed in a somewhat simplified and more intuitive form, i.e.,

$$ds_{eff}^2 = \frac{G_{vv}}{G_{rv}} dv^2 + 2dv dr + \frac{G_{ij}}{G_{rv}} dx^i dx^j \quad (4.5.12)$$

Using Eq. (4.5.9) and Eq. (4.5.10), and defining $\alpha = \lambda_2(d-4)(d-3)$, this finally reduces to,

$$ds_{eff}^2 = - \left(f(r,v) - \frac{2\alpha r \dot{f}(r,v)}{(d-3)r^2 + 2\alpha [(1-f(r,v))(d-5) - rf'(r,v)]} \right) dv^2 + 2dv dr + g(r,v) d\Omega_{d-2}^2 \quad (4.5.13)$$

where $g(r,v) = G_{ij}/G_v^v$. In five-dimensions, the effective metric takes the following form,

$$ds_{eff}^2 = - \left[f(r,v) - \frac{\alpha \dot{f}(r,v)}{r - \alpha f'(r,v)} \right] dv^2 + 2dv dr + \left(\frac{1 - \alpha f''(r,v)}{1 - \frac{\alpha f'(r,v)}{r}} \right) d\Omega_3^2 \quad (4.5.14)$$

The above expression of the effective graviton metric is analogous to Eq. (4.1.1). This allows us to obtain the evolution of the radius of graviton circular null orbit by proceeding in a similar approach developed in Section 4.1 for the case of a photon. In the static limit, we have $\dot{f}(r,v) = 0$ and one can check that the photon and graviton event horizon coincides, while the radius of the circular null orbit is different. This is in agreement with all the previous results [205, 206, 208]. Now, with the above form of the effective graviton metric (Eq. (4.5.14)), we study the evolution of the graviton sphere for various choices of mass functions.

4.5.1 Photon Vs. Graviton Sphere

Before addressing the more complicated case of graviton sphere, let us start by studying the dynamical evolution of photon sphere in the context of five-dimensional Einstein-Gauss-Bonnet theory. The Gauss-Bonnet term represents the second-order Lanczos-Lovelock correction to the Einstein-Hilbert action. Gauss-Bonnet theory admits exact spherically symmetric black hole solution, which in terms of the in-going coordinate has the form [48, 217, 218],

$$ds^2 = -f(r,v) dv^2 + 2dv dr + r^2 d\Omega_3^2 \quad (4.5.15)$$

where,

$$f(r,v) = 1 + \frac{r^2}{2\alpha} \left(1 - \sqrt{1 + \frac{4\alpha M(v)}{r^4}} \right) \quad (4.5.16)$$

Here $d\Omega_3^2 = d\theta^2 + \sin^2 \theta d\phi^2 + \sin^2 \theta \sin^2 \phi d\psi^2$, denotes the volume element on the three dimensional sphere (S^3) spanned by the angular coordinates (θ, ϕ, ψ) . And α represents the Gauss-Bonnet coupling constant in five-dimensions. Since the spacetime is spherically symmetric, we can always restrict to the equatorial orbits by setting $\theta = \psi = \pi/2$. In this case, the evolution equation for the photon sphere radius is of the same form as Eq. (4.1.2), with $f(r, v)$ replaced by Eq. (4.5.16). Further, for accreting matter, we solve this differential equation by imposing future boundary conditions $r_{\text{ph}}(v \rightarrow \infty) = \sqrt{2}(M^2 - M\alpha)^{1/4}$ and $\dot{r}_{\text{ph}}(v \rightarrow \infty) = 0$ to uniquely obtain the evolution of the [h]oton sphere around a Einstein-Gauss-Bonnet black hole. Analogously, for radiating case one can use a decreasing mass function and solve Eq. (4.1.4) w.r.t the past boundary conditions $r_{\text{ph}}(u \rightarrow -\infty) = \sqrt{2}(M^2 - M\alpha)^{1/4}$ and $\dot{r}_{\text{ph}}(u \rightarrow -\infty) = 0$. Finally, for the evolution of shadow we use Eq. (4.3.7) with the choice of $f(r, v)$ in Eq. (4.5.16). The results are illustrated in Fig. 4.13.

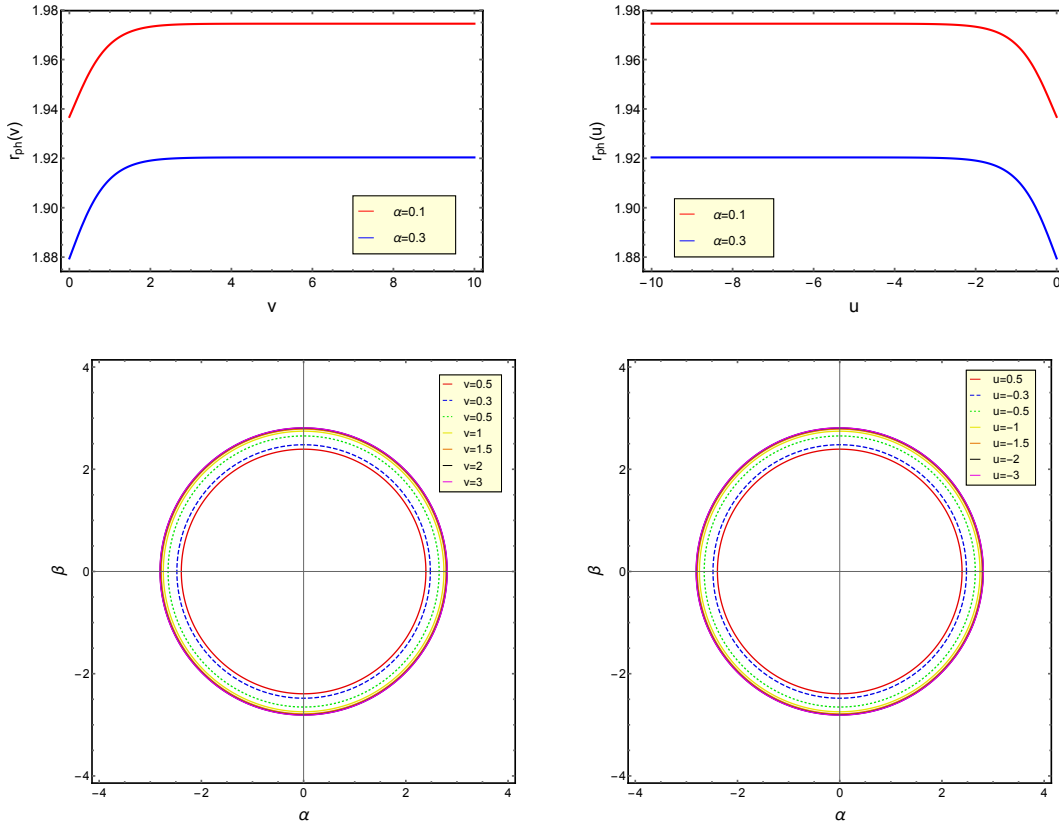


FIGURE 4.13: In this figure we depict the evolution of the photon sphere and shadow around a Gauss-Bonnet black hole in five-dimensions for various choice of coupling constants α . The top left and right panel shows the evolution of photon sphere for $m(v) = 1 + \tanh(v)$ and $m(v) = 1 - \tanh(u)$ respectively. In the bottom left and right panel we have plotted the corresponding evolution of shadow.

Having studied the dynamics of photon sphere for the five-dimensional Einstein-Gauss-Bonnet case, now we move to the more interesting case of graviton circular null orbit. Let us start with the effective graviton metric given in Eq. (4.5.14) which is of the form,

$$ds_{\text{eff}}^2 = -f_{\text{eff}}(r, v)dv^2 + 2dvdr + g(r, v), d\Omega_{d-2}^2 \quad (4.5.17)$$

By following an identical line of calculation described in [Section 4.1](#), we arrive at the following second-order differential equation that governs the dynamics of graviton sphere radius,

$$\ddot{r}_{\text{gr}}(v) + \frac{1}{2} [\dot{r}_{\text{gr}}(v)g'(r, v) - \dot{g}(r, v) - f_{\text{eff}}(r, v)g'(r, v)] \left(\frac{f_{\text{eff}}(r, v) - 2\dot{r}_{\text{gr}}}{g(r, v)} \right) - \frac{3}{2} \dot{r}_{\text{gr}}(v)f'_{\text{eff}}(r, v) \\ + \frac{1}{2} [f_{\text{eff}}(r, v)f'_{\text{eff}}(r, v) - \dot{f}_{\text{eff}}(r, v)] = 0 \quad (4.5.18)$$

As a consistency check, note that, when $g(r, v) = r^2$ we recover [Eq. \(4.1.2\)](#). We would like to understand the evolution of the graviton sphere radius and how it is different from that of the photon sphere. As emphasized earlier, we restrict our attention only to the small value of the coupling constant, α . This doesn't ruin any physical insights since the distinction between the photon and graviton sphere would be still significant. Hence in this limit we have,

$$f_{\text{eff}}(r, v) = 1 - \frac{M(v)}{r^2} + \left(\frac{M(v)^2}{r^6} - \frac{\dot{M}(v)}{r^3} \right) \alpha + \mathcal{O}(\alpha^2) \quad (4.5.19)$$

$$g(r, v) = r^2 + \frac{8M(v)\alpha}{r^2} + \mathcal{O}(\alpha^2) \quad (4.5.20)$$

Now we plug in these $\mathcal{O}(\alpha)$ expression of $f_{\text{eff}}(r, v)$ and $g(r, v)$ in [Eq. \(4.5.18\)](#) and study the evolution of the graviton sphere for a suitable choice smoothly increasing mass function. Further, in order to solve [Eq. \(4.5.18\)](#) numerically, we need to impose a set of future boundary conditions. To that end, let us derive an expression for the radius of graviton sphere in the static limit, i.e., by setting $\dot{f}_{\text{eff}}(r, v) = \dot{g}(r, v) = 0$ in [Eq. \(4.5.18\)](#), which further reduces to,

$$g(r)f'(r) - f(r)g'(r) \Big|_{r=R_{\text{gr}}} = 0 \quad (4.5.21)$$

Up to $\mathcal{O}(\alpha)$, this leads to the following algebraic equation,

$$r^6 - 2r^4 M - 8r^2 M \alpha + 4M^2 \alpha \Big|_{r=R_{\text{gr}}} = 0 \quad (4.5.22)$$

For consistency, one might check that when $\alpha = 0$, we obtain the photon sphere radius for five-dimensional Schwarzschild black hole, i.e., $R_{\text{gr}} = \sqrt{2M}$. Therefore, this allows us to expand the solution of the above algebraic equation around $\sqrt{2M}$ as,

$$R_{\text{gr}} = \sqrt{2M} + A\alpha + \mathcal{O}(\alpha^2) \quad (4.5.23)$$

where A is some unknown factor that can be determined by substituting R_{gr} in [Eq. \(4.5.22\)](#) and keeping terms up to linear order in α . This leads to,

$$R_{\text{gr}} = \sqrt{2M} + \frac{3\alpha}{2\sqrt{2M}} + \mathcal{O}(\alpha^2) \quad (4.5.24)$$

The above expression represents the radius of graviton circular null orbit around a static spherically symmetric five-dimensional Einstein-Gauss-Bonnet black hole in the small coupling limit. Now we impose the future boundary condition $r_{\text{gr}}(v \rightarrow \infty) = R_{\text{gr}}$ and $\dot{r}_{\text{gr}}(v \rightarrow \infty) = 0$ to solve [Eq. \(4.5.18\)](#). We illustrate this result in [Fig. 4.14](#) for the choice of mass function $M(v) = 1 + \tanh(v)$.

From [Fig. 4.14](#), we see a distinction between the evolution of photon and graviton sphere. Note that, when the Gauss-Bonnet coupling becomes smaller, the photon and graviton sphere approaches

each other. This is not surprising since the effective graviton metric contribution comes from the presence of higher curvature terms. Similarly, by following an identical approach developed in [Section 4.3](#), we obtain the following expression that governs the evolution of graviton shadow radius w.r.t the effective metric,

$$\alpha(v)^2 + \beta(v)^2 = \frac{g(r_g, v)}{f_e(r, v)} \left[1 - \left(\frac{\dot{r}_g(v)}{f_e(r, v) - \dot{r}_g(v)} \right)^2 \right] \quad (4.5.25)$$

Again, for consistency one might set $g(r, v) = r^2$ to recover the evolution equation of photon shadow. The shadow cast by the graviton lensing is clearly different than that of the photon and we illustrate this distinction in [Fig. 4.15](#).

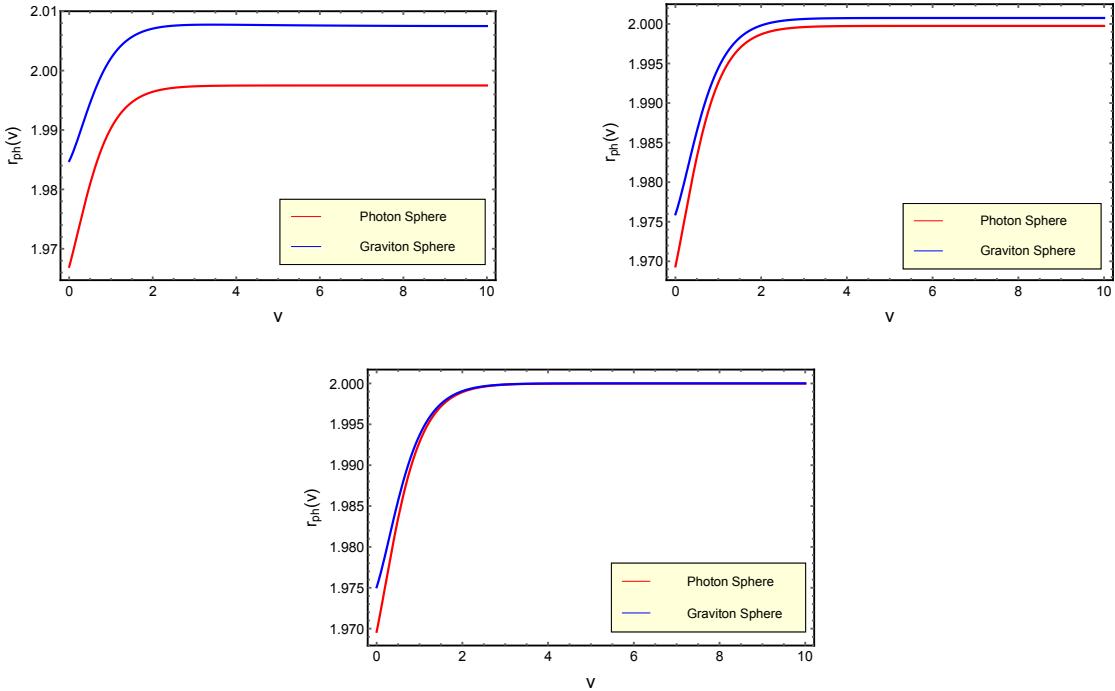


FIGURE 4.14: In this figure we compare the evolution of photon and graviton sphere around a five-dimensional Gauss-Bonnet black hole for the choice of mass function $M(v) = 1 + \tanh(v)$ and the coupling constant $\alpha = 0.01$ (top left), 0.001 (top right), 0.00001 (bottom) respectvly.

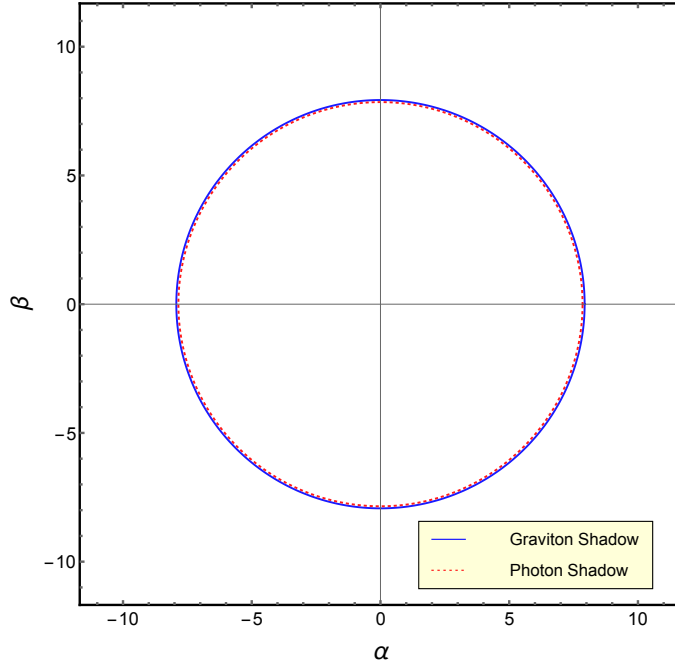


FIGURE 4.15: This figure represents a snapshot of the evolution of graviton and photon shadow at in-going time $v = 2$ w.r.t the mass function $M(v) = 1 + \tanh(v)$ and coupling constant $\alpha = 0.01$.

4.6 Summary

Compelling evidence are piling up towards the existence of black holes from a wide range of astrophysical data. The most notable ones among these observations are the detection of gravitational waves and the shadow of the super-massive object at the centre of the M87 galaxy captured by the event horizon telescope. The strong gravitational lensing effect in the vicinity of a black hole leads to the existence of circular null orbits, which further gives rise to a dark region around the black hole known as the shadow. Since most astrophysical black holes are not static, it is legitimate to understand the evolution of the photon sphere and shadow in the dynamical context. With this motivation, in the present chapter, we have carried out a detailed study of the dynamics of photon sphere and shadow around dynamical black holes. It is important to emphasize that, we consider only a simple toy model of spherically symmetric and slowly rotating dynamical spacetime, which does not reflect the reality.

We started our discussion from a spherically symmetric situation and derived the differential equation governing the evolution of the photon sphere radius. Subsequently, we have studied the case of Vaidya, Reissner-Nordström-Vaidya and de Sitter Vaidya black hole for various choices of mass and charge functions. For Vaidya spacetime, it is clear that as the mass function grows, the photon sphere also grows. However, for Reissner-Nordström-Vaidya spacetime, the situation is not straightforward. In this case, one can choose several well-behaved mass and charge functions which will violate the null energy condition. Then it appears that in those situations, besides the event and apparent horizon, the photon sphere also starts decreasing in radius. We have explicitly demonstrated this interesting relationship between the evolution of the photon sphere and violation of the null energy condition for various choices of mass and charge functions. Furthermore, we have extended this analysis to dynamical black holes in the presence of a positive cosmological constant,

namely the de Sitter Vaidya spacetime. Interestingly, in this case, the photon sphere radius strongly depends on the choice of the cosmological constant, unlike the Schwarzschild-de Sitter spacetime, where the photon sphere did not depend on the cosmological constant. Since the shadow structure strongly depends on the radius of the photon sphere, it is evident that, in the dynamical context, the black hole shadow would evolve in time. We have illustrated this result in the context of spherically symmetric and slowly rotating black holes.

So far, we have been considering dynamical black hole solutions within the framework of general relativity. We have generalized these results to incorporate the effect of higher curvature terms. In this work, we have concentrated on the black hole solutions of Einstein-Gauss-Bonnet theory, which represents the first non-trivial correction over and above general relativity, which keeps field equations second-order. We have obtained an expression of the effective graviton metric for five-dimensional Einstein-Gauss-Bonnet gravity and subsequently studied the evolution of photon and graviton sphere separately. The fact that photon and graviton sphere differs has been demonstrated explicitly, along with their evolution as the black hole accretes matter.

Chapter **5**

Overcharging a multi black hole system and the Weak Cosmic Censorship

This Chapter is based on, A. K. Mishra, S. Sarkar, Phys. Rev. D 100 (2019) 2, 024030 [[104](#)].

5.1 Introduction and Motivation

General relativity has passed all the observational and experimental tests with flying colours. However, as we have discussed previously, general relativity has been confronted by several challenges as well. One among such limitations is the existence of spacetime singularity. The basic notion of spacetime itself becomes ill-defined at the singularity, and the theory loses its predictive power. The spacetime singularities are best understood in terms of the geodesic incompleteness of causal curves [[3,4](#)]. Several efforts have been made over the years by numerous authors to understand the nature of gravitational singularities. The most definitive work in this regard is the Hawking and Penrose singularity theorems [[3,4](#)], which asserts that solutions of Einstein's equation with regular initial data would always evolve to a singularity via gravitational collapse. The weak cosmic censorship conjecture, first stated by Penrose, is the statement that singularities resulting from the gravitational collapse of an object may always be hidden inside the event horizon of a black hole. As a result, the singularity is not accessible to an exterior observer. The weak cosmic censorship is essential in ensuring the predictability of physical laws outside the black hole horizon. More precisely, it negates the existence of naked singularity solution, i.e., a spacetime singularity without an event horizon. For some excellent review on the subject refer to [[103,219,220](#)] and Refs. therein.

As it is almost impossible to come up with a general proof of the conjecture, the weak cosmic censorship remains a major open problem in classical general relativity till date. Nevertheless, one can approach the problem by studying possible counterexamples, and a significant amount of research has been done in this direction. The general strategy is to start with a black hole spacetime (extremal or non-extremal) as the initial state and look for any possible physical process that would give rise to a naked singularity in the final configuration. In his seminal paper [[102](#)], Wald pioneered this idea by studying the overcharging and overspinning of an extremal Kerr-Newman black hole by charged particle absorption. Interestingly, the electromagnetic repulsion between the black hole and the charged test particle turns out to be sufficient to prevent the black hole from capturing such

particle. The weak cosmic censorship conjecture is supported as well as challenged by several such examples and counterexamples. Studying the validity of weak cosmic censorship via the overcharging process have been performed for a wide range of black hole solutions in general relativity and modified theories [221–231]. In Ref [232], it has been shown that it is possible to obtain a naked singularity solution in the final configuration by starting with a slightly non-extremal charged black hole. Recently, in [233], a general analysis of the process of test particle absorption has been presented by taking into account up to a second-order variation of the parameters of the black hole. The key result of Ref. [233] is that overcharging of extremal as well as non-extremal black holes is not possible, as long as the matter stress-energy tensor satisfies the Null Energy Condition.

Given the current status of the problem, it is very much desirable to look for other possible tests of the weak cosmic censorship. It is important to emphasize that such tests as of now studied in the literature only involve overcharging a single charged black hole configuration. No such result exists for a system comprising more than one black hole. This motivates us to test the weak cosmic censorship in a multi black hole setting, which is the subject of this chapter. In particular, we attempt to study the overcharging problem via test particle absorption in the context of the well known Majumdar-Papapetrou configuration, which is a system of two extremal charged black hole in equilibrium [234–237]. The final configuration we are interested in is an equilibrium system of a non-extremal black hole and a naked singularity, which we refer to as a di-hole [238]. We would aim to understand whether one can obtain a stable di-hole configuration in the final state, starting from two extremal black holes in equilibrium. The condition for the stability of a di-hole configuration is more subtle as compared to a single black hole and requires additional constraint on the parameters involved, i.e., the mass(m_i), charge(q_i) and distance between the two sources [238]. Also, note that the spacetime symmetry of a di-hole configuration is vastly different from that of a single black hole. Therefore a priori, there is no reason to believe that the weak cosmic censorship would hold for such cases and this requires careful analysis.

5.2 Overcharging a Majumdar-Papapetrou configuration

The equilibrium system of multiple massive objects in general relativity is vastly different from Newtonian physics [239–244]. In general relativity, the only equilibrium configuration is either a system of two extremal black holes (Majumdar-Papapetrou solution) or a combination of one non-extremal black hole and a naked singularity (di-hole) [238]. The di-hole configuration is the only solution of Einstein-Maxwell equation in literature with two non-extremal sources in equilibrium. In this section, we begin by giving an overview of the di-hole spacetime geometry and further discuss the motion of test charged particle on such background. In terms of Weyl cylindrical coordinate, the line element can be written as [238],

$$ds^2 = -H(\rho, z)dt^2 + f(\rho, z)(d\rho^2 + dz^2) + \frac{\rho^2}{H}d\phi^2 \quad (5.2.1)$$

$$A_t = \Phi(\rho, z), \quad A_\rho = A_z = A_\phi = 0 \quad (5.2.2)$$

Here A_μ represents the electromagnetic gauge potential, and z is the symmetry axis. In the context of our problem, it is convenient to re-express the above line element in terms of bipolar coordinates

(r_1, θ_1) and (r_2, θ_2) , centred at both the sources, respectively, which spans the whole spacetime. To that end, we perform the following coordinate transformations,

$$\rho = \sqrt{(r_1 - m_1)^2 - \sigma_1^2} \sin \theta_1, \quad z = z_1 + (r_1 - m_1) \cos \theta_1 \quad (5.2.3)$$

$$\rho = \sqrt{(r_2 - m_2)^2 - \sigma_2^2} \sin \theta_2, \quad z = z_2 + (r_2 - m_2) \cos \theta_2 \quad (5.2.4)$$

The notations in the above expression are,

$$\sigma_1^2 = m_1^2 - e_1^2 + 2e_1\gamma, \quad \sigma_2^2 = m_2^2 - e_2^2 - 2e_2\gamma \quad (5.2.5)$$

$$\gamma = \frac{m_2 e_1 - m_1 e_2}{l + m_1 + m_2}, \quad l = z_2 - z_1 \quad (5.2.6)$$

Where (m_1, m_2) and (e_1, e_2) denotes the physical mass and electric charge associated with the two non-extreme Reissner-Nordström sources located at points z_1 and z_2 respectively on the symmetry axis and ' l ' is the distance between them. It is important to emphasize that the region between the two sources contains conical singularities (struts) at each point on the symmetry axis. However, the condition,

$$m_1 m_2 = (e_1 - \gamma)(e_2 + \gamma) \quad (5.2.7)$$

guarantees the equilibrium of the configuration without the presence of struts along the symmetry axis. Note that, in the absence of one source, the above condition for equilibrium is trivially satisfied. The metric components (H, f) and the electrostatic potential (Φ) in terms of the bi-polar coordinates is of the form [238],

$$H = \frac{[(r_1 - m_1)^2 - \sigma_1^2 + \gamma^2 \sin^2 \theta_2] \times [(r_2 - m_2)^2 - \sigma_2^2 + \gamma^2 \sin^2 \theta_1]}{[r_1 r_2 - (e_1 - \gamma - \gamma \sin \theta_1)(e_2 + \gamma - \gamma \sin \theta_2)]^2} \quad (5.2.8)$$

$$\Phi = -\frac{[(e_1 - \gamma)(r_2 - m_2) + (e_2 + \gamma)(r_1 - m_1) + \gamma(m_1 \cos \theta_1 + m_2 \cos \theta_2)]}{[r_1 r_2 - (e_1 - \gamma - \gamma \sin \theta_1)(e_2 + \gamma - \gamma \sin \theta_2)]} \quad (5.2.9)$$

$$f = \frac{[r_1 r_2 - (e_1 - \gamma - \gamma \sin \theta_1)(e_2 + \gamma - \gamma \sin \theta_2)]^2}{[(r_1 - m_1)^2 - \sigma_1^2 \cos^2 \theta_1] \times [(r_2 - m_2)^2 - \sigma_2^2 \cos^2 \theta_2]} \quad (5.2.10)$$

The extremal limit for both the sources is given by $\sigma_k^2 = 0$ ($k = 1, 2$) and the above configuration reduces to a Majumdar-Papapetrou spacetime consisting of two extremal black holes. For a di-hole configuration we have a non-extremal black hole ($\sigma_k^2 > 0$) and a naked singularity ($\sigma_k^2 < 0$). The location of the event horizon is obtained by solving $H = 0$, which corresponds to $r_1 = m_1$ and $r_2 = m_2$ in the extremal limit or equivalently $\rho = 0$.

Having discussed the geometry of a di-hole system, let us study the problem of overcharging and the weak cosmic censorship. We start with a Majumdar-Papapetrou configuration, i.e., a system of two extremal black holes ($\sigma_{1(i)}^2 = \sigma_{2(i)}^2 = 0, \gamma = 0$) as our initial configuration. Let the first extremal black hole absorb a charged test particle of mass δm_1 , electric charge δe_1 and turn into a non-extremal black hole of final mass and charge $m_1 + \delta m_1$ and $e_1 + \delta e_1$ respectively. Since we are considering the case of test particle absorption, we further have $\delta m_k \ll m_k$ and $\delta e_k \ll e_k$. A black hole in the final state is given by the condition $\sigma_{1(f)}^2 > 0$, which finally reduces to,

$$(\delta m_1 - \delta e_1) > -\delta\gamma \quad (5.2.11)$$

Furthermore, let the second extremal black hole absorb a test particle of mass and electric charge $(\delta m_2, \delta e_2)$ and turn into a naked singularity of final mass and charge $(m_2 + \delta m_2, e_2 + \delta e_2)$. For a naked singularity in the final configuration we have the condition $\sigma_{2(f)}^2 < 0$, which upon simplification reduces to,

$$(\delta m_2 - \delta e_2) < \delta\gamma \quad (5.2.12)$$

[Eq. \(5.2.11\)](#) and [Eq. \(5.2.12\)](#) are the conditions on the parameters of the test particles for which we have di-hole in the final configuration, which can be regarded as a potential violation of the weak cosmic censorship conjecture. Now we would like to understand whether the initial extremal black holes can capture these test particles while satisfying the above two conditions. To check this, we start by studying the motion of the first test particle with mass δm_1 and charge δe_1 on the above spacetime. For a time-like geodesic, with metric signature $diag(-, +, +, +)$ we have,

$$-1 = -H\dot{t}^2 + f(\dot{\rho}^2 + \dot{z}^2) + \frac{\rho^2}{H}\dot{\phi}^2 \quad (5.2.13)$$

where a ‘dot’ over any quantity represents derivative with respect to the proper time τ of the test particle. The energy of the particle is of the form,

$$-\delta m_1 = \delta e_1\Phi - \dot{t}H \quad (5.2.14)$$

We can eliminate \dot{t} in [Eq. \(5.2.13\)](#) and finally get,

$$(\delta m_1 + \delta e_1\Phi)^2 - H - \rho^2\dot{\phi}^2 = Hf(\dot{\rho}^2 + \dot{z}^2) \quad (5.2.15)$$

In terms of the bi-polar coordinate we have,

$$\dot{\rho} = \sqrt{(r_1 - m_1)^2 - \sigma_1^2} \cos\theta_1\dot{\theta}_1 + \frac{(r_1 - m_1)r_1}{\sqrt{(r_1 - m_1)^2 - \sigma_1^2}} \sin\theta_1 \quad (5.2.16)$$

$$\dot{z} = r_1 \cos\theta_1 - (r_1 - m_1) \sin\theta_1\dot{\theta}_1 \quad (5.2.17)$$

We can solve for δm_1 from [Eq. \(5.2.15\)](#) as,

$$\delta m_1 = -\delta e_1\Phi + H + \rho^2\dot{\phi}^2 + Hf(\dot{\rho}^2 + \dot{z}^2) \quad (5.2.18)$$

Since our initial configuration is a system of two extremal source we can use $HF = 1$. From [Eq. \(5.2.18\)](#) we further have,

$$\delta m_1 > -\delta e_1\Phi \quad (5.2.19)$$

At the extremal horizon ($r_1 = m_1$) of the first black hole, one has $\Phi = -1$. Therefore, if the test particle ever crosses the extremal horizon it must satisfy the condition $\delta m_1 > \delta e_1$. This is the condition on the mass and charge of the particle to get captured by the extremal black hole. Similarly, the second

particle must $\delta m_2 > \delta e_2$ to cross the horizon of the second extremal black hole.

As of now, we have not used the equilibrium condition for the final configuration. Now we shall study both the case of presence and absence of struts on the symmetry axis separately. Let us start with the case when the equilibrium condition holds in the final configuration, i.e., $m_{1(f)}m_{2(f)} = (e_{1(f)} - \gamma_f)(e_{2(f)} + \gamma_f)$. As we have discussed earlier, this condition is essential to ensure the absence of struts along the symmetry axis between the two sources. Further using the extremal condition $\gamma = 0$ for the initial black holes, the above equilibrium condition reduces to,

$$\gamma_f = \delta\gamma = \frac{m_1(\delta m_2 - \delta e_2) + m_2(\delta m_1 - \delta e_1)}{(m_1 - m_2)} \quad (5.2.20)$$

However, from the general expression in Eq. (5.2.6), by taking the first order variation of γ , we obtain,

$$\delta\gamma = \frac{m_1(\delta m_2 - \delta e_2) - m_2(\delta m_1 - \delta e_1)}{(l + m_1 + m_2)} \quad (5.2.21)$$

Now, assuming the equilibrium condition to hold in the final configuration, we equate Eq. (5.2.20) and Eq. (5.2.21) to solve for ' l ', in terms of the variations, which gives rise to,

$$\delta_1 + \delta_2 = -\frac{l(m_1\delta_2 + m_2\delta_1)}{2m_1m_2} \quad (5.2.22)$$

where, $\delta_1 = \delta m_1 - \delta e_1$ and $\delta_2 = \delta m_2 - \delta e_2$. From the above expression, it is evident that, as long as the test particles are crossing the extremal horizons, i.e., $\delta_1 > 0$ and $\delta_2 > 0$, Eq. (5.2.22) does not hold for the positive value of the length l , and as a result, the equilibrium condition will not be satisfied in the final configuration. Therefore, starting from an equilibrium system of two extremal black holes, it would not be possible to maintain the equilibrium in the final configuration via the process of test particle absorption. This rules out the possibility of obtaining any equilibrium system (two extremal black holes, a black hole & a naked singularity or two naked singularities) in the final state. Let us recall that the equilibrium here refers to the absence of conical singularities (struts) on the symmetry axis.

Now let us understand if we can have a naked singularity solution without demanding the equilibrium condition in the final configuration. More precisely, we would aim to see if one can produce a system of non-extremal black hole and naked singularity in the final state with struts on the symmetry axis. To that end, let us substitute the first-order variation of ' γ '(which doesn't use the equilibrium condition) from Eq. (5.2.21) in Eq. (5.2.11) and Eq. (5.2.12) to obtain,

$$(\delta m_1 - \delta e_1) > -\left(\frac{m_1}{l + m_1}\right)(\delta m_2 - \delta e_2) \quad (5.2.23)$$

$$(\delta m_2 - \delta e_2) < -\left(\frac{m_2}{l + m_2}\right)(\delta m_1 - \delta e_1) \quad (5.2.24)$$

Eq. (5.2.23) and Eq. (5.2.24) represents the conditions for obtaining a non-extremal black hole and a naked singularity respectively. From these expressions, it is clear that the condition of source '1' becoming a black hole depends explicitly on the constraint of the test particle entering the second source and vice-versa. Note that the condition for obtaining a non-extremal black hole is compatible with the condition of the test particle crossing the horizon. However, the condition for obtaining a naked singularity in the final configuration is not consistent with the test particle entering the

horizon. Thus, we conclude that it is impossible to have any naked singularity (with or without using the equilibrium condition) starting from an initial configuration of two extremal black holes. Therefore, the weak cosmic censorship conjecture holds for a Majumdar-Papapetrou configuration.

5.3 Summary

The weak cosmic censorship conjecture by Penrose is of the long standing puzzles in classical gravitational physics. One of the potential counterexample to the hypothesis is the possibility of overcharging a slightly non-extremal black hole to produce naked singularity. However, several follow up works suggests that such a process would not occur when the backreaction effect of the test particle is considered appropriately. Although the conjecture lacks general proof, there seems to be growing number of evidence in its favour. In this work, we extend these analyses to study the weak cosmic censorship in the context of a multi black hole configuration by test particle absorption. In particular, we started with a system of two extremal black holes, namely a Majumdar-Papapetrou solution, as our initial configuration and studied the overcharging problem via test particle absorption. If such a process leads to a di-hole configuration, this will correspond to a potential violation of the weak cosmic censorship. Since the spacetime structure is vastly different than that of a single charged black hole solution, *a priori*, it is not evident whether the weak cosmic censorship would hold for such non-trivial settings. However, surprisingly we have found that even in such a non-trivial setting, the cosmic censorship hypothesis remains intact.

Chapter **6**

Strong Cosmic Censorship in Higher Curvature Gravity

This Chapter is based on, A. K. Mishra, S. Chakraborty, Phys. Rev. D 101, 064041 (2020) [107] and A. K. Mishra, Gen. Rel. Grav. 52 (2020) 11, 106 [245].

6.1 Introduction and Motivation

The strong cosmic censorship is the statement that spacetimes in general relativity are globally hyperbolic manifolds [3,4]. This further ensures the deterministic nature of general relativity, i.e., the future of any event is uniquely determined from regular initial data on a Cauchy hypersurface. In other words, the initial value problem is well-posed. However, in the presence of spacetime singularities general relativity may no longer remain a deterministic theory. In particular, the existence of a timelike singularity indicates the presence of a Cauchy horizon, which is regarded as the boundary of the maximal development of initial data on a Cauchy hypersurface. Therefore the classical fate of any observer beyond the Cauchy horizon can not be uniquely determined from regular initial conditions, which in turn indicates a possible violation of the strong cosmic censorship. As a result, the breakdown of strong cosmic censorship conjecture or equivalently understanding the deterministic nature of the theory boils down to the question of whether the spacetime can be extended beyond the Cauchy horizon. The spacetime metric is regular at the Cauchy horizon, and in general, it is possible to construct a geodesic that smoothly extends beyond into regions where its further evolution cannot be uniquely determined [246]. This is a challenging situation and can be regarded as a potential violation of the strong cosmic censorship. One possible resolution to this problem in the context of asymptotically flat black holes, as initially suggested by Penrose, uses the unstable nature of the Cauchy horizon, a surface of infinite blue shift. More precisely, any perturbation approaching the Cauchy horizon attains an unbounded exponential blue shift $\Phi \sim e^{\kappa_- t}$ and further turns it into a curvature singularity, where κ_- is the surface gravity of Cauchy horizon. This phenomena is known as mass inflation [72,247–249].

A comparatively stronger and revised version of strong cosmic censorship conjecture as proposed by Christodoulou states that it is impossible to extend the spacetime beyond the Cauchy horizon with locally square integrable Christoffel connection, i.e., $\Gamma_{bc}^a \in L^2_{loc}$ [250]. Since the exponential growth of

any perturbation at the Cauchy horizon dominates the late-time power-law decay, the Christodoulou version of strong cosmic censorship conjecture turns out to be trivially satisfied for asymptotically flat spacetimes. However, for asymptotically de Sitter spacetimes, perturbations at late time attain an exponential decay, which has the possibility of balancing the exponential growth at the Cauchy horizon, leading to an extension of the spacetime beyond the Cauchy horizon [251, 252]. In other words, for the case of asymptotically de Sitter spacetimes, e.g., Reissner-Nordström-de Sitter black hole, the late time behaviour of the perturbation is of the form $\Phi \sim e^{-\alpha u}$, where $\alpha = -\text{Im}(\omega)$ is the spectral gap related to the lowest-lying quasi-normal frequency. Therefore, it is indeed possible, at least for a specific range of parameters, where the exponential decay of perturbation is cancelled by the exponential growth at the Cauchy horizon, thus avoiding any mass inflation singularity. Hence it is important to consider the relative ratio between the late time decay and the blueshift effect at the Cauchy horizon, which can be captured by the quantity, $\beta = \alpha/\kappa_-$. It turns out that, when $\beta > 1/2$, the late time exponential decay dominates over the blue shift effect at the Cauchy horizon and leads to a violation of the strong cosmic censorship conjecture. Recent interest in this area escalated after the work of Cardoso. et al., [106], where a violation of strong cosmic censorship conjecture was reported in the context of massless scalar perturbation on a Reissner-Nordström-de Sitter black hole spacetime. This approach has been used recently by several authors to test the validity of strong cosmic censorship conjecture for general relativity on various asymptotically de Sitter black hole spacetimes in four and higher dimensions with different test fields [253–264]. The central result of these analyses is the following: in the presence of a positive cosmological constant, the strong cosmic censorship conjecture is violated in the near extremal regime for non-rotating charged black holes, while for rotating black holes, the violation can be avoided. For black hole solutions in Born-Infeld-de Sitter and Horndeski theory, the strong cosmic censorship conjecture has also been recently studied in [265, 266].

Although general relativity successfully describes the gravitational phenomenon around us, it also has several limitations. We have provided a detailed discussion on various shortcomings of general relativity in [Chapter 1](#). The most notable among these is the non-renormalizability nature of Einstein-Hilbert gravitational action [46–49]. Thus it is reasonable to consider general relativity only as an effective theory, which may attain higher curvature corrections in the strong gravity regime. One of the simplest yet non-trivial generalizations of the Einstein-Hilbert action involving higher curvature corrections is the Lanczos-Lovelock gravity, containing at most second derivatives of the metric [51, 52]. This motivates us to study whether the strong cosmic censorship conjecture holds in the presence of higher curvature terms. In particular, our aim would be to understand whether the violation of strong cosmic censorship conjecture can be avoided by increasing the strength of higher curvature couplings.

As our first example, we consider the case of Einstein-Gauss-Bonnet gravity in five and higher spacetime dimensions, which is the second-order term of the Lanczos-Lovelock Lagrangian. The Einstein-Gauss-Bonnet theory admits spherically symmetric asymptotically de-Sitter charged black hole solution [267–271], which involves a Cauchy horizon. Our second example involves charged black hole solutions in pure Lovelock gravity [272–277] in dimensions $d \geq (3k + 1)$, with ‘ k ’ being the lovelock order. Here $k = 1$ represents general relativity while $k = 2$ is pure Gauss-Bonnet Gravity and so on. Finally, we study the recently proposed four-dimensional Einstein-Gauss-Bonnet theory. Although the above solutions may not represent a physical black hole spacetime, it provides a natural platform to study the effect of higher curvature terms on the violation of strong cosmic censorship

conjecture , which is the ultimate aim of this work.

The remainder of the chapter is organized as follows: In [Section 6.2](#) we start by discussing the relationship between the quasi-normal frequency corresponding to the photon sphere modes and the Lyapunov exponent associated with the photon sphere. Subsequently, in [Section 6.3](#), we discuss both the time and frequency domain methods of computing quasi-normal modes numerically. Next, in [Section 6.4](#) we study the validity of the strong cosmic censorship conjecture for several class of higher curvature theories, namely, Einstein-Gauss-Bonnet gravity in four and higher dimensions and pure Lovelock gravity. From all of our examples, we finally conclude that the violation of strong cosmic censorship conjecture becomes even stronger when higher curvature terms are added. Lastly, we conclude with a brief discussion in [Section 6.5](#).

6.2 Strong cosmic censorship conjecture and Quasi-normal modes: A brief overview

Computation of quasi-normal modes and understanding the stability of black hole solutions has been one of the major research subjects in gravitational physics. These modes are defined as the eigenfrequency of some perturbation with respect to a particular set of boundary conditions, i.e., purely ingoing modes at the event horizon and outgoing modes at spatial infinity (or cosmological horizon for de Sitter case). Since a black hole spacetime effectively works as a dissipative system, the corresponding eigenfrequencies are complex numbers. The real part of the quasi-normal mode determines the oscillation frequency, while the imaginary part represents the decay rate of the perturbation. The stability of a black hole spacetime w.r.t some perturbation is ultimately linked with the sign of the imaginary part of the quasi-normal mode frequency, ω . For most black hole space-times, because of the complex structure of the effective potential, it is often difficult to obtain an analytical expression for the quasi-normal modes by solving the perturbation equation. A relatively simpler approach is to obtain the quasi-normal frequency by solving the equation numerically. Several such techniques have been developed by numerous authors in the past few decades to compute the quasi-normal modes accurately. However, note that, in certain limiting cases, it is also possible to obtain an analytical expression of the quasi-normal mode frequency. One such limit is the ray optics approximation, also known as the eikonal limit or large angular momentum limit. In this approximation, both the real and imaginary part of the quasi-normal frequency are related to various geometric constructs associated with the photon sphere. This is not surprising since the effective potential experienced by a photon in a black hole spacetime is the same as the potential experienced by the test field in the large angular momentum limit, irrespective of the spin of the test field. More precisely, the imaginary part of the quasi-normal frequency is related to the Lyapunov exponent associated with the instability of the photon sphere, while the real part is related to the angular velocity of the photon sphere [278–280],

$$\omega_n = \Omega_{\text{ph}}\ell - i \left(n + \frac{1}{2} \right) \lambda_{\text{ph}} \quad (6.2.1)$$

where ℓ is the angular momentum and $n = 0, 1, 2, \dots$ represents the overtone number. We also refer the reader to [281, 282], where the above correspondence is discussed in the context of higher curvature gravity. In particular, in Ref. [281], the authors have shown that for gravitational quasi-normal modes in the presence of higher curvature terms, the above correspondence breaks. In this work, we

only restrict to test scalar perturbations.

The Lyapunov exponent λ_{ph} , associated with the photon sphere, is a measure of the rate at which a geodesic located at photon sphere diverge or converge with respect to a nearby geodesic. And, Ω_{ph} represents the angular velocity of a photon located at the maxima of the photon sphere. Let us start with a d -dimensional static spherically symmetric spacetime and obtain a general expression for the Lyapunov exponent in terms of the metric coefficients.

$$ds^2 = -f(r)dt^2 + f(r)^{-1}dr^2 + r^2d\Omega_{d-2}^2 \quad (6.2.2)$$

Since the spacetime under consideration is spherically symmetric, we can restrict our attention only to the equatorial plane ($\theta = \pi/2$) and hence the Lagrangian associated with the geodesic motion takes the form,

$$\mathcal{L} = \frac{1}{2} \left(-f(r)\dot{t}^2 + f(r)^{-1}\dot{r}^2 + r^2\dot{\phi}^2 \right) \quad (6.2.3)$$

where a ‘dot’ represents derivative with respect to the affine parameter. Also note that, here t and ϕ are cyclic coordinates and as a result the corresponding energy ($p_t = -E$) and angular momentum ($p_\phi = L$) are constants of motion. For photon orbits we have $\mathcal{L} = 0$ and the above equation reduces to,

$$\dot{r}^2 = V_{\text{eff}}(r) \quad (6.2.4)$$

where V_{eff} denotes the effective potential. The location of the photon sphere is determined by the equations $V'_{\text{eff}}(r_{\text{ph}}) = V''_{\text{eff}}(r_{\text{ph}}) = 0$. These equations further reduce to,

$$\begin{aligned} \frac{E^2}{L^2} &= \frac{f(r)}{r^2} \\ 2f(r) &= rf'(r) \end{aligned} \quad (6.2.5)$$

The Lyapunov exponent can be obtained by taking the variation of Eq. (6.2.4) as $r \rightarrow r_{\text{ph}} + \delta r$, which gives,

$$\delta r^2 = \frac{1}{2}V''_{\text{eff}}(r_{\text{ph}})\delta r^2 \quad (6.2.6)$$

The above equation has solution of the form $\delta r \sim \exp(\pm\lambda_{\text{ph}}t)$, where the Lyapunov exponent λ_{ph} has the following expression in terms of the effective potential [278],

$$\lambda_{\text{ph}} = \sqrt{\left. \frac{V''_{\text{eff}}}{2\dot{t}^2} \right|_{r=r_{\text{ph}}}} = \sqrt{\frac{f(r_{\text{ph}})}{2} \left(\frac{2f(r_{\text{ph}})}{r_{\text{ph}}^2} - f''(r_{\text{ph}}) \right)} \quad (6.2.7)$$

A positive Lyapunov exponent represents the divergence between two nearby geodesics, while a negative value represents convergence. According to our convention, the time dependence of the perturbation goes as $\exp(-i\omega_n t)$ and hence the imaginary part of the quasi-normal frequency must be negative to ensure stability. Since the longest-lived quasi-normal mode frequency correspond to the $n = 0$ mode in Eq. (6.2.1), the quantity of interest for strong cosmic censorship conjecture, i.e., $\beta \equiv \{-\min(\text{Im } \omega_n)/\kappa_{\text{ch}}\}$, is given by (from Eq. (6.2.1) and Eq. (6.2.7)),

$$\beta_{\text{ph}} = \frac{\lambda_{\text{ph}}}{2\kappa_{\text{ch}}} = \frac{1}{2\kappa_{\text{ch}}} \left\{ \sqrt{\frac{f(r_{\text{ph}})}{2} \left(\frac{2f(r_{\text{ph}})}{r_{\text{ph}}^2} - f''(r_{\text{ph}}) \right)} \right\} \quad (6.2.8)$$

So far, we have discussed one of the limiting case, namely the large ℓ limit, where one can explicitly

write down an analytic formula for the quasi-normal mode (Eq. (6.2.1)). Since the quasi-normal mode frequencies in this context solely depend on the photon sphere, these are generally referred to as the photon sphere modes. In the presence of electromagnetic charge and cosmological constant, the quasi-normal mode spectrum possesses two other sets of characteristic quasi-normal modes, namely, the de Sitter modes and the near extremal modes. The de Sitter mode becomes dominant when the cosmological horizon lies far away from the event horizon, i.e., in the limit when the cosmological constant goes to zero. The quasi-normal mode frequency associated with a de Sitter mode can be solely determined from the asymptotic structure of spacetime, which has the following form [283–286],

$$\omega_{n,\text{dS}} = -i(\ell + 2n)\kappa_c \quad (6.2.9)$$

Where κ_c represents the surface gravity of the cosmological horizon. The minimum value for the imaginary part of the quasi-normal mode frequency corresponds to $\omega_{n=0,\text{dS}} = -il\kappa_c$, which is the longest-lived mode. Note that the analytic expressions for various modes presented here are not exact and obtained with some approximations. However, for the computational accuracy of our result, we obtain the quasi-normal frequencies numerically in the subsequent sections and further compare with their corresponding analytical expressions given in this section. Finally, another set of modes that are important for our analysis are the near extremal modes. These appear when the Cauchy horizon and the event horizon approach each other. In the context of black holes in general relativity, it was possible to provide an analytical estimation for these modes. However, it turns out to be challenging to obtain an analytical expression for these modes in the present context. This is primarily because of the complicated structure of the equation determining the event horizon. Hence we will not attempt to write down any analytical expression for the near extremal modes; instead, we will compute it numerically.

Now let us see how the choice of β is related to the violation of strong cosmic censorship. Consider the field equation of a test scalar field on a static spherically symmetric background in d -dimensions, i.e., $\square\Phi = 0$. Because of the existence of a timelike Killing vector, the scalar field can be expanded as, $\Phi(t, r, \Omega) = e^{-i\omega t}R(r)h(\Omega)$, where $h(\Omega)$ denotes the spherical harmonics of the $(d-2)$ dimensional unit sphere. The function $R(r)$ satisfies a second-order differential equation, whose two independent solutions, regular at the Cauchy horizon reads,

$$\Phi^{(1)}(t, r, \Omega) = e^{-i\omega u}R^{(1)}(r)h(\Omega); \quad \Phi^{(2)}(r) = e^{-i\omega u}R^{(2)}(r)(r - r_{\text{ch}})^{i\omega_n/\kappa_{\text{ch}}}h(\Omega) \quad (6.2.10)$$

Here ω_n is the quasi-normal mode frequency, and κ_{ch} is the surface gravity associated with the Cauchy horizon. Therefore, the integral of the kinetic term w.r.t the scalar field corresponds to the integral of $(r - r_{\text{ch}})^{2(i\omega_n/\kappa_{\text{ch}} - 1)}$, which in turn corresponds to, $(r - r_{\text{ch}})^{2(\beta - 1)}$. As a result, when $\beta > (1/2)$, the scalar field Φ turns out to be regular at the Cauchy horizon and can be smoothly extended beyond. Hence the condition $\beta > (1/2)$ signifies whether the strong cosmic censorship conjecture is respected in the spacetime or not. Note that higher curvature terms in the field equation would lead to higher regularity requirement for the metric [266]. Hence the extension of metric perturbation across the Cauchy horizon, in this case, would yield a different bound on β . In this work, we only concentrate on scalar perturbations.

Also, note that, for the $\beta > (1/2)$ condition to have any relevance with the violation of the strong cosmic censorship conjecture , it is essential that the perturbation has a late time exponential decay, which is undoubtedly true for general relativity [287]. However, whether such an exponential

decay holds for asymptotically de Sitter black holes in higher curvature theory must be adequately addressed. This is an essential aspect in the analysis of strong cosmic censorship. Interestingly, such an exponential tail has already been reported for asymptotically de Sitter black holes in Einstein-Gauss-Bonnet gravity in [286]. In this work, we are also interested in asymptotically de Sitter black hole solutions of Einstein-Gauss-Bonnet gravity, and hence we can safely argue that the condition $\beta > (1/2)$ will characterize the violation of strong cosmic censorship. Since the properties of Gauss-Bonnet gravity, which is the second-order term in the Lovelock polynomial, closely matches with that of the higher-order Lovelock terms, it is reasonable to expect that the same exponential tail would appear even in the case of asymptotically de Sitter black holes in pure Lovelock gravity, which is also studied in this work. This is not surprising since the late time decay of any perturbation on a black hole spacetime solely depends on the asymptotic structure of the effective potential. We also perform a time-domain analysis to obtain the late time decay profile of scalar perturbations in these higher curvature theories to support these arguments.

In the subsequent sections, we will carry out the above analysis in the context of a scalar field perturbation on the charged Einstein-Gauss-Bonnet-de Sitter black hole background (in four and higher dimensions) and for a pure Lovelock black hole background. Our strategy would be identical to that of Ref. [106]. We start by computing the quasi-normal frequency associated with the photon sphere modes, de Sitter modes and near extremal modes numerically. Having obtained the full quasi-normal mode spectrum, we look for any possible violation of the strong cosmic censorship conjecture by computing β . The quasi-normal mode spectrum of test fields in Gauss-Bonnet and pure Lovelock theory are different than those in Einstein's gravity and strongly depends on the Gauss-Bonnet coupling constant [286, 288–294]. Therefore, it is expected that the fate of strong cosmic censorship conjecture in these theories would be vastly different from general relativity, and hence a detailed analysis is very important. For numerical computation, we follow the Mathematica package developed in [295]. Also, we use the Prony method and extract the quasi-normal frequencies from the time domain profile.

6.3 Numerical Analysis: Computation of quasi-normal modes

Having explained the necessary theoretical concepts, now we would like to understand the violation of strong cosmic censorship conjecture in higher curvature theories. As we have discussed previously, one of the most important ingredients in the analysis of strong cosmic censorship conjecture is the quasi-normal modes. In this section, we employ both the frequency and time domain analysis to numerically compute the quasi-normal frequency.

6.3.1 Frequency Domain

Let us start by describing the dynamics of a massless scalar field Φ on a d dimensional spherically symmetric black hole background as given in Eq. (6.2.2). The evolution of the perturbation is governed by the Klein-Gordon equation $\square\Phi = 0$, which takes the form,

$$\frac{d^2\Phi}{dt^2} - \frac{d^2\Phi}{dr_*^2} + V_{\text{eff}}(r)\Phi = 0 \quad (6.3.1)$$

Here $dr_* = \{dr/f(r)\}$ represents the tortoise coordinate and $V_{\text{eff}}(r)$ is the effective potential expressed above in terms of the metric coefficient $f(r)$. For spherically symmetric background, one

can always expand the field in terms of a natural basis on the $(d - 2)$ sphere, namely the spherical harmonics $\mathcal{Y}_{lm}(\theta, \phi)$ as follows,

$$\Phi(t, r, \Omega) = \sum_{\ell, m} e^{-i\omega t} \frac{\phi(r)}{r^{(d-2)/2}} \mathcal{Y}_{\ell m}(\theta, \phi) \quad (6.3.2)$$

which leads to the following master equation,

$$\left(\frac{\partial^2}{\partial r_*^2} + \omega^2 - V_{\text{eff}}(r) \right) \phi(r) = 0 \quad (6.3.3)$$

$$V_{\text{eff}}(r) = f(r) \left\{ \frac{\ell(\ell + d - 3)}{r^2} + \frac{(d-2)(d-4)}{4r^2} f(r) + \frac{(d-2)(1-s^2)}{2r} f'(r) \right\}$$

Here we have expressed the effective potential for a field perturbation of spin s . The quasi-normal mode frequency ω_n is defined as the eigenvalue of Eq. (6.3.3) that corresponds to ingoing modes at the event horizon, r_h and outgoing modes at the cosmological horizon, r_c , i.e.,

$$\phi(r \rightarrow r_h) \sim e^{-i\omega r_*} \quad \text{and} \quad \phi(r \rightarrow r_c) \sim e^{i\omega r_*} \quad (6.3.4)$$

Once the quasi-normal modes are obtained, the computation of β is straightforward. In the next section, we present the numerical value of β and discuss the violation of strong cosmic censorship conjecture in the context of various higher curvature theories.

6.3.2 Time Domain

The frequency-domain method discussed above is a boundary value problem, i.e., one needs to set suitable boundary conditions at the cosmological horizon and event horizon to solve the perturbation equation. However, one can also cast the perturbation equation as an initial value problem and numerically integrate the equation starting from regular initial data. This is known as the time-domain analysis. To discuss this method further, let us express Eq. (6.3.1) as follows,

$$\left(4 \frac{\partial^2}{\partial u \partial v} + V(u, v) \right) \Phi(u, v) = 0 \quad (6.3.5)$$

where $u = t - r_*$ and $v = t + r_*$ are the null cone variables. The above equation can be numerically solved in a straightforward manner on a null grid by adapting the following discretization scheme,

$$\Phi(u + h, v + h) = -\Phi(u, v) + \Phi(u + h, v) + \Phi(u, v + h) - \frac{h^2}{8} V(u, v) [\Phi(u + h, v) + \Phi(u, v + h)] \quad (6.3.6)$$

where h denotes the separation between grid points. Eq. (6.3.6) allows us to obtain the value of the field Φ on the entire null grid by starting from an initial data, which we take to be $\Phi(u, v_0) = \exp\left(\frac{-(v-12)^2}{10}\right)$. The time-domain profile provides the value of the field as a function of time, i.e., $\Phi(t_0), \Phi(t_0 + h), \Phi(t_0 + 2h)$...etc., which we use to compute the quasi-normal mode by a Prony fit algorithm [296]. In Fig. 6.1 we depict the time-domain evolution of a scalar perturbation on a five-dimensional Einstein-Gauss-Bonnet de Sitter black hole background for various choice of parameters.

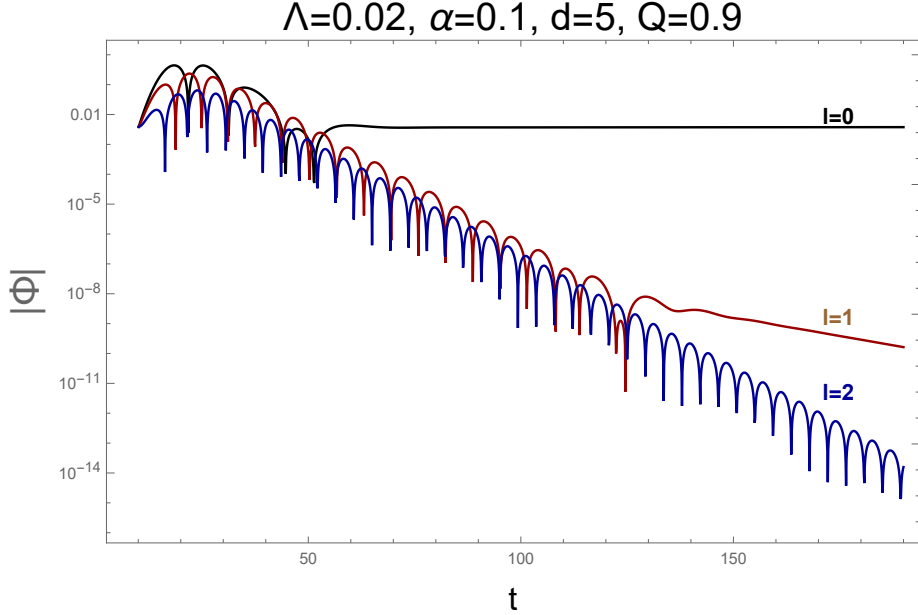


FIGURE 6.1: This figure represents the evolution of scalar perturbation as a function of time on a five dimensional Einstein-Gauss-Bonnet black hole spacetime. Further, the plot is represented in log scale and hence a straight line here corresponds to an exponential decay at late time.

6.4 Validity of Strong Cosmic Censorship

So far, the statement of strong cosmic censorship conjecture has been tested for several black hole solutions, but mostly within the realm of general relativity. Although, in certain cases influence of matter couplings are taken into account, the effects of higher curvature terms have not been explored. Since general relativity is expected to be supplemented by higher curvature corrections in the strong gravity regimes, it is crucial to study the effects of these terms on the strong cosmic censorship. In the previous section, we have described two frequently used numerical techniques in the literature to compute the quasi-normal modes. In this section, we employ these methods to obtain the values of β and subsequently check the validity of strong cosmic censorship conjecture for several class of higher curvature theories.

6.4.1 Higher dimensional Einstein-Gauss-Bonnet Gravity

In this work, we will be interested in the higher curvature corrections within the domain of Lanczos-Lovelock Lagrangian (Eq. (1.3.1)) since they represent the most general extension to general relativity in dimensions higher than four with field equations containing up to second derivatives of the metric. The Lanczos-Lovelock Lagrangian is a homogeneous polynomial in terms of the products of Riemann tensor, and the Einstein-Gauss-Bonnet theory is obtained by keeping terms up to second order, which is given by,

$$\mathcal{A} = \frac{1}{16\pi} \int d^d x \sqrt{-g} \left[R + \alpha \left(R^2 - 4R_{ab}R^{ab} + R_{abcd}R^{abcd} \right) - 2\Lambda - 4\pi F_{ab}F^{ab} \right], \quad (6.4.1)$$

where α is the Gauss-Bonnet coupling constant and Λ represents the cosmological constant. Also we have included a matter Lagrangian of the form $-(1/4)F_{ab}F^{ab}$. Interestingly, the theory possesses spherically symmetric and static black hole solution in d spacetime dimensions, with the line element

in the form presented in Eq. (6.2.2), where the function $f(r)$ is given by [268, 297–299],

$$f(r) = 1 + \frac{r^2}{2\tilde{\alpha}} \left[1 - \sqrt{1 + \frac{64\pi\tilde{\alpha}M}{(d-2)\Sigma_{d-2}r^{d-1}} - \frac{2\tilde{\alpha}Q^2}{(d-2)(d-3)r^{2d-4}} + \frac{8\tilde{\alpha}\Lambda}{(d-1)(d-2)}} \right]. \quad (6.4.2)$$

In the above expression, ‘ Q ’ denotes the electric charge of the black hole corresponding to the field tensor $F_{\mu\nu}$ and $\tilde{\alpha} = (d-3)(d-4)\alpha$ is the re-scaled Gauss-Bonnet coupling constant. M represents the ADM mass of the black hole. Further, Σ_{d-2} is the volume of a $(d-2)$ dimensional unit sphere. The location of the horizons are given by the equation $f(r) = 0$, which further reduces to,

$$\frac{4\Lambda}{(d-1)(d-2)} r^{(2d-4)} - 2r^{(2d-6)} - 2\alpha r^{(2d-8)} + \frac{32\pi M}{(d-2)\Sigma_{d-2}} r^{(d-3)} - \frac{Q^2}{(d-2)(d-3)} = 0 \quad (6.4.3)$$

Since for our analysis, we require the black hole under consideration to have three horizons, namely the event horizon, cosmological horizon and Cauchy horizon , Eq. (6.4.3) must give rise to three real positive roots. This is guaranteed from the Descarte rule of sign.

Given this black hole spacetime, which is an exact solution of the Einstein-Gauss-Bonnet field equation, we want to understand if there is any violation of strong cosmic censorship conjecture in this spacetime. Let us note that in the limit of $\alpha = 0$, i.e., in the absence of any higher curvature corrections, the above spacetime reduces to a Reissner-Nordström de Sitter configuration in d -dimensions and admits violation of strong cosmic censorship conjecture [255]. Therefore, it would be an interesting exercise to see whether, by adding higher curvature terms, one can avoid such violation. Now, for the above choice of $f(r)$, one can explicitly determine the quantity β for the photon sphere modes by computing the Lyapunov exponent and surface gravity at the Cauchy horizon following Eq. (6.2.8). However, as emphasized earlier, it is better to obtain β numerically for higher accuracy of our analysis.

For computing the quasi-normal modes numerically we solve Eq. (6.3.3) w.r.t the black hole boundary conditions (Eq. (6.3.4)). We follow the method and use the Mathematica package developed in [295] and also cross-check it with the quasi-normal modes computed using the Prony algorithm. As mentioned in the previous section, the complex part of the quasi-normal frequency is the first ingredient that goes into the definition of β . The computation of κ_{ch} can also be performed in a similar manner and hence the numerical estimation for $\{-(\text{Im } \omega_{n,\ell})/\kappa_{\text{ch}}\}$ can be obtained, whose minimum value would yield an estimation for β . We have presented the numerical values of β in Tab. 6.1 for the three modes of interest, namely the near extremal modes ($\ell = 0$), the de Sitter modes ($\ell = 1$) and the photon sphere modes ($\ell = 10$). Along with the numerical data, analytical estimations for $\{-(\text{Im } \omega_{n,\ell})/\kappa_{\text{ch}}\}$ has also been presented in Tab. 6.1. As evident, the numerical and analytical results matches quite well, within an error of 6%. Furthermore, from Tab. 6.1 one can see that the value of β crosses $(1/2)$ for near extremal values of the electric charge Q and as a result, the violation of strong cosmic censorship conjecture is evident in the Einstein-Gauss-Bonnet theory.

$\tilde{\alpha}$	Λ	Q/Q_{\max}	$\ell = 0$	$\ell = 1$	$\ell = 10$	$\ell = 10$ (analytical)
0.1	0.06	0.99	0.849266	0.467428	0.678101	0.6770764
		0.995	0.8860955	0.7059601	1.02414	1.018981
	0.1	0.99	0.850344	0.6296578	0.6674398	0.6661463
		0.995	0.8841346	0.9521732	1.00561	1.00365144
0.2	0.06	0.99	0.861229	0.510842	0.734559	0.7334486
		0.995	0.8952727	0.7683285	1.10481	1.09940317
	0.1	0.99	0.8608527	0.685808	0.7215474	0.7201545
		0.995	0.893013	1.0327756	1.0865954	1.0806729
0.3	0.06	0.99	0.8714403	0.555417	0.796272	0.79027861
		0.995	0.9035516	0.83237279	1.18615	1.1804926
	0.1	0.99	0.8703119	0.743391	0.776177	0.774676
		0.995	0.9010936	1.1544405	1.160704	1.1584423

TABLE 6.1: In this table we present the numerical values of $\{-(\text{Im } \omega_{n,\ell})/\kappa_{\text{ch}}\}$ for the lowest lying quasi-normal modes for different choices of ℓ . We have also presented them for various choices of the re-scaled Gauss-Bonnet coupling constant $\tilde{\alpha}$, cosmological constant Λ and re-scaled electric charge (Q/Q_{\max}) , for $M = 1$ and $d = 5$. The numerical estimation of β , for a given $\tilde{\alpha}$, Λ and (Q/Q_{\max}) would correspond to the lowest entry in that respective row. Here $\ell = 0$ values corresponds to the near-extremal modes (fourth column), while $\ell = 1$ is for the de Sitter modes (fifth column). Finally, the numerical estimation for $\{-(\text{Im } \omega_{n,\ell})/\kappa_{\text{ch}}\}$ associated with the photon sphere modes have been presented for $\ell = 10$. It is evident that, the analytical estimate of β provided in the last column are in strong agreement with that of the numerical ones.

Let us now study the violation of the strong cosmic censorship more explicitly. To that end, we plot $\{-(\text{Im } \omega_{n,\ell})/\kappa_{\text{ch}}\}$ (which for brevity have been labelled as β in the plots) w.r.t (Q/Q_{\max}) in Fig. 6.2, where Q_{\max} represents the extremal limit of the electric charge Q for a given cosmological constant and Gauss-Bonnet parameter α . In Fig. 6.2 we have plotted the β values w.r.t the photon sphere (left column), de Sitter modes (middle column) and near extremal modes (right-most column). It is evident that all the three class of modes cross the $\beta = (1/2)$ line, and hence the strong cosmic censorship conjecture is violated for charged de Sitter black hole in Einstein-Gauss-Bonnet theory. Furthermore, the violation gets severe as the Gauss-Bonnet coupling parameter α is increased, since the curves for β crosses the line $\beta = (1/2)$ earlier, thus allowing for a larger parameter space where the violation of strong cosmic censorship conjecture can be perceived. Also, for the photon sphere modes the violation becomes stronger as the spacetime dimension increases from $d = 5$ to $d = 6$ (see, the last row of Fig. 6.2), which is a reminiscent of the result presented in [255].

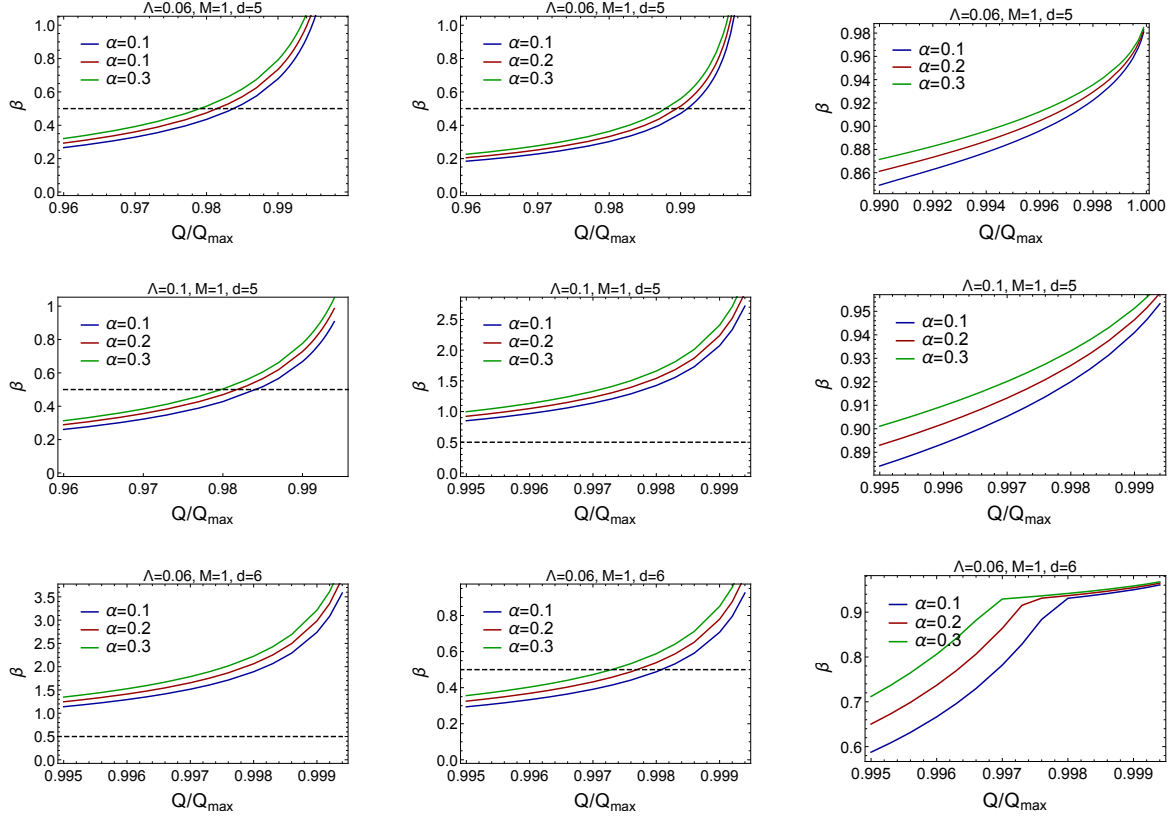


FIGURE 6.2: In this figure we plot the quantity $\{-(\text{Im } \omega_n) / \kappa_{\text{ch}}\}$, whose minima provides an estimation for β , against the ratio (Q/Q_{max}) for all the three quasi-normal modes of different origins. In the leftmost column, we illustrate the variation of $\{-(\text{Im } \omega_n) / \kappa_{\text{ch}}\}$ for the photon sphere modes, while the plots in the middle and rightmost column are for the de Sitter and near extremal modes respectively. Plots belonging to a particular row are for a fixed value of cosmological constant (Λ), and all the three curves in a given plot are for three choices of the rescaled Gauss-Bonnet parameter. See text for discussions.

Now, to see the above results from a different perspective, we have again plotted the ratio of the imaginary part of the quasi-normal and the surface gravity at the Cauchy horizon against (Q/Q_{max}) , but this time with all the three modes depicted in the same plot for various choices of the cosmological constant Λ and the Gauss-Bonnet Parameter α in Fig. 6.3 for $d = 5$. It is evident that for smaller values of the cosmological constant, the de Sitter modes dominates over the other two families of modes for small values of (Q/Q_{max}) . In the near extremal regime, i.e., in the limit $(Q/Q_{\text{max}}) \rightarrow 1$, the near extremal mode starts to dominate. Also, for larger values of the cosmological constant, the photon sphere dominates when (Q/Q_{max}) is small. The effect of higher curvature terms on the violation of strong cosmic censorship conjecture can also be easily realized from Fig. 6.3. As the Gauss-Bonnet coupling increases, the violation of strong cosmic censorship conjecture occurs at smaller values of (Q/Q_{max}) , which implies that the parameter space available for violating strong cosmic censorship conjecture in higher curvature theories is larger as compared to general relativity.

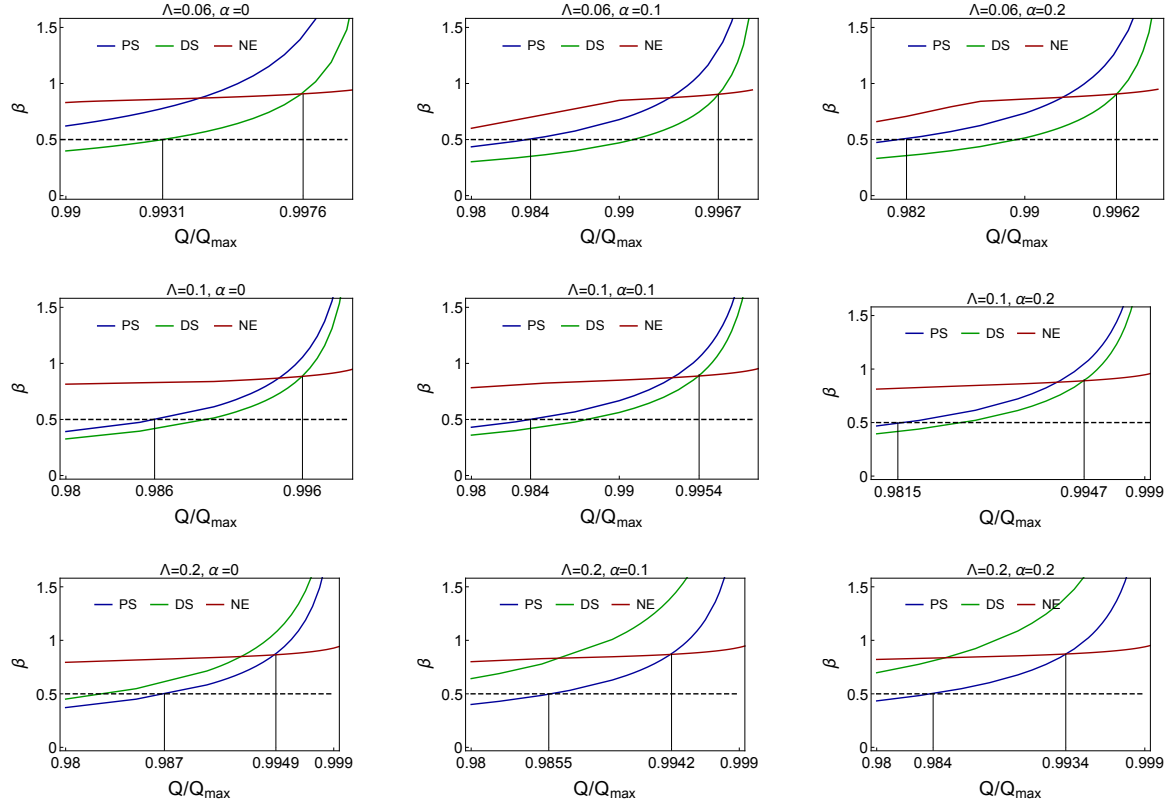


FIGURE 6.3: In this figure we have demonstrated the variation of $\{-(\text{Im } \omega_n)/\kappa_{\text{ch}}\}$, whose minima corresponds to the parameter β , with respect to (Q/Q_{max}) for all the three quasi-normal modes of interest in each single plots, namely the photon sphere modes (blue curves), de Sitter modes (green curves), near extremal modes (brown curves). Each of these plots here are for various choice of the cosmological constant Λ and Gauss-Bonnet parameter α . The first vertical line in each plot corresponds to the value of (Q/Q_{max}) , where β crosses the value $(1/2)$ for the first time, i.e., when the strong cosmic censorship conjecture is violated. While the second vertical line corresponds to the value of (Q/Q_{max}) , where the near extremal modes starts to dominate. In this figure, the spacetime dimensions is taken to be $d = 5$ and mass to be unity.

6.4.2 Pure Lovelock Gravity

In our previous example, we have studied the strong cosmic censorship conjecture in the context of Einstein-Gauss-Bonnet theory in spacetime dimensions higher than four. As we have illustrated, the Einstein-Gauss-Bonnet gravity leads to even stronger violation of strong cosmic censorship conjecture than that of a black hole solution in general relativity. To understand this effect further, in this section, we consider the case of pure Lovelock gravity [272, 273], which refers to a single term in the full Lovelock Lagrangian. More precisely, the k^{th} order pure Lovelock theory is given by the Lagrangian $\mathcal{L} = \sqrt{-g} L_k$ of the full Lovelock polynomial (Eq. (1.3.1)), without the sum. For example, the second-order pure Lovelock theory has the Lagrangian of the form, $\mathcal{L}_2 = \sqrt{-g} \{R^2 - 4R_{ab}R^{ab} + R_{abcd}R^{abcd}\}$, which is referred as the pure Gauss-Bonnet theory. Thus the action for such a theory with a positive cosmological constant term is given by,

$$\mathcal{A} = \frac{1}{16\pi} \int d^d x \sqrt{-g} \left[-2\Lambda + L_k - 4\pi F_{ab}F^{ab} \right] \quad (6.4.4)$$

This theory has spherically symmetric black hole solution in d dimensions with the line element expressed in the form of Eq. (6.2.2), where the function $f(r)$ is given by [300],

$$f(r) = 1 - \left(\tilde{\Lambda} r^{2k} + \frac{2M^k}{r^{d-2k-1}} - \frac{\tilde{Q}^2}{r^{2d-2k-4}} \right)^{\frac{1}{k}} \quad (6.4.5)$$

Where, $\tilde{\Lambda}$ and \tilde{Q} are some re-scaled version of the cosmological constant and electromagnetic charge associated with the Maxwell field. It is well known that such a black hole solution admits instabilities with respect to small perturbations in dimensions $d < (3k + 1)$ [272]. Therefore, in our analysis, we consider black hole solutions in dimensions $d \geq (3k + 1)$. In particular, we study the strong cosmic censorship conjecture for the pure Gauss-Bonnet solution ($k = 2$) in seven spacetime dimensions. To illustrate the effect of the pure Gauss-Bonnet term on the strong cosmic censorship, we compare it with the corresponding black hole solution of general relativity in seven dimensions, i.e., a Reissner-Nordström de Sitter solution. In $d = 7$, the metric component $f(r)$ for the charged pure Gauss-Bonnet-de Sitter and charged Einstein-de Sitter black hole solution takes the form,

$$f_{\text{GB}}(r) = 1 - \left(\tilde{\Lambda} r^4 + \frac{2M^2}{r^2} - \frac{\tilde{Q}^2}{r^6} \right)^{\frac{1}{2}}; \quad f_{\text{EH}}(r) = 1 - \left(\tilde{\Lambda} r^2 + \frac{2M}{r^4} - \frac{\tilde{Q}^2}{r^8} \right) \quad (6.4.6)$$

The horizons of both of these black hole solutions correspond to the solution of the equations $f_{\text{GB}}(r) = 0$ and $f_{\text{EH}}(r) = 0$. The existence of three positive real roots of these equations can be easily realized from the Descarte rule of sign applied to the solutions of the above equations.

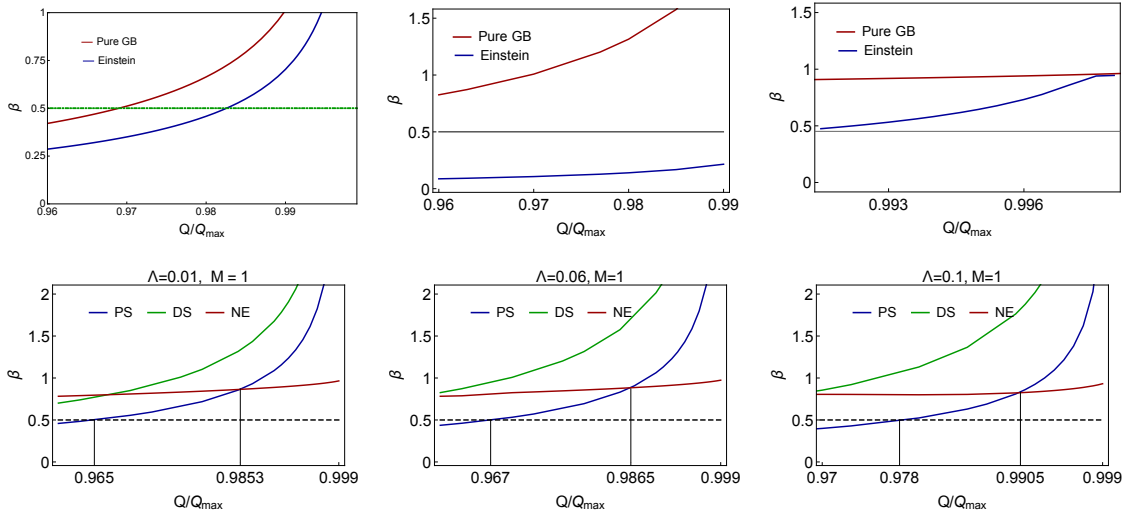


FIGURE 6.4: We have plotted $\{-(\text{Im } \omega_n)/\kappa_{\text{ch}}\}$ (for notational convenience, we have labeled the axis as β) for pure Gauss-Bonnet gravity as well as Einstein gravity, with the ratio (Q/Q_{max}) , for the photon sphere (top left), de Sitter (top middle) and near extremal (top right) modes. As evident, the strong cosmic censorship conjecture is violated in pure Gauss-Bonnet gravity. Furthermore, these plots also illustrate that the violation of strong cosmic censorship conjecture is stronger in pure Gauss-Bonnet gravity than the Einstein gravity in $d = 7$ dimensions. We have taken the mass to be unity and cosmological constant to be $\Lambda = 0.06$. In the bottom panel, we demonstrate the variation of $\{-(\text{Im } \omega_n)/\kappa_{\text{ch}}\}$ for seven-dimensional pure Gauss-Bonnet gravity with various choices of the cosmological constant. As this figure illustrates, the photon sphere mode always dominates for small values of (Q/Q_{max}) till the near extremal modes take over.

To study the validity of strong cosmic censorship in pure Lovelock theory, we follow an identical procedure adopted for the Einstein-Gauss-Bonnet case. We started by computing the quasi-normal modes and subsequently the ratio $\{-(\text{Im } \omega_n)/\kappa_{\text{ch}}\}$, whose minima provides an estimation for β . Then we plot the variation of β against electric charge (Q/Q_{max}) in Fig. 6.4 for all the three families of quasi-normal modes to illustrate the violation of strong cosmic censorship. The violation of strong cosmic censorship conjecture is clearly depicted in the above figure. To understand the effect of pure Lovelock terms further, we compared the value of $\{-(\text{Im } \omega_n)/\kappa_{\text{ch}}\}$ with that of general relativity. As evident from Fig. 6.4, the violation of strong cosmic censorship conjecture in a pure Lanczos-Lovelock theory occurs at smaller values of Q/Q_{max} in comparison with the similar solution for Einstein gravity in the same spacetime dimensions. Thus we can conclude that the violation of strong cosmic censorship is stronger in the presence of higher-order Lovelock terms. Initially, for smaller values of (Q/Q_{max}) the photon sphere modes dominates, while in the limit $(Q/Q_{\text{max}}) \rightarrow 1$, the near extremal mode takes over.

6.4.3 Four dimensional Einstein-Gauss-Bonnet Gravity

The Einstein-Gauss-Bonnet theory and its full Lovelock generalization discussed so far represents the low energy effective stringy correction over the Einstein-Hilbert action with the field equation containing the second derivative of the metric. The Gauss-Bonnet term in four dimensions turns out to be a total derivative, while in higher dimensions, it contributes to the gravitational field equation. However, recently the Einstein-Gauss-Bonnet theory in $d = 4$ has been reformulated as the $d \rightarrow 4$ limit of a higher dimensional theory after re-scaling the coupling constant as $\alpha \rightarrow \alpha/(d-4)$ [301]. The four-dimensional theory bypasses the Lovelock theorem and also is free of the Ostrogradsky instabilities. Note that several objections have been raised regarding the validity of the four-dimensional Gauss-Bonnet theory [302–304] and the regularization scheme used in Ref. [301], with all leading to the conclusion that no pure four-dimensional Einstein-Gauss-Bonnet theory exists. According to the Lovelock theorem, if there exists a consistent four dimensional version of Einstein-Gauss-Bonnet theory with two dynamical degrees of freedom, it must break the diffeomorphism invariance. In other words, the proposed four dimensional theory in Ref. [301] doesn't have a covariant prescription. Therefore, one possible approach to construct a consistent four dimensional Einstein-Gauss-Bonnet theory with two gravitational degrees of freedom as suggested in Ref. [305] would be to only demand invariance under three dimensional spatial diffeomorphism. In [305], the authors have proposed an ADM decomposition method to illustrate this idea and obtain a consistent four dimensional version of the Einstein-Gauss-Bonnet gravity. We refer the reader to Ref. [305] for more details. Several other regularization schemes have also been proposed with well defined $d \rightarrow 4$ limit [306–309].

The theory admits spherically symmetric charged black hole solutions in four dimensions and hence provides a natural alternative to general relativity [301, 306, 309, 310]. This has stimulated a series of recent work to further study several properties of the novel four-dimensional black hole solution in the Einstein-Gauss-Bonnet theory of gravity that includes thermodynamics, black hole shadow, stability, superradiance etc. [306, 311–319]. In this section, we extend our previous studies of the strong cosmic censorship in the presence of higher curvature terms to the regularized four-dimensional Einstein-Gauss-Bonnet gravity. Our study includes the case of both scalar and electromagnetic perturbations. Spherically symmetric black hole solutions of this theory is of the form Eq. (6.2.2), where the metric coefficients $f(r)$ is given by,

$$f(r) = 1 + \frac{r^2}{2\alpha} \left[1 - \sqrt{1 + 4\alpha \left(\frac{2M}{r^3} - \frac{Q^2}{r^4} + \frac{\Lambda}{3} \right)} \right] \quad (6.4.7)$$

The above spacetime admits three horizons namely the event horizon (r_+), the Cauchy horizon (r_-) and the cosmological horizon (r_c) given by the solution of the equation $f(r) = 0$, which is also ensured by the Descarte rule of sign. Given the above black hole solution, now we would like to understand the validity of strong cosmic censorship in the context of scalar and electromagnetic perturbations.

Scalar perturbation

To illustrate the validity of strong cosmic censorship conjecture in the four-dimensional Einstein-Gauss-Bonnet theory, we follow an identical line of approach taken for the previous two examples. Let us start by obtaining the quasi-normal modes of a test scalar perturbation on the above black hole background. To that end, we solve Eq. (6.3.3) w.r.t the black hole boundary condition by setting the spin parameter to be $s = 0$. We present the corresponding numerical values of $\{-(\text{Im } \omega_n)/\kappa_{\text{ch}}\}$ in Tab. 6.2 for all the three family of modes. The analytical results (obtained from the Lyapunov exponent) presented in the last column matches quite well with the numerical values of β . For each class of modes, β crosses the value (1/2) and hence the violation of strong cosmic censorship is evident.

α	Λ	Q/Q_{max}	$\ell = 0$	$\ell = 1$	$\ell = 10$	$\ell = 10$ (analytical)
0.1	0.01	0.99	0.83345	0.41607	0.61264	0.61042
		0.995	0.90112	0.63171	0.91967	0.92069
	0.05	0.99	0.80343	1.00052	0.56873	0.56829
		0.995	0.87892	1.52456	0.86028	0.86224
	0.2	0.99	0.86608	0.53995	0.76877	0.76847
		0.995	0.92425	0.80651	1.14142	1.11378
		0.99	0.88610	1.28742	0.75442	0.75292
		0.995	0.91084	1.93162	1.05611	1.06065
0.3	0.01	0.99	0.90122	0.68265	0.94530	0.93816
		0.995	0.94164	1.00844	1.39002	1.38595
	0.05	0.99	0.91747	1.61862	0.86334	0.86240
		0.995	0.93268	2.40133	1.28835	1.27295

TABLE 6.2: In this table we present the numerical values of $\beta \equiv \{-\min. (\text{Im } \omega_n)/\kappa_{\text{ch}}\}$ in the first three column ($\ell = 0, \ell = 1, \ell = 10$) for various choice of Gauss-Bonnet coupling constant (α), cosmological constant Λ and electric charge (Q/Q_{max}) for $M = 1$. In the last column we also give the value of β for the photon sphere modes computed from the corresponding analytical expression presented in earlier sections. The numerical and analytical value of β is clearly in close agreement.

Furthermore, we plot the variation of $\{-(\text{Im } \omega_n)/\kappa_{\text{ch}}\}$ with the ratio (Q/Q_m) in Fig. 6.5 for all the three family of modes to illustrate the violation of strong cosmic censorship conjecture in a more explicit manner. The photon sphere, de Sitter, and near extremal modes are depicted by blue, green and red lines, respectively. The de Sitter mode dominates the quasi-normal mode spectrum for smaller values of the cosmological constant, while in the extremal limit, the near extremal mode dominates. From Fig. 6.5, it is evident that the strong cosmic censorship conjecture is violated in

the near extremal region for charged de Sitter black hole (with respect to scalar perturbation) in four-dimensional Einstein-Gauss-Bonnet theory of gravity. Moreover, the effect of Gauss-Bonnet coupling constant on the violation of strong cosmic censorship is evident from both Tab. 6.2 and Fig. 6.5. The β value for the dominant mode appears to be increasing with the increasing strength of coupling α , suggesting that the violation of strong cosmic censorship conjecture is stronger for the larger value of the coupling.

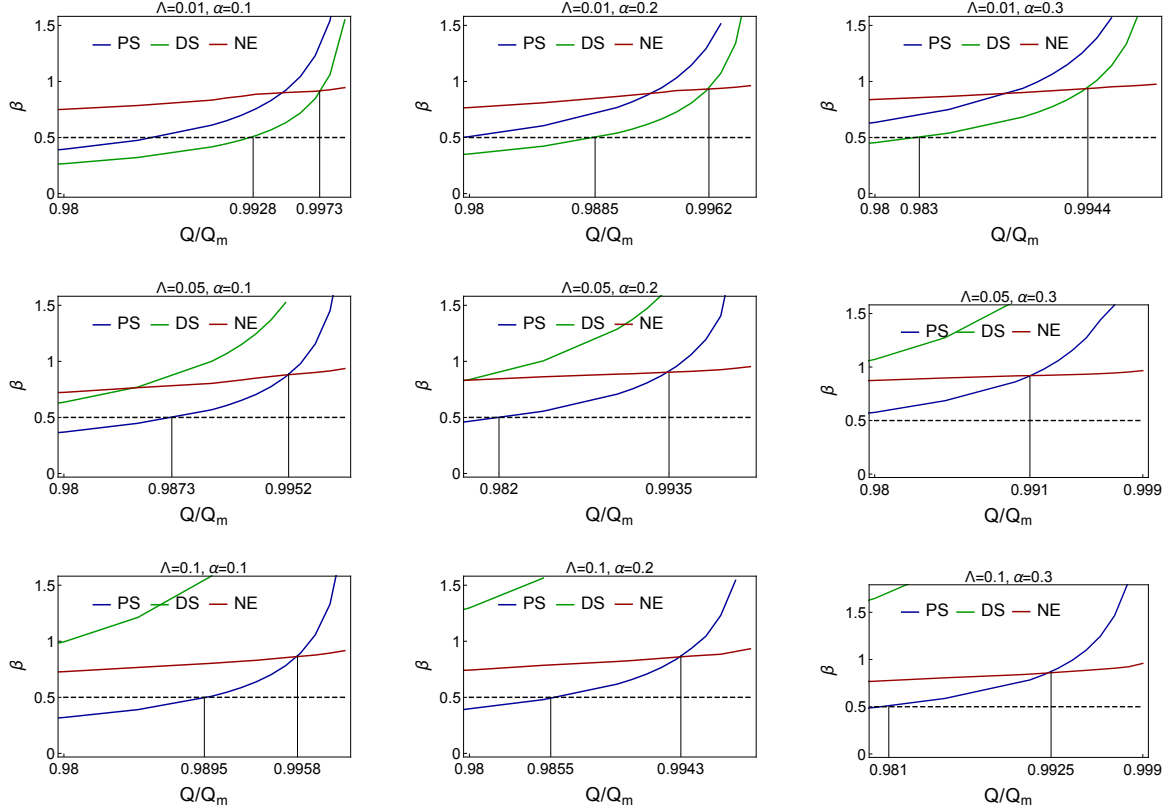


FIGURE 6.5: In this figure we demonstrate the variation of $\{-(\text{Im } \omega_n)/\kappa_{\text{ch}}\}$ against (Q/Q_m) for all three family of modes in the contest of scalar perturbation for various choice of cosmological constant(Λ) and the Gauss-Bonnet coupling constant(α). Mass of the black hole is taken to be unity.

Electromagnetic perturbation

Having studied the case of scalar perturbation, now we turn our attention to electromagnetic perturbation. For this case, one can obtain the quasi-normal modes by solving the master equation (Eq. (6.3.3)) with spin $s = 1$ and by imposing the black hole boundary conditions. Further we determine the β values (presented in Tab. 6.3) and plot is against (Q/Q_{\max}) in Fig. 6.6 to demonstrate the validity of strong cosmic censorship for both the photon sphere (blue) and de Sitter modes (green). Note that the quasi-normal mode spectrum for electromagnetic perturbation starts with the $\ell = 1$ mode. We find that the Christodulo version of the strong cosmic censorship conjecture is violated even for electromagnetic perturbation. Moreover, for the fixed charge ratio (Q/Q_m) and cosmological constant, the value of β corresponding to the dominant mode increases with increasing strength of the coupling constant. This further strengthens our earlier result that the violation of strong cosmic censorship conjecture is stronger in higher curvature theories irrespective of the spin of the perturbing field.

α	Λ	Q/Q_{\max}	$\ell = 1$	$\ell = 10$
0.1	0.01	0.99	0.83515	0.60985
		0.995	1.26678	0.91845
	0.05	0.99	2.02339	0.56784
		0.995	3.08332	0.85891
	0.2	0.99	1.08277	0.76770
		0.995	1.61730	1.14001
		0.99	2.60385	0.70718
		0.995	3.90682	1.05437
0.3	0.01	0.99	1.36892	0.94390
		0.995	2.02232	1.40167
	0.05	0.99	3.27373	0.86188
		0.995	4.85672	1.27599

TABLE 6.3: In this table we present the numerical values of $\beta \equiv \{-\min. (\text{Im } \omega_n)/\kappa_{\text{ch}}\}$ for the de Sitter modes ($\ell = 1$) and photon sphere modes ($\ell = 10$) corresponding to scalar perturbation for various choice of Gauss-Bonnet coupling constant (α), cosmological constant (Λ) and electric charge (Q/Q_{\max}). The mass (M) is taken to be unity.

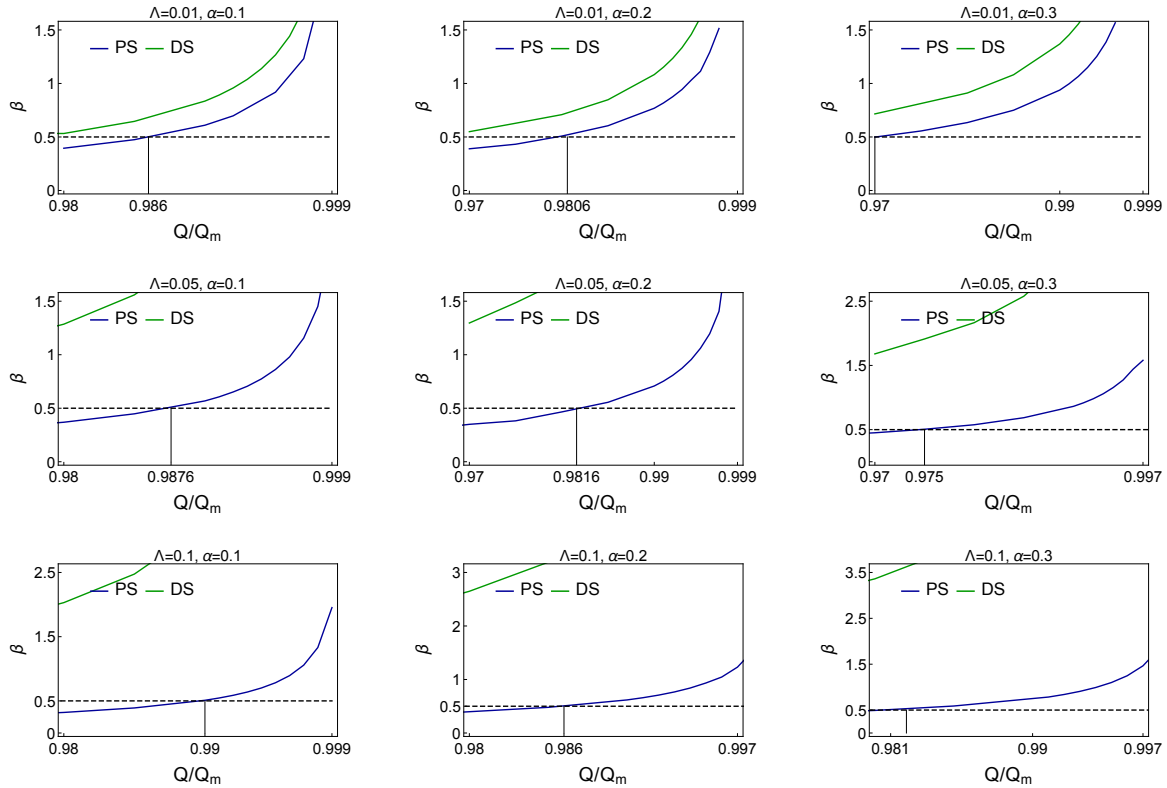


FIGURE 6.6: The variation of β is presented corresponding to electromagnetic perturbation for the de Sitter modes(green) and the photon sphere modes(blue) for various choice of cosmological constant(Λ) and the Gauss-Bonnet coupling constant(α). The vertical line represents the value of Q/Q_m where the violation of strong cosmic censorship conjecture occurs for the first time. The Mass parameter of the black hole is taken to be unity.

6.5 Summary

The strong cosmic censorship conjecture is an important theorem in mathematical relativity that ensures the deterministic nature of Einstein's theory. The conjecture is essentially the statement that any perturbation cannot be extended beyond the Cauchy horizon by keeping the Christoffel symbols as square-integrable functions. It further implies that spacetimes in general relativity are globally hyperbolic. However, in recent years it has appeared that the above version of strong cosmic censorship conjecture is violated for charged black hole spacetimes in the presence of a positive cosmological constant. This may imply that general relativity is not a deterministic theory, i.e., the classical fate of any observer is not completely determined from the initial data in general relativity. Since the higher curvature theories are one of the potential alternatives to general relativity, it would be interesting to understand the fate of strong cosmic censorship in such theories.

Following this motivation, in this chapter, we have presented a detailed analysis of the validity of strong cosmic censorship conjecture in the context of various higher curvature theories. In particular, we have considered asymptotically de Sitter black hole spacetimes in four and higher dimensional Einstein-Gauss-Bonnet gravity as well as the pure Lovelock gravity. We started by computing the quasi-normal modes in these spacetimes and subsequently obtained β corresponding to the lowest-lying modes. It is important to note that the Einstein-Gauss-Bonnet black hole solutions are only stable in the regime of small values of the coupling constant, which is the parameter space studied in this work. The violation of strong cosmic censorship conjecture has been illustrated by plotting β with the electromagnetic charge (Q/Q_{\max}). We find that the strong cosmic censorship conjecture is violated even in these theories. Moreover, our result also suggests that the violation of strong cosmic censorship conjecture seems to be stronger in higher curvature theories and the strength of violation increases with increasing strength of the higher curvature coupling constants. Since we have demonstrated this behaviour for three different class of higher curvature theories in four and higher dimensions, we can conjecture that the above result is a general property of any higher curvature theory of gravity.

Part II

Constraining Theories from Observations

Chapter **7**

Constraints on Higher Curvature Theories from Gravitational Wave Observations

This Chapter is based on, A. K. Mishra, M. Rahman, S. Sarkar, Constraints on higher curvature gravity from time delay between GW170817 and GRB 170817A, Phys. Rev. D 100 (2019) 8, 084054 [320].

The detection of gravitational waves by the LIGO Collaboration [13–18] in recent years has opened up a new paradigm of testing gravitational theories from strong field observations. This provides an unprecedented opportunity to constrain theories of gravity beyond general relativity. So far, no significant deviation from GR has been found in the weak-field regime through several precision tests [7]. However, the discoveries of gravitational waves allow us to test general relativity at the cosmological scales [321] as well as in the strong gravity regime. Such analysis often leads to interesting constraints on the strength of deviation from general relativity [15,322].

Among several observed gravitational wave signals by the LIGO-Virgo detectors, the GW 170817 [18] is the only binary neutron star merger event with an electromagnetic counterpart, namely the gamma-ray burst GRB 170817A [323]. Such a detection has marked the beginning of multimessenger astronomy, giving rise to interesting physics such as constraining gravitational theories beyond general relativity [132–140], probing the presence of extra dimensions [324,325]. The observed signal was from the merger of two neutron stars, with the total mass of the system being around $2.82^{+0.47}_{-0.09} M_{\odot}$. Also, the event was localized at a luminosity distance of 40 Mpc at redshift $z \sim 0.0099$. Interestingly, the Fermi gamma-ray space telescope detected the electromagnetic signal in the form of a short gamma-ray burst ~ 1.7 s after the gravitational wave signal. This time delay strongly constrain the difference in the speed of the gravitational wave and the electromagnetic signals to be less than $10^{-15}c$ [18]. As we have discussed previously in Chapter 1, the above difference in speed is indeed a non general relativity effect and often seen in theories with higher curvature corrections. Using this bound, constraints on several alternative theories were also obtained [132–140,326]. The possibility of explaining such a time delay by gravitational lensing was discussed in [327].

So far, general relativity has been proven to be tremendously successful in explaining gravitational interaction covering a wide range of length scales, particularly in the weak-field limit. However, despite such triumphs, there exist several motivations to look for physics beyond general relativity. We have discussed several such limitations of general relativity in [Chapter 1](#). As a result, the classical theory may only make sense as an effective theory, with higher curvature corrections in the low energy effective action [46, 47, 328]. Higher curvature theories represent one of the simplest possible modifications over general relativity, and various aspects of such theories have been extensively studied in the literature. Local tests involving the modification of Newton's law at short length scales, along with other astrophysical tests, has led to several interesting bounds on such theories [110–116]. The detection of gravitational waves provides another critical window to study the effect of higher curvature corrections at both cosmological scale and strong gravity regime.

In this chapter, we have developed a general formalism to constrain the higher curvature couplings using the observed time delay between GW 170817 and GRB 170817A. It is well known in the literature that, in a generic higher curvature theory, the gravitational and electromagnetic degree of freedom follows different geodesic while propagating on a curved spacetime [204–206, 208]. This effect may lead to a delay between gravitational and electromagnetic radiation. We study this phenomenon in detail and finally obtain a general expression for the time delay. As an illustration of our formalism, we consider the specific case of quadratic curvature theory in four dimensions and obtain a constraint on the coupling constant using the observed time delay. Our method is sufficiently general and can be extended to any higher curvature theory of gravity. Moreover, we also discuss how assumptions related to the intrinsic delay can influence the constraints.

7.1 A general framework for the time delay between Gravitational Wave and Electromagnetic signal

In this section, we provide a general expression for the time delay between the gravitational wave and electromagnetic signal. To arrive at our result, we follow an identical line of calculation developed in [208] and also discussed in [Appendix B](#). We start by considering the homogeneous and isotropic Friedmann–Lemaître–Robertson–Walker (FLRW) line element as the background spacetime metric, which is of the form,

$$ds^2 = -dt^2 + a^2(t) \left(dr^2 + r^2 d\Omega^2 \right) \quad (7.1.1)$$

where $a(t)$ represents the scale factor of the Universe and $d\Omega^2$ is the line element on S^2 . The electromagnetic signal travels along the null geodesics of the above metric. Note that the background spacetime is a solution of the field equation corresponding to the underlying theory of gravity. The causal structure of any theory of gravity is described by the characteristic hypersurfaces of the field equations. The characteristics hypersurface for general relativity turns out to a null surface, and as a result, the gravitational wave also follows the null geodesics of the metric given by [Eq. \(7.1.1\)](#). However, in the presence of higher curvature corrections, the study of characteristics of the perturbation equation shows that gravitational waves follow the null geodesic with respect to an effective metric instead of the physical metric [Eq. \(7.1.1\)](#) [204–206, 208]. In general, the effective graviton metric is of the following form,

$$ds_{\text{eff}}^2 = -U(t)dt^2 + a^2(t)V(t) \left(dr^2 + r^2 d\Omega^2 \right) \quad (7.1.2)$$

where $U(t)$ and $V(t)$ are functions of higher curvature terms and in the general relativity limit $U, V \rightarrow 1$.

Suppose that the electromagnetic signal is emitted from the source at the time t_E and is observed at t_O . Also, let the time delay between the observation of gravitational wave and electromagnetic signal be δt_O and let δt_E be the intrinsic delay in the emission of the gravitational wave at the source. Such an intrinsic delay may arise due to distinct emission processes of gravitational wave and electromagnetic radiations. As we shall demonstrate in subsequent sections, the intrinsic delay will play a significant role in constraining the theories beyond general relativity. According to our conventions, if the graviton arrives earlier, then δt_O is negative, while if it is emitted later then, δt_E is positive. By using the null geodesic w.r.t the background and the effective metric, one can finally arrive at the following expression,

$$\left(\frac{1}{a} \sqrt{\frac{U}{V}} \right) \Big|_{t_O} \delta t_O - \left(\frac{1}{a} \sqrt{\frac{U}{V}} \right) \Big|_{t_E} \delta t_E = \int_{t_E}^{t_O} \frac{1}{a} \left(1 - \sqrt{\frac{U}{V}} \right) dt \quad (7.1.3)$$

Also, we set the scale factor to be unity at the present time, i.e., $a(t_O) = 1$, and as a result, we have $a(t_E) = (1 + z_E)^{-1}$, where z_E refers to the redshift of the merger event. We can transform the time integral in Eq. (7.1.3) into a redshift integral and finally obtain,

$$\delta t_O = \delta t_E (1 + z_E) \sqrt{\frac{U_E V_O}{U_O V_E}} + \sqrt{\frac{V_O}{U_O}} \int_0^{z_E} \frac{dz}{H(z)} \left(1 - \sqrt{\frac{U(z)}{V(z)}} \right) \quad (7.1.4)$$

In the above expression we have used the notations $U(t_E) = U_E$, $V(t_E) = V_E$, $U(t_O) = U_O$, and $V(t_O) = V_O$. $H(z)$ is the Hubble parameter defined as $\dot{a}(t)/a(t)$ and expressed as a function of the redshift z . In the general relativity limit, the above expression for the time delay reduces to the redshifted intrinsic delay, as one would expect. Eq. (7.1.4) represents our main expression which will be used later in the chapter to set constraints on the modification over general relativity. Now our strategy would be to explicitly calculate the functions $U(z)$ and $V(z)$ for a particular theory of interest and compare the computed time delay with the observations.

In our analysis we consider the theory with the Lagrangian of the form,

$$\mathcal{L} = R + a R^2 + b R_{ab} R^{ab} + c R_{abcd} R^{abcd} \quad (7.1.5)$$

In four dimensions, one can use the Gauss-Bonnet theorem to express the last term in terms of the other two terms. Furthermore, a pure Ricci scalar² term does not change the causal structure of the theory. Therefore, in four dimensions, we need to consider the following theory:

$$\mathcal{L} = R + \alpha R_{ab} R^{ab} \quad (7.1.6)$$

The higher curvature coupling constant α is of the dimensions length². Note that any higher curvature theory, such as above, has many pathological features. Such theories in four dimensions suffer from perturbative ghosts [329], and as a result, the initial value problem may not be well-posed. In this work, we will treat the higher curvature terms to be the first-order correction of an effective

theory. Therefore, we will expand everything till the first order in α , neglecting the higher-order contributions. Following the general strategy discussed above, first, we will obtain the time delay up to the first order in α , and further, compare it with the observed delay. The formalism is completely general, and as evident, it can be repeated for any class of modified gravity with a small deviation from general relativity.

7.2 Time delay in higher curvature gravity

Having developed a general framework in the previous section, now we study the time delay in the context of a particular class of higher curvature theory described by the Lagrangian in Eq. (7.1.6). In this theory, the components of the effective metric take the form [330],

$$\begin{aligned} U &= \frac{1}{1 + \alpha H^2 \left(-3(1+z) \frac{HH'}{H^2} + 5 \right)} \\ V &= \frac{1}{1 + \alpha H^2 \left(-(1+z) \frac{HH'}{H^2} + 5 \right)} \end{aligned} \quad (7.2.1)$$

where we have expressed everything in terms of the redshift z , and a prime here denotes derivative with respect to z . To further obtain the time delay, we use the above expression of the components of effective graviton metric (Eq. (7.2.1)) and expand it as a power series in α . Note that, at each order in α , the metric coefficients can be computed by perturbatively solving the Friedmann equation of the higher curvature theory (Eq. (7.1.6)). Since the redshift z is an observable, we will take it as our variable to express various quantities. Therefore we express the Friedmann equation completely as a function of z and solve it perturbatively order by order in α . We assume the Hubble parameter $H(z)$ to admit the following expansion:

$$H(z) = H_G(z) + \alpha h(z) + \mathcal{O}(\alpha^2) \quad (7.2.2)$$

At zeroth-order, we have $H(z) = H_G(z)$, which is the Hubble parameter for general relativity. The first-order perturbation $h(z)$ can be obtained by solving the Friedmann equation of the quadratic curvature theory (Eq. (7.1.6)) with the boundary condition $h(0) = 0$. This is equivalent to the assumption that the theory at the present epoch is predominantly general relativity and the effects of higher curvature terms are dominant at higher redshifts. Most importantly, this guarantees that the present day density parameter for dark energy (Ω_Λ) is equal to 0.7 and that of the matter (Ω_m) to be 0.3. We would like to emphasize here that the above boundary condition is only a particular choice. However, since we are only interested in results up to $\mathcal{O}(\alpha)$, the explicit form of $h(z)$ is not required for our analysis. The final results up to linear order in α can be expressed in terms of the general relativity solution $H_G(z)$ only, i.e., we need not solve the full Friedmann equation of the quadratic curvature theory under consideration.

Since α has the dimension of length², it is convenient to construct a dimensionless small parameter $\eta = \alpha H_G^2(0)$ in the natural units and expand everything in terms of η . In the general relativity limit, we have $\eta = 0$ and any non-vanishing value of η would measure the strength of higher curvature coupling α with respect to the characteristic size of the background universe. We hope to

constraint this dimensionless parameter from the time delay observation. Note that the intrinsic delay may also depend on the higher curvature coupling. Further assuming that δt_O and δt_E admits series expansion in terms of η , and equating terms at various order in Eq. (7.1.4), one finally arrives at the following expressions,

$$\begin{aligned} \text{Order } \eta^{(0)} : \quad & \delta t_O^{(0)} = \delta t_E^{(0)}(1 + z_E) \\ \text{Order } \eta^{(1)} : \quad & \delta t_O^{(1)} = - \int_0^{z_E} (1+z) H'_G dz + \delta t_E^{(1)}(1 + z_E) \\ & + \delta t_E^{(0)}(1 + z_E) \left(H'_G(z_E) H_G(z_E) - H'_G(0) H_G(0) \right) \end{aligned} \quad (7.2.3)$$

where the numbers in superscripts represent perturbation order. The $\mathcal{O}(\eta^0)$ equation represents the general relativity case where no contribution from the higher curvature terms appears, and as a result, the observed time delay is nothing but the redshifted value of the intrinsic time delay. The $\mathcal{O}(\eta)$ equation represents the first-order correction to the general relativity expression of the time delay. As we have discussed earlier, the net observed delay between the gravitational wave and electromagnetic signal can originate from two sources. The first one is purely astrophysical and depends on the detailed mechanism of gamma-ray bursts. The other source of such delay could be either from the presence of higher curvature terms, Shapiro effect or lensing. The former one involves the complex emission mechanism of the gamma-ray burst, which is not a completely understood phenomenon. Among several models of the gamma-ray burst process, the relativistic fireball model is the most accepted one. In the fireball framework, part of the gravitational energy released due to the merger process is assumed to be utilized to form a fireball which comprised of e^\pm , baryons and gamma rays. The fireball must also expand relativistically with a high Lorentz factor (Γ), with respect to the central engine, to avoid depletion due to $\gamma\gamma$ interactions [331, 332]. As a result, the gamma-ray emission can occur from a position away from the central core. Interestingly, this distance appropriately converted to time by taking the Lorentz factor into account can attribute to an intrinsic time delay [333].

In the absence of a complete understanding of the gamma-ray emission process, an independent estimation of the intrinsic delay is difficult to obtain. Therefore in our analysis, we assume that the intrinsic delay can be completely accounted for by keeping a term like δt_E in Eq. (7.2.5) and concentrate more on the part of the delay arising from the presence of higher curvature terms. However, note that the intrinsic time delay cannot be separated completely from the delay arising due to the modification of gravity. This is because of the fact that the intrinsic delay undergoes a redshift due to cosmological expansion that depends on the underlying theory of gravity. Nevertheless, to obtain an initial estimate, we can start with the assumption that the intrinsic delay does not depend on the higher curvature coupling constant α . This is the case when the astrophysical processes discussed above does not depend on the theory of gravity. In this assumption, we have the following simplified expression for the observed time delay,

$$\delta t_O = \delta t_E(1 + z_E) [1 + \alpha (H'_G(z_E) H_G(z_E) - H'_G(0) H_G(0))] - \alpha \int_0^{z_E} (1+z) H'_G dz \quad (7.2.4)$$

The above equation relates the intrinsic delay and the observed delay up to the first order in η . Given

the intrinsic delay, δt_E at the source, Eq. (7.2.5) can be used to determine the quantity η . Further upon substituting $H_G(z) = H_G(0)\sqrt{\Omega_m(1+z)^3 + \Omega_\Lambda}$ and putting various parameters for the GW 170817 merger event, we obtain,

$$\eta = \frac{\delta t_O - 1.0099 \delta t_E}{0.00904275 \delta t_E - 0.00451145 t_H} \quad (7.2.5)$$

where the quantity $t_H = 1/H_G(0)$. In the absence of any prior knowledge of the intrinsic time delay, we can only get an estimate of η for various trial values of δt_E . Let us start with an initial guess of $\delta t_E = 0$, which will provide an estimate of the upper bound for η . Then, using the appropriate factors for the speed of light c , one obtains

$$\eta = \frac{\alpha H_G^2(0)}{c^2} \leq 8.5 \times 10^{-16} \quad (7.2.6)$$

The above bound on η translates into an upper bound on the coupling constant as $\alpha \leq 10^{36} m^2$, which is obviously a weak bound. Several other precession experiments involving local and astrophysical tests have led to even stronger bounds on various modified gravity models [110–116, 334]. A similar weak constrain was also obtained in [326] by using the bound on the speed of the gravitational wave in the context of Born Infeld theory of gravity, where matter and gravity are non linearly coupled.

Although the bound obtained in this work is a weak constraint, our result is important due to the following reasons: Firstly, this is a bound directly coming from cosmological considerations that constraints the coupling constant compared to the scale of the Universe, while most of the other bounds involve local tests. For example, in the Newtonian approximation, the contribution to the gravitational potential coming from the higher curvature terms are of Yukawa type. The Eöt-Wash experiment attempts to verify such Yukawa-like corrections by measuring possible departure from the Newtonian potential in the Laboratory. In fact, the $R_{ab}R^{ab}$ theory also introduces a similar additional term [109]. The Eöt-Wash experiment puts an upper bound $\lesssim 2 \times 10^{-9} m^2$ on the parameter in the Yukawa term [110]. However, these experiments cannot uniquely constrain the coupling of $R_{ab}R^{ab}$ theory since the contribution to the Yukawa type correction will come from all possible higher curvature interactions of the form given in Eq. (7.1.5). On the other hand, our analysis provides the possibility of obtaining a constraint on the coupling strength of $R_{ab}R^{ab}$ term only. Moreover, if we use the bound obtained from the Eöt-Wash experiment in our formula, we get $\delta t_O - \delta t_E \sim 10^{-52} s$, which implies that the observed time delay is entirely due to the redshifted intrinsic delay. Similarly, planetary precession rates put the upper bound $\lesssim 1.2 \times 10^{18} m^2$ on the coupling of the Ricci scalar² theory. Using such bound in our analysis leads to $\delta t_O - \delta t_E \sim 10^{-19} s$. Note that the above bounds are obtained in the context of a pure $f(R)$ theory of gravity, which we are using here to obtain a rough estimate of the intrinsic time delay. To the best of our knowledge, Eq. (7.2.6) is the only bound so far available for the $R_{ab}R^{ab}$ theory alone. A relatively simpler version of our analysis could be comparing the velocities of gravitational wave and electromagnetic radiation, as performed in most previous works. The velocity of gravitational wave obtained from Eq. (7.1.2) is given by $\sqrt{U/V}$. Since this is a function of the redshift parameter z , one needs to integrate over the entire path to arrive at the final expression for the time delay, which has been done in our analysis. However, a rough estimation can be obtained as follows. Since the maximum deviation from general relativity occurs at $z = z_E$, one can obtain a bound on η or α by equating this value with the observed difference between the speed of the gravitational wave and light ($10^{-15} c$), i.e., by setting $\eta \Omega_m(1+z_E)^2 \approx 10^{-15}$. This will further

lead to a bound of the same order as we have obtained in this work. However, for comparatively more accuracy, one needs to perform the full integration appropriate for sources at higher redshifts.

7.3 Summary

Higher curvature theories are one of the most straightforward extensions of general relativity. It is expected that the low energy effective action of a fully consistent quantum theory of gravity would contain higher curvature invariants as corrections over the Einstein-Hilbert action functional. These terms will be dominant at higher energy scales giving rise to new phenomenological effects. One such interesting non general relativity effect is the difference in the speed of gravitational waves and electromagnetic radiation. In this chapter, we consider one of the simplest models of higher curvature theory given by Eq. (7.1.6), which contributes to the path difference between gravitational wave and electromagnetic wave. Such a path difference further results in a time delay between the arrival of gravitational waves and the associated electromagnetic radiation at the Earth-based detectors. The recently observed event GW 170817 and the corresponding electromagnetic counterpart GRB 170817A is a model system where we can study this effect. It was observed that the electromagnetic radiation arrived around 1.7 s after the gravitational wave detected by the LIGO-Virgo detectors. We started our analysis by obtaining a general expression for the time delay up to first order in the higher curvature coupling. We also assume the existence of an intrinsic delay at the source due to various astrophysical effects, and the net observed time delay is given by Eq. (7.2.5). This expression for the time delay is sufficiently general and can be applied to any source of gravitational waves with a known electromagnetic counterpart.

To obtain the higher curvature coupling accurately using Eq. (7.2.5), we need to know the intrinsic delay at the source. However, our limited understanding of the process of gamma-ray burst is not sufficient to provide such information accurately. Therefore, to proceed further, we use various reasonable physical assumptions to obtain an upper bound on the strength of coupling constant α compared to the characteristic scale of the Universe, i.e., in terms of the present day Hubble constant. Unlike various other local experiments, which puts bound on a particular combination of the couplings of R^2 and $R_{ab}R^{ab}$ terms, our result can uniquely bound the coefficient of $R_{ab}R^{ab}$ term. This is because a theory with R^2 modification cannot cause any path difference, at least in the linear order of the coupling parameter. Although we cannot determine the intrinsic delay accurately, the mechanisms which led to such a delay indicates that the gravitational wave should be emitted before the electromagnetic radiation. As per our convention, this would correspond to $\delta t_E < 0$. Furthermore, if we also assume the coupling constant to be positive i.e., $\alpha > 0$, from Eq. (7.2.5) we obtain $|\delta t_E(1 + z_E)| \leq |\delta t_O|$ with the equality sign representing general relativity. This is because in a higher curvature theory with a positive value of the coupling constant, the gravitational wave propagates faster than the electromagnetic radiation. So both the effects are working in the same direction.

Note that, as we have discussed previously, the intrinsic delay might also depend on the higher curvature coupling. One must then be able to expand it as a function of η , and the terms $\delta t_E^0, \delta t_E^1, \dots$, in Eq. (7.2.3) can be identified as the coefficient of such expansion. Although we have not taken this into account in obtaining our final result, Eq. (7.2.3) has this case incorporated. In this case, the contribution to the observed delay (δt_O) from the higher curvature terms will crucially depend on an intrinsic scale set by the gamma-ray burst physics. It would be an interesting exercise to understand this case in detail where there are two scales at play, one being the scale of the higher

curvature corrections set by the coupling constant α , and an intrinsic scale, set by the physics of gamma-ray burst process. Using the parameters of the binary neutron star merger event GW170817, Eq. (7.2.5) provides a weak constraint on the strength of higher curvature coupling. However, it is expected that the formalism developed in the present chapter would result in a much stronger bound in the future when we have more sources of simultaneous gravitational wave and electromagnetic radiation emissions. Also, the methodology can be extended to any modified theory of gravity for which the form of the effective graviton metric is known. At the same time, the result can be used to precisely estimate the intrinsic delay. This could be very useful to understand the complex physics of gamma-ray bursts.

Chapter 8

Constraining the tidal charge parameter of a Braneworld Black hole

8.1 Introduction and Motivation

In the previous chapters, we have explored various interesting aspects of modified gravity with higher curvature corrections over general relativity. In this chapter, we concentrate on the modification of general relativity due to the presence of extra spatial dimensions. In the framework of string theory, gravity is described as a higher-dimensional interaction that appears to be effectively four-dimensional in the low energy limit. Such ideas have lead to the proposal of several brane-world models which describes the four-dimensional Universe to be embedded in a higher-dimensional spacetime [335–337]. In this terminology, the higher dimensional spacetime is known as the bulk, while the four-dimensional spacetime is referred to be the brane. In the brane-world scenario, all the non-gravitational matter fields are confined to the brane, whereas gravity alone can probe the extra dimensions. Unlike the five-dimensional Randall-Sundaram model [338,339], the extra dimension in the brane-world scenario need not be compact and, in general, can be arbitrarily large.

The gravitational dynamics on the brane is governed by the four-dimensional field equation, which is the projection of the bulk Einstein's equations on the brane. Interestingly, the field equations possess exact localized black hole solutions on the brane, which resemble the identical structure of the Reissner-Nordström and Kerr-Newman solution of general relativity with the crucial difference being the electromagnetic charge getting replaced by a tidal charge [335,340–342]. Unlike the electric charge, the tidal charge parameter takes only negative values and carries an imprint of the bulk Weyl tensor. In the general relativity limit, the tidal charge parameter vanishes.

The primary motivation for introducing brane-world models was to resolve the hierarchy problem, i.e., to explain the origin of the large discrepancy between the weak force and gravity [338,339,343,344]. However, later studies have resulted into various interesting applications of the brane-world models in the context of black holes [255,345–348], cosmology, gravitational waves [349–352] etc. Several previous works have also reported interesting constraints on the tidal charge parameter [352–357]. In this article, we develop a general formalism to constrain the tidal charge parameter of a rotating brane-world black hole from gravitational wave observations. In particular, by using

the quasi-normal mode spectrum corresponding to the GW 150914 event [15], we obtain a novel upper bound on the strength of the tidal charge. Our strategy would be to compute the quasi-normal mode frequency of the dominant gravitational perturbation ($\ell = 2, m = 2, n = 0$ mode) on a rotating brane-world black hole background for various values of the tidal charge and compare it with the observed quasi-normal mode spectrum of the GW 150914 event.

The rest of the article is arranged as follows: In [Section 8.2](#) we review the brane-world models and discuss the rotating black hole solutions. Then we compute the quasi-normal frequency using the continued fraction method in [Section 8.3](#). Finally, comparison with the GW 150914 event and the resulting constraint has been presented in [Section 8.4](#). We conclude with a discussion on our results and possible future directions.

8.2 Brief review of rotating braneworld black hole

Let us start with a brief overview of the effective gravitational field equations on the brane and the spacetime geometry of rotating black hole solution arising out of these field equations. In this scenario, the gravitational dynamics in the five-dimensional bulk spacetime is described by Einstein gravity. The effective four-dimensional field equation on the brane is the projection of the bulk Einstein's equation with appropriate projector, i.e., of the form $h_B^A = \delta_B^A - n^A n_B$, where n_A is the unit normal to the brane hypersurface, satisfying $n_A n^A = 1$. This results into the following effective gravitational field equations on the brane,

$${}^{(4)}G_{\mu\nu} + E_{\mu\nu} = 8\pi G T_{\mu\nu} + \Pi_{\mu\nu} \quad (8.2.1)$$

Here, $E_{\mu\nu} = W_{ABCD} n^A e_\mu^B n^C e_\nu^D$ is the modification over the Einstein's equation with W_{ABCD} being the bulk Weyl tensor and $T_{\mu\nu}$ represents the matter-energy tensor on the brane. Additionally, the tensor $\Pi_{\mu\nu}$ appearing in the effective gravitational field equations presented above, is a quadratic combination of $T_{\mu\nu}$ (e.g., it involves terms like, $T_{\mu\alpha} T_\nu^\alpha$, $T T_{\mu\nu}$ etc). Since we will be interested in vacuum solutions, we work with $T_{\mu\nu} = 0$ and as a result, the field equation on the brane reduces to,

$${}^{(4)}G_{\mu\nu} + E_{\mu\nu} = 0 \quad (8.2.2)$$

Note that, due to the symmetries of the Weyl tensor, $E_{\mu\nu}$ is traceless, and due to Bianchi identity, it is also divergence free. Both of these properties hold true for the electromagnetic stress-tensor as well. As a result, the black hole solutions of the above field equations resemble the Kerr Newman family of black holes. However, there is one crucial sign difference. The electromagnetic stress-energy tensor appears on the right-hand side of the field equations, while in this case, $E_{\mu\nu}$ appears on the left-hand side. Interestingly, [Eq. \(8.2.2\)](#) admits exact rotating black hole solution of the form,

$$ds^2 = -\frac{\Delta}{\Sigma}(dt - a \sin^2 \theta d\phi)^2 + \Sigma \left[\frac{dr^2}{\Delta} + d\theta^2 \right] + \frac{\sin^2 \theta}{\Sigma} \left[a dt - (r^2 + a^2)d\phi \right]^2 \quad (8.2.3)$$

where, $\Delta \equiv r^2 + a^2 - 2Mr + \beta$ and $\Sigma \equiv r^2 + a^2 \cos^2 \theta$. For the case of Kerr-Newman black hole, the tidal charge parameter β can be identified with the square of the black hole charge, i.e., $\beta|_{KN} = Q^2$. However, in the braneworld scenario, β can take negative values as well. This is the key feature for the braneworld black holes, which we wish to explore in detail in this work from the perspective of

quasi-normal modes.

Let us briefly discuss some other interesting properties of these solutions. The above braneworld black hole has two horizon located at, $r_{\pm} = M \pm \sqrt{M^2 - a^2 - \beta}$. In the non-rotating case with $\beta < 0$, there is only *one* horizon, which is in contrast with the case of Reissner-Nordström black hole. Also, in the rotating case, the parameters must satisfy $(a/M)^2 \leq 1 - (\beta/M^2)$ for the existence of horizons. For negative values of β , (a/M) can be larger than unity, which is again in sharp contrast with the Kerr-Newman black hole. Furthermore, a negative value of the tidal charge has implications in various other astrophysical scenarios. In this work, we concentrate on the effect of the tidal charge on the quasi-normal mode spectrum. For this purpose, we present the computation of the quasi-normal modes for braneworld black holes in the next section.

8.3 Quasi-normal modes of a rotating braneworld black hole

We discussed the spacetime geometry of a rotating braneworld black hole in the previous section. Here we shall present the numerical method for obtaining quasi-normal modes. For simplicity, we shall assume $2M = 1$ in this section, and all the factors involving the mass of the black hole will be restored later. The perturbation equation of a spin ' s ' filed on the above black hole background is separable. The decoupled radial and angular equation takes the following form,

$$\frac{d}{du} \left[\left(1 - u^2\right) \frac{dS_{\ell m}}{du} \right] + \left[(a\omega u)^2 - 2a\omega su + s + A_{\ell m} - \frac{(m+su)^2}{1-u^2} \right] S_{\ell m} = 0 \quad (8.3.1)$$

$$\begin{aligned} \Delta \left(\frac{d^2 R_{\ell m}}{dr^2} \right) + (s+1)(2r-1) \left(\frac{dR_{\ell m}}{dr} \right) + & \left[- \left\{ a^2 + \beta + (r-1)r \right\} \left\{ A_{\ell m} + \omega \left(a^2\omega - 2am - 4irs \right) \right\} \right. \\ & \left. - i(2r-1)s \left\{ \omega \left(a^2 + r^2 \right) - am \right\} + \left\{ am - \omega \left(a^2 + r^2 \right) \right\}^2 \right] R_{\ell m} = 0 \end{aligned} \quad (8.3.2)$$

The spin parameter s takes values $(0, -1, -2)$ for scalar, electromagnetic and gravitational perturbations respectively and $u \equiv \cos \theta$. $A_{\ell m}$ is the separation constant which reduces to $\ell(\ell+1) - s(s+1)$ in the limit of vanishing rotation parameter a .

The above pair of differential equations can be solved to obtain $(\omega, A_{\ell m})$ by setting appropriate regularity and boundary conditions. For the angular equation, the relevant boundary condition are the finiteness of $S_{\ell m}$ at the regular singular points of the equation, i.e., at $(u = 1, -1)$. With this, we can employ Leaver's method, which is equivalent to finding a series solution of the angular equation. Given the regular singular points, the series solution to the angular equation can be expressed as,

$$S_{\ell m}(u) = e^{a\omega u} (1+u)^{k_1} (1-u)^{k_2} \sum_{n=0}^{\infty} c_n (1+u)^n \quad (8.3.3)$$

where, $k_1 = \frac{1}{2}|m-s|$ and $k_2 = \frac{1}{2}|m+s|$. The expansion coefficients c_n in the above series solution, are related by the following three term recurrence relation,

$$\alpha_n^{(\theta)} c_{n+1} + \beta_n^{(\theta)} c_n + \gamma_n^{(\theta)} c_{n-1} = 0, \quad (n = 1, 2, 3, \dots) \quad (8.3.4)$$

The coefficients $\alpha_n^{(\theta)}$, $\beta_n^{(\theta)}$ and $\gamma_n^{(\theta)}$, appearing in the above recurrence relation are of the following form,

$$\alpha_n^{(\theta)} = -2(n+1)(2k_1+n+1) \quad (8.3.5)$$

$$\begin{aligned} \beta_n^{(\theta)} &= -\left[a^2\omega^2 + (s+1)s + A_{\ell m}\right] + 2n(-2a\omega + k_1 + k_2 + 1) \\ &\quad - [2a\omega(2k_1+s+1) - (k_1+k_1)(k_1+k_1+1)] + (n-1)n \end{aligned} \quad (8.3.6)$$

$$\gamma_n^{(\theta)} = 2a\omega(k_1+k_2+n+s) \quad (8.3.7)$$

The series solution to the radial equation can be obtained by setting the black hole boundary conditions — perturbations are purely ingoing at the event horizon and purely outgoing at spatial infinity. Thus the series solution, with regular singular points at $r = r_{\pm}$, takes the following form,

$$R_{\ell m}(r) = e^{i\omega r} (r - r_+)^{-s-i\sigma_+} (r - r_-)^{-1-s+i\omega+i\sigma_+} \sum_{n=0}^{\infty} d_n \left(\frac{r - r_+}{r - r_-}\right)^n \quad (8.3.8)$$

where, $r_{\pm} = (1/2)(1 \pm b)$ are the horizon locations. Here, $b \equiv \sqrt{1-4(a^2+\beta)}$ and $\sigma_+ \equiv (1/b)[\omega(r_+ - \beta) - am]$. By substituting the above series solution in the radial equation (Eq. (8.3.2)), we obtain the following three term recurrence relation,

$$\alpha_n^{(r)} d_{n+1} + \beta_n^{(r)} d_n + \gamma_n^{(r)} d_{n-1} = 0, \quad (n = 1, 2, 3, \dots). \quad (8.3.9)$$

with the coefficients $\alpha_n^{(r)}$, $\beta_n^{(r)}$ and $\gamma_n^{(r)}$ are given by,

$$\begin{aligned} \alpha_n^{(r)} &= (n+1) \left[-2i\beta\omega\sqrt{-4a^2-4\beta+1} + i\omega\sqrt{-4a^2-4\beta+1} - 2iam\sqrt{-4a^2-4\beta+1} \right. \\ &\quad \left. + (n+1)(4a^2+4\beta-1) \right] - (n+1)(4a^2+4\beta-1)(s+i\omega) \end{aligned} \quad (8.3.10)$$

$$\begin{aligned} \beta_n^{(r)} &= -4a^4\omega^2 - 8a^3m\omega - 4\omega^2\sqrt{-4a^2-4\beta+1} + 12\beta\omega^2\sqrt{-4a^2-4\beta+1} \\ &\quad - 2i\omega\sqrt{-4a^2-4\beta+1} + 6i\beta\omega\sqrt{-4a^2-4\beta+1} - 4in\omega\sqrt{-4a^2-4\beta+1} \\ &\quad + 2am \left[i\sqrt{-4a^2-4\beta+1} + 2\sqrt{-4a^2-4\beta+1}(\omega+in) - 4\beta\omega + \omega \right] \\ &\quad + 12i\beta n\omega\sqrt{-4a^2-4\beta+1} + (1-4\beta)[A_{\ell m} + 2n(n+1)+s+1] \\ &\quad - 4(4\beta^2-5\beta+1)\omega^2 + 2i(4\beta-1)(2n+1)\omega \\ &\quad + a^2 \left\{ \omega \left(8\sqrt{-4a^2-4\beta+1} - 20\beta + 17 \right) + 4i \left(\sqrt{-4a^2-4\beta+1} + 2 \right) \right\} \\ &\quad + 8in \left\{ \omega \left(\sqrt{-4a^2-4\beta+1} + 2 \right) + i \right\} \Big] - (4A_{\ell m} + 8n^2 + 4s + 4)a^2 \end{aligned} \quad (8.3.11)$$

$$\begin{aligned} \gamma_n^{(r)} &= (n-2i\omega) \left[-2i\beta\omega\sqrt{-4a^2-4\beta+1} + i\omega\sqrt{-4a^2-4\beta+1} - 2iam\sqrt{-4a^2-4\beta+1} \right. \\ &\quad \left. + 4a^2(n+s-i\omega) \right] + (n-2i\omega)(4\beta-1)(n+s-i\omega) \end{aligned} \quad (8.3.12)$$

Now we can solve the radial and angular three term recurrence relation simultaneously to obtain the separation constant ($A_{\ell m}$) and the quasinormal frequencies (ω) by using the continued fraction method. Note that, the real part of the quasinormal frequency represents oscillation frequency, while the imaginary part is related to the decay time. Following [358], we use,

$$f_{\ell mn}(\text{Hz}) = \frac{1}{2\pi} \frac{c^3 \omega}{2GM(1+z)} \quad \text{and} \quad \tau(\text{ms}) = \frac{2GM(1+z)}{c^3 \omega} \times 10^3 \quad (8.3.13)$$

The numerical values of the quasinormal frequencies and corresponding oscillation frequency and decay time are shown in Tab. 8.1 for gravitational perturbation($s=-2$) for various values of tidal charge parameter β . The spin and mass of the final black hole are taken to be $a = 0.67^{+0.05}_{-0.07}$ and $M = 62^{+4}_{-4} M_\odot$, i.e., the remnant of the GW 150914 event. We discuss this observation in detail subsequently. The redshift of the event is given by $z = 0.093^{+0.030}_{-0.036}$.

ℓ, m	$-\beta$	ω_r	$-\omega_i$	Decay time scale(ms)	Frequency(Hz)
$\ell = 2, m = 2$	0	1.039711	0.163690	4.069	248.395
	0.05	0.963809	0.163932	4.063	230.261
	0.1	0.905704	0.162635	4.096	216.380
	0.15	0.858954	0.160679	4.146	205.211
	0.2	0.820065	0.158443	4.204	195.920
	0.25	0.786925	0.156107	4.267	188.002
	0.3	0.758165	0.153765	4.332	181.131
	0.35	0.732845	0.151463	4.398	175.082
	0.4	0.710292	0.149226	4.464	169.694
	0.45	0.690011	0.147066	4.529	164.849
	0.5	0.671623	0.144988	4.594	160.456
	0.55	0.654837	0.142992	4.658	156.446
	0.6	0.639422	0.141076	4.722	152.763
	0.65	0.625192	0.139238	4.784	149.363
	0.7	0.611995	0.137475	4.845	146.210
	0.75	0.599706	0.135782	4.906	143.274
	0.8	0.58822	0.134157	4.965	140.530
$\ell = 3, m = 3$	0	1.64959	0.168181	3.92107	394.109
	0.05	1.54121	0.16998	3.91915	348.185
	0.1	1.45737	0.169987	3.91899	348.185
	0.15	1.38932	0.169127	3.93892	331.927
	0.2	1.33226	0.167821	3.96959	318.295
	0.25	1.283312	0.166279	4.00638	306.003
	0.3	1.240552	0.164621	4.04673	296.384
	0.35	1.20269	0.162912	4.08919	287.339
	0.4	1.168812	0.161192	4.13282	279.244
	0.45	1.138176	0.159484	4.17708	271.924
	0.5	1.11029	0.157804	4.22155	265.263
	0.55	1.08473	0.156166	4.26599	259.071
	0.6	1.061172	0.154556	4.31027	253.528
	0.65	1.035172	0.152688	4.36321	247.316
	0.7	1.01904	0.151478	4.39785	243.462
	0.75	1.000172	0.150121	4.43941	238.930
	0.8	0.982296	0.148577	4.48372	234.684

TABLE 8.1: In this table we present the numerical values of the quasi-normal frequency corresponding to the modes ($n=0, l=m=2$) and ($n=0, l=m=3$) for gravitational perturbation($s=-2$). We have taken the spin parameter to be $a = 0.67$ and mass of the remnant as $M = 62M_\odot$. The redshift factor (z) here is 0.093.

For completeness, let us plot the associated quasi-normal frequencies. Fig. 8.1 shows the real and imaginary part of the quasi-normal modes corresponding to different values of β and the spin parameter.

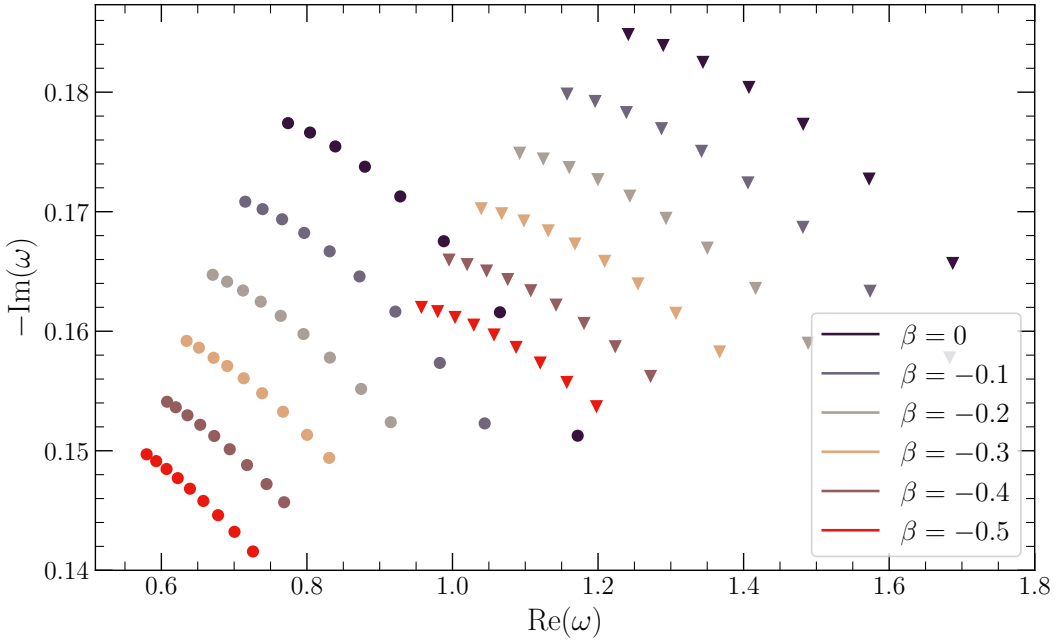


FIGURE 8.1: In this figure we have plotted the real and imaginary parts of the quasi-normal frequency $\omega_{n\ell m}$ for different choices of the tidal charge β . The left side of the plot is for the fundamental $\ell = 2 = m$ mode (denoted by circular dots), while the plot on the right is for the excited $\ell = 3 = m$ mode (denoted by triangles). For each value of β , the points refer to the spin parameter having values, $a = 0.1, 0.2, 0.3, \dots, 0.9$ (left to right). As evident, with the increase of $|\beta|$, the decrease in $(\text{Re } \omega_{n\ell m})$ is smaller than the decrease in $(\text{Im } \omega_{n\ell m})$.

8.4 Bounds from GW 150914

The observation of gravitational waves by the LIGO-Virgo detectors in the last five years has allowed us to test predictions of general relativity in the highly dynamical strong-field regimes of gravity. One particular class of such tests focus on measuring properties of the remnant black hole, like the final mass, spin and the quasi-normal frequencies. These measurements can further be confronted with the predicted values from general relativity or any modified theory of gravity. In Ref. [1, 2, 359] two complementary Bayesian techniques have been developed to measure the remnant properties of black holes. The first method, called PyRing ([359], Section VII A.1 in [2]) infers the remnant mass and rotation parameter by fitting a damped-sinusoid template with the ringdown phase of the observed signal. One can further obtain the quasi-normal mode frequencies from the final mass and spin using appropriate relations [358]. Unlike the PyRing method, the second approach called the pSEOBNRv4HM analysis ([360], Section VII A.2 in [2]) uses the full waveform to predict the final mass and spin by fitting with a parameterized spinning effective one body (EOB) waveform. So far, these methods have reported strong constraints on the remnant properties [359]. In this section, we use these publicly available measurements of the binary black holes remnant properties to provide a preliminary bound on the tidal charge parameter, β . From Section 8.3, we know:

$$f_{lmn} = f_{lmn}(M, a, \beta) \quad (8.4.1a)$$

$$\tau_{lmn} = \tau_{lmn}(M, a, \beta) \quad (8.4.1b)$$

With these relations, one can predict the frequency and damping time from the measured values of final mass and spin for a given β . These frequency and damping time can further be compared

with that of the values inferred from the pSEOBNRv4HM and IMR analysis. For general relativity, we have $\beta = 0$, and hence the predicted and measured frequencies should be consistent with each other. However, for nonzero values of β , the predicted frequencies would be expected to show inconsistency with the observed ones. This allows us to put an upper bound on β within measurement uncertainties. More precisely, our aim would be to find the value of β for which the above inconsistency occurs. We carry out this analysis in the context of the first gravitational wave observation, GW 150914, by restricting ourselves to the least damped ($\ell = 2, m = 2$) quasi-normal mode.

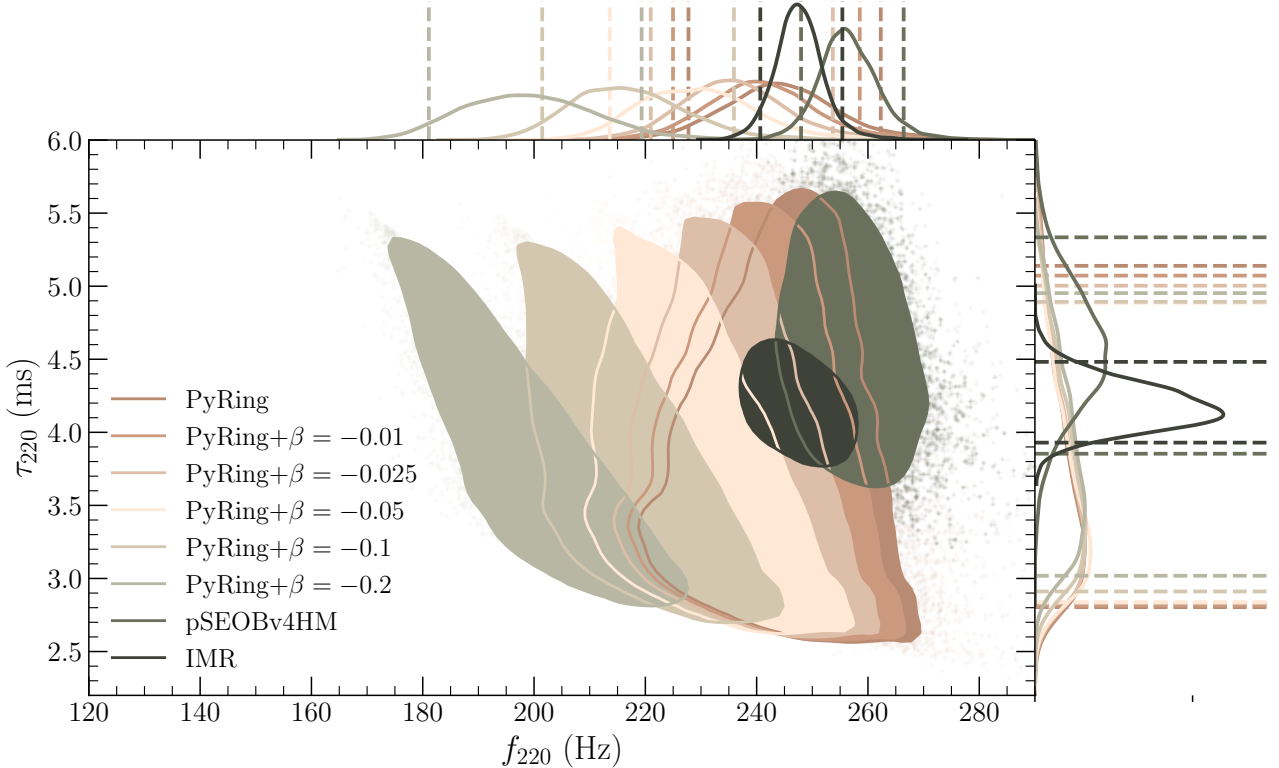


FIGURE 8.2: 90% credible interval of the 2D posterior probability distributions of the frequency and damping time of the (2,2) quasi-normal modes. The labels refers to the LIGO-Virgo analysis used for the corresponding distribution. For the ‘PyRing’ distributions, the mass and spin samples from the GW150914 PyRing analysis were used to predict the distributions on (f_{220}, τ_{220}) for a given value of β . The pSEOBNRv4HM posterior is from [1] and the ‘IMR’ posterior is from [2].

[Fig. 8.2](#) illustrates the two-dimensional posterior distribution of the oscillation frequency and damping time corresponding to the $(\ell = 2, m = 2)$ mode. It is evident that with the increasing magnitude of the tidal charge parameter β , the predicted posterior distributions of (f_{220}, τ_{220}) becomes progressively more inconsistent with the pSEOBNRv4HM and the IMR posteriors. For $\beta = -0.01, -0.025$, we find the predictions of the quasi-normal mode frequencies are consistent, at the 90% credible interval with both the pSEOBNRv4HM and IMR measurements ([Fig. 8.2](#)). However, already for $\beta = -0.05$ we start to see the disagreement with the pSEOBNRv4HM measurements, although there remains partial overlap with the IMR measurements. For values of $\beta \leq -0.05$, the predictions and independent measurements start to become inconsistent. Hence, at current measurement uncertainties, one would assume values of the tidal parameter $\beta < -0.05$ to be unlikely.

8.5 Conclusion

With the advancement of gravitational wave detectors, we have the unprecedented opportunity to test gravitational theories against strong field observations. These tests are expected to provide strong constraints on parameters beyond general relativity. In this chapter, we developed such a framework to obtain a bound on the tidal charge parameter of rotating braneworld black hole. In particular, we used the two-dimensional posterior distribution of (f_{220}, τ_{220}) inferred from the GW 150914 event and compared with that of the values obtained numerically to constrain β . This formalism is entirely general and can be extended to other theories by computing the quasi-normal mode spectrum. As an extension of our work, it would be an interesting exercise to constrain the length scale of the extra dimension in the braneworld context from the bound on β . However, in this case, we need to know the entire bulk spacetime geometry. This can be achieved by numerically evolving the braneworld solution along the extra dimension using numerical relativity algorithms, which is beyond the scope of this work.

Chapter **9**

Conclusion and Future Outlook

Gravity is vastly different from other fundamental interactions and best described in the framework of general relativity as the curvature of spacetime. The theory has been astonishingly successful in explaining various gravitational phenomena, and no significant deviation from general relativity has been observed to date. However, as emphasized in the introduction, despite such triumphs, general relativity is still plagued with several theoretical challenges and cannot be regarded as a complete theory of gravity. These limitations have led to the development of several alternative theories of gravity over the past few decades. The primary focus of this thesis has been to study several aspects of various modified theories of gravity with application in some of the contemporary research areas in gravitational physics such as black hole thermodynamics, shadow around compact objects, quasi-normal modes, gravitational waves etc. The thesis is comprised of two parts, which we classify as theoretical and observational studies. In Part I, we carry out studies of several interesting theoretical problems in black hole physics within the framework of general relativity and modified theories. Part II mostly deals with constraining theories of gravity from gravitational-wave observations. In this chapter, we finally conclude by presenting a concise summary of various interesting problems this thesis has attempted to address.

To begin with, we have prepared [Chapter 1](#) as a warm-up for the rest of the thesis. We started by providing some of the fundamentals of general relativity and further discussed its limitations. In the subsequent sections, we present an in-depth overview of various modified theories of gravity. This includes the case of Lanczos-Lovelock gravity, quadratic curvature theories, $f(R)$ theories etc. Furthermore, we review some of the interesting results of black hole physics in the context of general relativity (black hole horizon topology, thermodynamics of black holes, photon sphere and shadow, cosmic censorship conjectures etc.), which has been studied in detail in the successive chapters.

The topology theorem of Hawking is considered to be one of the central results in mathematical relativity. It states that the admissible horizon topology of asymptotically flat black hole solutions of general relativity in four dimensions is either spherical (S^2) or toroidal ($S^1 \times S^1$). The theorem explicitly uses Einstein's equation and assumes the stress-energy tensor to obey the dominant energy condition. Galloway and Schoen have studied the higher dimensional version of this theorem. Since the solution space of the modified gravity theories is expected to be larger as compared to that of general relativity, it would be an interesting exercise to obtain possible restrictions on the geometry of black holes in such theories. Motivated by these ideas, in [Chapter 2](#) we have studied the horizon topology of black holes in $f(R)$ gravity. In particular, we have derived a sufficient condition on the

form of $f(R)$, i.e., $\square f'(R) \geq 0$ (along with the dominant energy condition) for which the horizon cross-section has topology identical as that of general relativity. We have also extended our analysis to higher dimensions. Interestingly, the same sufficient condition also restricts the topology of higher-dimensional black holes in $f(R)$ gravity. A generalization of our result to other class of modified theories would be interesting to pursue.

The subject of black hole thermodynamics has been studied for decades and still remain an active area of research in gravitational physics. The black hole horizon is attributed with various thermodynamic properties and follows certain equations that resemble the four laws of thermodynamics. The area-entropy proportionality relation in general relativity is one of the characteristics property of black holes, which has led to the proposals of holographic principles. Furthermore, linearized perturbation of the horizon area due to influx of matter can be expressed in a form (Eq. (1.4.4)) identical to the first law of thermodynamics. This is known as the physical process version of the first law. However, as one deviates from general relativity, the entropy is no longer proportional to the horizon area. In a general context, for an arbitrary diffeomorphism invariant theory of gravity, the horizon entropy has been shown to be the Noether charge associated with the Killing isometry of the spacetime and given by the Wald entropy formula. If the black hole spacetime is dynamical, which is the case in the presence of a perturbation, the Wald entropy suffers from ambiguities and cannot be considered as a viable measure of the horizon entropy. In Chapter 3 we have studied the PPFL for an arbitrary diffeomorphism invariant theory of gravity and attempted to understand the effect of ambiguities on the formulation of PPFL. Some of the central outcomes of this chapters are as follows,

- Firstly, we have obtained a general expression for the variation of black hole entropy in an arbitrary theory of gravity with diffeomorphism invariance.
- Furthermore, we have illustrated that for linear order perturbations, the presence of ambiguities does not affect the PPFL when the variation is taken between an initial bifurcation surface and a future stationary slice.
- We have also studied the variation of entropy between two arbitrary non-stationary slices and expressed it in the form of first law with the introduction of an additional term corresponding to the horizon membrane energy. We have demonstrated this result in the context of Lanczos-Lovelock theories of gravity.

Having understood the first law for an arbitrary diffeomorphism theory of gravity in detail, our next goal would be to study the second law in such theories. This would be an useful analysis to classify certain classes of theories that are at least theoretically consistent. Another possible study could be to go beyond the linear order and understand the effect of dissipative terms.

The deflection of light by gravitating objects, namely the gravitational lensing effect, was one of the initial predictions of general relativity. The existence of the photon sphere and shadow around black holes are immediate consequences of such an effect. In Chapter 4 we study the dynamical evolution of the circular photon orbits and shadow radius around black holes accreting or radiating matter. This is an interesting study since astrophysical black holes strongly interact with the surrounding accretion disk and cannot be represented by a stationary spacetime ansatz. The key results obtained in this chapter are,

- The location of the photon sphere in a dynamical spacetime is governed by a second-order differential equation, unlike the static case where it is given by an algebraic equation. We started by providing a detailed derivation of the differential equation.

- Further, to study the evolution of the photon sphere, we solve the differential equation numerically for various dynamical black hole models in the context of general relativity and also Einstein-Gauss-Bonnet gravity. We illustrated a novel relationship between the null energy condition of the accreting matter and the photon sphere radius. We have also demonstrated that the photon sphere radius for a dynamical Schwarzschild de Sitter black hole explicitly depends on the choice of the cosmological constant, unlike the static case.
- In the subsequent sections, we obtained an expression for the black hole shadow when the spacetime is dynamical. This result has been extended to slowly rotating black hole spacetimes as well.
- Finally, we extend our analysis to theories beyond general relativity. In particular, we studied dynamical black holes in the context of Einstein-Gauss-Bonnet theory of gravity. By obtaining an expression for the effective graviton metric, we demonstrated the dynamics of photon and graviton circular null orbits.

As an extension of this work, we aim to include physically more relevant spacetimes in our analysis. In particular, one can study the dynamics of photon sphere and shadow around a rapidly rotating dynamical black hole. Also, studying the evolution of shadow by considering different models of accretion disk would be an interesting future prospect. Note that, in the static case, the quasi-normal modes of a perturbation (scalar, electromagnetic or gravitational) in the eikonal limit is related to the Lyapunov exponent associated with the photon sphere. It would be interesting see if such an analogy holds even in the dynamical case.

In [Chapter 5](#) we have analyzed the weak cosmic censorship conjecture in the context of a multi charged black hole setting, whereas most of the earlier studies on this subject has been for single black holes. We started by studying the process of test particle absorption in a Majumdar-Papapetrou spacetime, representing the only known equilibrium configuration of two extremal charged black holes. If such a process leads to the formation of a di-hole in the final configuration (with or without equilibrium condition), it would be regarded as a potential violation of the weak cosmic censorship. This is not a straightforward problem since the Majumdar-Papapetrou spacetime is completely different from that of a single Reissner-Nordström source. However, we have explicitly shown that those test particles which would expose the naked singularity would not be able to cross the event horizon, and as a result, the weak cosmic censorship is not violated. This is an interesting result and, at the same time, strong evidence for the validity of weak cosmic censorship. A further possible generalization of this work could be to carry out such analysis for a system of N -extremal charged black holes.

The strong cosmic censorship is a mathematical statement about the predictability nature of general relativity. However, several recent studies suggest that the conjecture is violated for asymptotically de Sitter charged black hole spacetimes in general relativity. This is an alarming situation since it immediately indicates that general relativity as a classical theory is not deterministic. The general approach adopted in these studies has been to look for possible parameter space for which a small perturbation can be smoothly extended beyond the Cauchy horizon. Note that the time evolution of the perturbation beyond the Cauchy horizon can not be uniquely determined as the Cauchy horizon represents the boundary of maximal evolution of an initial hyper-surface. In [Chapter 6](#), we study the validity of strong cosmic censorship conjecture in the presence of higher curvature corrections over the Einstein-Hilbert action. In particular, we have considered the Lanczos-Lovelock class of theories

and explicitly studied the effect of the higher curvature coupling constant on the violation of strong cosmic censorship. Firstly, we have shown that the Christdul version of strong cosmic censorship conjecture is violated even in higher curvature theories. Furthermore, the violation in higher curvature theories seems to be stronger as compared to general relativity. We have illustrated these results for all three families of quasi-normal modes. As a future outlook, one may consider a similar situation in the context of rotating black holes in higher curvature theories. Also, extending our results to gravitational perturbation would be an interesting exercise.

The LIGO-Virgo collaborations have reported several observations of binary coalescence in the past five years. Such observational success of the gravitational wave detectors have opened up exciting avenues for testing and constraining theories of gravity beyond general relativity. In the second part of this thesis, we have developed two general methodologies to constrain modified theories from gravitational-wave observations. In [Chapter 7](#) we start with a quadratic curvature theory in four dimensions described by the action as given in [Eq. \(7.1.6\)](#). The causal structure in such theories are vastly different from general relativity, and as a result, gravitational wave and electromagnetic signal follow different null geodesic. This effect is a distinctive property of any theory with higher curvature terms. This further predicts that there must be a time delay between the arrival of gravitational wave and electromagnetic signal at an Earth-based detector. Interestingly, such a time delay of 1.7 s was observed in the GW 170817 event, the only binary neutron star merger. We have explicitly computed the time delay using the effective graviton metric of the quadratic curvature theory and compared it with the observed delay to obtain an upper bound on the coupling constant $\alpha \leq 10^{36} m^2$ or the dimensionless parameter $\eta = \frac{\alpha H_G^2(0)}{c^2} \leq 8.5 \times 10^{-16}$. Note that the constrain on α is obtained from cosmological considerations, whereas the previous bounds are based on local experiments. The formalism we have developed is completely general and can be used to constrain the parameters of any class of modified theories. An interesting extension of this analysis would be to consider theories with non-minimal coupling between matter and curvature.

In the last chapter ([Chapter 8](#)), we study theories with correction over general relativity due to the presence of extra spatial dimensions. Interestingly, the effective field equation on the brane admits rotating black hole solutions that resemble the structure of a Kerr Newman black hole of general relativity. However, instead of the electromagnetic charge, the braneworld solution has a tidal charge as an additional parameter, which can take negative values. In this chapter, we have developed a formalism to constrain the tidal charge parameter from gravitational-wave observations. In particular, by using the quasi-normal mode spectrum of the GW 150914 event, we have placed an bound of $\beta > -0.05$ within the range of measurement uncertainties. Note that the effective correction to the gravitational dynamics on the brane is linked with the bulk Weyl tensor. Therefore, we expect that the bound on β would ultimately constrain the length scale of the extra dimension. However, to arrive at such a result, one must know the full bulk solution a priori, which can only be obtained by numerically evolving the solution on the brane along the additional dimension. This requires a full numerical relativity framework, which we leave for the future. Also, our analysis can be extended to other class gravitational theories.

Although general relativity is in excellent agreement with observations over a wide range of length scales, there still remains ample parameter space where the theory may attain modifications. However, in the absence of a fully consistent quantum gravity framework, the exact form of such corrections are not clear. In this context, one possible approach could be to perform several consistency

checks of the low energy theory. With such motivation, in this thesis, we have presented some novel studies involving black holes and gravitational waves in general relativity and modified theories. We hope that the analysis presented in this thesis would be a valuable addition towards constraining various modified theory of gravity from both theoretical and observational considerations.

Appendix **A**

Derivation of the Evolution Equation for photon sphere (Chapter 4)

In this section we provide a complete derivation of the evolution equation of the photon sphere, i.e., Eq. (4.1.2). For in-going case we have $r_{\text{ph}} = r_{\text{ph}}(v)$. Hence,

$$dr_{\text{ph}}(v) = \frac{\partial r_{\text{ph}}(v)}{\partial v} dv = \dot{r}_{\text{ph}}(v) dv \quad (\text{A.0.1})$$

For null orbits we now put $ds^2 = 0$ from Eq. (4.1.1) but keeping in mind that, now we don't have $dr_{\text{ph}} = 0$ rather dr_{ph} is given by Eq. (A.0.1). This leads to the expression,

$$\left(\frac{d\phi}{dv}\right)^2 = \frac{1}{r_{\text{ph}}(v)^2} f(r_{\text{ph}}(v), v) - \frac{2}{r_{\text{ph}}(v)^2} \dot{r}_{\text{ph}}(v) \quad (\text{A.0.2})$$

Now for the metric in Eq. (4.1.1) we have the following non-vanishing components of the Christoffel connection,

$$\Gamma_{vv}^v = \frac{1}{2} f'(r, v), \quad \Gamma_{vv}^r = \frac{1}{2} [\dot{f}(r, v) + f(r, v) f'(r, v)], \quad \Gamma_{rv}^v = -\frac{1}{2} f'(r, v)$$

$$\Gamma_{\theta\theta}^v = -r, \quad \Gamma_{r\theta}^r = \frac{1}{r}, \quad \Gamma_{\phi\phi}^v = -r \sin^2 \theta, \quad \Gamma_{r\phi}^\phi = \frac{1}{r} \quad \Gamma_{\phi\phi}^\theta = -\cos \theta \sin \theta, \quad \Gamma_{\theta\phi}^\phi = \cot \theta$$

and the geodesic equations can be written as,

$$\frac{d^2r}{d\lambda^2} - \frac{\partial f}{\partial r} \left(\frac{dr}{d\lambda} \right) \left(\frac{dv}{d\lambda} \right) + \frac{1}{2} \left(f \frac{\partial f}{\partial r} - \frac{\partial f}{\partial v} \right) \left(\frac{dv}{d\lambda} \right)^2 - rf \left(\frac{d\phi}{d\lambda} \right)^2 = 0 \quad (\text{A.0.3})$$

$$\frac{d^2v}{d\lambda^2} + \frac{1}{2} \frac{\partial f}{\partial r} \left(\frac{dv}{d\lambda} \right)^2 - r \left(\frac{d\phi}{d\lambda} \right)^2 = 0 \quad (\text{A.0.4})$$

Now we set $r = r_{\text{ph}}(v)$ for the evolution of the radius of photon sphere. From Eq. (A.0.1) we obtain,

$$\frac{d^2r_{\text{ph}}(v)}{d\lambda^2} = \dot{r}_{\text{ph}}(v) \frac{d^2v}{d\lambda^2} + \ddot{r}_{\text{ph}}(v) \left(\frac{dv}{d\lambda} \right)^2$$

$$= \dot{r}_{\text{ph}}(v) \left[r_{\text{ph}}(v) \left(\frac{d\phi}{d\lambda} \right)^2 - \frac{1}{2} \frac{\partial f}{\partial r} \Big|_{r_{\text{ph}}(v), v} \left(\frac{dv}{d\lambda} \right)^2 \right] + \ddot{r}_{\text{ph}}(v) \left(\frac{dv}{d\lambda} \right)^2 \quad (\text{A.05})$$

Now we plug in [Eq. \(A.0.2\)](#) and [Eq. \(A.0.5\)](#) in [Eq. \(A.0.3\)](#) to obtain

$$\begin{aligned} & \ddot{r}_{\text{ph}}(v) + \dot{r}_{\text{ph}}(v) \left[\frac{3}{r_{\text{ph}}(v)} f(r_{\text{ph}}, v) - \frac{3}{2} \frac{\partial f}{\partial r} \Big|_{r_{\text{ph}}(v), v} \right] - \frac{2}{r_{\text{ph}}(v)} \dot{r}_{\text{ph}}(v)^2 \\ & + \frac{1}{2} \left(f \frac{\partial f}{\partial r} \Big|_{r_{\text{ph}}(v), v} - \frac{\partial f}{\partial v} \Big|_{r_{\text{ph}}(v), v} \right) - \frac{1}{r_{\text{ph}}(v)} f(r_{\text{ph}}(v), v)^2 = 0 \end{aligned} \quad (\text{A.06})$$

Similar procedure can be carried out for the evolution equation of photon sphere in terms of outgoing coordinate, i.e., [Eq. \(4.1.3\)](#) to obtain [Eq. \(4.1.4\)](#).

Appendix **B**

Derivation of the effective graviton metric (Chapter 4)

We shall start with the G_v^v component, for which we set $b = d = v$ in Eq. (4.5.3) and obtain the correction as,

$$\lambda_2(\delta_{qvc_1d_1}^{pava_1b_1} - \delta_q^p \delta_{cvc_1d_1}^{ava_1b_1})R_{a_1b_1}{}^{c_1d_1}\nabla_v\nabla^v h_a^c = \lambda_2(\delta_{\hat{q}\hat{c}\hat{c}_1\hat{d}_1}^{\hat{p}\hat{a}\hat{d}_1\hat{b}_1} - \delta_q^p \delta_{\hat{c}\hat{c}_1\hat{d}_1}^{\hat{a}\hat{d}_1\hat{b}_1})R_{\hat{a}_1\hat{b}_1}{}^{\hat{c}_1\hat{d}_1}\nabla_v\nabla^v h_{\hat{a}}^{\hat{c}} \quad (\text{B.0.1})$$

Here $\hat{a}, \hat{b} = 1, 2, \dots, d-1$, are the spatial indexes, i.e., the radial coordinate r and angular coordinates. We shall denote the angular coordinates as $i, j = 1, 2, \dots, d-2$. In the above result we've used the identity,

$$\delta_{b_1 b_2 v \dots b_k}^{a_1 a_2 v \dots a_k} = \delta_{\hat{b}_1 \hat{b}_2 \dots \hat{b}_k}^{\hat{a}_1 \hat{a}_2 \dots \hat{a}_k} \quad (\text{B.0.2})$$

Hence Eq. (B.0.1) becomes,

$$\begin{aligned} & \lambda_2 \left(4\delta_{\hat{q}\hat{c}r\hat{d}_1}^{\hat{p}\hat{a}r\hat{b}_1} R_{r\hat{b}_1}{}^{r\hat{d}_1} + \delta_{\hat{q}\hat{c}\hat{c}_1\hat{d}_1}^{\hat{p}\hat{a}\hat{d}_1\hat{b}_1} R_{\hat{a}_1\hat{b}_1}{}^{\hat{c}_1\hat{d}_1} - 4\delta_q^p \delta_{\hat{c}r\hat{d}_1}^{\hat{a}r\hat{b}_1} R_{r\hat{b}_1}{}^{r\hat{d}_1} - \delta_q^p \delta_{\hat{c}\hat{c}_1\hat{d}_1}^{\hat{a}\hat{d}_1\hat{b}_1} R_{\hat{a}_1\hat{b}_1}{}^{\hat{c}_1\hat{d}_1} \right) \\ &= \lambda_2 \left(4\delta_{\hat{q}\hat{c}rj}^{\hat{p}\hat{a}ri} R_{ri}{}^{rj} + \delta_{\hat{q}\hat{c}kl}^{\hat{p}\hat{a}ij} R_{ij}{}^{kl} - 4\delta_q^p \delta_{\hat{c}rj}^{\hat{a}ri} R_{ri}{}^{rj} - \delta_q^p \delta_{\hat{c}kl}^{\hat{a}ij} R_{ij}{}^{kl} \right) \nabla_v \nabla^v h_{\hat{a}}^{\hat{c}} \end{aligned}$$

Note that, we are using gauge-invariant transverse and traceless tensor perturbation, i.e., $h^{\mu\nu} = h^{\mu i} = h_i^i = \nabla_i h^{ij} = 0$, where $\mu, \nu = r, v$. To understand the calculation further, let us concentrate on the first term, i.e., $\delta_{\hat{q}\hat{c}rj}^{\hat{p}\hat{a}ri}$. Note that, because of the antisymmetric properties of δ tensor, it can not have two same indexes either in the contravariant or in the covariant position. Hence all other indexes in this term apart from r are angular coordinates and so on for other terms. Now we put the component of Riemann tensor from Eq. (4.5.5), Eq. (4.5.6), Eq. (4.5.7) to obtain,

$$\begin{aligned} & \lambda_2 \left[4\delta_{\hat{q}\hat{c}rj}^{\hat{p}\hat{a}ri} \left(\frac{-f'}{2r} \right) \delta_i^j + \delta_{\hat{q}\hat{c}kl}^{\hat{p}\hat{a}ij} \left(\frac{1-f}{r^2} \right) \delta_{ij}^{kl} - 4\delta_q^p \delta_{\hat{c}rj}^{\hat{a}ri} \left(\frac{-f'}{2r} \right) \delta_i^j - \delta_q^p \delta_{\hat{c}kl}^{\hat{a}ij} \left(\frac{1-f}{r^2} \right) \delta_{ij}^{kl} \right] \nabla_v \nabla^v h_{\hat{a}}^{\hat{c}} \\ &= \lambda_2 \left[4\delta_{\hat{q}\hat{c}i}^{\hat{p}\hat{a}i} \left(\frac{-f'}{2r} \right) + 2\delta_{\hat{q}\hat{c}ij}^{\hat{p}\hat{a}ij} \left(\frac{1-f}{r^2} \right) - 4\delta_q^p \delta_{\hat{c}i}^{\hat{a}i} \left(\frac{-f'}{2r} \right) - 2\delta_q^p \delta_{\hat{c}ij}^{\hat{a}ij} \left(\frac{1-f}{r^2} \right) \right] \nabla_v \nabla^v h_{\hat{a}}^{\hat{c}} \\ &= \lambda_2 \left[4\delta_{\hat{q}\hat{c}}^{\hat{p}\hat{a}} (d-4) \left(\frac{-f'}{2r} \right) + 2\delta_{\hat{q}\hat{c}}^{\hat{p}\hat{a}} (d-4)(d-5) \left(\frac{1-f}{r^2} \right) - 4\delta_q^p \delta_{\hat{c}}^{\hat{a}} (d-3) \left(\frac{-f'}{2r} \right) - 2\delta_q^p \delta_{\hat{c}}^{\hat{a}} (d-3)(d-4) \left(\frac{1-f}{r^2} \right) \right] \nabla_v \nabla^v h_{\hat{a}}^{\hat{c}} \end{aligned}$$

Here it is understood that f is a function of r and v , i.e., $f = f(r, v)$, which we've considered for simplicity. Deriving the above result we've used the following identities,

$$\delta_{klm}^{ijm} = (d-4)\delta_{kl}^{ij} \quad (\text{B.0.3})$$

$$\delta_{klmn}^{ijmn} = (d-4)(d-5)\delta_{kl}^{ij} \quad (\text{B.0.4})$$

$$\delta_{jmn}^{imn} = (d-3)(d-4)\delta_j^i \quad (\text{B.0.5})$$

$$\delta_{jm}^{im} = (d-3)\delta_j^i \quad (\text{B.0.6})$$

$$\delta_{klmno}^{ijmno} = (d-4)(d-5)(d-6)\delta_{kl}^{ij} \quad (\text{B.0.7})$$

Note that, the last two terms in the above expression doesn't contribute, because they contain a $\delta_{\hat{c}}^{\hat{a}}$ term, which multiplies with $h_{\hat{a}}^{\hat{c}}$ to give zero from the traceless condition. Hence we are left with only,

$$\lambda_2 \left[4\delta_{\hat{q}\hat{c}}^{\hat{p}\hat{a}}(d-4) \left(\frac{-f'}{2r} \right) + 2\delta_{\hat{q}\hat{c}}^{\hat{p}\hat{a}}(d-4)(d-5) \left(\frac{1-f}{r^2} \right) \right] \nabla_v \nabla^v h_{\hat{a}}^{\hat{c}}$$

$$= \lambda_2 \left[4 \left(\delta_{\hat{q}}^{\hat{p}} \delta_{\hat{c}}^{\hat{a}} - \delta_{\hat{c}}^{\hat{p}} \delta_{\hat{q}}^{\hat{a}} \right) (d-4) \left(\frac{-f'}{2r} \right) + 2 \left(\delta_{\hat{q}}^{\hat{p}} \delta_{\hat{c}}^{\hat{a}} - \delta_{\hat{c}}^{\hat{p}} \delta_{\hat{q}}^{\hat{a}} \right) (d-4)(d-5) \left(\frac{1-f}{r^2} \right) \right] \nabla_v \nabla^v h_{\hat{a}}^{\hat{c}}$$

Again using the fact that, $\delta_{\hat{c}}^{\hat{a}}$ term doesn't contribute, we further get,

$$\lambda_2 \left[2\delta_{\hat{c}}^{\hat{p}} \delta_{\hat{q}}^{\hat{a}}(d-4) \left(\frac{f'}{r} \right) - 2\delta_{\hat{c}}^{\hat{p}} \delta_{\hat{q}}^{\hat{a}}(d-4)(d-5) \left(\frac{1-f}{r^2} \right) \right] \nabla_v \nabla^v h_{\hat{a}}^{\hat{c}}$$

$$= \lambda_2 \left[2(d-4) \left(\frac{f'}{r} \right) - 2(d-4)(d-5) \left(\frac{1-f}{r^2} \right) \right] \nabla_v \nabla^v h_{\hat{q}}^{\hat{p}}$$

The coefficient of the kinetic term we identify as the correction to the background metric and hence the (v, v) component of the effective metric is given by,

$$G_v^v = 1 - 2\lambda_2 \left[(d-4) \left(\frac{f'}{r} \right) - (d-4)(d-5) \left(\frac{1-f}{r^2} \right) \right] \quad (\text{B.0.8})$$

Now let us calculate G_v^r component. For this we set $b = r, d = v$ in [Eq. \(4.5.3\)](#) to obtain,

$$\lambda_2(\delta_{qcrc_1d_1}^{pava_1b_1} - \delta_q^p \delta_{crc_1d_1}^{ava_1b_1}) R_{a_1b_1}{}^{c_1d_1} \nabla_v \nabla^v h_a^c$$

$$= \lambda_2 \left[4\delta_{qcrvj}^{pavri} R_{vi}{}^{rj} + \delta_{qcrkl}^{pavij} R_{ij}{}^{kl} - 4\delta_q^p \delta_{crvj}^{avri} R_{vi}{}^{rj} - \delta_q^p \delta_{crkl}^{avij} R_{ij}{}^{kl} \right] \nabla_v \nabla^v h_a^c$$

Note that $\delta_{qcrvj}^{pavri} = -\delta_{qcj}^{pai}$ and $\delta_{qcrkl}^{pavij} = 0$ in the above expression. The first identity is because of antisymmetric properties of δ tensor. The second identity is because all other indexes apart from ' v ' in the contravariant position and index apart from ' r ' in the covariant position are angular index. This gives zero when the determinant is taken. Using this and by replacing the components of Riemann tensor, the above expression becomes,

$$\lambda_2 \left[-4\delta_{qcj}^{pai} \left(\frac{-\dot{f}}{2r} \delta_i^j \right) - 4\delta_q^p \delta_{cj}^{ai} \left(\frac{-\dot{f}}{2r} \delta_i^j \right) \right] \nabla_v \nabla^v h_a^c$$

$$\begin{aligned}
&= \lambda_2 \left[2\delta_{qci}^{pai} \left(\frac{\dot{f}}{r} \right) + 2\delta_q^p \delta_{ci}^{ai} \left(\frac{\dot{f}}{r} \right) \right] \nabla_v \nabla^v h_a^c \\
&= \lambda_2 \left[2\delta_{qc}^{pa} (d-4) \left(\frac{\dot{f}}{r} \right) + 2\delta_q^p \delta_c^a (d-3) \left(\frac{\dot{f}}{r} \right) \right] \nabla_v \nabla^v h_a^c
\end{aligned}$$

The last term again doesn't contribute because of the traceless condition, and finally, we have [204],

$$G_v^r = 2\lambda_2(d-4) \frac{\dot{f}}{r} \quad (\text{B.0.9})$$

Bibliography

- [1] A. Ghosh, R. Brito, and A. Buonanno, “Constraints on quasi-normal-mode frequencies with LIGO-Virgo binary-black-hole observations,” [arXiv:2104.01906 \[gr-qc\]](https://arxiv.org/abs/2104.01906).
- [2] **LIGO Scientific, Virgo** Collaboration, R. Abbott *et al.*, “Tests of General Relativity with Binary Black Holes from the second LIGO-Virgo Gravitational-Wave Transient Catalog,” [arXiv:2010.14529 \[gr-qc\]](https://arxiv.org/abs/2010.14529).
- [3] S. W. Hawking and G. F. R. Ellis, *The Large Scale Structure of Space-Time*. Cambridge Monographs on Mathematical Physics. Cambridge University Press, 1973.
- [4] R. M. Wald, *General Relativity*. Chicago Univ. Pr., Chicago, USA, 1984.
- [5] S. Chandrasekhar, *The mathematical theory of black holes*. 1985.
- [6] K. Schwarzschild, “On the gravitational field of a mass point according to Einstein’s theory,” *Sitzungsber. Preuss. Akad. Wiss. Berlin (Math. Phys.)* **1916** (1916) 189–196, [arXiv:physics/9905030](https://arxiv.org/abs/physics/9905030).
- [7] C. M. Will, “The Confrontation between General Relativity and Experiment,” *Living Rev. Rel.* **17** (2014) 4, [arXiv:1403.7377 \[gr-qc\]](https://arxiv.org/abs/1403.7377).
- [8] J. B. Griffiths and J. Podolský, *Exact Space-Times in Einstein’s General Relativity*. Cambridge Monographs on Mathematical Physics. Cambridge University Press, 2009.
- [9] R. P. Kerr, “Gravitational field of a spinning mass as an example of algebraically special metrics,” *Phys. Rev. Lett.* **11** (Sep, 1963) 237–238.
<https://link.aps.org/doi/10.1103/PhysRevLett.11.237>.
- [10] M. Heusler, *Black Hole Uniqueness Theorems*. Cambridge Lecture Notes in Physics. Cambridge University Press, 1996.
- [11] W. Israel, “Event horizons in static vacuum space-times,” *Phys. Rev.* **164** (Dec, 1967) 1776–1779. <https://link.aps.org/doi/10.1103/PhysRev.164.1776>.
- [12] B. Carter, “Axisymmetric black hole has only two degrees of freedom,” *Phys. Rev. Lett.* **26** (Feb, 1971) 331–333. <https://link.aps.org/doi/10.1103/PhysRevLett.26.331>.
- [13] **LIGO Scientific, Virgo** Collaboration, B. P. Abbott *et al.*, “Observation of Gravitational Waves from a Binary Black Hole Merger,” *Phys. Rev. Lett.* **116** no. 6, (2016) 061102, [arXiv:1602.03837 \[gr-qc\]](https://arxiv.org/abs/1602.03837).

- [14] **LIGO Scientific, Virgo** Collaboration, B. P. Abbott *et al.*, “Properties of the Binary Black Hole Merger GW150914,” *Phys. Rev. Lett.* **116** no. 24, (2016) 241102, [arXiv:1602.03840 \[gr-qc\]](https://arxiv.org/abs/1602.03840).
- [15] **LIGO Scientific, Virgo** Collaboration, B. P. Abbott *et al.*, “Tests of general relativity with GW150914,” *Phys. Rev. Lett.* **116** no. 22, (2016) 221101, [arXiv:1602.03841 \[gr-qc\]](https://arxiv.org/abs/1602.03841). [Erratum: Phys.Rev.Lett. 121, 129902 (2018)].
- [16] **LIGO Scientific, Virgo** Collaboration, B. P. Abbott *et al.*, “GW151226: Observation of Gravitational Waves from a 22-Solar-Mass Binary Black Hole Coalescence,” *Phys. Rev. Lett.* **116** no. 24, (2016) 241103, [arXiv:1606.04855 \[gr-qc\]](https://arxiv.org/abs/1606.04855).
- [17] **LIGO Scientific, VIRGO** Collaboration, B. P. Abbott *et al.*, “GW170104: Observation of a 50-Solar-Mass Binary Black Hole Coalescence at Redshift 0.2” *Phys. Rev. Lett.* **118** no. 22, (2017) 221101, [arXiv:1706.01812 \[gr-qc\]](https://arxiv.org/abs/1706.01812). [Erratum: Phys. Rev. Lett. 121,no.12,129901(2018)].
- [18] **LIGO Scientific, Virgo** Collaboration, B. P. Abbott *et al.*, “GW170817: Observation of Gravitational Waves from a Binary Neutron Star Inspiral,” *Phys. Rev. Lett.* **119** no. 16, (2017) 161101, [arXiv:1710.05832 \[gr-qc\]](https://arxiv.org/abs/1710.05832).
- [19] **Event Horizon Telescope** Collaboration, K. Akiyama *et al.*, “First M87 Event Horizon Telescope Results. I. The Shadow of the Supermassive Black Hole,” *Astrophys. J.* **875** no. 1, (2019) L1, [arXiv:1906.11238 \[astro-ph.GA\]](https://arxiv.org/abs/1906.11238).
- [20] **Event Horizon Telescope** Collaboration, K. Akiyama *et al.*, “First M87 Event Horizon Telescope Results. IV. Imaging the Central Supermassive Black Hole,” *Astrophys. J. Lett.* **875** no. 1, (2019) L4, [arXiv:1906.11241 \[astro-ph.GA\]](https://arxiv.org/abs/1906.11241).
- [21] **Event Horizon Telescope** Collaboration, K. Akiyama *et al.*, “First M87 Event Horizon Telescope Results. V. Physical Origin of the Asymmetric Ring,” *Astrophys. J. Lett.* **875** no. 1, (2019) L5, [arXiv:1906.11242 \[astro-ph.GA\]](https://arxiv.org/abs/1906.11242).
- [22] **Event Horizon Telescope** Collaboration, K. Akiyama *et al.*, “First M87 Event Horizon Telescope Results. VI. The Shadow and Mass of the Central Black Hole,” *Astrophys. J. Lett.* **875** no. 1, (2019) L6, [arXiv:1906.11243 \[astro-ph.GA\]](https://arxiv.org/abs/1906.11243).
- [23] R. Penrose, “Gravitational collapse and space-time singularities,” *Phys. Rev. Lett.* **14** (Jan, 1965) 57–59. <https://link.aps.org/doi/10.1103/PhysRevLett.14.57>.
- [24] R. Penrose, “Gravitational collapse: The role of general relativity,” *Riv. Nuovo Cim.* **1** (1969) 252–276.
- [25] A. Ashtekar, “Singularity Resolution in Loop Quantum Cosmology: A Brief Overview,” *J. Phys. Conf. Ser.* **189** (2009) 012003, [arXiv:0812.4703 \[gr-qc\]](https://arxiv.org/abs/0812.4703).
- [26] K. Blanchette, S. Das, S. Hergott, and S. Rastgoo, “Black hole singularity resolution via the modified Raychaudhuri equation in Loop Quantum Gravity,” [arXiv:2011.11815 \[gr-qc\]](https://arxiv.org/abs/2011.11815).
- [27] **Planck** Collaboration, N. Aghanim *et al.*, “Planck 2018 results. VI. Cosmological parameters,” *Astron. Astrophys.* **641** (2020) A6, [arXiv:1807.06209 \[astro-ph.CO\]](https://arxiv.org/abs/1807.06209).
- [28] S. Weinberg, *Cosmology*. 9, 2008.
- [29] G. Goldhaber and D. B. Cline, “The acceleration of the expansion of the universe: A brief early history of the supernova cosmology project (scp),” *AIP Conference Proceedings* (2009) . <http://dx.doi.org/10.1063/1.3232196>.

- [30] S. Perlmutter, G. Aldering, G. Goldhaber, R. A. Knop, P. Nugent, P. G. Castro, S. Deustua, S. Fabbro, A. Goobar, D. E. Groom, I. M. Hook, A. G. Kim, M. Y. Kim, J. C. Lee, N. J. Nunes, R. Pain, C. R. Pennypacker, R. Quimby, C. Lidman, R. S. Ellis, M. Irwin, R. G. McMahon, P. Ruiz-Lapuente, N. Walton, B. Schaefer, B. J. Boyle, A. V. Filippenko, T. Matheson, A. S. Fruchter, N. Panagia, H. J. M. Newberg, W. J. Couch, and T. S. C. Project, “Measurements of ω and λ from 42 high-redshift supernovae,” *The Astrophysical Journal* **517** no. 2, (Jun, 1999) 565–586. <https://doi.org/10.1086/307221>.
- [31] A. G. Riess, A. V. Filippenko, P. Challis, A. Clocchiatti, A. Diercks, P. M. Garnavich, R. L. Gilliland, C. J. Hogan, S. Jha, R. P. Kirshner, B. Leibundgut, M. M. Phillips, D. Reiss, B. P. Schmidt, R. A. Schommer, R. C. Smith, J. Spyromilio, C. Stubbs, N. B. Suntzeff, and J. Tonry, “Observational evidence from supernovae for an accelerating universe and a cosmological constant,” *The Astronomical Journal* **116** no. 3, (Sep, 1998) 1009–1038. <https://doi.org/10.1086/300499>.
- [32] S. Weinberg, “The cosmological constant problem,” *Rev. Mod. Phys.* **61** (Jan, 1989) 1–23. <https://link.aps.org/doi/10.1103/RevModPhys.61.1>.
- [33] T. Padmanabhan, “Cosmological constant: The Weight of the vacuum,” *Phys. Rept.* **380** (2003) 235–320, [arXiv:hep-th/0212290](https://arxiv.org/abs/hep-th/0212290).
- [34] S. M. Carroll, “The Cosmological constant,” *Living Rev. Rel.* **4** (2001) 1, [arXiv:astro-ph/0004075](https://arxiv.org/abs/astro-ph/0004075).
- [35] J. Martin, “Everything You Always Wanted To Know About The Cosmological Constant Problem (But Were Afraid To Ask),” *Comptes Rendus Physique* **13** (2012) 566–665, [arXiv:1205.3365 \[astro-ph.CO\]](https://arxiv.org/abs/1205.3365).
- [36] L. Amendola, R. Gannouji, D. Polarski, and S. Tsujikawa, “Conditions for the cosmological viability of $f(r)$ dark energy models,” *Phys. Rev. D* **75** (Apr, 2007) 083504. <https://link.aps.org/doi/10.1103/PhysRevD.75.083504>.
- [37] L. Amendola and S. Tsujikawa, “Phantom crossing, equation-of-state singularities, and local gravity constraints in $f(r)$ models,” *Physics Letters B* **660** no. 3, (2008) 125 – 132. [http://www.sciencedirect.com/science/article/pii/S0370269308000221](https://www.sciencedirect.com/science/article/pii/S0370269308000221).
- [38] S. A. Appleby and R. A. Battye, “Do consistent $F(R)$ models mimic General Relativity plus Λ ?,” *Phys. Lett. B* **654** (2007) 7–12, [arXiv:0705.3199 \[astro-ph\]](https://arxiv.org/abs/0705.3199).
- [39] G. Cognola, E. Elizalde, S. Nojiri, S. D. Odintsov, L. Sebastiani, and S. Zerbini, “Class of viable modified $f(r)$ gravities describing inflation and the onset of accelerated expansion,” *Phys. Rev. D* **77** (Feb, 2008) 046009. <https://link.aps.org/doi/10.1103/PhysRevD.77.046009>.
- [40] N. Deruelle, M. Sasaki, and Y. Sendouda, ““detuned” $f(r)$ gravity and dark energy,” *Phys. Rev. D* **77** (Jun, 2008) 124024. <https://link.aps.org/doi/10.1103/PhysRevD.77.124024>.
- [41] W. Hu and I. Sawicki, “Models of $f(r)$ cosmic acceleration that evade solar system tests,” *Phys. Rev. D* **76** (Sep, 2007) 064004. <https://link.aps.org/doi/10.1103/PhysRevD.76.064004>.
- [42] E. V. Linder, “Exponential gravity,” *Phys. Rev. D* **80** (Dec, 2009) 123528. <https://link.aps.org/doi/10.1103/PhysRevD.80.123528>.

- [43] A. A. Starobinsky, “Disappearing cosmological constant in $f(r)$ gravity,” *JETP Letters* **86** no. 3, (Oct, 2007) 157–163. <http://dx.doi.org/10.1134/S0021364007150027>.
- [44] S. Tsujikawa, “Observational signatures of $f(r)$ dark energy models that satisfy cosmological and local gravity constraints,” *Phys. Rev. D* **77** (Jan, 2008) 023507. <https://link.aps.org/doi/10.1103/PhysRevD.77.023507>.
- [45] N. Birrell and P. Davies, *Quantum Fields in Curved Space*. Cambridge Monographs on Mathematical Physics. Cambridge Univ. Press, Cambridge, UK, 2, 1984.
- [46] R. Utiyama and B. S. DeWitt, “Renormalization of a classical gravitational field interacting with quantized matter fields,” *J. Math. Phys.* **3** (1962) 608–618.
- [47] K. S. Stelle, “Renormalization of higher-derivative quantum gravity,” *Phys. Rev. D* **16** (Aug, 1977) 953–969.
- [48] D. G. Boulware and S. Deser, “String-generated gravity models,” *Phys. Rev. Lett.* **55** (Dec, 1985) 2656–2660. <https://link.aps.org/doi/10.1103/PhysRevLett.55.2656>.
- [49] B. Zwiebach, “Curvature squared terms and string theories,” *Physics Letters B* **156** no. 5, (1985) 315 – 317. <http://www.sciencedirect.com/science/article/pii/0370269385916168>.
- [50] C. Lanczos, “A Remarkable property of the Riemann-Christoffel tensor in four dimensions,” *Annals Math.* **39** (1938) 842–850.
- [51] D. Lovelock, “The Einstein tensor and its generalizations,” *J. Math. Phys.* **12** (1971) 498–501.
- [52] T. Padmanabhan and D. Kothawala, “Lanczos-Lovelock models of gravity,” *Phys. Rept.* **531** (2013) 115–171, [arXiv:1302.2151 \[gr-qc\]](https://arxiv.org/abs/1302.2151).
- [53] A. De Felice and S. Tsujikawa, “ $f(R)$ theories,” *Living Rev. Rel.* **13** (2010) 3, [arXiv:1002.4928 \[gr-qc\]](https://arxiv.org/abs/1002.4928).
- [54] T. P. Sotiriou and V. Faraoni, “ $f(R)$ Theories Of Gravity,” *Rev. Mod. Phys.* **82** (2010) 451–497, [arXiv:0805.1726 \[gr-qc\]](https://arxiv.org/abs/0805.1726).
- [55] M. B. Mijić, M. S. Morris, and W.-M. Suen, “The R^2 cosmology: Inflation without a phase transition,” *Phys. Rev. D* **34** (Nov, 1986) 2934–2946. <https://link.aps.org/doi/10.1103/PhysRevD.34.2934>.
- [56] A. A. Starobinsky, “A New Type of Isotropic Cosmological Models Without Singularity,” *Adv. Ser. Astrophys. Cosmol.* **3** (1987) 130–133.
- [57] J. Audretsch, A. Economou, and C. O. Lousto, “Topological defects in gravitational theories with nonlinear Lagrangians,” *Phys. Rev. D* **47** (1993) 3303–3311, [arXiv:gr-qc/9301024](https://arxiv.org/abs/gr-qc/9301024).
- [58] M. Campanelli, C. O. Lousto, and J. Audretsch, “Perturbative metric of charged black holes in quadratic gravity,” *Phys. Rev. D* **51** (1995) 6810–6815, [arXiv:gr-qc/9412001](https://arxiv.org/abs/gr-qc/9412001).
- [59] J. Matyjasek and D. Tryniecki, “Charged black holes in quadratic gravity,” *Phys. Rev. D* **69** (2004) 124016, [arXiv:gr-qc/0402098](https://arxiv.org/abs/gr-qc/0402098).
- [60] W. Berej, J. Matyjasek, D. Tryniecki, and M. Woronowicz, “Regular black holes in quadratic gravity,” *Gen. Rel. Grav.* **38** (2006) 885–906, [arXiv:hep-th/0606185](https://arxiv.org/abs/hep-th/0606185).

- [61] S. Bhattacharjee, S. Sarkar, and A. C. Wall, “Holographic entropy increases in quadratic curvature gravity,” *Phys. Rev. D* **92** no. 6, (2015) 064006, [arXiv:1504.04706 \[gr-qc\]](https://arxiv.org/abs/1504.04706).
- [62] L. Alvarez-Gaume, A. Kehagias, C. Kounnas, D. Lüst, and A. Riotto, “Aspects of Quadratic Gravity,” *Fortsch. Phys.* **64** no. 2-3, (2016) 176–189, [arXiv:1505.07657 \[hep-th\]](https://arxiv.org/abs/1505.07657).
- [63] S. W. Hawking, “Black holes in general relativity,” *Comm. Math. Phys.* **25** no. 2, (1972) 152–166. <https://projecteuclid.org:443/euclid.cmp/1103857884>.
- [64] J. L. Friedman, K. Schleich, and D. M. Witt, “Topological censorship,” *Phys. Rev. Lett.* **71** (Sep, 1993) 1486–1489. <https://link.aps.org/doi/10.1103/PhysRevLett.71.1486>.
- [65] G. J. Galloway and R. Schoen, “A Generalization of Hawking’s black hole topology theorem to higher dimensions,” *Commun. Math. Phys.* **266** (2006) 571–576, [arXiv:gr-qc/0509107](https://arxiv.org/abs/gr-qc/0509107).
- [66] G. J. Galloway, *Constraints on the topology of higher dimensional black holes*, pp. 159–179. 2012. [arXiv:1111.5356 \[gr-qc\]](https://arxiv.org/abs/1111.5356).
- [67] A. K. Mishra, M. Rahman, and S. Sarkar, “Black Hole Topology in $f(R)$ Gravity,” *Class. Quant. Grav.* **35** no. 14, (2018) 145011, [arXiv:1806.06596 \[gr-qc\]](https://arxiv.org/abs/1806.06596).
- [68] J. D. Bekenstein, “Black holes and the second law,” *Lett. Nuovo Cim.* **4** (1972) 737–740.
- [69] J. D. Bekenstein, “Black holes and entropy,” *Phys. Rev. D* **7** (1973) 2333–2346.
- [70] S. W. Hawking, “Particle creation by black holes,” *Comm. Math. Phys.* **43** no. 3, (1975) 199–220. <https://projecteuclid.org:443/euclid.cmp/1103899181>.
- [71] J. M. Bardeen, B. Carter, and S. W. Hawking, “The Four laws of black hole mechanics,” *Commun. Math. Phys.* **31** (1973) 161–170.
- [72] E. Poisson, *A Relativist’s Toolkit: The Mathematics of Black-Hole Mechanics*. Cambridge University Press, 2004.
- [73] S. W. Hawking and J. B. Hartle, “Energy and angular momentum flow into a black hole,” *Comm. Math. Phys.* **27** no. 4, (1972) 283–290. <https://projecteuclid.org:443/euclid.cmp/1103858289>.
- [74] R. M. Wald, *Quantum Field Theory in Curved Space-Time and Black Hole Thermodynamics*. Chicago Lectures in Physics. University of Chicago Press, Chicago, IL, 10, 1995.
- [75] R. M. Wald, “The thermodynamics of black holes,” *Living Rev. Rel.* **4** (2001) 6, [arXiv:gr-qc/9912119](https://arxiv.org/abs/gr-qc/9912119).
- [76] S. Sarkar, “Black Hole Thermodynamics: General Relativity and Beyond,” *Gen. Rel. Grav.* **51** no. 5, (2019) 63, [arXiv:1905.04466 \[hep-th\]](https://arxiv.org/abs/1905.04466).
- [77] A. Einstein, “Lens-Like Action of a Star by the Deviation of Light in the Gravitational Field,” *Science* **84** (1936) 506–507.
- [78] M. Bartelmann, “Gravitational Lensing,” *Class. Quant. Grav.* **27** (2010) 233001, [arXiv:1010.3829 \[astro-ph.CO\]](https://arxiv.org/abs/1010.3829).
- [79] P. V. P. Cunha and C. A. R. Herdeiro, “Shadows and strong gravitational lensing: a brief review,” *Gen. Rel. Grav.* **50** no. 4, (2018) 42, [arXiv:1801.00860 \[gr-qc\]](https://arxiv.org/abs/1801.00860).

- [80] S. Liebes, “Gravitational lenses,” *Phys. Rev.* **133** (Feb, 1964) B835–B844.
<https://link.aps.org/doi/10.1103/PhysRev.133.B835>.
- [81] M. Sereno, A. Sesana, A. Bleuler, P. Jetzer, M. Volonteri, and M. C. Begelman, “Strong lensing of gravitational waves as seen by lisa,” *Phys. Rev. Lett.* **105** (Dec, 2010) 251101.
<https://link.aps.org/doi/10.1103/PhysRevLett.105.251101>.
- [82] N. Seto, “Strong gravitational lensing and localization of merging massive black hole binaries with lisa,” *Phys. Rev. D* **69** (Jan, 2004) 022002.
<https://link.aps.org/doi/10.1103/PhysRevD.69.022002>.
- [83] V. Bozza, “Gravitational Lensing by Black Holes,” *Gen. Rel. Grav.* **42** (2010) 2269–2300,
[arXiv:0911.2187 \[gr-qc\]](https://arxiv.org/abs/0911.2187).
- [84] S. Frittelli and E. T. Newman, “Exact universal gravitational lensing equation,” *Phys. Rev. D* **59** (Apr, 1999) 124001. <https://link.aps.org/doi/10.1103/PhysRevD.59.124001>.
- [85] S. Chakraborty and S. SenGupta, “Strong gravitational lensing — A probe for extra dimensions and Kalb-Ramond field,” *JCAP* **1707** no. 07, (2017) 045, [arXiv:1611.06936 \[gr-qc\]](https://arxiv.org/abs/1611.06936).
- [86] A. K. Mishra, S. Chakraborty, and S. Sarkar, “Understanding photon sphere and black hole shadow in dynamically evolving spacetimes,” *Phys. Rev. D* **99** no. 10, (2019) 104080,
[arXiv:1903.06376 \[gr-qc\]](https://arxiv.org/abs/1903.06376).
- [87] S. E. Vazquez and E. P. Esteban, “Strong field gravitational lensing by a Kerr black hole,” *Nuovo Cim.* **B119** (2004) 489–519, [arXiv:gr-qc/0308023 \[gr-qc\]](https://arxiv.org/abs/gr-qc/0308023).
- [88] R. Shaikh, P. Kocherlakota, R. Narayan, and P. S. Joshi, “Shadows of spherically symmetric black holes and naked singularities,” *Mon. Not. Roy. Astron. Soc.* **482** (2019) 52,
[arXiv:1802.08060 \[astro-ph.HE\]](https://arxiv.org/abs/1802.08060).
- [89] P. V. P. Cunha, C. A. R. Herdeiro, and M. J. Rodriguez, “Does the black hole shadow probe the event horizon geometry?,” *Phys. Rev. D* **97** no. 8, (2018) 084020, [arXiv:1802.02675 \[gr-qc\]](https://arxiv.org/abs/1802.02675).
- [90] N. Tsukamoto, “Black hole shadow in an asymptotically-flat, stationary, and axisymmetric spacetime: The Kerr-Newman and rotating regular black holes,” *Phys. Rev. D* **97** no. 6, (2018) 064021, [arXiv:1708.07427 \[gr-qc\]](https://arxiv.org/abs/1708.07427).
- [91] S. V. Repin, D. A. Kompaneets, I. D. Novikov, and V. A. Mityagina, “Shadow of rotating black holes on a standard background screen,” [arXiv:1802.04667 \[gr-qc\]](https://arxiv.org/abs/1802.04667).
- [92] A. Abdjabbarov, M. Amir, B. Ahmedov, and S. G. Ghosh, “Shadow of rotating regular black holes,” *Phys. Rev. D* **93** no. 10, (2016) 104004, [arXiv:1604.03809 \[gr-qc\]](https://arxiv.org/abs/1604.03809).
- [93] R. Kumar and S. G. Ghosh, “Black hole parameters estimation from its shadow,”
[arXiv:1811.01260 \[gr-qc\]](https://arxiv.org/abs/1811.01260).
- [94] P. V. P. Cunha, C. A. R. Herdeiro, and M. J. Rodriguez, “Shadows of Exact Binary Black Holes,” *Phys. Rev. D* **98** no. 4, (2018) 044053, [arXiv:1805.03798 \[gr-qc\]](https://arxiv.org/abs/1805.03798).
- [95] D. Ayzenberg and N. Yunes, “Black Hole Shadow as a Test of General Relativity: Quadratic Gravity,” *Class. Quant. Grav.* **35** no. 23, (2018) 235002, [arXiv:1807.08422 \[gr-qc\]](https://arxiv.org/abs/1807.08422).

- [96] M. Rahman and A. A. Sen, “Astrophysical Signatures of Black holes in Generalized Proca Theories,” [arXiv:1810.09200 \[gr-qc\]](https://arxiv.org/abs/1810.09200).
- [97] F. Atamurotov, A. Abdujabbarov, and B. Ahmedov, “Shadow of rotating non-Kerr black hole,” *Phys. Rev.* **D88** no. 6, (2013) 064004.
- [98] F. Atamurotov, S. G. Ghosh, and B. Ahmedov, “Horizon structure of rotating Einstein?Born?Infeld black holes and shadow,” *Eur. Phys. J.* **C76** no. 5, (2016) 273, [arXiv:1506.03690 \[gr-qc\]](https://arxiv.org/abs/1506.03690).
- [99] M. Mars, C. F. Paganini, and M. A. Oancea, “The fingerprints of black holes-shadows and their degeneracies,” *Class. Quant. Grav.* **35** no. 2, (2018) 025005, [arXiv:1710.02402 \[gr-qc\]](https://arxiv.org/abs/1710.02402).
- [100] B. Carter, “Global structure of the Kerr family of gravitational fields,” *Phys. Rev.* **174** (1968) 1559–1571.
- [101] V. P. Frolov and A. Zelnikov, *Introduction to black hole physics*. Oxford Univ. Press, Oxford, 2011. <https://cds.cern.ch/record/1418196>.
- [102] R. .Wald, “Gedanken experiments to destroy a black hole,” *Annals Phys.* **82** (1974) 548–556.
- [103] R. M. Wald, “Gravitational collapse and cosmic censorship,” in *Black Holes, Gravitational Radiation and the Universe: Essays in Honor of C.V. Vishveshwara*, pp. 69–85. 1997. [arXiv:gr-qc/9710068 \[gr-qc\]](https://arxiv.org/abs/gr-qc/9710068).
- [104] A. K. Mishra and S. Sarkar, “Overcharging a multi black hole system and cosmic censorship,” *Phys. Rev. D* **100** no. 2, (2019) 024030, [arXiv:1905.00394 \[gr-qc\]](https://arxiv.org/abs/1905.00394).
- [105] J. Isenberg, “On Strong Cosmic Censorship,” [arXiv:1505.06390 \[gr-qc\]](https://arxiv.org/abs/1505.06390).
- [106] V. Cardoso, J. a. L. Costa, K. Destounis, P. Hintz, and A. Jansen, “Quasinormal modes and strong cosmic censorship,” *Phys. Rev. Lett.* **120** (Jan, 2018) 031103. <https://link.aps.org/doi/10.1103/PhysRevLett.120.031103>.
- [107] A. K. Mishra and S. Chakraborty, “Strong Cosmic Censorship in higher curvature gravity,” *Phys. Rev. D* **101** no. 6, (2020) 064041, [arXiv:1911.09855 \[gr-qc\]](https://arxiv.org/abs/1911.09855).
- [108] S. Capozziello, “Newtonian limit of extended theories of gravity,” [arXiv:gr-qc/0412088](https://arxiv.org/abs/gr-qc/0412088).
- [109] S. Capozziello and A. Stabile, “The Newtonian limit of metric gravity theories with quadratic Lagrangians,” *Class. Quant. Grav.* **26** (2009) 085019, [arXiv:0903.3238 \[gr-qc\]](https://arxiv.org/abs/0903.3238).
- [110] C. P. L. Berry and J. R. Gair, “Linearized f(R) Gravity: Gravitational Radiation and Solar System Tests,” *Phys. Rev. D* **83** (2011) 104022, [arXiv:1104.0819 \[gr-qc\]](https://arxiv.org/abs/1104.0819). [Erratum: *Phys. Rev. D* 85, 089906 (2012)].
- [111] C. D. Hoyle, D. J. Kapner, B. R. Heckel, E. G. Adelberger, J. H. Gundlach, U. Schmidt, and H. E. Swanson, “Submillimeter tests of the gravitational inverse-square law,” *Phys. Rev. D* **70** (Aug, 2004) 042004. <https://link.aps.org/doi/10.1103/PhysRevD.70.042004>.
- [112] D. J. Kapner, T. S. Cook, E. G. Adelberger, J. H. Gundlach, B. R. Heckel, C. D. Hoyle, and H. E. Swanson, “Tests of the gravitational inverse-square law below the dark-energy length scale,” *Phys. Rev. Lett.* **98** (Jan, 2007) 021101. <https://link.aps.org/doi/10.1103/PhysRevLett.98.021101>.

- [113] K. Yagi, "New constraint on scalar gauss-bonnet gravity and a possible explanation for the excess of the orbital decay rate in a low-mass x-ray binary," *Phys. Rev. D* **86** (Oct, 2012) 081504. <https://link.aps.org/doi/10.1103/PhysRevD.86.081504>.
- [114] E. Berti *et al.*, "Testing General Relativity with Present and Future Astrophysical Observations," *Class. Quant. Grav.* **32** (2015) 243001, [arXiv:1501.07274 \[gr-qc\]](https://arxiv.org/abs/1501.07274).
- [115] A. Maselli, P. Pani, R. Cotesta, L. Gualtieri, V. Ferrari, and L. Stella, "Geodesic models of quasi-periodic-oscillations as probes of quadratic gravity," *The Astrophysical Journal* **843** no. 1, (Jun, 2017) 25. <https://doi.org/10.3847/1538-4357/aa72e2>.
- [116] D. Ayzenberg and N. Yunes, "Black Hole Continuum Spectra as a Test of General Relativity: Quadratic Gravity," *Class. Quant. Grav.* **34** no. 11, (2017) 115003, [arXiv:1701.07003 \[gr-qc\]](https://arxiv.org/abs/1701.07003).
- [117] Z. Carson and K. Yagi, "Testing General Relativity with Gravitational Waves," [arXiv:2011.02938 \[gr-qc\]](https://arxiv.org/abs/2011.02938).
- [118] K. Chamberlain and N. Yunes, "Theoretical physics implications of gravitational wave observation with future detectors," *Physical Review D* **96** no. 8, (Oct, 2017) . [http://dx.doi.org/10.1103/PhysRevD.96.084039](https://dx.doi.org/10.1103/PhysRevD.96.084039).
- [119] N. Yunes and F. Pretorius, "Fundamental Theoretical Bias in Gravitational Wave Astrophysics and the Parameterized Post-Einsteinian Framework," *Phys. Rev. D* **80** (2009) 122003, [arXiv:0909.3328 \[gr-qc\]](https://arxiv.org/abs/0909.3328).
- [120] S. Tahura and K. Yagi, "Parametrized post-einsteinian gravitational waveforms in various modified theories of gravity," *Phys. Rev. D* **98** (Oct, 2018) 084042. <https://link.aps.org/doi/10.1103/PhysRevD.98.084042>.
- [121] Z. Carson and K. Yagi, "Parameterized and Consistency Tests of Gravity with GravitationalWaves: Current and Future," *MDPI Proc.* **17** no. 1, (2019) 5, [arXiv:1908.07103 \[gr-qc\]](https://arxiv.org/abs/1908.07103).
- [122] S. Tahura, K. Yagi, and Z. Carson, "Testing Gravity with Gravitational Waves from Binary Black Hole Mergers: Contributions from Amplitude Corrections," *Phys. Rev. D* **100** no. 10, (2019) 104001, [arXiv:1907.10059 \[gr-qc\]](https://arxiv.org/abs/1907.10059).
- [123] B. Abbott, R. Abbott, T. Abbott, M. Abernathy, F. Acernese, K. Ackley, C. Adams, T. Adams, P. Addesso, R. Adhikari, and et al., "Properties of the binary black hole merger gw150914," *Physical Review Letters* **116** no. 24, (Jun, 2016) . [http://dx.doi.org/10.1103/PhysRevLett.116.241102](https://dx.doi.org/10.1103/PhysRevLett.116.241102).
- [124] A. Ghosh, A. Ghosh, N. K. Johnson-McDaniel, C. K. Mishra, P. Ajith, W. Del Pozzo, D. A. Nichols, Y. Chen, A. B. Nielsen, C. P. L. Berry, and L. London, "Testing general relativity using golden black-hole binaries," *Phys. Rev. D* **94** (Jul, 2016) 021101. <https://link.aps.org/doi/10.1103/PhysRevD.94.021101>.
- [125] A. Ghosh, N. K. Johnson-McDaniel, A. Ghosh, C. K. Mishra, P. Ajith, W. D. Pozzo, C. P. L. Berry, A. B. Nielsen, and L. London, "Testing general relativity using gravitational wave signals from the inspiral, merger and ringdown of binary black holes," *Classical and Quantum Gravity* **35** no. 1, (Nov, 2017) 014002. [http://dx.doi.org/10.1088/1361-6382/aa972e](https://dx.doi.org/10.1088/1361-6382/aa972e).

- [126] Z. Carson and K. Yagi, “Probing string-inspired gravity with the inspiral–merger–ringdown consistency tests of gravitational waves,” *Class. Quant. Grav.* **37** no. 21, (2020) 215007, [arXiv:2002.08559 \[gr-qc\]](https://arxiv.org/abs/2002.08559).
- [127] Z. Carson and K. Yagi, “Probing beyond-kerr spacetimes with inspiral-ringdown corrections to gravitational waves,” *Phys. Rev. D* **101** (Apr, 2020) 084050.
<https://link.aps.org/doi/10.1103/PhysRevD.101.084050>.
- [128] B. Abbott, R. Abbott, T. Abbott, S. Abraham, F. Acernese, K. Ackley, C. Adams, R. Adhikari, V. Adya, C. Affeldt, and et al., “Tests of general relativity with the binary black hole signals from the ligo-virgo catalog gwtc-1,” *Physical Review D* **100** no. 10, (Nov, 2019) .
<http://dx.doi.org/10.1103/PhysRevD.100.104036>.
- [129] C. de Rham, J. T. Deskins, A. J. Tolley, and S.-Y. Zhou, “Graviton Mass Bounds,” *Rev. Mod. Phys.* **89** no. 2, (2017) 025004, [arXiv:1606.08462 \[astro-ph.CO\]](https://arxiv.org/abs/1606.08462).
- [130] C. M. Will, “Solar system versus gravitational-wave bounds on the graviton mass,” *Class. Quant. Grav.* **35** no. 17, (2018) 17LT01, [arXiv:1805.10523 \[gr-qc\]](https://arxiv.org/abs/1805.10523).
- [131] S. Perkins and N. Yunes, “Probing screening and the graviton mass with gravitational waves,” *Classical and Quantum Gravity* **36** no. 5, (Feb, 2019) 055013.
<http://dx.doi.org/10.1088/1361-6382/aafce6>.
- [132] D. Bettoni, J. M. Ezquiaga, K. Hinterbichler, and M. Zumalacárregui, “Speed of gravitational waves and the fate of scalar-tensor gravity,” *Phys. Rev. D* **95** (Apr, 2017) 084029.
<https://link.aps.org/doi/10.1103/PhysRevD.95.084029>.
- [133] J. M. Ezquiaga and M. Zumalacárregui, “Dark energy after gw170817: Dead ends and the road ahead,” *Phys. Rev. Lett.* **119** (Dec, 2017) 251304.
<https://link.aps.org/doi/10.1103/PhysRevLett.119.251304>.
- [134] T. Baker, E. Bellini, P. G. Ferreira, M. Lagos, J. Noller, and I. Sawicki, “Strong constraints on cosmological gravity from gw170817 and grb 170817a,” *Phys. Rev. Lett.* **119** (Dec, 2017) 251301.
<https://link.aps.org/doi/10.1103/PhysRevLett.119.251301>.
- [135] J. Sakstein and B. Jain, “Implications of the neutron star merger gw170817 for cosmological scalar-tensor theories,” *Phys. Rev. Lett.* **119** (Dec, 2017) 251303.
<https://link.aps.org/doi/10.1103/PhysRevLett.119.251303>.
- [136] P. Creminelli and F. Vernizzi, “Dark energy after gw170817 and grb170817a,” *Phys. Rev. Lett.* **119** (Dec, 2017) 251302. <https://link.aps.org/doi/10.1103/PhysRevLett.119.251302>.
- [137] S. Nojiri and S. D. Odintsov, “Cosmological Bound from the Neutron Star Merger GW170817 in scalar-tensor and $F(R)$ gravity theories,” *Phys. Lett. B* **779** (2018) 425–429, [arXiv:1711.00492 \[astro-ph.CO\]](https://arxiv.org/abs/1711.00492).
- [138] Y. Akrami, P. Brax, A.-C. Davis, and V. Vardanyan, “Neutron star merger gw170817 strongly constrains doubly coupled bigravity,” *Phys. Rev. D* **97** (Jun, 2018) 124010.
<https://link.aps.org/doi/10.1103/PhysRevD.97.124010>.
- [139] S. Boran, S. Desai, E. O. Kahya, and R. P. Woodard, “Gw170817 falsifies dark matter emulators,” *Phys. Rev. D* **97** (Feb, 2018) 041501.
<https://link.aps.org/doi/10.1103/PhysRevD.97.041501>.

- [140] S. Bahamonde, K. F. Dialektopoulos, V. Gakis, and J. Levi Said, “Reviving Horndeski theory using teleparallel gravity after GW170817,” *Phys. Rev. D* **101** no. 8, (2020) 084060, [arXiv:1907.10057 \[gr-qc\]](https://arxiv.org/abs/1907.10057).
- [141] A. Casalino, M. Rinaldi, L. Sebastiani, and S. Vagnozzi, “Mimicking dark matter and dark energy in a mimetic model compatible with GW170817,” *Phys. Dark Univ.* **22** (2018) 108, [arXiv:1803.02620 \[gr-qc\]](https://arxiv.org/abs/1803.02620).
- [142] A. Casalino, M. Rinaldi, L. Sebastiani, and S. Vagnozzi, “Alive and well: mimetic gravity and a higher-order extension in light of GW170817,” *Class. Quant. Grav.* **36** no. 1, (2019) 017001, [arXiv:1811.06830 \[gr-qc\]](https://arxiv.org/abs/1811.06830).
- [143] R. Emparan and H. S. Reall, “Black Holes in Higher Dimensions,” *Living Rev. Rel.* **11** (2008) 6, [arXiv:0801.3471 \[hep-th\]](https://arxiv.org/abs/0801.3471).
- [144] T. Jacobson and S. Venkataramani, “Topology of event horizons and topological censorship,” *Class. Quant. Grav.* **12** (1995) 1055–1062, [arXiv:gr-qc/9410023](https://arxiv.org/abs/gr-qc/9410023).
- [145] T. Jacobson and G. Kang, “Conformal invariance of black hole temperature,” *Class. Quant. Grav.* **10** (1993) L201–L206, [arXiv:gr-qc/9307002](https://arxiv.org/abs/gr-qc/9307002).
- [146] E. Gourgoulhon and J. L. Jaramillo, “A 3+1 perspective on null hypersurfaces and isolated horizons,” *Phys. Rept.* **423** (2006) 159–294, [arXiv:gr-qc/0503113](https://arxiv.org/abs/gr-qc/0503113).
- [147] D. Wands, “Extended gravity theories and the Einstein-Hilbert action,” *Class. Quant. Grav.* **11** (1994) 269–280, [arXiv:gr-qc/9307034](https://arxiv.org/abs/gr-qc/9307034).
- [148] T. Jacobson, G. Kang, and R. C. Myers, “Increase of black hole entropy in higher curvature gravity,” *Phys. Rev. D* **52** (1995) 3518–3528, [arXiv:gr-qc/9503020](https://arxiv.org/abs/gr-qc/9503020).
- [149] T. Jacobson, G. Kang, and R. C. Myers, “Black hole entropy in higher curvature gravity,” in *16th Annual MRST (Montreal-Rochester-Syracuse-Toronto) Meeting on High-energy Physics: What Next? Exploring the Future of High-energy Physics.* 5, 1994. [arXiv:gr-qc/9502009](https://arxiv.org/abs/gr-qc/9502009).
- [150] P. Cañate, L. G. Jaime, and M. Salgado, “Spherically symmetric black holes in $f(R)$ gravity: Is geometric scalar hair supported ?,” *Class. Quant. Grav.* **33** no. 15, (2016) 155005, [arXiv:1509.01664 \[gr-qc\]](https://arxiv.org/abs/1509.01664).
- [151] J. F. M. Delgado, C. A. R. Herdeiro, E. Radu, and H. Runarsson, “Kerr-Newman black holes with scalar hair,” *Phys. Lett. B* **761** (2016) 234–241, [arXiv:1608.00631 \[gr-qc\]](https://arxiv.org/abs/1608.00631).
- [152] C. A. R. Herdeiro and E. Radu, “Kerr black holes with scalar hair,” *Phys. Rev. Lett.* **112** (2014) 221101, [arXiv:1403.2757 \[gr-qc\]](https://arxiv.org/abs/1403.2757).
- [153] J. D. Bekenstein, “Black holes: Classical properties, thermodynamics and heuristic quantization,” in *9th Brazilian School of Cosmology and Gravitation.* 7, 1998. [arXiv:gr-qc/9808028](https://arxiv.org/abs/gr-qc/9808028).
- [154] M.-l. Cai and G. J. Galloway, “On the Topology and area of higher dimensional black holes,” *Class. Quant. Grav.* **18** (2001) 2707–2718, [arXiv:hep-th/0102149](https://arxiv.org/abs/hep-th/0102149).
- [155] L. Andersson, M. Mars, and W. Simon, “Stability of marginally outer trapped surfaces and existence of marginally outer trapped tubes,” *Adv. Theor. Math. Phys.* **12** no. 4, (08, 2008) 853–888. <https://projecteuclid.org:443/euclid.atmp/1216046746>.

- [156] G. Huang, “Rigidity of riemannian manifolds with positive scalar curvature,” 2017.
- [157] L. Ambrozio, “On static three-manifolds with positive scalar curvature,” 2015.
- [158] M. Hallam and V. Mathai, “Positive scalar curvature via end-periodic manifolds,” *K Theory* **5** (2020) 639–676, [arXiv:1706.09354 \[math.DG\]](https://arxiv.org/abs/1706.09354).
- [159] A. A. Starobinsky, “Spectrum of relict gravitational radiation and the early state of the universe,” *JETP Lett.* **30** (1979) 682–685.
- [160] A. Kehagias, A. Moradinezhad Dizgah, and A. Riotto, “Remarks on the Starobinsky model of inflation and its descendants,” *Phys. Rev. D* **89** no. 4, (2014) 043527, [arXiv:1312.1155 \[hep-th\]](https://arxiv.org/abs/1312.1155).
- [161] T. Asaka, S. Iso, H. Kawai, K. Kohri, T. Noumi, and T. Terada, “Reinterpretation of the Starobinsky model,” *PTEP* **2016** no. 12, (2016) 123E01, [arXiv:1507.04344 \[hep-th\]](https://arxiv.org/abs/1507.04344).
- [162] M. Artymowski, Z. Lalak, and M. Lewicki, “Inflationary scenarios in Starobinsky model with higher order corrections,” *JCAP* **06** (2015) 032, [arXiv:1502.01371 \[hep-th\]](https://arxiv.org/abs/1502.01371).
- [163] A. Mishra, S. Chakraborty, A. Ghosh, and S. Sarkar, “On the physical process first law for dynamical black holes,” *JHEP* **09** (2018) 034, [arXiv:1709.08925 \[gr-qc\]](https://arxiv.org/abs/1709.08925).
- [164] T. Jacobson, “Thermodynamics of space-time: The Einstein equation of state,” *Phys. Rev. Lett.* **75** (1995) 1260–1263, [arXiv:gr-qc/9504004](https://arxiv.org/abs/gr-qc/9504004).
- [165] A. J. Amsel, D. Marolf, and A. Virmani, “Physical process first law for bifurcate killing horizons,” *Physical Review D* **77** no. 2, (Jan, 2008) .
<http://dx.doi.org/10.1103/PhysRevD.77.024011>.
- [166] S. Bhattacharjee and S. Sarkar, “Physical process first law and caustic avoidance for rindler horizons,” *Physical Review D* **91** no. 2, (Jan, 2015) .
<http://dx.doi.org/10.1103/PhysRevD.91.024024>.
- [167] S. Chakraborty and T. Padmanabhan, “Thermodynamical interpretation of the geometrical variables associated with null surfaces,” *Physical Review D* **92** no. 10, (Nov, 2015) .
<http://dx.doi.org/10.1103/PhysRevD.92.104011>.
- [168] R. M. Wald, “Black hole entropy is the noether charge,” *Phys. Rev. D* **48** (Oct, 1993) R3427–R3431. <https://link.aps.org/doi/10.1103/PhysRevD.48.R3427>.
- [169] V. Iyer and R. M. Wald, “Some properties of the noether charge and a proposal for dynamical black hole entropy,” *Phys. Rev. D* **50** (Jul, 1994) 846–864.
<https://link.aps.org/doi/10.1103/PhysRevD.50.846>.
- [170] T. Jacobson, G. Kang, and R. C. Myers, “On black hole entropy,” *Phys. Rev. D* **49** (Jun, 1994) 6587–6598. <https://link.aps.org/doi/10.1103/PhysRevD.49.6587>.
- [171] C. Fairoos, A. Ghosh, and S. Sarkar, “Black hole entropy production and transport coefficients in lovelock gravity,” *Phys. Rev. D* **98** (Jul, 2018) 024036.
<https://link.aps.org/doi/10.1103/PhysRevD.98.024036>.
- [172] S. Bhattacharjee, A. Bhattacharyya, S. Sarkar, and A. Sinha, “Entropy functionals and c -theorems from the second law,” *Phys. Rev. D* **93** (May, 2016) 104045.
<https://link.aps.org/doi/10.1103/PhysRevD.93.104045>.

- [173] K. S. Thorne, R. H. Price, and D. A. Macdonald, eds., *BLACK HOLES: THE MEMBRANE PARADIGM*. 1986.
- [174] G. W. Gibbons and S. W. Hawking, “Action integrals and partition functions in quantum gravity,” *Phys. Rev. D* **15** (May, 1977) 2752–2756.
<https://link.aps.org/doi/10.1103/PhysRevD.15.2752>.
- [175] K. Parattu, S. Chakraborty, and T. Padmanabhan, “Variational principle for gravity with null and non-null boundaries: a unified boundary counter-term,” *The European Physical Journal C* **76** no. 3, (Mar, 2016) . <http://dx.doi.org/10.1140/epjc/s10052-016-3979-y>.
- [176] M. K. Parikh and F. Wilczek, “An action for black hole membranes,” *Phys. Rev. D* **58** (Aug, 1998) 064011. <https://link.aps.org/doi/10.1103/PhysRevD.58.064011>.
- [177] R. H. Price and K. S. Thorne, “Membrane Viewpoint on Black Holes: Properties and Evolution of the Stretched Horizon,” *Phys. Rev. D* **33** (1986) 915–941.
- [178] T. Jacobson, A. Mohd, and S. Sarkar, “Membrane paradigm for Einstein-Gauss-Bonnet gravity,” *Phys. Rev. D* **95** no. 6, (2017) 064036, [arXiv:1107.1260 \[gr-qc\]](https://arxiv.org/abs/1107.1260).
- [179] S. Kolekar and D. Kothawala, “Membrane Paradigm and Horizon Thermodynamics in Lanczos-Lovelock gravity,” *JHEP* **02** (2012) 006, [arXiv:1111.1242 \[gr-qc\]](https://arxiv.org/abs/1111.1242).
- [180] T.-Y. Zhao and T. Wang, “Membrane paradigm of black holes in Chern-Simons modified gravity,” *JCAP* **06** (2016) 019, [arXiv:1512.01919 \[gr-qc\]](https://arxiv.org/abs/1512.01919).
- [181] T. Padmanabhan, “Entropy density of spacetime and the Navier-Stokes fluid dynamics of null surfaces,” *Phys. Rev. D* **83** (2011) 044048, [arXiv:1012.0119 \[gr-qc\]](https://arxiv.org/abs/1012.0119).
- [182] S. Kolekar and T. Padmanabhan, “Action Principle for the Fluid-Gravity Correspondence and Emergent Gravity,” *Phys. Rev. D* **85** (2012) 024004, [arXiv:1109.5353 \[gr-qc\]](https://arxiv.org/abs/1109.5353).
- [183] C. Eling and Y. Oz, “A Novel Formula for Bulk Viscosity from the Null Horizon Focusing Equation,” *JHEP* **06** (2011) 007, [arXiv:1103.1657 \[hep-th\]](https://arxiv.org/abs/1103.1657).
- [184] S. Bhattacharya and S. Shankaranarayanan, “Fluctuations in horizon-fluid lead to negative bulk viscosity,” *Phys. Rev. D* **93** no. 6, (2016) 064030, [arXiv:1511.01377 \[gr-qc\]](https://arxiv.org/abs/1511.01377).
- [185] S. Kolekar, T. Padmanabhan, and S. Sarkar, “Entropy Increase during Physical Processes for Black Holes in Lanczos-Lovelock Gravity,” *Phys. Rev. D* **86** (2012) 021501, [arXiv:1201.2947 \[gr-qc\]](https://arxiv.org/abs/1201.2947).
- [186] T. Jacobson and R. C. Myers, “Black hole entropy and higher curvature interactions,” *Phys. Rev. Lett.* **70** (Jun, 1993) 3684–3687.
<https://link.aps.org/doi/10.1103/PhysRevLett.70.3684>.
- [187] A. Chatterjee and S. Sarkar, “Physical process first law and increase of horizon entropy for black holes in Einstein-Gauss-Bonnet gravity,” *Phys. Rev. Lett.* **108** (2012) 091301, [arXiv:1111.3021 \[gr-qc\]](https://arxiv.org/abs/1111.3021).
- [188] A. M. Ghez *et al.*, “Measuring Distance and Properties of the Milky Way’s Central Supermassive Black Hole with Stellar Orbits,” *Astrophys. J.* **689** (2008) 1044–1062, [arXiv:0808.2870 \[astro-ph\]](https://arxiv.org/abs/0808.2870).

- [189] R. Schodel *et al.*, “A Star in a 15.2 year orbit around the supermassive black hole at the center of the Milky Way,” *Nature* (2002) , arXiv:astro-ph/0210426 [astro-ph]. [Nature419,694(2002)].
- [190] J. Kormendy and L. C. Ho, “Coevolution (Or Not) of Supermassive Black Holes and Host Galaxies,” *Ann. Rev. Astron. Astrophys.* **51** (2013) 511–653, arXiv:1304.7762 [astro-ph.CO].
- [191] C.-M. Claudel, K. S. Virbhadra, and G. F. R. Ellis, “The Geometry of photon surfaces,” *J. Math. Phys.* **42** (2001) 818–838, arXiv:gr-qc/0005050 [gr-qc].
- [192] S. Hod, “Spherical null geodesics of rotating Kerr black holes,” *Phys. Lett.* **B718** (2013) 1552–1556, arXiv:1210.2486 [gr-qc].
- [193] Y. Decanini, A. Folacci, and B. Raffaelli, “Unstable circular null geodesics of static spherically symmetric black holes, Regge poles and quasinormal frequencies,” *Phys. Rev.* **D81** (2010) 104039, arXiv:1002.0121 [gr-qc].
- [194] A. A. Shoom, “Metamorphoses of a photon sphere,” *Phys. Rev.* **D96** no. 8, (2017) 084056, arXiv:1708.00019 [gr-qc].
- [195] T. Johannsen, “Photon Rings around Kerr and Kerr-like Black Holes,” *Astrophys. J.* **777** (2013) 170, arXiv:1501.02814 [astro-ph.HE].
- [196] E. Teo, “Spherical photon orbits around a kerr black hole,” *General Relativity and Gravitation* **35** no. 11, (Nov, 2003) 1909–1926. <https://doi.org/10.1023/A:1026286607562>.
- [197] E. Gallo and J. R. Villanueva, “Photon spheres in Einstein and Einstein-Gauss-Bonnet theories and circular null geodesics in axially-symmetric spacetimes,” *Phys. Rev.* **D92** no. 6, (2015) 064048, arXiv:1509.07379 [gr-qc].
- [198] S. Mukherjee, S. Chakraborty, and N. Dadhich, “On some novel features of the Kerr-Newman-NUT spacetime,” *Eur. Phys. J.* **C79** no. 2, (2019) 161, arXiv:1807.02216 [gr-qc].
- [199] A. A. Abdujabbarov, L. Rezzolla, and B. J. Ahmedov, “A coordinate-independent characterization of a black hole shadow,” *Mon. Not. Roy. Astron. Soc.* **454** no. 3, (2015) 2423–2435, arXiv:1503.09054 [gr-qc].
- [200] Z. Younsi, A. Zhidenko, L. Rezzolla, R. Konoplya, and Y. Mizuno, “New method for shadow calculations: Application to parametrized axisymmetric black holes,” *Phys. Rev.* **D94** no. 8, (2016) 084025, arXiv:1607.05767 [gr-qc].
- [201] C. Goddi *et al.*, “BlackHoleCam: Fundamental physics of the galactic center,” *Int. J. Mod. Phys.* **D26** no. 02, (2016) 1730001, arXiv:1606.08879 [astro-ph.HE]. [1,863(2017)].
- [202] C. Aragone, “STRINGY CHARACTERISTICS OF EFFECTIVE GRAVITY,” in *SILARG 6: 6th Latin American Symposium on Relativity and Gravitation Rio de Janeiro, Brazil, July 13-18, 1987*, pp. 60–69. 1987.
- [203] Y. Choquet-Bruhat, “The Cauchy Problem for Stringy Gravity,” *J. Math. Phys.* **29** (1988) 1891–1895.
- [204] K. Izumi, “Causal Structures in Gauss-Bonnet gravity,” *Phys. Rev.* **D90** no. 4, (2014) 044037, arXiv:1406.0677 [gr-qc].

- [205] H. Reall, N. Tanahashi, and B. Way, “Causality and Hyperbolicity of Lovelock Theories,” *Class. Quant. Grav.* **31** (2014) 205005, [arXiv:1406.3379 \[hep-th\]](https://arxiv.org/abs/1406.3379).
- [206] G. Papallo and H. S. Reall, “Graviton time delay and a speed limit for small black holes in Einstein-Gauss-Bonnet theory,” *JHEP* **11** (2015) 109, [arXiv:1508.05303 \[gr-qc\]](https://arxiv.org/abs/1508.05303).
- [207] H. S. Reall, N. Tanahashi, and B. Way, “Shock Formation in Lovelock Theories,” *Phys. Rev. D* **91** no. 4, (2015) 044013, [arXiv:1409.3874 \[hep-th\]](https://arxiv.org/abs/1409.3874).
- [208] R. Brustein and Y. Sherf, “Causality Violations in Lovelock Theories,” *Phys. Rev. D* **97** no. 8, (2018) 084019, [arXiv:1711.05140 \[hep-th\]](https://arxiv.org/abs/1711.05140).
- [209] T. Andrade, E. Caceres, and C. Keeler, “Boundary causality versus hyperbolicity for spherical black holes in Gauss?Bonnet gravity,” *Class. Quant. Grav.* **34** no. 13, (2017) 135003, [arXiv:1610.06078 \[hep-th\]](https://arxiv.org/abs/1610.06078).
- [210] A. B. Nielsen, “The Spatial relation between the event horizon and trapping horizon,” *Class. Quant. Grav.* **27** (2010) 245016, [arXiv:1006.2448 \[gr-qc\]](https://arxiv.org/abs/1006.2448).
- [211] P. C. Vaidya, “Nonstatic solutions of einstein’s field equations for spheres of fluids radiating energy,” *Phys. Rev.* **83** (Jul, 1951) 10–17.
<https://link.aps.org/doi/10.1103/PhysRev.83.10>.
- [212] E. Caceres, A. Kundu, J. F. Pedraza, and W. Tangarife, “Strong Subadditivity, Null Energy Condition and Charged Black Holes,” *JHEP* **01** (2014) 084, [arXiv:1304.3398 \[hep-th\]](https://arxiv.org/abs/1304.3398).
- [213] Z. Stuchlík and S. Hledík, “Some properties of the schwarzschild-de sitter and schwarzschild-anti-de sitter spacetimes,” *Phys. Rev. D* **60** (Jul, 1999) 044006.
<https://link.aps.org/doi/10.1103/PhysRevD.60.044006>.
- [214] M. Murenbeeld and J. R. Trollope, “Slowly rotating radiating sphere and a kerr-vaidya metric,” *Phys. Rev. D* **1** (Jun, 1970) 3220–3223.
<https://link.aps.org/doi/10.1103/PhysRevD.1.3220>.
- [215] J. M. Bardeen, W. H. Press, and S. A. Teukolsky, “Rotating black holes: Locally nonrotating frames, energy extraction, and scalar synchrotron radiation,” *Astrophys. J.* **178** (1972) 347.
- [216] C. W. Misner, K. S. Thorne, and J. A. Wheeler, *Gravitation*. Physics Series. W. H. Freeman, San Francisco, first edition ed., Sept., 1973. <http://www.worldcat.org/isbn/0716703440>.
- [217] D. L. Wiltshire, “Black Holes in String Generated Gravity Models,” *Phys. Rev. D* **38** (1988) 2445.
- [218] J. T. Wheeler, “Symmetric Solutions to the Gauss-Bonnet Extended Einstein Equations,” *Nucl. Phys.* **B268** (1986) 737–746.
- [219] P. S. JOSHI, “Cosmic censorship: A current perspective,” *Modern Physics Letters A* **17** no. 15n17, (2002) 1067–1079.
- [220] C. J. S. Clarke, “A title of cosmic censorship,” *Classical and Quantum Gravity* **11** no. 6, (Jun, 1994) 1375–1386. <https://doi.org/10.1088%2F0264-9381%2F11%2F6%2F003>.
- [221] I. Semiz, “Dyon black holes do not violate cosmic censorship,” *Class. Quant. Grav.* **7** (1990) 353–359.

- [222] S. Hod, “Black hole polarization and cosmic censorship,” *Phys. Rev.* **D60** (1999) 104031, [arXiv:gr-qc/9907001 \[gr-qc\]](https://arxiv.org/abs/gr-qc/9907001).
- [223] S. Hod, “Weak Cosmic Censorship: As Strong as Ever,” *Phys. Rev. Lett.* **100** (2008) 121101, [arXiv:0805.3873 \[gr-qc\]](https://arxiv.org/abs/0805.3873).
- [224] G. Chirco, S. Liberati, and T. P. Sotiriou, “Gedanken experiments on nearly extremal black holes and the Third Law,” *Phys. Rev.* **D82** (2010) 104015, [arXiv:1006.3655 \[gr-qc\]](https://arxiv.org/abs/1006.3655).
- [225] A. Saa and R. Santarelli, “Destroying a near-extremal Kerr-Newman black hole,” *Phys. Rev.* **D84** (2011) 027501, [arXiv:1105.3950 \[gr-qc\]](https://arxiv.org/abs/1105.3950).
- [226] C. Fairoos, A. Ghosh, and S. Sarkar, “Massless charged particles: Cosmic censorship, and the third law of black hole mechanics,” *Phys. Rev.* **D96** no. 8, (2017) 084013, [arXiv:1709.05081 \[gr-qc\]](https://arxiv.org/abs/1709.05081).
- [227] K. S. Revelar and I. Vega, “Overcharging higher-dimensional black holes with point particles,” *Phys. Rev.* **D96** no. 6, (2017) 064010, [arXiv:1706.07190 \[gr-qc\]](https://arxiv.org/abs/1706.07190).
- [228] J. An, J. Shan, H. Zhang, and S. Zhao, “Five-dimensional Myers-Perry black holes cannot be overspun in gedanken experiments,” *Phys. Rev.* **D97** no. 10, (2018) 104007, [arXiv:1711.04310 \[hep-th\]](https://arxiv.org/abs/1711.04310).
- [229] S. Jana, R. Shaikh, and S. Sarkar, “Overcharging black holes and cosmic censorship in Born-Infeld gravity,” *Phys. Rev.* **D98** no. 12, (2018) 124039, [arXiv:1808.09656 \[gr-qc\]](https://arxiv.org/abs/1808.09656).
- [230] S. Shaymatov, N. Dadhich, and B. Ahmedov, “The higher dimensional Myers-Perry black hole with single rotation always obeys the Cosmic Censorship Conjecture,” [arXiv:1809.10457 \[gr-qc\]](https://arxiv.org/abs/1809.10457).
- [231] R. Ghosh, C. Fairoos, and S. Sarkar, “Overcharging higher curvature black holes,” *Phys. Rev. D* **100** no. 12, (2019) 124019, [arXiv:1906.08016 \[gr-qc\]](https://arxiv.org/abs/1906.08016).
- [232] V. E. Hubeny, “Overcharging a black hole and cosmic censorship,” *Phys. Rev.* **D59** (1999) 064013, [arXiv:gr-qc/9808043 \[gr-qc\]](https://arxiv.org/abs/gr-qc/9808043).
- [233] J. Sorce and R. M. Wald, “Gedanken experiments to destroy a black hole. II. Kerr-Newman black holes cannot be overcharged or overspun,” *Phys. Rev.* **D96** no. 10, (2017) 104014, [arXiv:1707.05862 \[gr-qc\]](https://arxiv.org/abs/1707.05862).
- [234] S. D. Majumdar, “A class of exact solutions of einstein’s field equations,” *Phys. Rev.* **72** (Sep, 1947) 390–398. <https://link.aps.org/doi/10.1103/PhysRev.72.390>.
- [235] A. Papapetrou, “A static solution of the equations of the gravitational field for an arbitrary charge-distribution,” *Proceedings of the Royal Irish Academy. Section A: Mathematical and Physical Sciences* **51** (1945) 191–204. <http://www.jstor.org/stable/20488481>.
- [236] J. B. Hartle and S. W. Hawking, “Solutions of the einstein-maxwell equations with many black holes,” *Comm. Math. Phys.* **26** no. 2, (1972) 87–101. <https://projecteuclid.org:443/euclid.cmp/1103858037>.
- [237] O. Semerk and M. Basovnk, “Geometry of deformed black holes. I. Majumdar-Papapetrou binary,” *Phys. Rev.* **D94** no. 4, (2016) 044006, [arXiv:1608.05948 \[gr-qc\]](https://arxiv.org/abs/1608.05948).

- [238] G. A. Alekseev and V. A. Belinski, “Equilibrium configurations of two charged masses in General Relativity,” *Phys. Rev.* **D76** (2007) 021501, [arXiv:0706.1981 \[gr-qc\]](https://arxiv.org/abs/0706.1981).
- [239] W. B. Bonnor, “The Equilibrium of Two Charged Masses in General Relativity,” *Phys. Lett.* **A83** (1981) 414–416.
- [240] T. Ohta and T. Kimura, “Static Balance of Two Charged Particles in General Relativity,” *Prog. Theor. Phys.* **68** (1982) 1175.
- [241] A. Tomimatsu, “Condition for Equilibrium of Two Reissner-Nordström Black Holes,” *Prog. Theor. Phys.* **71** (1984) 409–412.
- [242] T. Azuma and T. Koikawa, “Equilibrium condition in the axisymmetric N-Reissner-Nordstrom solution,” *Prog. Theor. Phys.* **92** (1994) 1095–1104.
- [243] D. Bini, A. Geralico, and R. Ruffini, “On the equilibrium of a charged massive particle in the field of a Reissner-Nordstrom black hole,” *Phys. Lett.* **A360** (2007) 515–517, [arXiv:gr-qc/0608139 \[gr-qc\]](https://arxiv.org/abs/gr-qc/0608139).
- [244] V. S. Manko, “The Double-Reissner-Nordstrom solution and the interaction force between two spherically symmetric charged particles,” *Phys. Rev.* **D76** (2007) 124032, [arXiv:0710.2158 \[gr-qc\]](https://arxiv.org/abs/0710.2158).
- [245] A. K. Mishra, “Quasinormal modes and strong cosmic censorship in the regularised 4D Einstein–Gauss–Bonnet gravity,” *Gen. Rel. Grav.* **52** no. 11, (2020) 106, [arXiv:2004.01243 \[gr-qc\]](https://arxiv.org/abs/2004.01243).
- [246] J. L. Costa, P. M. Girão, J. Natário, and J. D. Silva, “On the global uniqueness for the Einstein–Maxwell–scalar field system with a cosmological constant: I. Well posedness and breakdown criterion,” *Class. Quant. Grav.* **32** no. 1, (2015) 015017, [arXiv:1406.7245 \[gr-qc\]](https://arxiv.org/abs/1406.7245).
- [247] A. Ori, “Inner structure of a charged black hole: An exact mass-inflation solution,” *Phys. Rev. Lett.* **67** (Aug, 1991) 789–792. <https://link.aps.org/doi/10.1103/PhysRevLett.67.789>.
- [248] E. Poisson and W. Israel, “Internal structure of black holes,” *Phys. Rev. D* **41** (Mar, 1990) 1796–1809. <https://link.aps.org/doi/10.1103/PhysRevD.41.1796>.
- [249] S. Bhattacharjee, S. Sarkar, and A. Virmani, “Internal Structure of Charged AdS Black Holes,” *Phys. Rev.* **D93** no. 12, (2016) 124029, [arXiv:1604.03730 \[hep-th\]](https://arxiv.org/abs/1604.03730).
- [250] D. Christodoulou, “The Formation of Black Holes in General Relativity,” in *On recent developments in theoretical and experimental general relativity, astrophysics and relativistic field theories. Proceedings, 12th Marcel Grossmann Meeting on General Relativity, Paris, France, July 12–18, 2009. Vol. 1–3*, pp. 24–34. 2008. [arXiv:0805.3880 \[gr-qc\]](https://arxiv.org/abs/0805.3880).
- [251] R. H. Price, “Nonspherical perturbations of relativistic gravitational collapse. i. scalar and gravitational perturbations,” *Phys. Rev. D* **5** (May, 1972) 2419–2438. <https://link.aps.org/doi/10.1103/PhysRevD.5.2419>.
- [252] Y. Angelopoulos, S. Aretakis, and D. Gajic, “Late-time asymptotics for the wave equation on spherically symmetric, stationary spacetimes,” *Adv. Math.* **323** (2018) 529–621, [arXiv:1612.01566 \[math.AP\]](https://arxiv.org/abs/1612.01566).

- [253] Y. Mo, Y. Tian, B. Wang, H. Zhang, and Z. Zhong, “Strong cosmic censorship for the massless charged scalar field in the Reissner-Nordstrom-de Sitter spacetime,” *Phys. Rev.* **D98** no. 12, (2018) 124025, [arXiv:1808.03635 \[gr-qc\]](https://arxiv.org/abs/1808.03635).
- [254] O. J. C. Dias, H. S. Reall, and J. E. Santos, “Strong cosmic censorship for charged de Sitter black holes with a charged scalar field,” *Class. Quant. Grav.* **36** no. 4, (2019) 045005, [arXiv:1808.04832 \[gr-qc\]](https://arxiv.org/abs/1808.04832).
- [255] M. Rahman, S. Chakraborty, S. SenGupta, and A. A. Sen, “Fate of Strong Cosmic Censorship Conjecture in Presence of Higher Spacetime Dimensions,” *JHEP* **03** (2019) 178, [arXiv:1811.08538 \[gr-qc\]](https://arxiv.org/abs/1811.08538).
- [256] K. Destounis, “Charged Fermions and Strong Cosmic Censorship,” *Phys. Lett.* **B795** (2019) 211–219, [arXiv:1811.10629 \[gr-qc\]](https://arxiv.org/abs/1811.10629).
- [257] B. Gwak, “Strong Cosmic Censorship under Quasinormal Modes of Non-Minimally Coupled Massive Scalar Field,” *Eur. Phys. J.* **C79** no. 9, (2019) 767, [arXiv:1812.04923 \[gr-qc\]](https://arxiv.org/abs/1812.04923).
- [258] Y. Gim and B. Gwak, “Charged Particle and Strong Cosmic Censorship in Reissner-Nordström-de Sitter Black Holes,” [arXiv:1901.11214 \[gr-qc\]](https://arxiv.org/abs/1901.11214).
- [259] H. Liu, Z. Tang, K. Destounis, B. Wang, E. Papantonopoulos, and H. Zhang, “Strong Cosmic Censorship in higher-dimensional Reissner-Nordström-de Sitter spacetime,” *JHEP* **03** (2019) 187, [arXiv:1902.01865 \[gr-qc\]](https://arxiv.org/abs/1902.01865).
- [260] M. Rahman, “On the validity of Strong Cosmic Censorship Conjecture in presence of Dirac fields,” [arXiv:1905.06675 \[gr-qc\]](https://arxiv.org/abs/1905.06675).
- [261] H. Guo, H. Liu, X.-M. Kuang, and B. Wang, “Strong Cosmic Censorship in Charged de Sitter spacetime with Scalar Field Non-minimally Coupled to Curvature,” [arXiv:1905.09461 \[gr-qc\]](https://arxiv.org/abs/1905.09461).
- [262] O. J. C. Dias, H. S. Reall, and J. E. Santos, “The BTZ black hole violates strong cosmic censorship,” [arXiv:1906.08265 \[hep-th\]](https://arxiv.org/abs/1906.08265).
- [263] V. Cardoso, J. L. Costa, K. Destounis, P. Hintz, and A. Jansen, “Strong cosmic censorship in charged black-hole spacetimes: still subtle,” *Phys. Rev.* **D98** no. 10, (2018) 104007, [arXiv:1808.03631 \[gr-qc\]](https://arxiv.org/abs/1808.03631).
- [264] O. J. C. Dias, F. C. Eperon, H. S. Reall, and J. E. Santos, “Strong cosmic censorship in de Sitter space,” *Phys. Rev.* **D97** no. 10, (2018) 104060, [arXiv:1801.09694 \[gr-qc\]](https://arxiv.org/abs/1801.09694).
- [265] Q. Gan, G. Guo, P. Wang, and H. Wu, “Strong Cosmic Censorship for a Scalar Field in a Born-Infeld-de Sitter Black Hole,” [arXiv:1907.04466 \[hep-th\]](https://arxiv.org/abs/1907.04466).
- [266] K. Destounis, R. D. B. Fontana, F. C. Mena, and E. Papantonopoulos, “Strong Cosmic Censorship in Horndeski Theory,” [arXiv:1908.09842 \[gr-qc\]](https://arxiv.org/abs/1908.09842).
- [267] R.-G. Cai and Q. Guo, “Gauss-Bonnet black holes in dS spaces,” *Phys. Rev.* **D69** (2004) 104025, [arXiv:hep-th/0311020 \[hep-th\]](https://arxiv.org/abs/hep-th/0311020).
- [268] X.-Y. Guo, H.-F. Li, and L.-C. Zhang, “Entropy of Higher Dimensional Charged Gauss-Bonnet Black hole in de Sitter Space,” [arXiv:1803.09456 \[gr-qc\]](https://arxiv.org/abs/1803.09456).

- [269] R.-G. Cai, L.-M. Cao, L. Li, and R.-Q. Yang, “P-V criticality in the extended phase space of Gauss-Bonnet black holes in AdS space,” *JHEP* **09** (2013) 005, [arXiv:1306.6233 \[gr-qc\]](https://arxiv.org/abs/1306.6233).
- [270] S. H. Hendi, B. E. Panah, and S. Panahiyan, “Black Hole Solutions in Gauss?Bonnet?Massive Gravity in the Presence of Power?Maxwell Field,” *Fortsch. Phys.* **66** no. 3, (2018) 1800005, [arXiv:1708.02239 \[hep-th\]](https://arxiv.org/abs/1708.02239).
- [271] S.-W. Wei and Y.-X. Liu, “Critical phenomena and thermodynamic geometry of charged Gauss-Bonnet AdS black holes,” *Phys. Rev. D* **87** no. 4, (2013) 044014, [arXiv:1209.1707 \[gr-qc\]](https://arxiv.org/abs/1209.1707).
- [272] R. Gannouji, Y. Rodríguez Baez, and N. Dadhich, “Pure Lovelock black holes in dimensions $d = 3n + 1$ are stable,” *Phys. Rev. D* **100** (Oct, 2019) 084011. <https://link.aps.org/doi/10.1103/PhysRevD.100.084011>.
- [273] N. Dadhich and J. M. Pons, “Static pure Lovelock black hole solutions with horizon topology $S^{(n)} \times S^{(n)}$,” *JHEP* **05** (2015) 067, [arXiv:1503.00974 \[gr-qc\]](https://arxiv.org/abs/1503.00974).
- [274] N. Dadhich and S. Chakraborty, “Buchdahl compactness limit for a pure Lovelock static fluid star,” *Phys. Rev. D* **95** no. 6, (2017) 064059, [arXiv:1606.01330 \[gr-qc\]](https://arxiv.org/abs/1606.01330).
- [275] S. Chakraborty and N. Dadhich, “ $1/r$ potential in higher dimensions,” *Eur. Phys. J. C* **78** no. 1, (2018) 81, [arXiv:1605.01961 \[gr-qc\]](https://arxiv.org/abs/1605.01961).
- [276] N. Dadhich, R. Durka, N. Merino, and O. Miskovic, “Dynamical structure of Pure Lovelock gravity,” *Phys. Rev. D* **93** no. 6, (2016) 064009, [arXiv:1511.02541 \[hep-th\]](https://arxiv.org/abs/1511.02541).
- [277] R. Gannouji and N. Dadhich, “Stability and existence analysis of static black holes in pure Lovelock theories,” *Class. Quant. Grav.* **31** (2014) 165016, [arXiv:1311.4543 \[gr-qc\]](https://arxiv.org/abs/1311.4543).
- [278] V. Cardoso, A. S. Miranda, E. Berti, H. Witek, and V. T. Zanchin, “Geodesic stability, lyapunov exponents, and quasinormal modes,” *Phys. Rev. D* **79** (Mar, 2009) 064016. <https://link.aps.org/doi/10.1103/PhysRevD.79.064016>.
- [279] S. Hod, “Black-hole quasinormal resonances: Wave analysis versus a geometric-optics approximation,” *Phys. Rev. D* **80** (Sep, 2009) 064004. <https://link.aps.org/doi/10.1103/PhysRevD.80.064004>.
- [280] B. Mashhoon, “Stability of charged rotating black holes in the eikonal approximation,” *Phys. Rev. D* **31** (Jan, 1985) 290–293. <https://link.aps.org/doi/10.1103/PhysRevD.31.290>.
- [281] R. A. Konoplya and Z. Stuchlík, “Are eikonal quasinormal modes linked to the unstable circular null geodesics?,” *Phys. Lett. B* **771** (2017) 597–602, [arXiv:1705.05928 \[gr-qc\]](https://arxiv.org/abs/1705.05928).
- [282] R. A. Konoplya, A. F. Zinhailo, and Z. Stuchlík, “Quasinormal modes, scattering, and Hawking radiation in the vicinity of an Einstein-dilaton-Gauss-Bonnet black hole,” *Phys. Rev. D* **99** no. 12, (2019) 124042, [arXiv:1903.03483 \[gr-qc\]](https://arxiv.org/abs/1903.03483).
- [283] D.-P. Du, B. Wang, and R.-K. Su, “Quasinormal modes in pure de sitter spacetimes,” *Phys. Rev. D* **70** (Sep, 2004) 064024. <https://link.aps.org/doi/10.1103/PhysRevD.70.064024>.
- [284] A. Lopez-Ortega, “On the quasinormal modes of the de Sitter spacetime,” *Gen. Rel. Grav.* **44** (2012) 2387–2400, [arXiv:1207.6791 \[gr-qc\]](https://arxiv.org/abs/1207.6791).

- [285] E. Abdalla, K. H. C. Castello-Branco, and A. Lima-Santos, “Support of ds/cft correspondence from space-time perturbations,” *Phys. Rev. D* **66** (Nov, 2002) 104018.
<https://link.aps.org/doi/10.1103/PhysRevD.66.104018>.
- [286] E. Abdalla, R. A. Konoplya, and C. Molina, “Scalar field evolution in Gauss-Bonnet black holes,” *Phys. Rev. D* **72** (2005) 084006, [arXiv:hep-th/0507100 \[hep-th\]](https://arxiv.org/abs/hep-th/0507100).
- [287] P. Hintz and A. Vasy, “Analysis of linear waves near the Cauchy horizon of cosmological black holes,” *J. Math. Phys.* **58** no. 8, (2017) 081509, [arXiv:1512.08004 \[math.AP\]](https://arxiv.org/abs/1512.08004).
- [288] R. Konoplya, “Quasinormal modes of the charged black hole in Gauss-Bonnet gravity,” *Phys. Rev. D* **71** (2005) 024038, [arXiv:hep-th/0410057 \[hep-th\]](https://arxiv.org/abs/hep-th/0410057).
- [289] R. A. Konoplya and A. Zhidenko, “(In)stability of D-dimensional black holes in Gauss-Bonnet theory,” *Phys. Rev. D* **77** (2008) 104004, [arXiv:0802.0267 \[hep-th\]](https://arxiv.org/abs/0802.0267).
- [290] M. A. Cuyubamba, R. A. Konoplya, and A. Zhidenko, “Quasinormal modes and a new instability of Einstein-Gauss-Bonnet black holes in the de Sitter world,” *Phys. Rev. D* **93** no. 10, (2016) 104053, [arXiv:1604.03604 \[gr-qc\]](https://arxiv.org/abs/1604.03604).
- [291] R. A. Konoplya and A. Zhidenko, “Eikonal instability of Gauss-Bonnet-(anti)-de Sitter black holes,” *Phys. Rev. D* **95** no. 10, (2017) 104005, [arXiv:1701.01652 \[hep-th\]](https://arxiv.org/abs/1701.01652).
- [292] R. A. Konoplya and A. Zhidenko, “The portrait of eikonal instability in Lovelock theories,” *JCAP* **1705** no. 05, (2017) 050, [arXiv:1705.01656 \[hep-th\]](https://arxiv.org/abs/1705.01656).
- [293] S. Nojiri and S. D. Odintsov, “Anti-de Sitter black hole thermodynamics in higher derivative gravity and new confining deconfining phases in dual CFT,” *Phys. Lett. B* **521** (2001) 87–95, [arXiv:hep-th/0109122 \[hep-th\]](https://arxiv.org/abs/hep-th/0109122). [Erratum: *Phys. Lett.B*542,301(2002)].
- [294] S. Nojiri, S. D. Odintsov, and S. Ogushi, “Cosmological and black hole brane world universes in higher derivative gravity,” *Phys. Rev. D* **65** (2002) 023521, [arXiv:hep-th/0108172 \[hep-th\]](https://arxiv.org/abs/hep-th/0108172).
- [295] A. Jansen, “Overdamped modes in Schwarzschild-de Sitter and a Mathematica package for the numerical computation of quasinormal modes,” *Eur. Phys. J. Plus* **132** no. 12, (2017) 546, [arXiv:1709.09178 \[gr-qc\]](https://arxiv.org/abs/1709.09178).
- [296] R. A. Konoplya and A. Zhidenko, “Quasinormal modes of black holes: From astrophysics to string theory,” *Rev. Mod. Phys.* **83** (2011) 793–836, [arXiv:1102.4014 \[gr-qc\]](https://arxiv.org/abs/1102.4014).
- [297] R.-G. Cai, “Gauss-Bonnet black holes in AdS spaces,” *Phys. Rev. D* **65** (2002) 084014, [arXiv:hep-th/0109133 \[hep-th\]](https://arxiv.org/abs/hep-th/0109133).
- [298] M. Cvetic, S. Nojiri, and S. D. Odintsov, “Black hole thermodynamics and negative entropy in de Sitter and anti-de Sitter Einstein-Gauss-Bonnet gravity,” *Nucl. Phys. B* **628** (2002) 295–330, [arXiv:hep-th/0112045 \[hep-th\]](https://arxiv.org/abs/hep-th/0112045).
- [299] S. H. Hendi, S. Panahiyan, and B. Eslam Panah, “Charged Black Hole Solutions in Gauss-Bonnet-Massive Gravity,” *JHEP* **01** (2016) 129, [arXiv:1507.06563 \[hep-th\]](https://arxiv.org/abs/1507.06563).
- [300] S. Chakraborty and N. Dadhich, “Black Holes in pure Lovelock gravity,” *work in progress* (2019).

- [301] D. Glavan and C. Lin, “Einstein-Gauss-Bonnet gravity in 4-dimensional space-time,” *Phys. Rev. Lett.* **124** no. 8, (2020) 081301, [arXiv:1905.03601 \[gr-qc\]](#).
- [302] M. Gurses, T. C. Sisman, and B. Tekin, “Is there a novel Einstein-Gauss-Bonnet theory in four dimensions?”, [arXiv:2004.03390 \[gr-qc\]](#).
- [303] F.-W. Shu, “Vacua in novel 4D Einstein-Gauss-Bonnet Gravity: pathology and instability?”, [arXiv:2004.09339 \[gr-qc\]](#).
- [304] W.-Y. Ai, “A note on the novel 4D Einstein-Gauss-Bonnet gravity,” [arXiv:2004.02858 \[gr-qc\]](#).
- [305] K. Aoki, M. A. Gorji, and S. Mukohyama, “A consistent theory of $D \rightarrow 4$ Einstein-Gauss-Bonnet gravity,” *Phys. Lett. B* **810** (2020) 135843, [arXiv:2005.03859 \[gr-qc\]](#).
- [306] H. Lu and Y. Pang, “Horndeski Gravity as $D \rightarrow 4$ Limit of Gauss-Bonnet,” [arXiv:2003.11552 \[gr-qc\]](#).
- [307] T. Kobayashi, “Effective scalar-tensor description of regularized Lovelock gravity in four dimensions,” [arXiv:2003.12771 \[gr-qc\]](#).
- [308] P. G. Fernandes, P. Carrilho, T. Clifton, and D. J. Mulryne, “Derivation of Regularized Field Equations for the Einstein-Gauss-Bonnet Theory in Four Dimensions,” [arXiv:2004.08362 \[gr-qc\]](#).
- [309] R. A. Hennigar, D. Kubiznak, R. B. Mann, and C. Pollack, “On Taking the $D \rightarrow 4$ limit of Gauss-Bonnet Gravity: Theory and Solutions,” [arXiv:2004.09472 \[gr-qc\]](#).
- [310] Z.-C. Lin, K. Yang, S.-W. Wei, Y.-Q. Wang, and Y.-X. Liu, “Is the four-dimensional novel EGB theory equivalent to its regularized counterpart in a cylindrically symmetric spacetime?”, [arXiv:2006.07913 \[gr-qc\]](#).
- [311] R. A. Konoplya and A. F. Zinhailo, “Quasinormal modes, stability and shadows of a black hole in the novel 4D Einstein-Gauss-Bonnet gravity,” [arXiv:2003.01188 \[gr-qc\]](#).
- [312] P. G. S. Fernandes, “Charged Black Holes in AdS Spaces in 4D Einstein Gauss-Bonnet Gravity,” [arXiv:2003.05491 \[gr-qc\]](#).
- [313] M. Guo and P.-C. Li, “The innermost stable circular orbit and shadow in the novel 4D Einstein-Gauss-Bonnet gravity,” [arXiv:2003.02523 \[gr-qc\]](#).
- [314] R. A. Konoplya and A. Zhidenko, “Black holes in the four-dimensional Einstein-Lovelock gravity,” [arXiv:2003.07788 \[gr-qc\]](#).
- [315] R. Kumar and S. G. Ghosh, “Rotating black holes in the novel 4D Einstein-Gauss-Bonnet gravity,” [arXiv:2003.08927 \[gr-qc\]](#).
- [316] S. G. Ghosh and S. D. Maharaj, “Radiating black holes in the novel 4D Einstein-Gauss-Bonnet gravity,” [arXiv:2003.09841 \[gr-qc\]](#).
- [317] S. G. Ghosh and R. Kumar, “Generating black holes in the novel 4D Einstein-Gauss-Bonnet gravity,” [arXiv:2003.12291 \[gr-qc\]](#).
- [318] R. A. Konoplya and A. Zhidenko, “(In)stability of black holes in the 4D Einstein-Gauss-Bonnet and Einstein-Lovelock gravities,” [arXiv:2003.12492 \[gr-qc\]](#).

- [319] M. S. Churilova, “Quasinormal modes of the Dirac field in the novel 4D Einstein-Gauss-Bonnet gravity,” [arXiv:2004.00513 \[gr-qc\]](https://arxiv.org/abs/2004.00513).
- [320] A. Ghosh, S. Jana, A. K. Mishra, and S. Sarkar, “Constraints on higher curvature gravity from time delay between GW170817 and GRB 170817A,” *Phys. Rev. D* **100** no. 8, (2019) 084054, [arXiv:1906.08014 \[gr-qc\]](https://arxiv.org/abs/1906.08014).
- [321] M. Ishak, “Testing General Relativity in Cosmology,” *Living Rev. Rel.* **22** no. 1, (2019) 1, [arXiv:1806.10122 \[astro-ph.CO\]](https://arxiv.org/abs/1806.10122).
- [322] N. Yunes, K. Yagi, and F. Pretorius, “Theoretical Physics Implications of the Binary Black-Hole Mergers GW150914 and GW151226,” *Phys. Rev. D* **94** no. 8, (2016) 084002, [arXiv:1603.08955 \[gr-qc\]](https://arxiv.org/abs/1603.08955).
- [323] **LIGO Scientific, Virgo, Fermi-GBM, INTEGRAL** Collaboration, B. P. Abbott *et al.*, “Gravitational Waves and Gamma-rays from a Binary Neutron Star Merger: GW170817 and GRB 170817A,” *Astrophys. J. Lett.* **848** no. 2, (2017) L13, [arXiv:1710.05834 \[astro-ph.HE\]](https://arxiv.org/abs/1710.05834).
- [324] L. Visinelli, N. Bolis, and S. Vagnozzi, “Brane-world extra dimensions in light of gw170817,” *Phys. Rev. D* **97** (Mar, 2018) 064039.
<https://link.aps.org/doi/10.1103/PhysRevD.97.064039>.
- [325] H. Yu, B.-M. Gu, F. P. Huang, Y.-Q. Wang, X.-H. Meng, and Y.-X. Liu, “Probing extra dimension through gravitational wave observations of compact binaries and their electromagnetic counterparts,” *Journal of Cosmology and Astroparticle Physics* **2017** no. 02, (Feb, 2017) 039–039. <https://doi.org/10.1088/1475-7516/2017/02/039>.
- [326] S. Jana, G. K. Chakravarty, and S. Mohanty, “Constraints on born-infeld gravity from the speed of gravitational waves after gw170817 and grb 170817a,” *Phys. Rev. D* **97** (Apr, 2018) 084011. <https://link.aps.org/doi/10.1103/PhysRevD.97.084011>.
- [327] P. Cremonese and E. Mörtzell, “The lensing time delay between gravitational and electromagnetic waves,” [arXiv:1808.05886 \[astro-ph.HE\]](https://arxiv.org/abs/1808.05886).
- [328] R. C. Myers, “Higher-derivative gravity, surface terms, and string theory,” *Phys. Rev. D* **36** (Jul, 1987) 392–396. <https://link.aps.org/doi/10.1103/PhysRevD.36.392>.
- [329] R. P. Woodard, “Ostrogradsky’s theorem on Hamiltonian instability,” *Scholarpedia* **10** no. 8, (2015) 32243, [arXiv:1506.02210 \[hep-th\]](https://arxiv.org/abs/1506.02210).
- [330] Y. Sherf, “Hyperbolicity Constraints in Extended Gravity Theories,” *Phys. Scripta* **94** no. 8, (2019) 085005, [arXiv:1806.09984 \[gr-qc\]](https://arxiv.org/abs/1806.09984).
- [331] P. Meszaros, “Gamma-Ray Bursts,” *Rept. Prog. Phys.* **69** (2006) 2259–2322, [arXiv:astro-ph/0605208](https://arxiv.org/abs/astro-ph/0605208).
- [332] P. Kumar and B. Zhang, “The physics of gamma-ray bursts & relativistic jets,” *Phys. Rept.* **561** (2014) 1–109, [arXiv:1410.0679 \[astro-ph.HE\]](https://arxiv.org/abs/1410.0679).
- [333] I. M. Shoemaker and K. Murase, “Constraints from the time lag between gravitational waves and gamma rays: Implications of GW170817 and GRB 170817A,” *Phys. Rev. D* **97** no. 8, (2018) 083013, [arXiv:1710.06427 \[astro-ph.HE\]](https://arxiv.org/abs/1710.06427).

- [334] L. Amendola, C. Charmousis, and S. C. Davis, “Solar System Constraints on Gauss-Bonnet Mediated Dark Energy,” *JCAP* **10** (2007) 004, [arXiv:0704.0175 \[astro-ph\]](#).
- [335] T. Shiromizu, K.-i. Maeda, and M. Sasaki, “The Einstein equation on the 3-brane world,” *Phys. Rev. D* **62** (2000) 024012, [arXiv:gr-qc/9910076](#).
- [336] R. Maartens, “Brane world gravity,” *Living Rev. Rel.* **7** (2004) 7, [arXiv:gr-qc/0312059](#).
- [337] P. Kanti, “Black holes in theories with large extra dimensions: A Review,” *Int. J. Mod. Phys. A* **19** (2004) 4899–4951, [arXiv:hep-ph/0402168](#).
- [338] L. Randall and R. Sundrum, “A Large mass hierarchy from a small extra dimension,” *Phys. Rev. Lett.* **83** (1999) 3370–3373, [arXiv:hep-ph/9905221](#).
- [339] L. Randall and R. Sundrum, “An Alternative to compactification,” *Phys. Rev. Lett.* **83** (1999) 4690–4693, [arXiv:hep-th/9906064](#).
- [340] N. Dadhich, R. Maartens, P. Papadopoulos, and V. Rezania, “Black holes on the brane,” *Phys. Lett. B* **487** (2000) 1–6, [arXiv:hep-th/0003061](#).
- [341] A. N. Aliev and A. E. Gumrukcuoglu, “Charged rotating black holes on a 3-brane,” *Phys. Rev. D* **71** (2005) 104027, [arXiv:hep-th/0502223](#).
- [342] A. N. Aliev and P. Talazan, “Gravitational Effects of Rotating Braneworld Black Holes,” *Phys. Rev. D* **80** (2009) 044023, [arXiv:0906.1465 \[gr-qc\]](#).
- [343] I. Antoniadis, N. Arkani-Hamed, S. Dimopoulos, and G. R. Dvali, “New dimensions at a millimeter to a Fermi and superstrings at a TeV,” *Phys. Lett. B* **436** (1998) 257–263, [arXiv:hep-ph/9804398](#).
- [344] N. Arkani-Hamed, S. Dimopoulos, and G. R. Dvali, “The Hierarchy problem and new dimensions at a millimeter,” *Phys. Lett. B* **429** (1998) 263–272, [arXiv:hep-ph/9803315](#).
- [345] B. Toshmatov, Z. Stuchlík, J. Schee, and B. Ahmedov, “Quasinormal frequencies of black hole in the braneworld,” *Phys. Rev. D* **93** no. 12, (2016) 124017, [arXiv:1605.02058 \[gr-qc\]](#).
- [346] R. Dey, S. Biswas, and S. Chakraborty, “Ergoregion instability and echoes for braneworld black holes: Scalar, electromagnetic and gravitational perturbations,” [arXiv:2010.07966 \[gr-qc\]](#).
- [347] E. S. de Oliveira, “Tidal-charge effects on the superradiance of rotating black holes,” *Eur. Phys. J. C* **80** no. 11, (2020) 1048, [arXiv:2004.10122 \[gr-qc\]](#).
- [348] R. Dey, S. Chakraborty, and N. Afshordi, “Echoes from braneworld black holes,” *Phys. Rev. D* **101** no. 10, (2020) 104014, [arXiv:2001.01301 \[gr-qc\]](#).
- [349] L. Visinelli, N. Bolis, and S. Vagnozzi, “Brane-world extra dimensions in light of GW170817,” *Phys. Rev. D* **97** no. 6, (2018) 064039, [arXiv:1711.06628 \[gr-qc\]](#).
- [350] S. Chakraborty, K. Chakravarti, S. Bose, and S. SenGupta, “Signatures of extra dimensions in gravitational waves from black hole quasinormal modes,” *Phys. Rev. D* **97** no. 10, (2018) 104053, [arXiv:1710.05188 \[gr-qc\]](#).
- [351] K. Chakravarti, S. Chakraborty, S. Bose, and S. SenGupta, “Tidal Love numbers of black holes and neutron stars in the presence of higher dimensions: Implications of GW170817,” *Phys. Rev. D* **99** no. 2, (2019) 024036, [arXiv:1811.11364 \[gr-qc\]](#).

- [352] K. Chakravarti, S. Chakraborty, K. S. Phukon, S. Bose, and S. SenGupta, “Constraining extra-spatial dimensions with observations of GW170817,” *Class. Quant. Grav.* **37** no. 10, (2020) 105004, [arXiv:1903.10159 \[gr-qc\]](https://arxiv.org/abs/1903.10159).
- [353] Z. Horvath and L. A. Gergely, “Black hole tidal charge constrained by strong gravitational lensing,” *Astron. Nachr.* **334** (2013) 1047–1050, [arXiv:1203.6576 \[gr-qc\]](https://arxiv.org/abs/1203.6576).
- [354] A. F. Zakharov, “Constraints on tidal charge of the supermassive black hole at the Galactic Center with trajectories of bright stars,” *Eur. Phys. J. C* **78** no. 8, (2018) 689, [arXiv:1804.10374 \[gr-qc\]](https://arxiv.org/abs/1804.10374).
- [355] I. Banerjee, S. Chakraborty, and S. SenGupta, “Decoding signatures of extra dimensions and estimating spin of quasars from the continuum spectrum,” *Phys. Rev. D* **100** no. 4, (2019) 044045, [arXiv:1905.08043 \[gr-qc\]](https://arxiv.org/abs/1905.08043).
- [356] I. Banerjee, S. Chakraborty, and S. SenGupta, “Silhouette of M87*: A New Window to Peek into the World of Hidden Dimensions,” *Phys. Rev. D* **101** no. 4, (2020) 041301, [arXiv:1909.09385 \[gr-qc\]](https://arxiv.org/abs/1909.09385).
- [357] J. C. S. Neves, “Constraining the tidal charge of brane black holes using their shadows,” *Eur. Phys. J. C* **80** no. 8, (2020) 717, [arXiv:2005.00483 \[gr-qc\]](https://arxiv.org/abs/2005.00483).
- [358] E. Berti, V. Cardoso, and C. M. Will, “On gravitational-wave spectroscopy of massive black holes with the space interferometer LISA,” *Phys. Rev. D* **73** (2006) 064030, [arXiv:gr-qc/0512160](https://arxiv.org/abs/gr-qc/0512160).
- [359] G. Carullo, W. Del Pozzo, and J. Veitch, “Observational Black Hole Spectroscopy: A time-domain multimode analysis of GW150914,” *Phys. Rev. D* **99** no. 12, (2019) 123029, [arXiv:1902.07527 \[gr-qc\]](https://arxiv.org/abs/1902.07527). [Erratum: Phys.Rev.D 100, 089903 (2019)].
- [360] R. Cotesta, A. Buonanno, A. Bohé, A. Taracchini, I. Hinder, and S. Ossokine, “Enriching the symphony of gravitational waves from binary black holes by tuning higher harmonics,” *Phys. Rev. D* **98** (Oct, 2018) 084028. <https://link.aps.org/doi/10.1103/PhysRevD.98.084028>.